UTRECHT MICROPALEONTOLOGICAL BULLETINS

A. J. T. ROMEIN

LINEAGES IN EARLY PALEOGENE CALCAREOUS NANNOPLANKTON

22

UTRECHT MICROPALEONTOLOGICAL BULLETINS

Editor C. W. Drooger
Department of Stratigraphy and Paleontology
State University of Utrecht
Budapestlaan 4, Postbus 80.021
3508 TA Utrecht, Netherlands

In the series have been published:

Bull. 1. T. FREUDENTHAL – Stratigraphy of Neogene deposits in the Khania Province, Crete, with special reference to foraminifera of the family Planorbulinidae and the genus *Heterostegina*. 208 p., 15 pl., 33 figs. (1969) *f* 32,–

Bull. 2. J. E. MEULENKAMP – Stratigraphy of Neogene deposits in the Rethymnon Province, Crete, with special reference to the phylogeny of uniserial *Uvigerina* from the Mediterranean region. 172 p., 6 pl., 53 figs. (1969) *f* 29,–

Bull. 3. J. G. VERDENIUS – Neogene stratigraphy of the Western Guadalquivir basin, S. Spain. 109 p., 9 pl., 12 figs. (1970) *f* 28,–

Bull. 4. R. C. TJALSMA – Stratigraphy and foraminifera of the Neogene of the Eastern Guadalquivir basin, S. Spain. 161 p., 16 pl., 28 figs. (1971) *f* 44,–

Bull. 5. C. W. DROOGER, P. MARKS, A. PAPP et al. – Smaller radiate *Nummulites* of northwestern Europe. 137 p., 5 pl., 50 figs. (1971) *f* 37,–

Bull. 6. W. SISSINGH – Late Cenozoic Ostracoda of the South Aegean Island arc. 187 p., 12 pl., 44 figs. (1972) *f* 57,–

Bull. 7. author's edition. F. M. GRADSTEIN – Mediterranean Pliocene *Globorotalia*, a biometrical approach. 128 p., 8 pl., 44 figs. (1974) *f* 39,–

Bull. 8. J. A. BROEKMAN – Sedimentation and paleoecology of Pliocene lagoonal-shallow marine deposits on the island of Rhodos (Greece). 148 p., 7 pl., 9 figs. (1974) *f* 47,–

Bull. 9. D. S. N. RAJU – Study of Indian Miogypsinidae. 148 p., 8 pl., 39 figs. (1974) *f* 38,–

Bull. 10. W. A. VAN WAMEL – Conodont biostratigraphy of the Upper Cambrian and Lower Ordovician of north-western Öland, south-eastern Sweden. 128 p., 8 pl., 25 figs. (1974) *f* 40,–

Bull. 11. W. J. ZACHARIASSE – Planktonic foraminiferal biostratigraphy of the Late Neogene of Crete (Greece). 171 p., 17 pl., 23 figs. (1975) *f* 52,–

Bull. 12. J. T. VAN GORSEL – Evolutionary trends and stratigraphic significance of the Late Cretaceous *Helicorbitoides-Lepidorbitoides* lineage. 100 p., 15 pl., 14 figs. (1975) *f* 37,–

Bull. 13. E. F. J. DE MULDER – Microfauna and sedimentary-tectonic history of the Oligo-Miocene of the Ionian Islands and western Epirus (Greece). 140 p., 4 pl., 47 figs. (1975) *f* 45,–

Bull. 14. R. T. E. SCHÜTTENHELM – History and modes of Miocene carbonate deposition in the interior of the Piedmont Basin, NW Italy. 208 p., 5 pl., 54 figs. (1976) *f* 56,–

(continued on back cover)

LINEAGES IN EARLY PALEOGENE CALCAREOUS NANNOPLANKTON

A. J. T. ROMEIN

Printed in the Netherlands by Loonzetterij Abé, Hoogeveen
23 november 1979

CONTENTS

50 text-figures, 10 plates

ABSTRACT

A detailed study of the ultrastructure of Paleocene-Middle Eocene calcareous nannofossils has led to the recognition of evolutionary lineages comprising 16 genera and 110 species. The lineages have been established on the basis of evidence from floras derived from closely sampled sections in Spain, Israel, Denmark and Sweden.

Information about the ultrastructure of species, and the relations between species, was gained by investigating selected specimens in the Scanning Electron Microscope, and by studying others with a polarization microscope equipped with a gypsum plate. The latter microscope showed up the extinction- and colour patterns of the specimens. The principles and applicability of the latter technique are discussed.

It is argued that statements about the evolution of calcareous nannoplankton are necessarily speculative due to the nature of the fossil material and the method of study.

Attention was given to the floras in the Cretaceous/Tertiary boundary interval. In this paper it is proposed to define the lower boundary of the lowest nannofossil zone of the Tertiary by the mass occurrence of *Braarudosphaera bigelowii* and/or *Thoracosphaera operculata.* With a few possible exceptions, efforts to detect the Cretaceous ancestors of Tertiary taxa were fruitless.

The Standard Zonation for the Tertiary was applied for the biostratigraphic subdivision of the investigated sequences. The established lineages added to the refinement of this zonation, as most of the zonal markers belong to the lineages.

Additional and, in some cases, new information is given about the ultrastructure and optical behaviour of all taxa encountered. Several new descriptive terms are introduced and some new combinations are made. Nine new species are described: *Biscutum parvulum, Braarudosphaera alta, Cruciplacolithus edwardsii, Cruciplacolithus latipons, Fasciculithus bitectus, Fasciculithus magnicordis, Rhomboaster intermedia, Rhomboaster bitrifida* and *Zygodiscus clausus.*

Chapter I

INTRODUCTION

The term calcareous nannofossils is a collective name for fossils which are smaller than about 30 μ and which are composed of one or more calcite elements.

Most of these fossils are sub-elliptical or circular in distal and proximal views, and are made up of one or more cycles of elements. These forms are interpreted as *coccoliths*: composite calcareous platelets which are secreted today by a certain group of predominantly marine, unicellular, biflagellate, golden-brown algae (Haptophyceae).

In the Recent representatives of this group of algae, the coccoliths are formed by calcification of organic scales, generated in the cisternae of the Golgi-body. After mineralization, the coccoliths are extruded from this body to the cell surface where together they form a coccosphere. The function of these coccoliths is still a subject of speculation; they have been interpreted as by-products of photosynthesis, as lenses, as buoyancy devices or as protective covers.

At present the continuous record of coccoliths ranges from the Lower Jurassic up to the Recent.

Within the size-range of coccoliths and coccospheres, and associated with these, are found calcareous bodies of variable size and shape (rosettes, cubes, spheres, vases) which are probably also of organic origin. Recent organisms forming these kinds of structures are not known, but their organic origin is indicated not only by their construction but also by their limited stratigraphic distribution.

Purpose of the investigation

The aim of the present study is to search for changes within, and relationships between, calcareous nanofossil species. Such a study is likely to yield information which will be primarily of interest to biostratigraphers. Most of the existing nannofossil zonations are based on the entries and exits of a certain number of rather arbitrarily chosen species with unknown ancestor-descendant relationships. A better understanding of relationships adds to the recognizability of the zones.

The investigation was focused on the Lower Paleogene for various reasons: (1) The fossils from this interval are generally somewhat larger than those

from the Mesozoic or the higher Cenozoic and thus easier to study in the L.M.*, (2) a large part of the floras is well illustrated in the literature with L.M., S.E.M.* and T.E.M.* photographs, and (3) the chance of detecting lineages is relatively high, as in the Lower Paleogene a completely new flora came into existence after the extinctions at the end of the Cretaceous.

Previous investigations

Although the need for the detection of evolutionary lineages has been emphasized by several authors and preliminary assumptions have been given in the literature, there is still only a limited number of papers dealing with this subject for the Lower Paleogene.

The first quantitative investigation of an evolutionary trend was made by Moshkovitz (1967) in a short study of the number of rays in *Discoaster multiradiatus* in two samples from the Negev Desert. This trend is worked out in the present study.

Evolutionary lineages within a genus were first published by Gartner (1970). His publication on the genus *Chiasmolithus* is the first in the nannofossil literature to be based on a thorough study of the ultrastructure of the fossils. In the present paper most of Gartner's ideas are corroborated, although a different opinion is expressed about the origin of the genus.

Hekel (1968) elaborated the relationship between the genera *Rhomboaster* and *Marthasterites,* which had already been indicated by Stradner and Papp (1961). It appears that several more taxa can be placed in this lineage.

The origin of, and the lineages in, the genus *Discoaster* formed the subject of a study by Prins (1971). In the opinion of the present author *Discoaster* is a "biphyletic" genus and, as a consequence, the lineages presented here differ from Prins' suggestions.

Haq (1973b) described evolutionary lineages in the genus *Helicopontosphaera.* Only the early part of these lineages falls within the studied interval; information will be given about the origin of the genus.

Methods

The assemblages have been examined with the aid of both the L.M. and the S.E.M. As the gathering of observations with the S.E.M. is extremely time-consuming and as much of the material showed a variable degree of calcite overgrowth, most of the information presented is based on the in-

* = Light Microscope, Scanning Electron Microscope, Transmission Electron Microscope.

vestigations with the L.M.

We used a Leitz Orthoplan microscope, with polarization equipment, a gypsum plate and a revolving object table with a graduated scale. The oculars were provided with a micrometer and cross-hairs, parallel to the polarization directions. The specimens were viewed with a magnification of 1250 ×.

S.E.M.-studies were carried out with a Cambridge Mark II microscope at a high tension of 30 Kilovolts. The specimens were coated with gold in a Polaron Sputter apparatus for four minutes at a high tension of 2 Kilovolts.

Preparation of the samples

For investigations in the L.M. a standard quantity of each sediment sample (about 1 cm^3) was allowed to disintegrate in distilled water for 24 hours. Smear slides were prepared from the resulting suspension. The nannofossil fraction was not concentrated, since this might distort the composition of the assemblages. Canada balsam was used as the embedding medium for the fixed mounts. For special studies (side views) mobile mounts were prepared, Castor oil being used as the viscous fluid.

For the examination of selected nannofossil species in the S.E.M., the required size-fraction was concentrated by means of the settling method. We tried to clean the fossil material using various techniques (repeated centrifugation, ultrasonic treatment, adding of H_2O_2) but had little success.

Although laborious, the method described by Moshkovitz (1974) and Hansen et al. (1975) and used to study the same object in the L.M. and the S.E.M. proved to be very useful. Instead of alcohol, M.I.B.K. was used as the volatile medium in the L.M. because it evaporates less quickly.

L.M. Investigation Technique

For routine studies of nannofossil assemblages and specimens (especially for secondarily overgrown ones) the L.M. is, and will remain the most obvious instrument. In the present study we made extensive use of cross-polarized light and the gypsum plate to obtain a maximum amount of information.

a. Information gained in cross-polarized light

Coccoliths (and supposedly related calcareous nannofossils) are composed of one or more modified calcite rhombohedrons which may be arranged in superposed cycles.

Calcite is a uni-axial, negative mineral (fig. 1a). When a crystal thinner than 10 μ, such as is found in nannofossils, is placed between crossed nicols it will show interference-colours if the optical axis makes an angle with the

vibration directions of the nicols (fig. 1b). The crystal becomes dark when the optical axis coincides with the microscopical axis or when the optical axis is parallel to the vibration direction of one of the polarizers (fig. 1c).

In calcareous nannofossils the optical behaviour is the result of the thickness and the orientation of the elements and of the number of superposed elements. In most nannofossils that are placed between crossed nicols the areas showing interference-colours are larger than those showing extinction. The latter zones are called extinction lines, and together these lines form a cross-like pattern (in distal and proximal view). In coccoliths the extinction lines can be observed best in the central area, the wall and the proximal shield.

The shape of the extinction lines, the angles formed by them, and the angles between the lines and the polarization directions are variable. Three

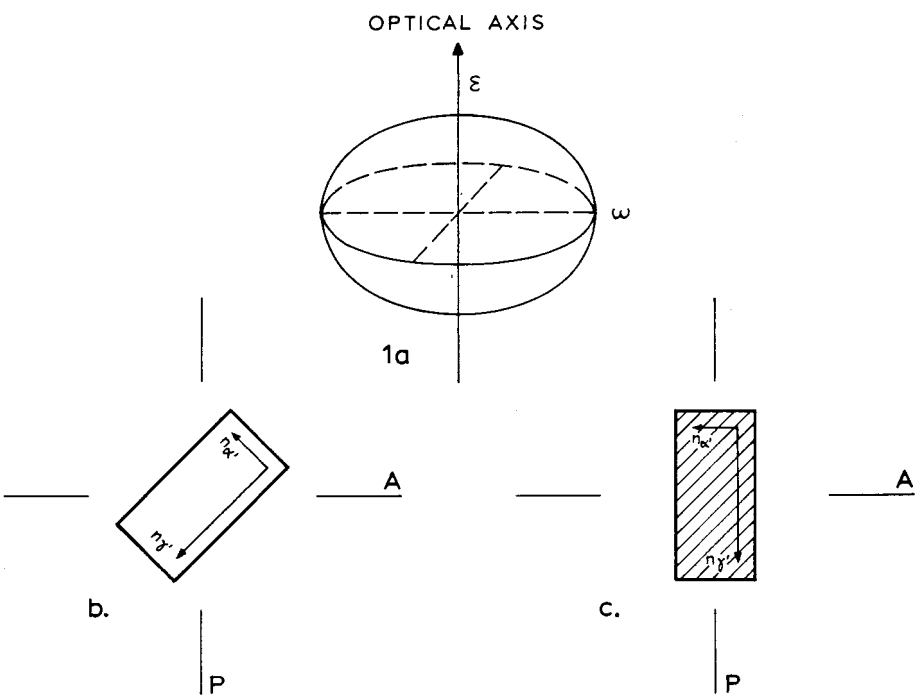

Fig. 1 a. Indicatrix of a uni-axial, negative mineral; n_ω ordinary ray; n_ϵ extraordinary ray.
b. The refractive indices of the crystal make an angle with the nicols; the crystal shows interference (A: analyzer, P. polarizer, n_α: smaller refractive index; n_γ: larger refractive index).
c. The refractive indices of the crystal are parallel to the nicols; the crystal shows extinction.

general types of extinction crosses can be discerned in the assemblages from the Lower Paleogene:

Type I. The extinction crosses are composed of straight lines; the lines are parallel to the polarization directions (fig. 2a) (Fasciculithaceae, Sphenolithaceae).

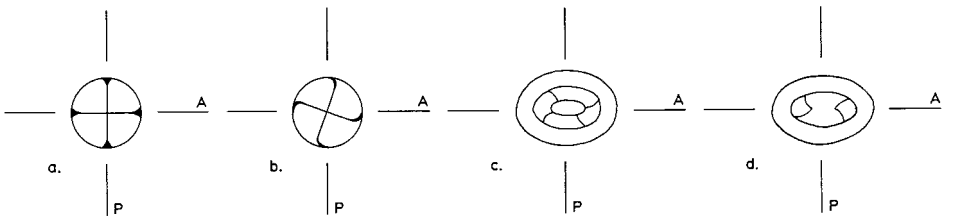

Fig. 2 Types of extinction crosses (all distal views):
a. Straight lines, parallel to the polarizers.
b. Straight lines making an angle of about 20° in clockwise direction with the polarizers, and curved only marginally (laevogyre).
c. d. Curved lines; c: laevogyre, d: dextrogyre.

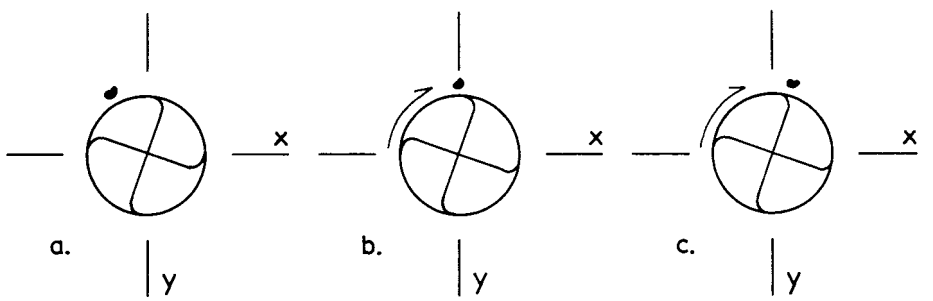

Fig. 3 Method to determine the angle between the extinction lines and the polarization directions (X, Y: cross-hairs, parallel to the polarizers; distal view).
a. Find object in the vicinity of the nannofossil,
b. Rotate clockwise until the object is in line with one of the cross-hairs; read scale (a),
c. Rotate further, until the object is in line with the (straight) part of an extinction line; read scale (b); a minus b gives the desired angle.

Type II. The extinction crosses are composed of lines which are straight over most of their length and curved only near the margin. The lines are normal to each other, but the straight parts make an angle with the polarization directions (fig. 2b) (Discoasteraceae, Heliolithaceae). This angle is measured clockwise in distal view (fig. 3).

Type III. The extinction crosses are composed of curved lines which are not normal to each other. The lines are called laevogyre if they bend to the

left (Coccolithaceae), dextrogyre if they bend in the opposite direction (Noëlaerhabdaceae, Zygodiscaceae, Pontosphaeraceae, Biscutaceae, Ellipsagelosphaeraceae, both in distal view (figs. 2c, d, respectively).

Each irregularity in the extinction lines is indicative of a change in the orientation of the elements, which permits the distinction of very narrow cycles of elements. Once the extinction pattern of a species is established, very small or heavily calcified specimens can readily be recognized and it is easy to decide which side of a specimen is lying upwards. The latter is of importance in the measurement of angles.

When the centre of a nannofossil is examined in side view under the microscope, the different cycles can be distinguished better in cross-polarized light than in normal light, as some cycles will show interference-colours while others are dark. The light penetration is reversed when the table is rotated over 90°.

In the course of the investigation it appeared that the extinction patterns are constant at the species and genus level, and in some cases even at the family level. The patterns thus are a helpful tool for determination and classification.

b. Information gained in cross-polarized light with a gypsum plate inserted in the light-beam

Depending on the orientation of the calcite crystal with regard to the microscope axis, the interference-colour becomes higher or lower after the

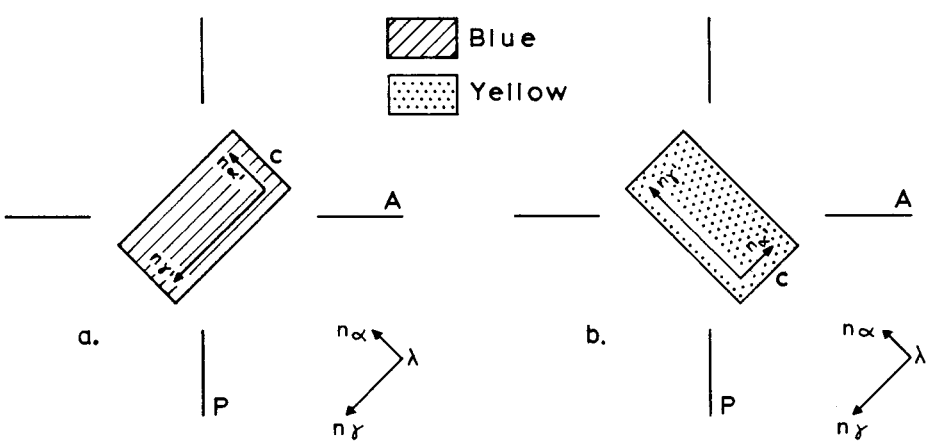

Fig. 4 Behaviour of a crystal thinner than 10 μ between crossed polarizers and with a gypsum plate (1 λ) inserted in the light-beam.
a. The colours are "added", the crystal becomes blue.
b. The colours are "substracted", the crystal becomes yellow.

insertion in the light-beam of the gypsum plate (first order red) at an angle of 45° with the polarization directions.

A crystal (thinner than 10 μ) becomes blue when the smaller refractive index of the gypsum plate (n_α) is parallel to the smaller refractive index ($n_{\alpha'}$) of the crystal ("the colours are added", fig. 4a). The crystal becomes yellow when the corresponding indices are at an angle of 90° ("the colours are substracted", fig. 4b).

When the gypsum plate is inserted, nannofossils show sectors, limited by extinction lines; these sectors are alternately blue and yellow (second order yellow, third order blue, Carl Zeiss colour table after M. Lévy). The colours are helpful for observing the configuration of the extinction lines, especially in very small forms or in forms with vague extinction lines.

One can determine at a glance which side of a specimen is lying upwards (fig. 5a).

The colour distribution permits the distinction of even the narrowest cycle of elements in distal, proximal or in side view. Structures which belong to the same unit will display the same colour (fig. 5b). In the course of the investigation it was found that homologous structures have the same colour (in side view) in different species or genera; this observation made it possible to "follow" structures and their transformation in time (fig. 5c).

The species concept

Species of calcareous nannofossils are defined typologically. As a consequence of this species concept two morphologically different, fossil coccoliths will be assigned to two species. Morphologically distinct specimens may, however, well have belonged to a single coccosphere, as it is known that Recent coccospheres may bear several types of coccoliths and that the types of coccoliths may change considerably in successive phases of the life cycle of a species (Parke and Adams, 1960). In addition, morphological differences in coccoliths of Recent species may be the result of differences in temperature (Watabe and Wilbur, 1966). Thus, a fossil species and a living species are different entities.

Frequencies of species

On the range charts for the various sections, the frequencies of the species are indicated by subjective notations. A more precise quantitative approach was considered to be beyond the scope of the study. It appeared that species important for the establishing of lineages are often rare. They would fall outside the fixed-number counts, especially in the highly diverse floras of the

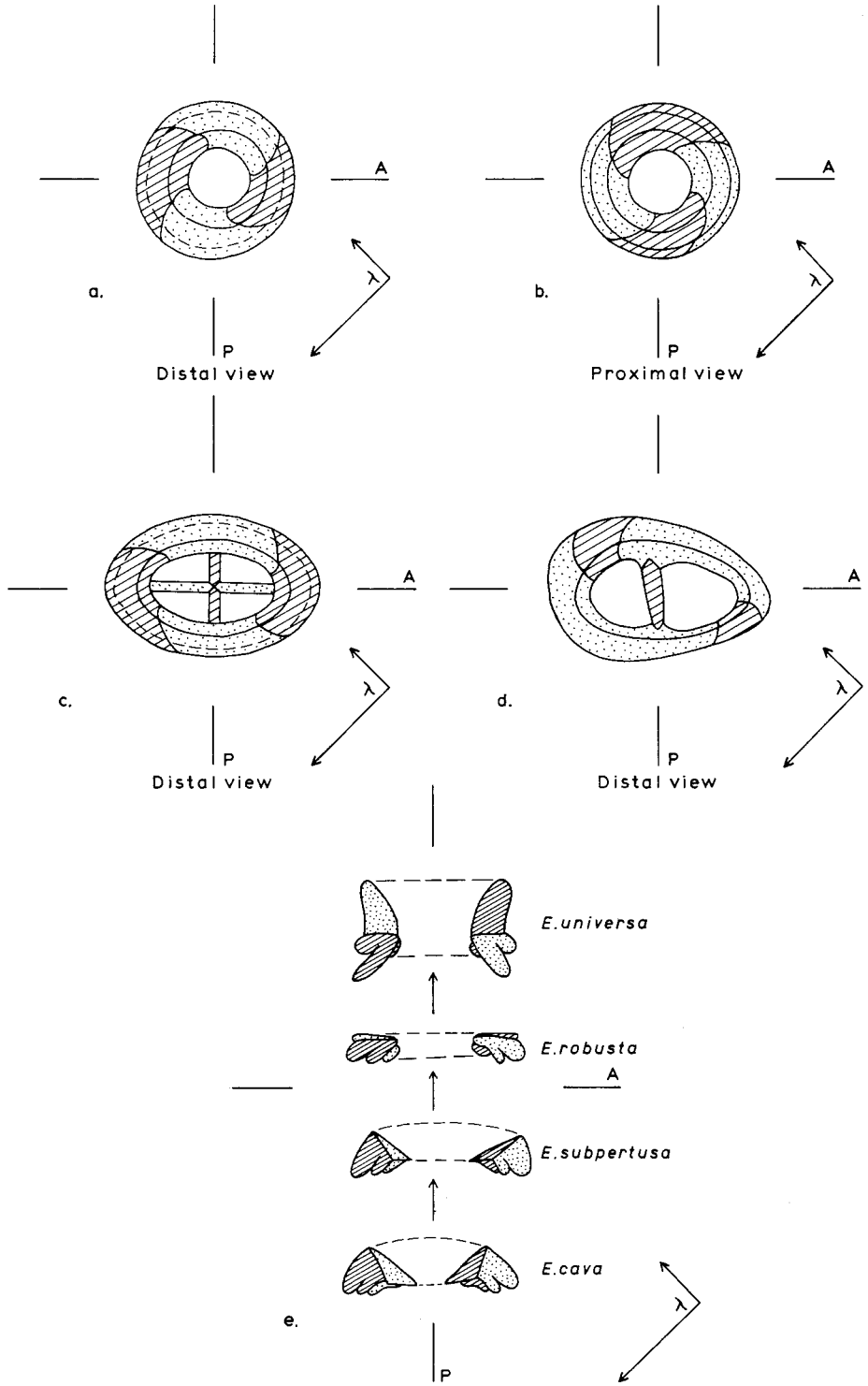
a.
A
λ
P
Distal view
b.
A
λ
P
Proximal view
c.
A
λ
P
Distal view
d.
A
λ
P
Distal view
E.universa
E.robusta
A
E.subpertusa
E.cava
e.
λ
P

Upper Paleocene and Lower Eocene.

The following relative frequency categories are discerned: (a) Rare: one or two specimens per hundred fields, (b) Few: 1 specimen per ten fields, (c) Common: about one specimen in every field, (d) Abundant: tens of specimens per field.

Acknowledgements

The author wishes to express his thanks to the following persons: C. W. Drooger for his critical reading of the manuscript, R. R. Schmidt for introducing him to the study of calcareous nannofossils and his assistance in the field, A. von Hillebrandt and J. Smit for providing some of the material from the Caravaca section, Z. Reiss and C. M. Benjamini for their hospitality and for fruitful discussions, B. Prins for suggesting the use of the "gypsum-red method" and for many valuable comments, C. Bakker for his assistance at the S.E.M., and the members of the "Vakgroep voor Electronenmicroscopie en moleculaire cytologie" of the University of Amsterdam for providing facilities, J. P. van der Linden, A. van Doorn and P. Hoonhout for the careful drawing of the text-figures, and M. Y. Asperslag for typing the manuscript.

The financial support from the Netherlands Organization for the advancement of Pure Research (Z.W.O.) is gratefully acknowledged.

Fig. 5 Information gained with the aid of a gypsum plate is cross-polarized light.

a. Distal and proximal view of a coccolith, showing the different colour distribution in the wall and the proximal shield in these views.

b. In the left species, the cross-bars and the wall show opposite colours, while the colours in the distal shield are mixed; this indicates the presence of at least three, ultrastructurally different components.
In the right species, the wall and the flange show the same colours, indicating the presence of a single, continuous structure.

c. Lineage in the genus *Ericsonia,* showing that the colours of the separate structural units are constant, while their position is changing.

Chapter II

EVOLUTION IN CALCAREOUS NANNOFOSSILS

At first sight calcareous nannofossils appear to be eminently suitable for evolutionary studies: we can deal with huge "populations" of, often well preserved fossils, from stratigraphically closely spaced samples over widespread areas. Several authors have in fact used the term evolution in connection with calcareous nannofossils (Gartner, 1970; Bukry,1971a; Prins, 1971). In the papers of these authors, however, little or no attention is given to concepts and methods in evolutionary studies or to whether sequences of calcareous nannofossils really reflect evolution. We think that such matters should be discussed if we are to delimit the framework within which our statements in Chapter V should be read.

Evolution

One could define the evolution of organisms as the modification through time of genes and gene frequencies. In paleontology we can study only the morphology of fossils, which means the phenotypic expression of the genotype and the modifications enacted by the environment. In evolutionary studies of paleontology we deal with morphology and the morphological transformations that occur in the course of time.

Calcareous nannofossil species

In most groups of fossils a species consists of remains of complete *individuals* (e.g. Gastropods, Foraminifera). In the case of calcareous nannofossil species we find ourselves in a different situation. As the coccospheres of most species are unknown, a nannofossil species consists of similar isolated *anatomical parts* of individuals. When we find a fossil coccolith, we know nothing of the actual individual coccosphere; we do not know its size, its shape, or the number of coccoliths in the sphere. We cannot even be sure that different coccoliths belonged to different individuals or to different biospecies.

Calcareous nannofossil assemblages

Thanatocoenoses give an imperfect, distorted image of the biocoenoses. First of all it is known from studies of Recent coccospheres that the number of fossilizable species is considerably lower than the number of living species

(Honjo and Okada, 1974). This is due to the low degree of mineralization of the organic scales in many species. Furthermore it is known that the coccoliths of fossilizable species may be strongly affected by dissolution and calcification during and after sedimentation (Adelseck et al., 1973; Roth and Berger, 1975).

One should be very careful in drawing conclusions from the relative frequencies of coccolith species in death assemblages. When, for instance, coccoliths of species A are more frequent in an assemblage than coccoliths of species B, several interpretations are possible: (a) the number of coccospheres of species A was higher than that of species B, (b) the species had roughly the same frequencies, but the spheres of species A were composed of more coccoliths than those of species B, (c) whatever the original frequencies, the coccoliths of species B were more susceptible to dissolution owing to their construction.

Evolution of calcareous nannoplankton

Although the facts mentioned in the foregoing paragraphs do not affect the use that can be made of calcareous nannofossils in biostratigraphic subdivisions, they do have a distinct bearing on statements on phylogeny. It is emphasized that in a strict sense we cannot speak of the evolution of calcareous nannoplankton; populations evolved, not anatomical parts of individuals. Thus, any statement about the phylogeny of calcareous nannoplankton can be based only on a supposed evolution, because of the nature of our fossils.

The establishment of ancestor-descendant relationships in calcareous nannofossils appears to give rise to "cladistic" patterns: new species do not replace the ancestor, but they range upwards side by side at least for some time.

Speciation

Recent populations of calcareous nannoplankton species consist of innumerable individuals, and they are spread over a large part of the oceanic realm. It is hard to imagine how repeated "cladogenesis" can take place in such assumedly large interbreeding (?) populations.

Polyploidy is a possible explanation, but as long as this phenomenon has not been observed in living coccospheres it is hardly acceptable.

Some sort of isolation is always involved in models for speciation (Eldredge and Gould, 1972, 1977; Sylvester-Bradley, 1977). In which way(s) can nannoplankton populations become isolated?

First of all it should be noted that the life cycles of Recent calcareous

nannoplankton species are still poorly understood; both sexual and asexual reproduction have been observed, but little is known about the periodicity in the alternation of sexual and asexual generations (Klaveness, 1972). It might well be that we are not dealing with large interbreeding populations, but with large clones, reproducing asexually for many generations, which, after a longer period find themselves sexually isolated from each other.

An example of isolation through land barriers was recently postulated by Gartner and Keany (1978). These authors proposed that "Danian" coccolithophores developed during the Late Maastrichtian in an isolated Arctic Ocean. It seems unlikely, however, that earlier and later diversifications are the result of repeated isolations of this geographical type.

Speciation through geographical isolation, i.e. isolation in a remote area, and subsequent migration might explain the sudden appearance of many species in the stratigraphical record. "Cladistic" speciation following a period of isolation, however, cannot account for the relatively frequent co-occurrence of ancestral species, descendant species and transitional forms.

In our opinion ecological separation is a more likely type of isolation. From in vitro studies of cells (Outka and Williams, 1971) it is known that reproduction, coccolith formation and coccolith shape are highly influenced by temperature, salinity, light intensity and nutrients. It is conceivable that (shifts in) barriers created by these factors resulted in laterally, as well as vertically isolated populations. Isolation and subsequent speciation at different depths in the photic zone might serve as an explanation for the co-occurrence, in assemblages, of ancestral and descendant species, and transitional forms.

The words cladogenesis and cladistic are placed between quotation marks as we are well aware that these terms apply to populations of individuals, not to parts of individuals.

Trends and morphoclines

The words trend and morphocline occur frequently in the literature on evolution and are used in a variety of ways. In the present paper the term trend is used with the meaning of tendency; i.e. morphological change in a particular direction. The term morphocline is used with the meaning of a morphological gradient linked to a certain lapse of time. The term applies to gradients within a species as well as to gradients in a line of descent in which more than one species is involved. Thus we speak of a trend towards larger size in the morphocline of a species, and of a trend towards larger size in a morphocline formed by successive morphologically stable species in a line of descent.

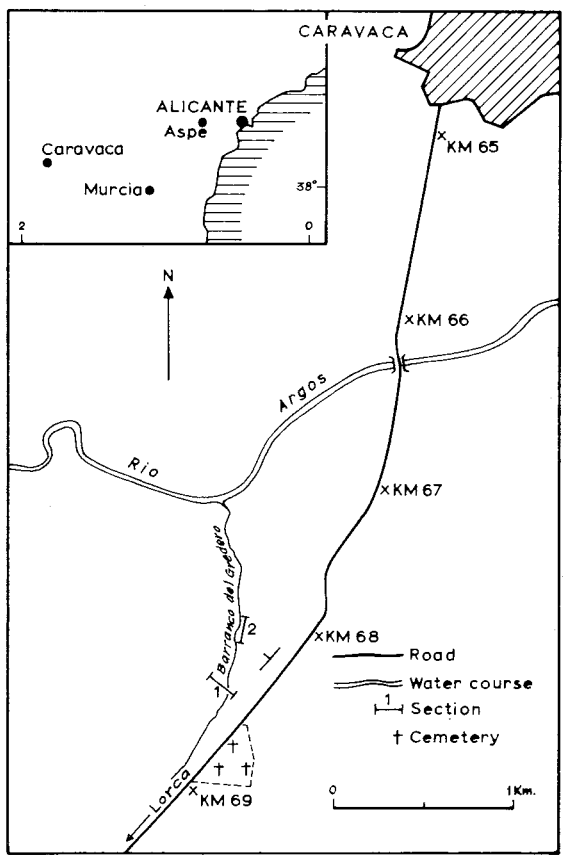

Fig. 6 Sketch maps showing the investigated localities in S.E. Spain, and the location of the Caravaca section (after Van Veen, 1969; Von Hillebrandt, 1974).

Chapter III

PROVENANCE OF THE MATERIAL; BIOSTRATIGRAPHY

Theoretically the study of evolution of any group of fossils should be based on closely spaced samples from many continuous, and lithologically uniform sequences in different parts of the world. If such a study concerns calcareous nannofossils, two more requirements must be fulfilled: (a) the sediment should disintegrate in water, and (b) the degree of solution or of calcite overgrowth of the fossils should not vary beyond certain narrow limits.

In practice such stratigraphic sequences are hard to find, especially if only land sections are taken into consideration.

Three longer sections that fulfil at least some of the above requirements have been investigated. They are located in S.E. Spain (sections Caravaca and Aspe) and Israel (section Nahal Avdat). Several shorter sections covering the Lower Paleocene in Denmark and Sweden were also taken into account so that the floras from Boreal regions could be compared with those from the Tethys realm.

S.E. SPAIN

Section Caravaca

Location and geological setting

The investigated sequence is to be found in the Barranco del Gredero, four kilometres South of the town of Caravaca. The sediments are exposed in the walls of this barranco (steep-sided gully), which runs almost parallel to the road from Lorca to Caravaca (fig. 6).

Structurally the sequence is located in the Subbetic Zone of the Betic Cordilleras, which is the Alpine mountain chain extending in a WSW-ENE direction from Cadiz to the area South of Valencia. The Subbetic Zone comprises folded and overthrust, neritic and pelagic sediments of Triassic to Late Tertiary age.

The deposits exposed in the Barranco del Gredero form part of a relatively undisturbed sequence which Paquet (1962) called the Loma de Solana Unit. Van Veen (1969) placed these deposits in his Jorquera Formation, which consists of a 225 m thick succession of light-coloured calcilutites and marls, with intercalated calcarenites (probably the result of mass-transport).

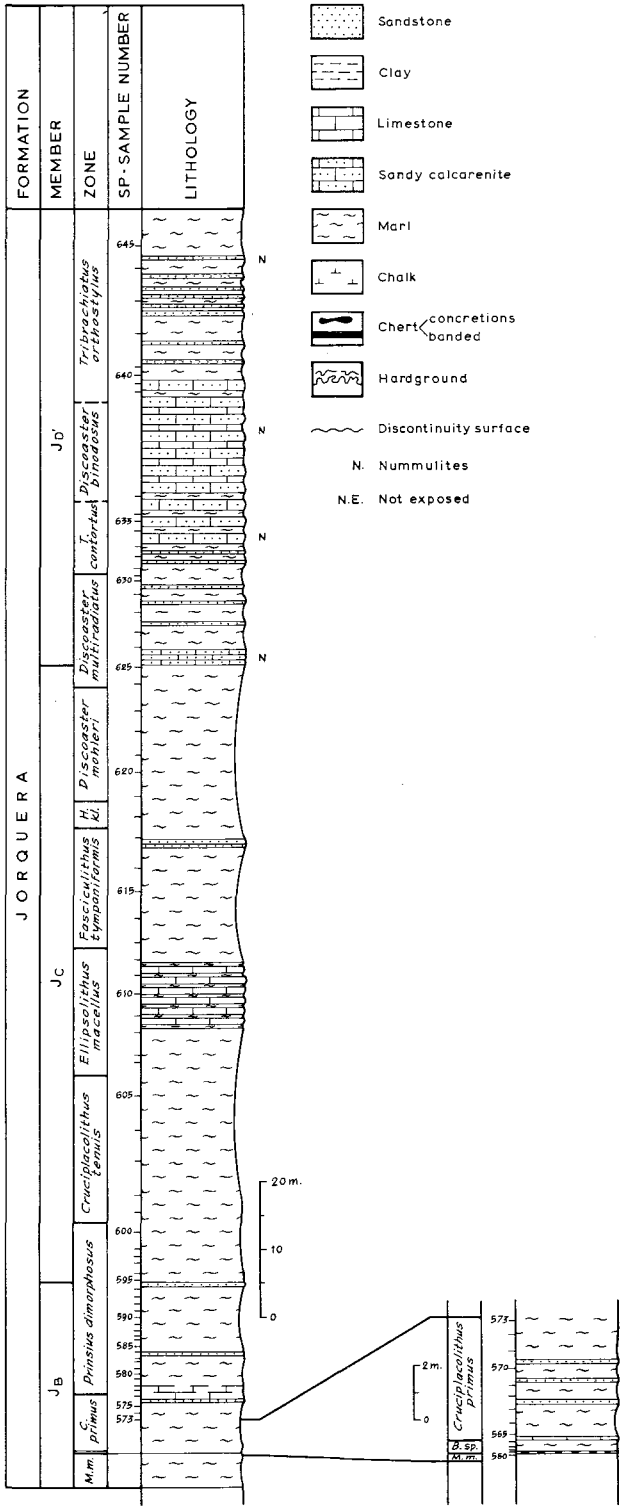

Fig. 7 Section Caravaca; lithology, position of samples and biozonation.

Lithostratigraphy

Van Veen divided the formation into four "somewhat artificial" members, J_a–J_d; for the present study only the uppermost part of member J_b, and members J_c and J_d are of importance (fig. 7).

We started our sampling at the Cretaceous/Tertiary boundary, which is known to be situated at the base of a 20 cm thick, dark-green clay in the upper part of the J_b member (Smit, 1977; Romein, 1977). The overlying part of this member (25 m) consists predominantly of greenish marls.

The J_c member (90 m), composed of olive-green marls, contains a 5 m thick interval of alternating red to yellow marls and hard calcilutites (faciès Couches Rouges).

The J_d member (65 m) is formed by light olive-green marls alternating with medium- to thick-bedded, slightly arenaceous calcarenites.

Sampling was stopped in the uppermost part of the J_d member because the overlying strata (belonging to Van Veen's Gredero Formation) are poorly exposed and are tectonically disturbed.

Biostratigraphy (fig. 8)

The upper part of the J_b member comprises the *Biantholithus sparsus* Zone, the *Cruciplacolithus primus* Zone, and most of the *Prinsius dimorphosus* Zone.

The J_c member corresponds to the uppermost part of the *Prinsius dimorphosus* Zone, the *Cruciplacolithus tenuis* Zone, the *Ellipsolithus macellus* Zone, the *Fasciculithus tympaniformis* Zone, the *Heliolithus kleinpellii* Zone, the *Discoaster mohleri* Zone and the lower part of the *Discoaster multiradiatus* Zone. The faciès Couches Rouges falls completely within the *Ellipsolithus macellus* Zone.

The J_d member encompasses the upper part of the *Discoaster multiradiatus* Zone, the *Tribrachiatus contortus* Zone, the *Discoaster binodosus* Zone and the *Tribrachiatus orthostylus* Zone.

Remarks

All samples, except those from the lower part of the J_d member (= upper part of the *Discoaster multiradiatus* Zone and the lower part of the *Tribrachiatus contortus* Zone), contained rich nannofossil floras. Most specimens showed a moderate calcite overgrowth.

The flora of sample SP 560, collected just below the Cretaceous/Tertiary boundary, indicated the presence of the *Micula murus* Zone of Late Maastrichtian Age (Romein 1977). *Nephrolithus frequens* was not present in the assemblage.

Tribrachiatus contortus did not occur in the Lower Eocene floras from

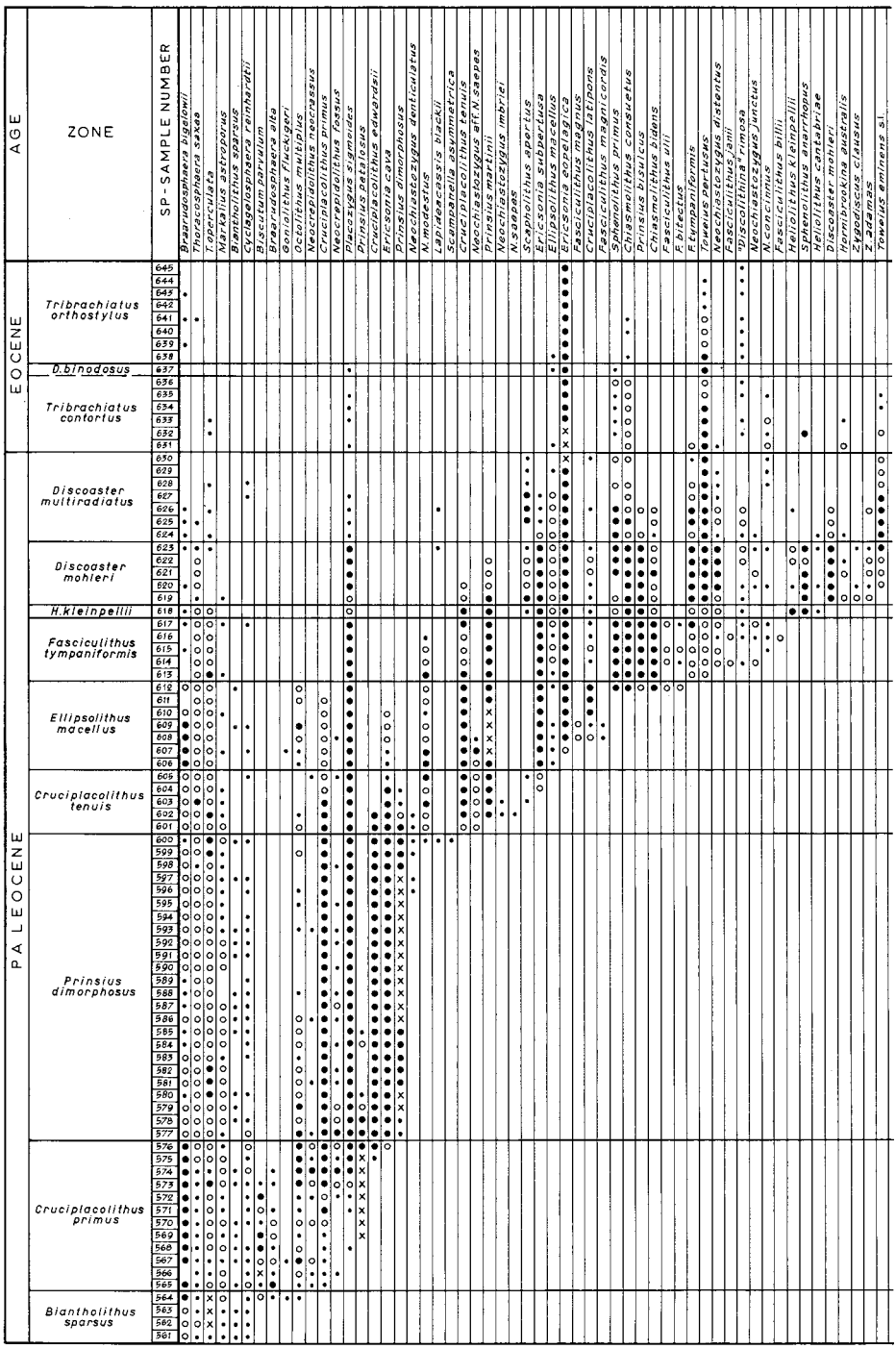

Fig. 8 Distribution of species in the Caravaca section.

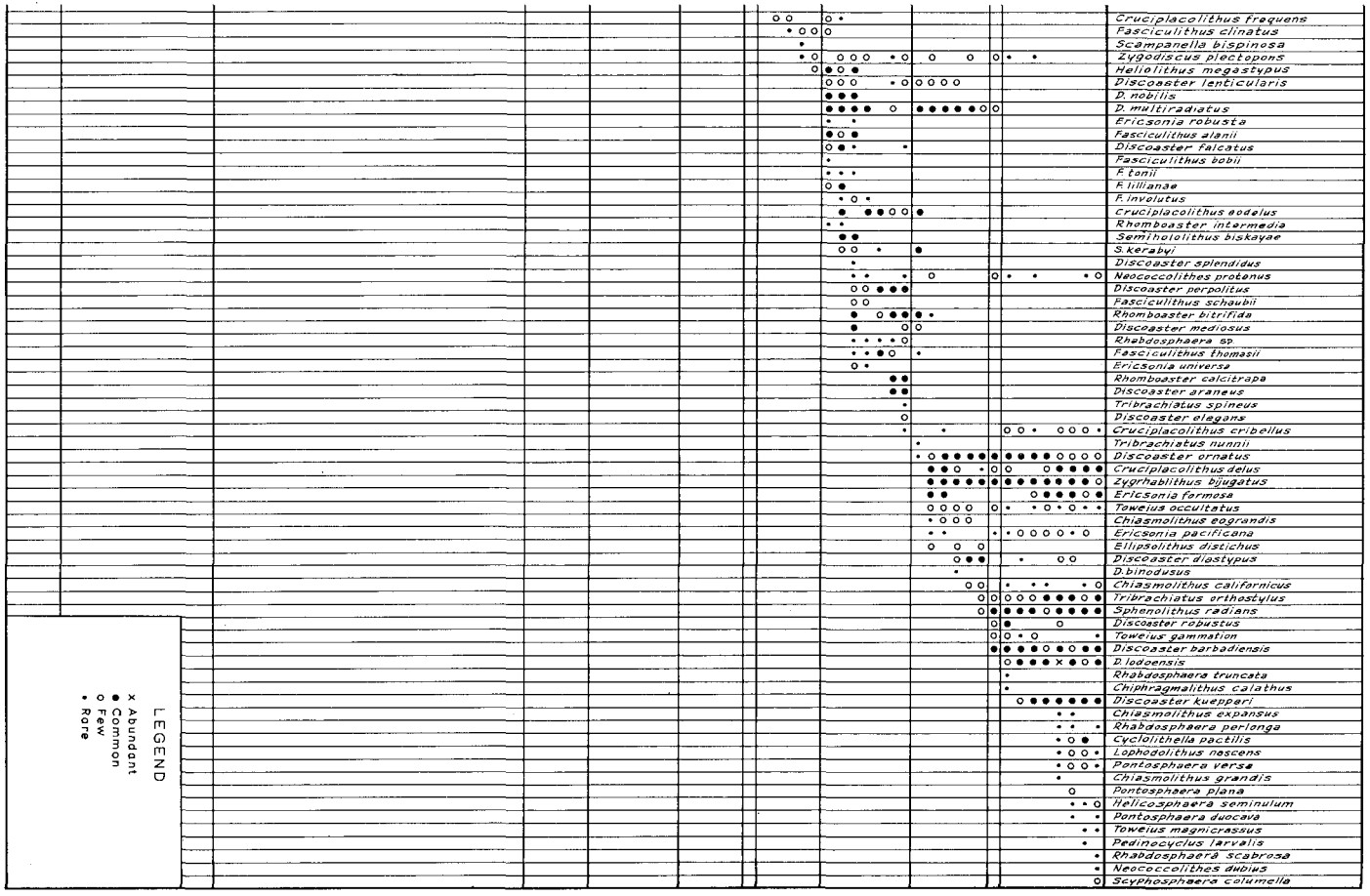
Cruciplacolithus frequens
Fasciculithus clinatus
Scampanella bispinosa
Zygodiscus plectopons
Heliolithus megastypus
Discoaster lenticularis
D. nobilis
D. multiradiatus
Ericsonia robusta
Fasciculithus alanii
Discoaster falcatus
Fasciculithus bobii
F. tonii
F. hillianae
F. involutus
Cruciplacolithus eodelus
Rhomboaster intermedia
Semihololithus biskayae
S. kerabyi
Discoaster splendidus
Neococcolithes protenus
Discoaster perplitus
Fasciculithus schaubii
Rhomboaster bitrifida
Discoaster mediosus
Rhabdosphaera sp.
Fasciculithus thomasii
Ericsonia universa
Rhomboaster calcitrapa
Discoaster araneus
Tribrachiatus spineus
Discoaster elegans
Cruciplacolithus cribellus
Tribrachiatus nunnii
Discoaster ornatus
Cruciplacolithus delus
Zygrhablithus bijugatus
Ericsonia formosa
Toweius occultatus
Chiasmolithus eograndis
Ericsonia pacificana
Ellipsolithus distichus
Discoaster diastypus
D. binodusus
Chiasmolithus californicus
Tribrachiatus orthostylus
Sphenolithus radians
Discoaster rapusus
Toweius gammation
Discoaster barbadiensis
D. lodoensis
Rhabdosphaera truncata
Chiphragmalithus calathus
Discoaster kuepperi
Chiasmolithus expansus
Rhabdosphaera perlonga
Cyclolithella pactilis
Lophodolithus nascens
Pontosphaera versa
Chiasmolithus grandis
Pontosphaera plana
Helicosphaera seminulum
Pontosphaera duocava
Toweius magnicrassus
Pedinocyclus larvalis
Rhabdosphaera scabrosa
Neococcolithes dubius
Scyphosphaera columella
LEGEND
x Abundant
● Common
o Few
• Rare

this sequence; the boundary between the *T. contortus* Zone and the *Discoaster binodosus* Zone has been arbitrarily drawn between the appearance of *T. orthostylus* and the entry of *Discoaster barbadiensis* (based on evidence from the Nahal Avdat section, Israel).

Previous investigations

Papers dealing with the geological setting and the planktonic and (smaller and larger) benthonic foraminifera of this sequence have been presented by Fallot et al. (1958), Durand Delga and Magné (1959), Paquet (1962, 1967), Van Veen (1969), Von Hillebrandt (1974, 1976) and Abtahi (1975). A detailed account of the Cretaceous/Tertiary boundary interval was given by Smit (1977, foraminifera) and Romein (1977, nannofossils).

Section Aspe

Location and geological setting

Upper Cretaceous and Paleogene, Subbetic rocks are exposed in the hills South of Aspe in an area delimited by the roads leading from Aspe to Crevillente and from Aspe to Elche. The section lies SW of the Km. 3 markerstone of the latter road (fig. 9).

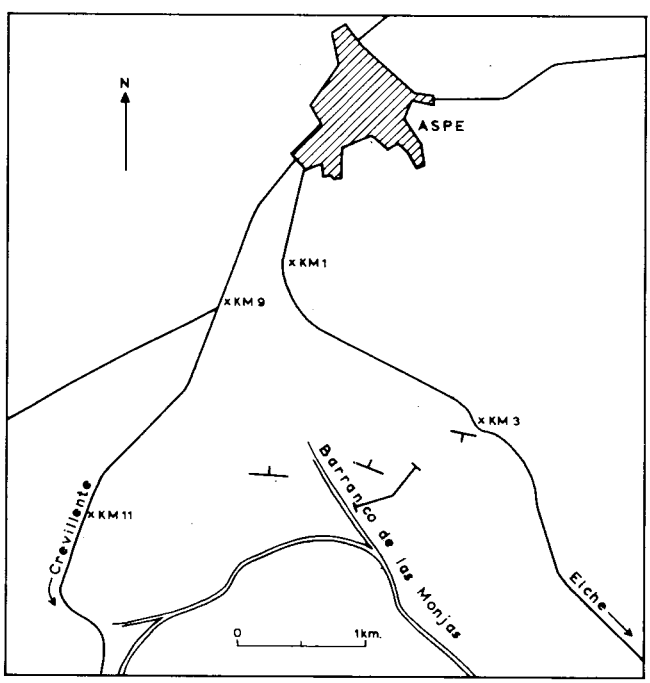

Fig. 9 Sketch map showing the location of the Aspe section (after Von Hillebrandt, 1974). For legend, see Fig. 6.

Lithostratigraphy

The succession of Cretaceous to Oligocene sediments was subdivided by Von Hillebrandt (1974) into six lithological units. Only the sediments of units 4 and 5 are taken into consideration (fig. 10), as the units 1 to 3, consisting of rocks of Late Maastrichtian to Late Paleocene age, contain several hiatuses.

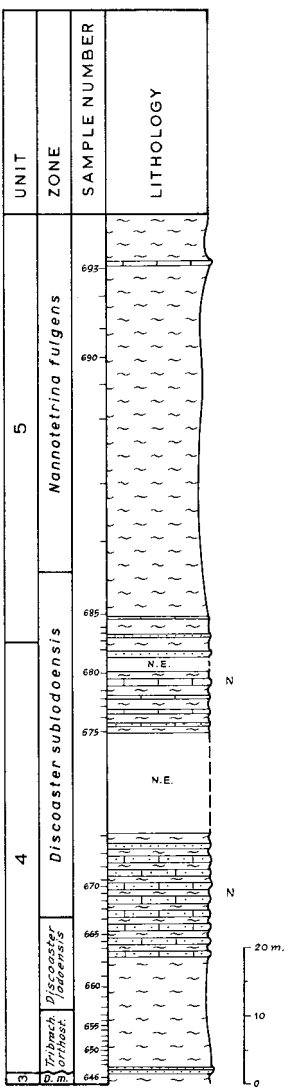

Fig. 10 Section Aspe; lithology, position of samples and biozonation. For legend, see Fig. 7.

Unit 4 (62.5 m) is composed of marls, sandstones and limestones. Brownish to olive-green marls occur in the lower part. The upper part of the unit is composed of an alternation of thin- to thick-bedded, fine grained sandstones, marls and limestones. Many beds contain larger benthonic foraminifera.

Unit 5 (about 60 m) is composed mainly of greenish to brownish marls. The unit was subdivided by Von Hillebrandt into a lower and an upper part, separated by an 85 cm thick, bioclastic limestone. Only the lower part of the unit was sampled for the present study.

Biostratigraphy (fig. 11)

Unit 4 contains the *Tribrachiatus orthostylus* Zone, the *Discoaster lodoensis* Zone and most of the *Discoaster sublodoensis* Zone.

The lower part of unit 5 corresponds to the upper part of the *Discoaster sublodoensis* Zone and at least the lower part of the *Nannotetrina fulgens* Zone.

The presence of "*Cyclolithella*" *pactilis, Neococcolithes dubius* and *Helicosphaera seminulum* in the lowermost sample of the section in the *Tribrachiatus orthostylus* Zone, indicates that there is a small gap between the sections Caravaca and Aspe.

Remarks

The floras from this sequence are well diversified, but most specimens showed an inconveniently high degree of secondary calcification.

An examination of the assemblages from units 2 and 3 indicated the presence of the *Micula murus* Zone, the *Cruciplacolithus tenuis* Zone and the *Discoaster multiradiatus* Zone, pointing to several gaps in the Lower and Middle Paleocene and immediately below unit 4.

Previous investigations

The planktonic and larger benthonic foraminifera of this section were investigated by Von Hillebrandt (1974).

ISRAEL

Section Nahal Avdat

Location and geological setting

The investigated sequence is exposed in the canyon formed by the Nahal Avdat, some 3 km South of the Kibbutz of Sde Boquer in the Northern Negev, Israel (fig. 12). The canyon cuts about 2 km into the Avdat Plateau in a NNE-SSW direction. This plateau is part of the slightly NNW-dipping flank of the so-called Ramon anticline. This area in the Northern part of

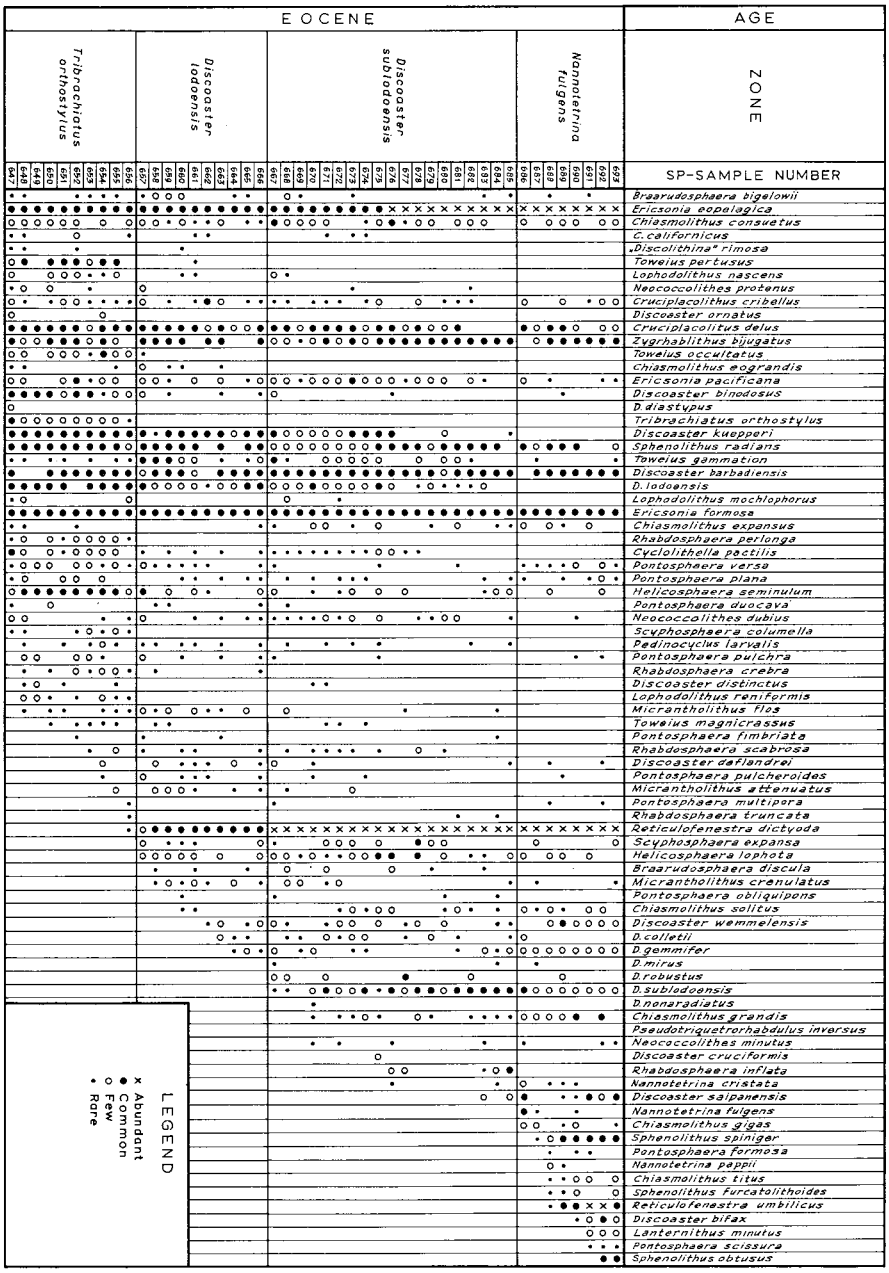

Fig. 11 Distribution of species in the Aspe section.

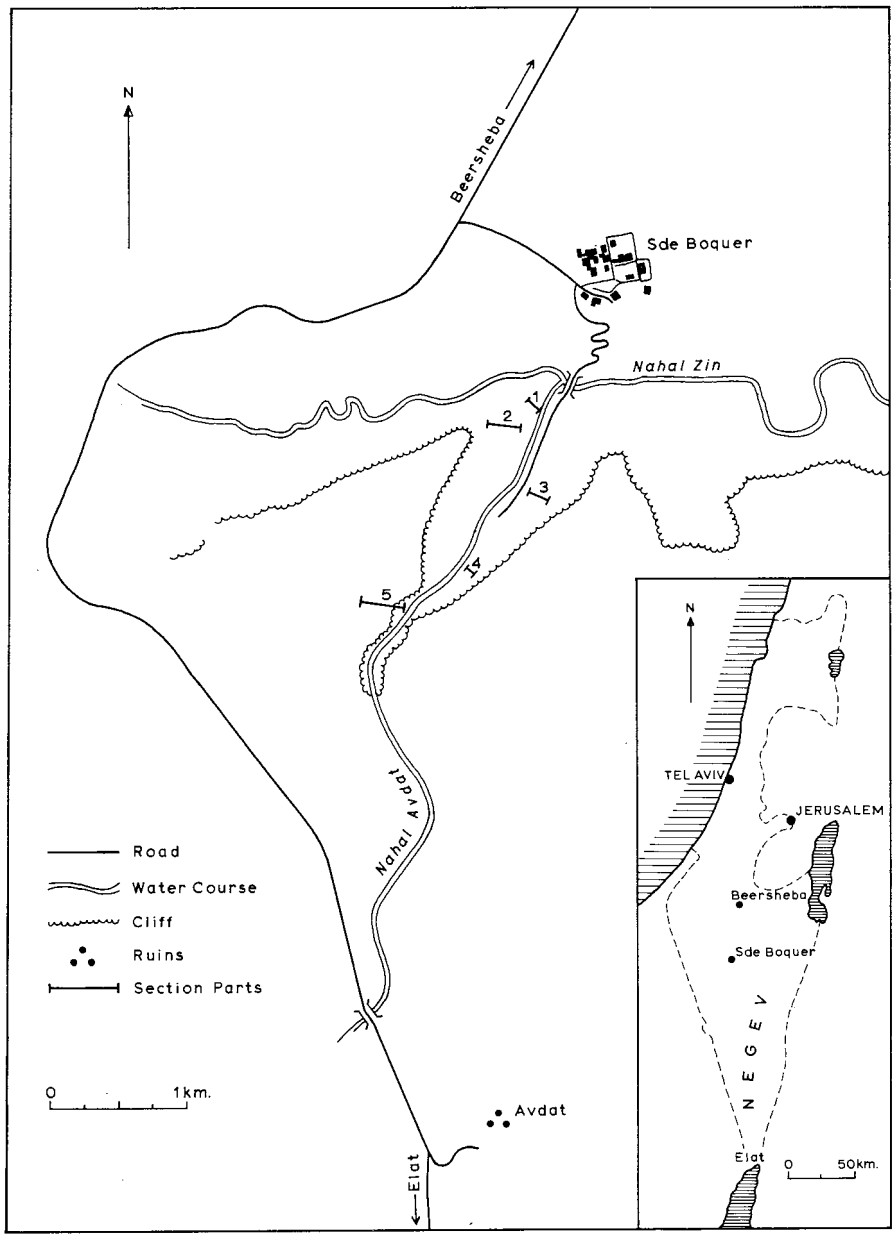

Fig. 12 Sketch maps showing the location of the section Nahal Avdat.

the Central Negev Mountain Area is characterized by several large anticlinal and synclinal structures separated from each other by strike-slip faults; it forms part of a belt of folds, striking E-W to NE-SW, and high-angle reverse faults, collectively known as the Syrian Arc.

Lithostratigraphy

The marls, clays and chalks exposed in the Avdat Canyon and surrounding areas are well known in the literature; the sequence (fig. 13) has been assigned to the following units in stratigraphic order: the Taqiye Formation (Shaw, 1947), the Mor Formation (Bentor and Vroman, 1964) and the

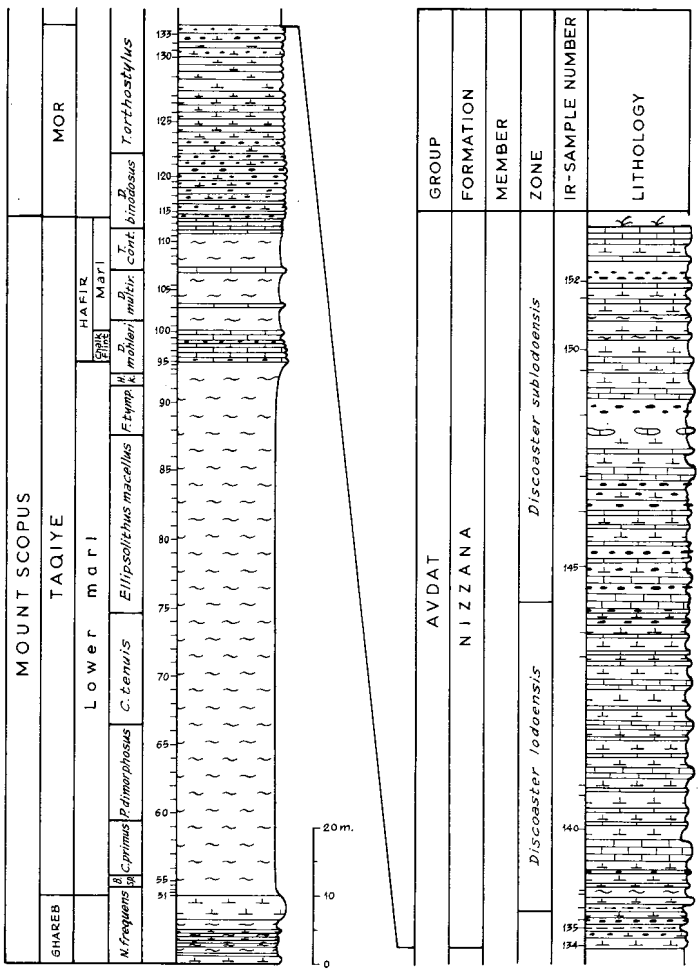

Fig. 13 Section Nahal Avdat, lithology, position of samples and biozonation. For legend, see Fig. 7.

Nizzana Formation (Bentor and Vroman, 1964). The Taqiye Formation forms the upper part of the Mount Scopus Group (Flexer, 1968, emend. Bartov et al., 1972), while the latter two formations constitute the lower part of the Avdat Group (Braun, 1967). The Taqiye and Mor Formations as defined in Israel are widespread and extend into the adjacent countries where they have other, local names (see Arkin et al., 1972).

The Taqiye Formation (about 100 m) consists of a monotonous succession of bluish to green-grey marls and clays rich in gypsum veins and (oxidized) pyrite concretions. In the Northern Negev the formation has been subdivided into the Lower Marl Member and the Hafir Member (Bentor and Vroman, 1964; Arkin et al., 1972). The Hafir Member has, in turn, been subdivided into a chalk-with-flint unit and an overlying marl unit (Arkin et al., 1972). In the Nahal Avdat the lower, cliff-forming chalk has a thickness of 5 m, but elsewhere it is totally absent, so the formation consists entirely of marls.

In the Nahal Avdat the Taqiye Formation is conformably overlain by the Mor Formation (27.5 m), which is composed of thin- to thick-bedded yellowish-brown chalk and intercalated layers of silicified chalk with flint concretions parallel to the bedding planes. These concretions are concentrated in the lower part of the formation. Bituminous horizons, up to 10 cm thick, are found in the middle and upper parts of the Mor Formation.

The youngest formation exposed in the Nahal Avdat is the Nizzana Formation, which conformably overlies the Mor Formation. This formation is composed of thin- to thick-bedded yellowish to brownish chalks and limestones with flint concretions. In the lower part of the formation the bedding-planes are flat and parallel, but in the middle and upper parts there are beds the upper surface of which is convex upwards and others which wedge out laterally. Locally, the chalks and limestones are extremely rich in larger benthonic foraminifera (*Nummulites, Discocyclina, Asterocyclina*). The base of the formation has been placed at the lowest mass-occurrence of these foraminifera. The boundary with the overlying Horsha Formation (Bentor and Vroman, 1964) is not exposed in the Nahal Avdat. The exposed part of the Nizzana Formation has a thickness of 105 m.

Biostratigraphy (fig. 14)

We started our sampling at the base of the Taqiye Formation, just above the thick chalk bed (3.5 m) which forms the top of the underlying Ghareb Formation (Shaw, 1947). The lowermost three samples (IR 51–53) contained a flora, typical for the Upper Maastrichtian *Nephrolithus frequens* Zone. The next higher sample (IR 54), taken from a level 150 cm above the base of the formation, contained a flora indicative of the Lower Paleocene *Bian-*

tholithus sparsus Zone. The Cretaceous/Tertiary boundary thus lies well above the base of the formation; lithologically the boundary corresponds to no more than a slight change in the colour of the marls.

The overlying part of the Lower Marl Member corresponds to the *Biantholithus sparsus* Zone, the *Cruciplacolithus primus* Zone, the *Prinsius dimorphosus* Zone, the *Cruciplacolithus tenuis* Zone, the *Ellipsolithus macellus* Zone, the *Fasciculithus tympaniformis* Zone and the *Heliolithus kleinpellii* Zone. The base of the Hafir Member lies in the lower part of the *Discoaster mohleri* Zone, and the chalk-with-flint unit of this member falls completely within this zone. The marl unit of the Hafir Member corresponds to the top part of the *Discoaster mohleri* Zone, the *Discoaster multiradiatus* Zone, the *Tribrachiatus contortus* Zone and the lower part of the *Discoaster binodosus* Zone. The Paleocene/Eocene boundary lies in the marl unit of the Hafir Member, 7.5 m below the base of the Mor Formation.

The Mor Formation yields the larger part of the *Discoaster binodosus* Zone and most of the *Tribrachiatus orthostylus* Zone.

The Nizzana Formation, on top, corresponds to the uppermost part of the *Tribrachiatus orthostylus* Zone, the *Discoaster lodoensis* Zone and at least the lower part of the *Discoaster sublodoensis* Zone.

Remarks

The samples from the Nahal Avdat contained well-diversified nannofossil associations. The nannofloras from the Nizzana Formation showed a considerable overgrowth. The associations from the Nahal Avdat differ from the succession of associations found in the Caravaca section by (a) the near-absence of *Braarudosphaera bigelowii,* especially in the Cretaceous/Tertiary boundary interval, (b) the presence of *Nephrolithus frequens* in this interval, and (c) the presence of *Tribrachiatus contortus.*

Previous and current investigations

The planktonic foraminifera of the Taqiye Formation have been studied by Hamaoui and Reiss (1963). Moshkovitz (1967) published the details of the calcareous nannofossil assemblages in two samples from the Hafir Member. Reports dealing with the regional distribution and depositional history of the Nizzana Formation and overlying formations, and with the planktonic and larger benthonic foraminifera of these formations will be given by C. Benjamini (in press) and W. J. J. Fermont (in preparation).

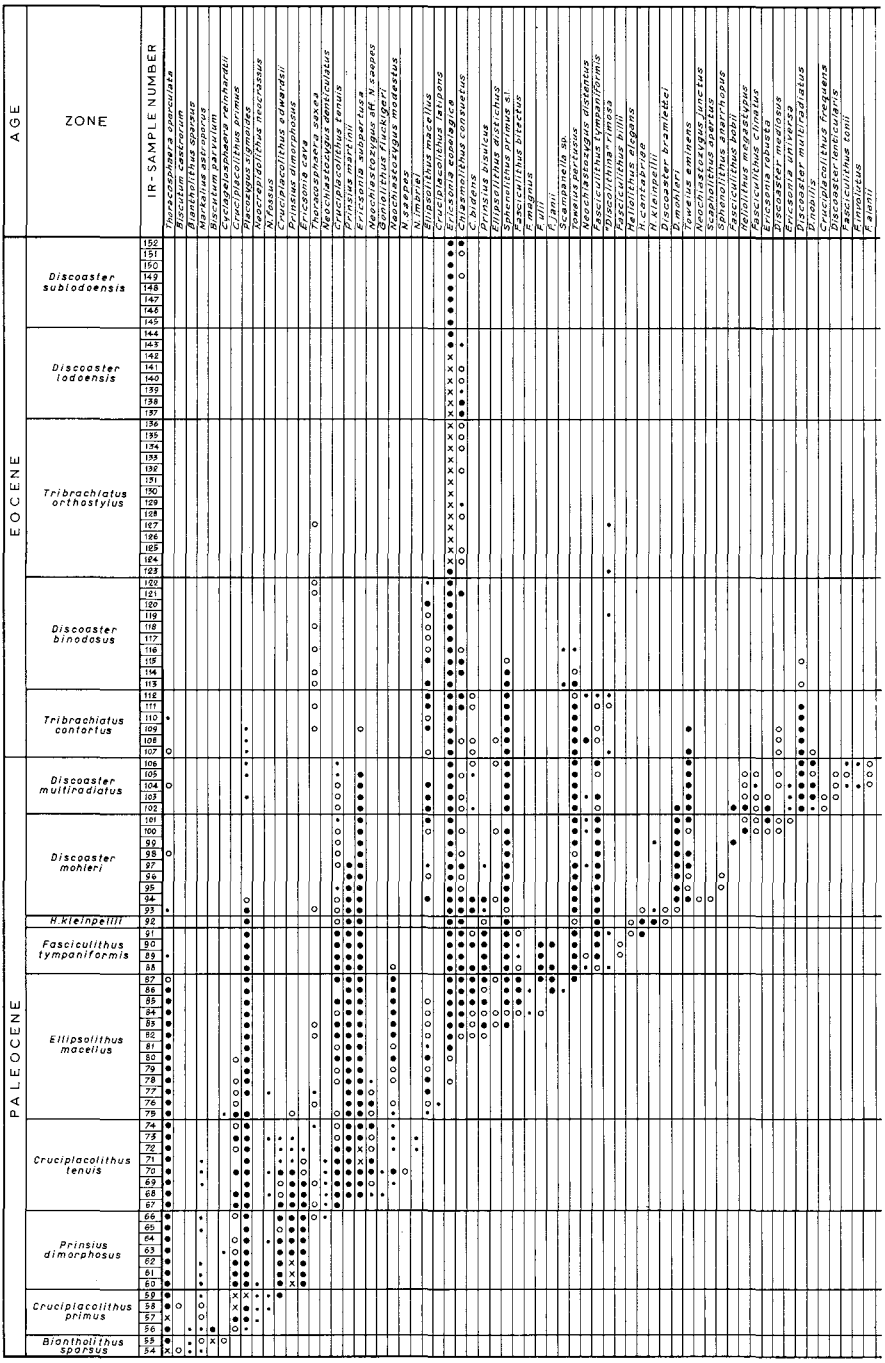

Fig. 14 Distribution of species in the section Nahal Avdat.

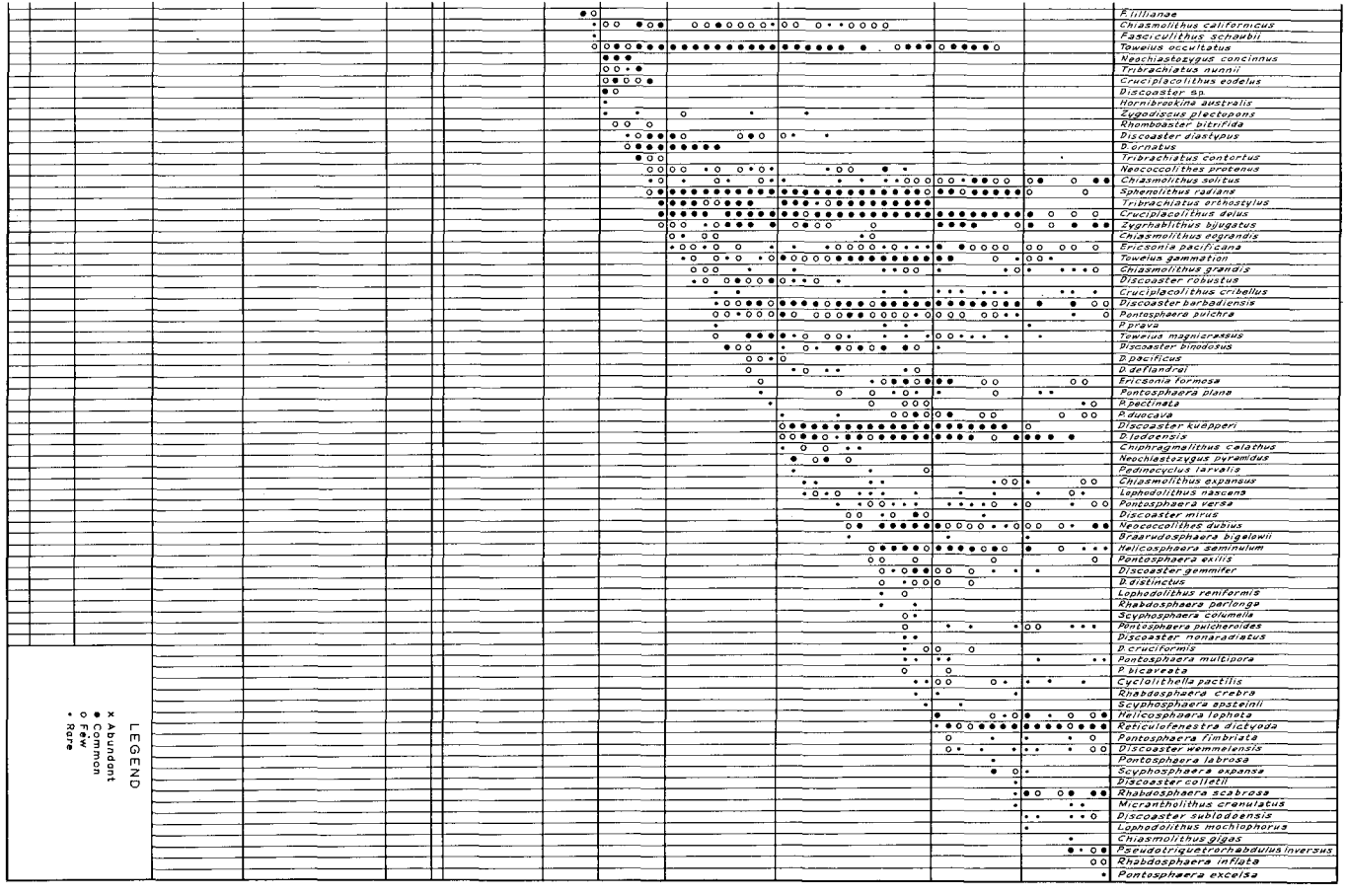
F. lillianae
Chiasmolithus californicus
Fasciculithus schaubii
Toweius occultatus
Neochiastozygus concinnus
Tribrachiatus nunnii
Cruciplacolithus eodelus
Discoaster sp.
Hornibrookina australis
Zygodiscus plectopons
Rhomboaster bitrifida
Discoaster diastypus
D. ornatus
Tribrachiatus contortus
Neococcolithes protenus
Chiasmolithus solitus
Sphenolithus radians
Tribrachiatus orthostylus
Cruciplacolithus delus
Zygrhablithus bijugatus
Chiasmolithus eograndis
Ericsonia pacificana
Toweius gammation
Chiasmolithus grandis
Discoaster robustus
Cruciplacolithus cribellus
Discoaster barbadiensis
Pontosphaera pulchra
P. prava
Toweius magniarassus
Discoaster binodosus
D. pacificus
D. deflandrei
Ericsonia formosa
Pontosphaera plana
P. pectinata
P. duocava
Discoaster kuepperi
D. laddensis
Chiphragmalithus calathus
Neochiastozygus pyramidus
Pedinocyclus larvalis
Chiasmolithus expansus
Lophodolithus nascens
Pontosphaera versa
Discoaster mirus
Neococcolithes dubius
Braarudosphaera bigelowii
Helicosphaera seminulum
Pontosphaera exilis
Discoaster gemmifer
D. distinctus
Lophodolithus reniformis
Rhabdosphaera parlonga
Scyphosphaera columella
Pontosphaera pulchroides
Discoaster nonaradiatus
D. cruciformis
Pontosphaera multipora
P. bicavrata
Cyclolithella pactilis
Rhabdosphaera crebra
Scyphosphaera apsteinii
Helicosphaera lophota
Reticulofenestra dictyoda
Pontosphaera fimbriata
Discoaster weimmelensis
Pontosphaera labrosa
Scyphosphaera expansa
Discoaster colletii
Rhabdosphaera scabrosa
Micrantholithus granulatus
Discoaster subladoensis
Lophodolithus mochlophorus
Chiasmolithus gigas
Pseudotriquetrorhabdulus inversus
Rhabdosphaera inflata
Pontosphaera excelsa
LEGEND
x Abundant
● Common
o Few
• Rare

Location and geological setting

Limestones, marls and greensands were deposited during the Early Paleocene in the part of the North Sea basin known in the literature as the Danish-Scandian depression. Today these sediments occur in a syncline trending roughly NW-SE over Jutland, Sealand and the most Southwesterly part of Sweden, below a thin Pleistocene cover.

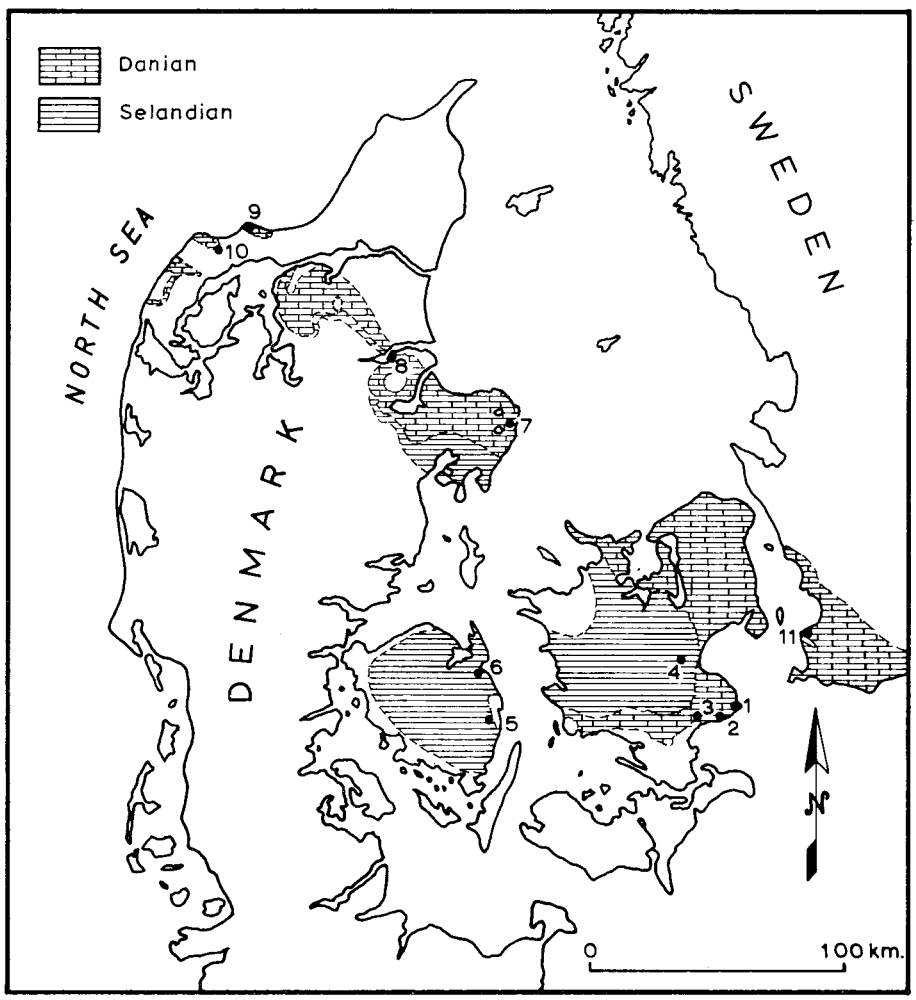

Fig. 15 Sampling stations in Denmark and Sweden and distribution of Danian and Paleocene formations below the Pleistocene (after Sorgenfrei, 1957).
1. Stevns Klint, 2. Boesdal, 3. Fakse, 4. Lellinge Creek, 5. Klintholm, 6. Kerteminde, 7. Bredstrup Klint, 8. Dania, 9. Bulbjerg, 10. Kjølby Gaard, 11. Limhamn.

Stage names introduced for these sediments are Danian (introduced by Desor in 1846 for the limestones exposed at Fakse and Stevns Klint) and Selandian (proposed by Rosenkrantz in 1924 for the Paleocene deposits above the Danian limestone and below the formation of volcanic tuff beds). For the litho- and biostratigraphy of these stages the reader is referred to Brotzen (1948, 1959), Berggren (1962, 1969) and Malmgren (1974).

Good exposures of the Danian and Selandian are rather scarce. Several of these exposures were visited and sampled during the XV-th European Micropaleontological Colloquium in Denmark (1977). The localities are indicated in figure 15; for extensive descriptions of these localities the reader is referred to the guide-books issued in connection with the XXI International Geological Congress (1960), and Hofker (1966).

Stevns Klint (fig. 16)

At this classical locality, samples were taken from the uppermost Maastrichtian Chalk, the Fish-Clay, the *Cerithium*-Limestone and the lower part of the

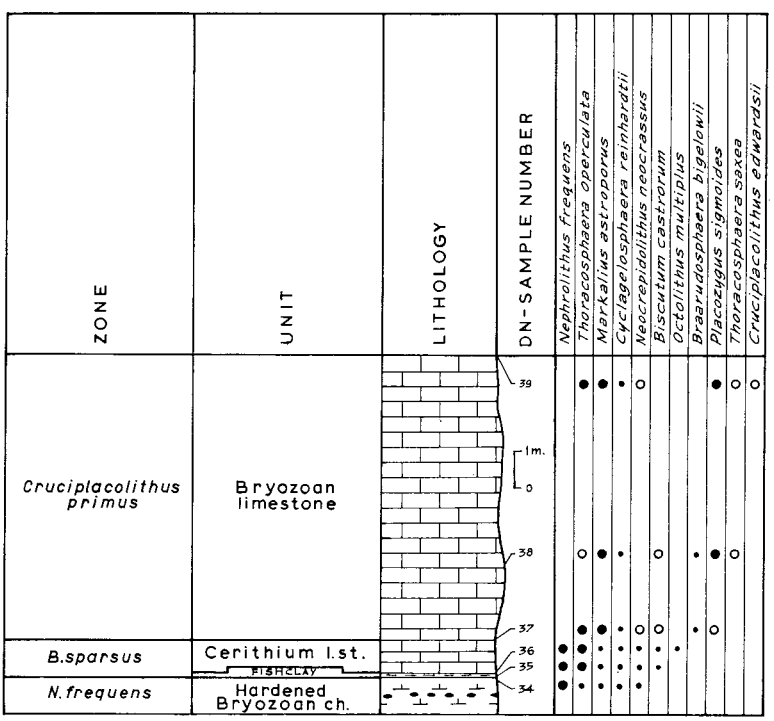

Fig. 16 Lithology, distribution of species and biozonation of the middle part of the section at Stevns Klint near Højerup. For legend of this figure and the figures 17–25, see Fig. 7.

Bryozoan Limestone. Sample DN34, collected just below the Fish-Clay is placed in the Upper Maastrichtian *Nephrolithus frequens* Zone. The assemblage from the Fish-Clay (DN35) differs from the preceding one in that it contains *Biscutum castrorum,* and has a higher frequency of *Thoracosphaera operculata*. This sample, and the next higher one (DN36) from the base of the *Cerithium*-Limestone are assigned to the *Biantholithus sparsus* Zone, although *B. sparsus* does not occur in the assemblages.

Sample DN 37 from the base of the Bryozoan Limestone, and sample DN38 taken 2 m above this base, are placed in the *Cruciplacolithus primus* Zone, because of the presence of *Placozygus sigmoides*; the zonal marker was not found. The highest sample (DN39), taken about 7 m above the base of the Bryozoan Limestone, contains *Cruciplacolithus edwardsii*, which justifies its assignment to the *Cruciplacolithus primus* Zone.

Dania (fig. 17)

In the quarry of the Dania Cement Works the Maastrichtian Chalk is superposed by approximately 10 m of Danian Bryozoan Limestone. The

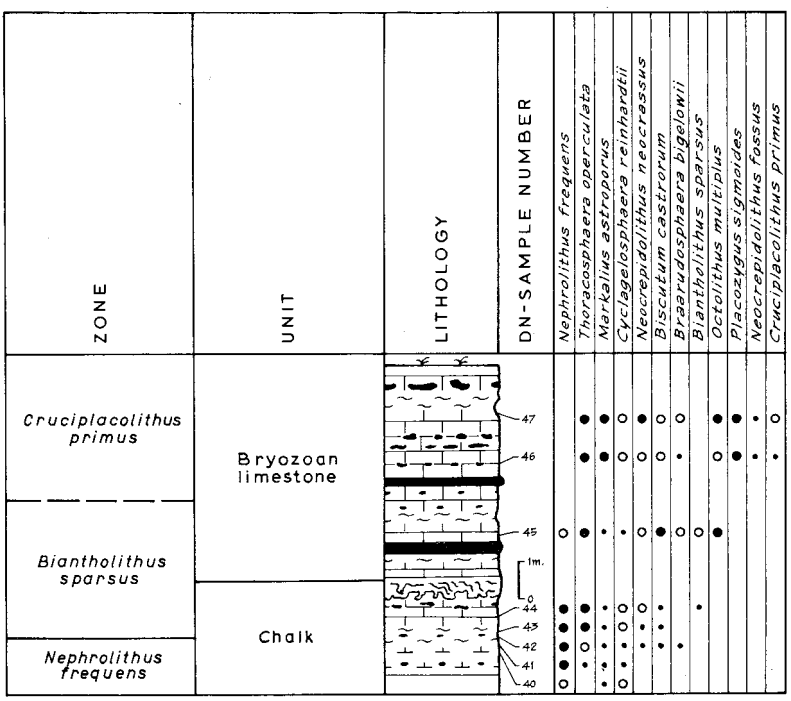

Fig. 17 Section in the quarry of the Dania Cement Works; lithology, distribution of species and biozonation.

Cretaceous/Tertiary boundary is generally placed at the base of a 40 cm marl layer. The samples DN40 and DN41 from the top of the Chalk, and sample DN42 from the base of the marl contain floras that are typical of the Upper Maastrichtian *Nephrolithus frequens* Zone.

There is a marked increase in the frequency of *Thoracospheara operculata* in sample DN43, collected 20 cm above the base of the marl. This sample, and the next two higher ones (DN44, DN45) from the Bryozoan Limestone are assigned to the *Biantholithus sparsus* Zone; *B. sparsus* occurs only in the latter two samples.

The uppermost two samples (DN46, DN47) are placed in the *Cruciplacolithus primus* Zone because of the presence of the zonal marker in association with *Placozygus sigmoides*.

Kjølby Gaard (fig. 18)

In the section at Kjølby Gaard the chalk facies persists well into the Danian. The Danian sequence starts with a 20 cm conglomeratic marl layer. Sample DN48, collected just below this layer, yields a flora typical of the *Nephrolithus frequens* Zone. Sample DN49 from the marl contains *B. sparsus*. This sample and samples DN50 and DN51 from the base of the overlying chalk are rich in *Thoracosphaera operculata*; they are placed in the *Bian-*

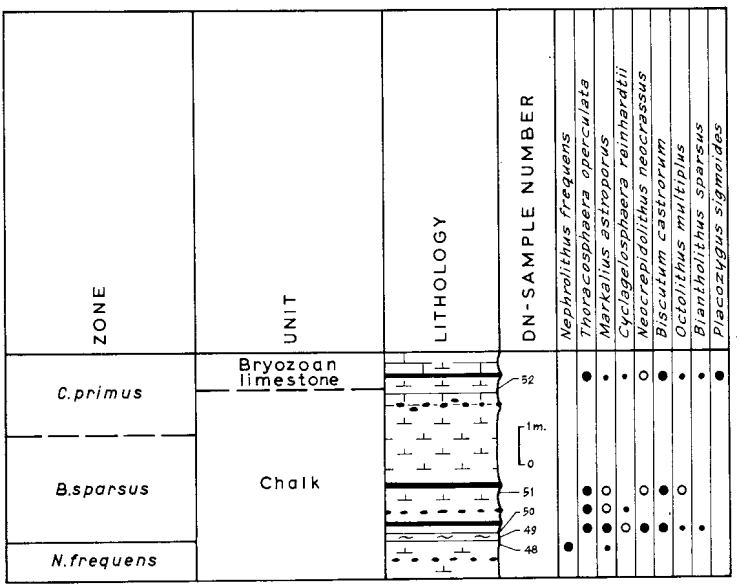

Fig. 18 Section Kjølby Gaard; lithology, distribution of species and biozonation.

tholithus sparsus Zone. Sample DN52, collected about 4 m above the marl layer contains *Placozygus sigmoides* and is therefore assigned to the *Cruciplacolithus primus* Zone.

Bulbjerg (fig. 19)

Danian Bryozoan Limestone is exposed in the coastal cliffs at Bulbjerg. The lowermost sample from this sequence (DN53) is rich in *Thoracosphaera operculata,* while *Placozygus sigmoides* and *Cruciplacolithus primus* are absent. The sample is assigned to the *Biantholithus sparsus* Zone.

All higher samples (DN54–DN59) are assigned to the *Cruciplacolithus primus* Zone, because of the presence of *Placozygus sigmoides* in all samples and the occurrence of *Cruciplacolithus edwardsii* in the uppermost sample.

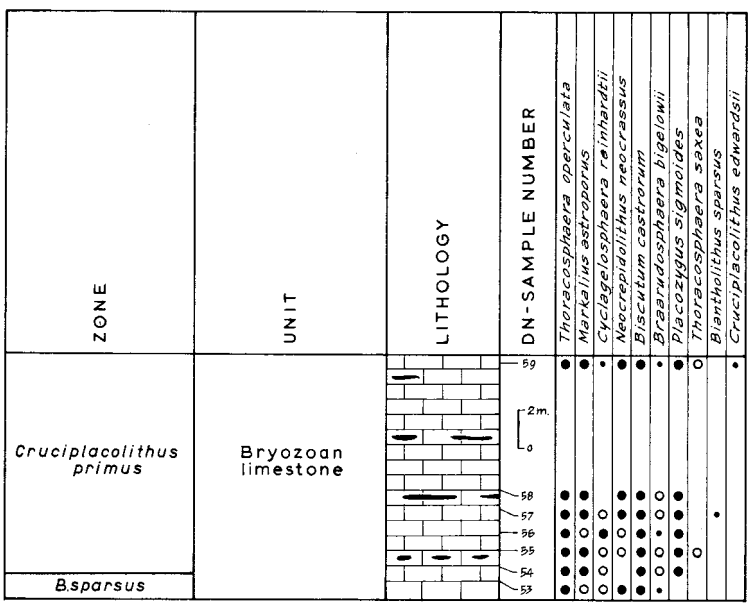

Fig. 19 Lithology, distribution of species and biozonation of the section at Bulbjerg.

Boesdal (fig. 20)

About 20 m of Bryozoan Limestone are exposed in a quarry near Boesdal in the vicinity of Stevns Klint. All samples (DN60–DN66) contain *Placozygus sigmoides* and are assigned to the *Cruciplacolithus primus* Zone, although the name-giving species was not found.

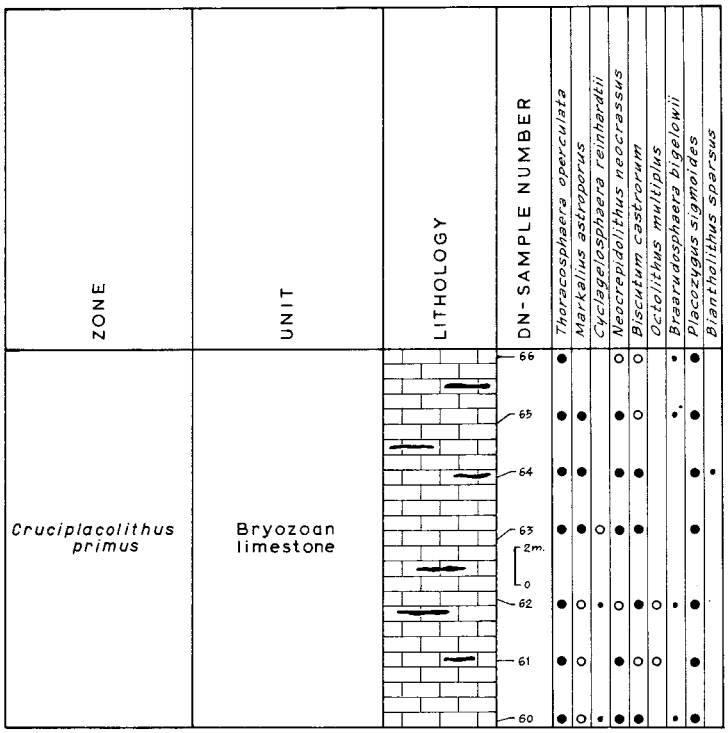

Fig. 20 Section Boesdal; lithology, distribution of species and biozonation.

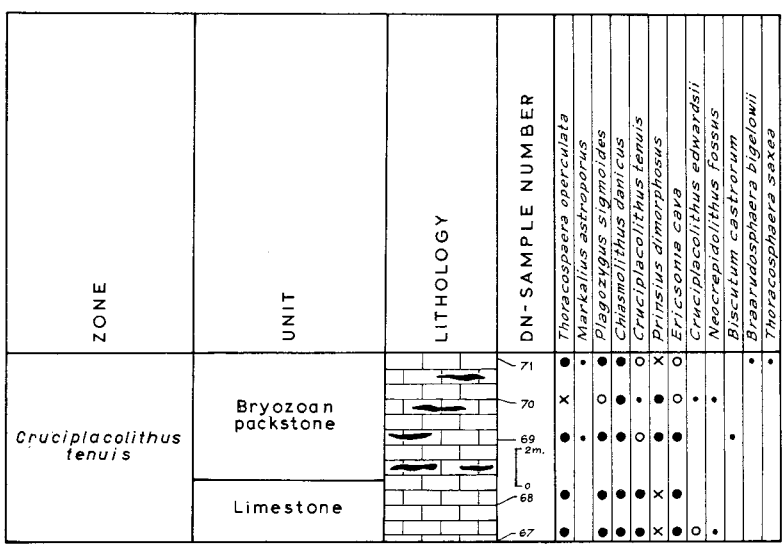

Fig. 21 Upper part of the section in the Fakse quarry; lithology, distribution of species and zonal assignment.

Fakse (fig. 21)

In the large quarry of Fakse only the upper part of the exposed Bryozoan Limestone could be sampled. The elements of wackestones and Bryozoan packstones in this upper part are supposed to have undergone only limited transport. All samples (DN67–DN71) contain *Prinsius dimorphosus, Cruciplacolithus tenuis* and *Chiasmolithus danicus,* which justifies the assignment of these samples to the *Cruciplacolithus tenuis* Zone.

Bredstrup Klint (fig. 22)

All samples from the Bryozoan Limestone of this locality (DN72–DN77) contain *Cruciplacolithus tenuis, Chiasmolithus danicus* and *Prinsius dimorphosus,* indicative of the *Cruciplacolithus tenuis* Zone.

Klintholm (fig. 23)

In the quarry at Klintholm the eroded top of the Danian Bryozoan Limestone is overlain by the Selandian Kerteminde Marl. The samples from both the limestone and the marl (DN78–DN80) contain *Prinsius martinii,* while *Chiasmolithus bidens* is absent. The samples can be assigned to the upper part of the *Cruciplacolithus tenuis* Zone and/or to the lower part of the *Ellipsolithus macellus* Zone.

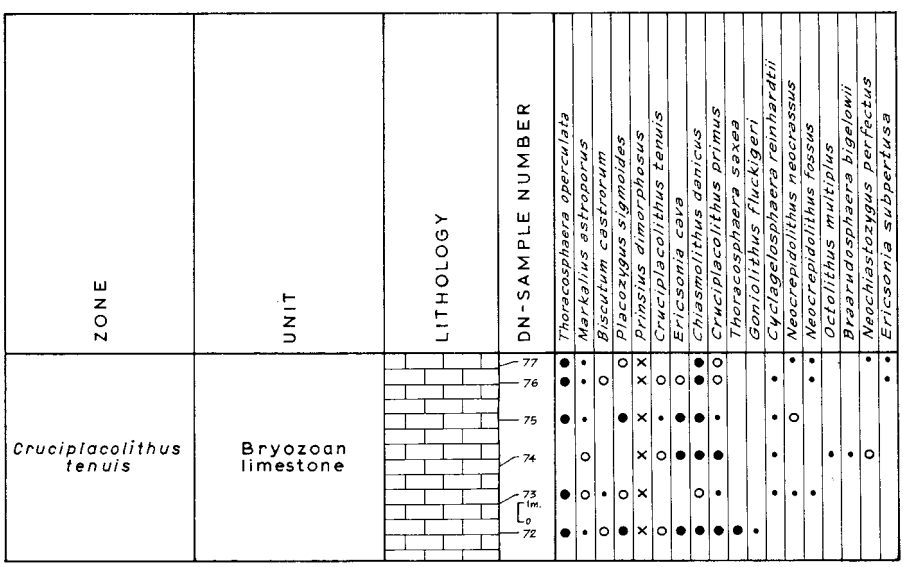

Fig. 22 Section Bredstrup Klint; lithology, distribution of species and zonal assignment.

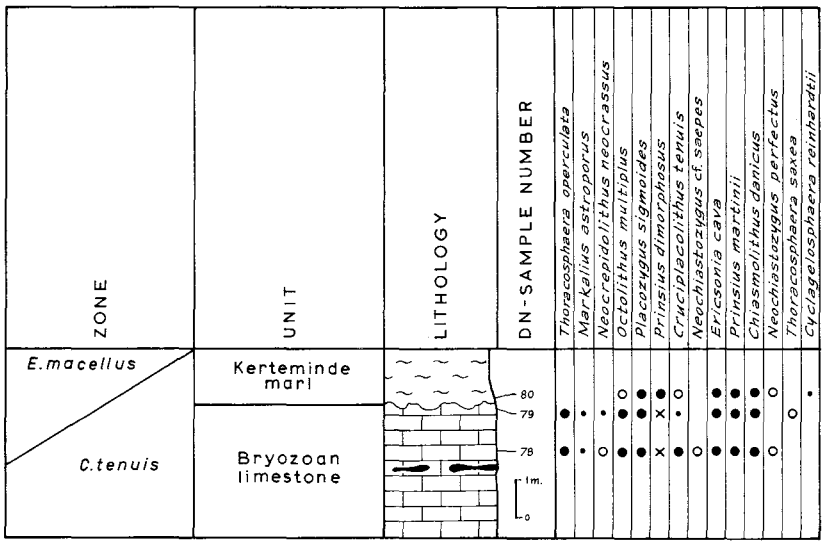

Fig. 23 Section Klintholm; lithology, distribution of species and biozonation.

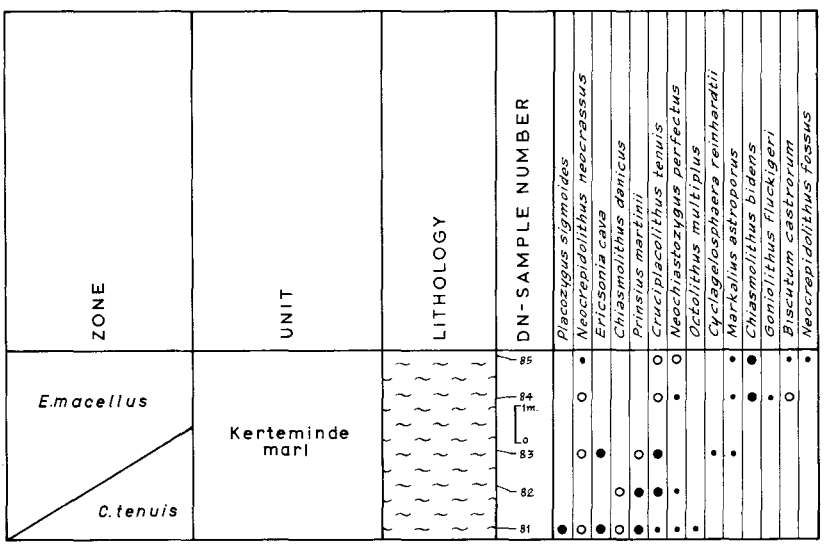

Fig. 24 Section Kerteminde; lithology, distribution of species and biozonation.

Kerteminde (fig. 24)

The five samples from the type locality of the Kerteminde Marl (Selandian) at Lundsgards Cliff cover an interval of about five metres. The lower three samples contain *Prinsius martinii,* while *Chiasmolithus bidens* is absent; these samples can be placed in the top of the *Cruciplacolithus tenuis* Zone and/or in the lower part of the *Ellipsolithus macellus* Zone. The upper two samples containing *Chiasmolithus bidens* can be assigned with certainty to the *Ellipsolithus macellus* Zone.

Lellinge Creek (fig. 25)

Four samples (DN86–DN89) were collected from two small outcrops of Selandian marls, limestones and greensands at Lellinge Creek. *Chiasmolithus bidens* and *Prinsius martinii* are present in all samples, which are assigned to the *Ellipsolithus macellus* Zone.

Sweden, Limhamn Quarry (fig. 26)

In the Limhamn Quarry, South of Malmö, the uppermost part of the Maastrichtian Chalk, and the Danian Bryozoan Limestone are exposed. Biozonations of the Danian at this locality have been presented by Brotzen (1959), Berggren (1962, 1969) and Malmgren (1974).

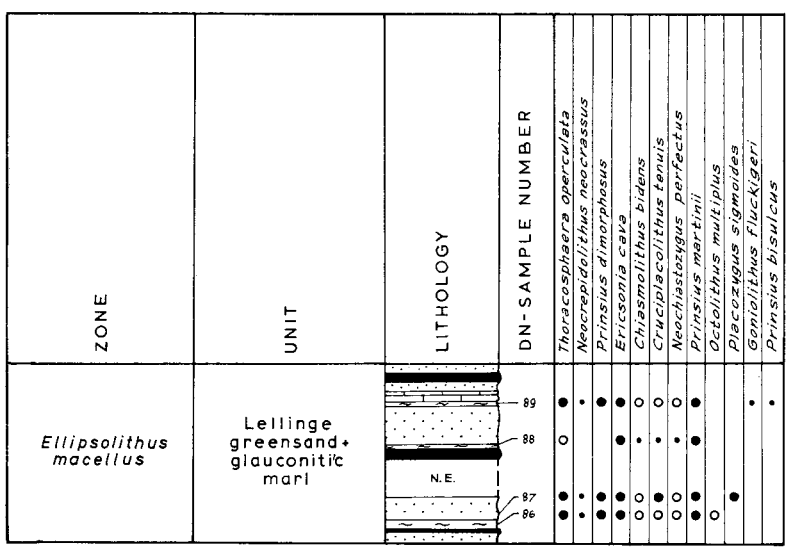

Fig. 25 Section Lellinge Creek; lithology, distribution of species and biozonation.

Only seven samples were collected from the roughly sixty metre sequence. The lithostratigraphic subdivision is that given by Brotzen (1959). The lowermost sample (S132), taken from the Chalk at about 2 m below the unconformity marking the Cretaceous/Tertiary boundary, is assigned to the *Nephrolithus frequens* Zone. Owing to bad exposure, the boundary interval could not be sampled in detail. The samples S133–S135 from Bioherm Group I already contain *Placozygus sigmoides,* indicative of the *Cruciplacolithus primus* Zone. Sample S136 from the base of Bioherm Group II is assigned to the *Cruciplacolithus tenuis* Zone because of the presence of the zonal marker. *Chiasmolithus danicus* has its first occurrence in sample S137 from the upper part of Bioherm Group II; this sample and sample S138 from the Limhamn Limestones are also assigned to the *Cruciplacolithus tenuis* Zone.

The absence of the *Biantholithus sparsus* Zone and of the *Prinsius dimorphosus* Zone in this record is due either to hiatuses or to too wide spacing of the samples.

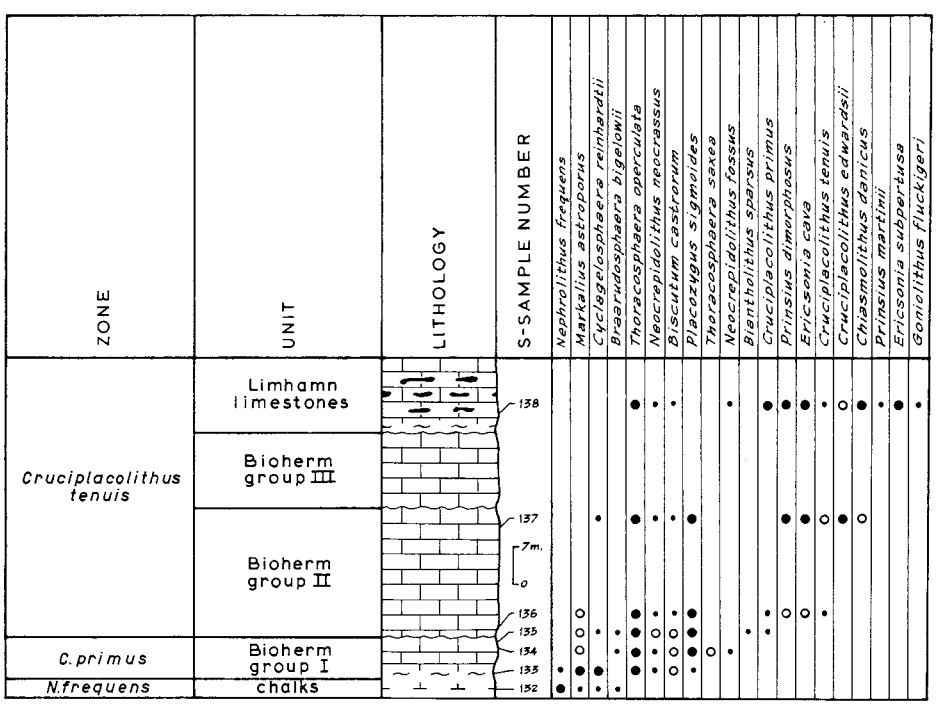

Fig. 26 Section Limhamn quarry; lithology, distribution of species and biozonation (lithological subdivision after Brotzen, 1959).

Remarks

The investigated Scandinavian assemblages show a large number of species; this diversity is the result of the presence of many, supposedly reworked, Cretaceous species. The specimens generally show a moderate degree of overgrowth.

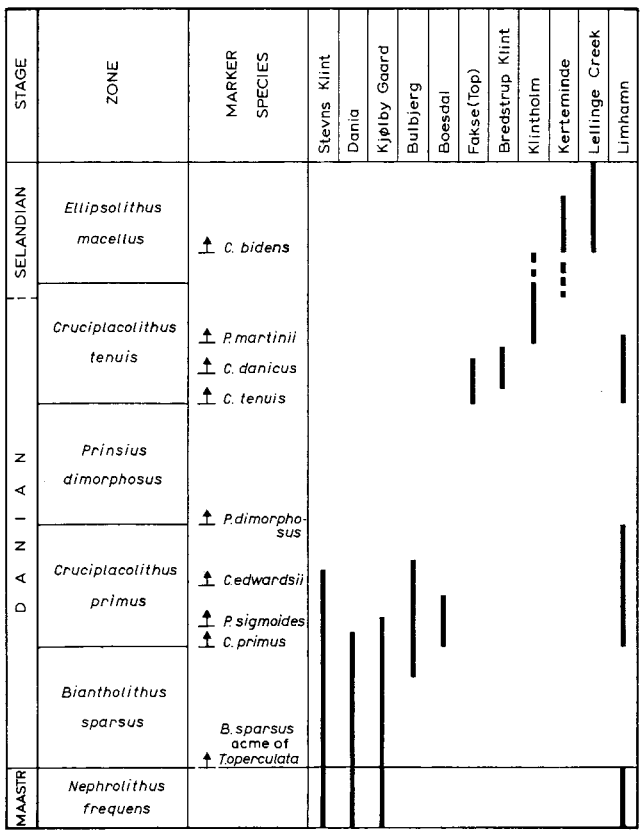

Fig. 27 Correlation of the investigated sequences in Denmark and Sweden.

The biostratigraphic correlation of the above mentioned sequences is given in figure 27. Index species for the correlation are (in order of first occurrence): *Thoracosphaera operculata, Placozygus sigmoides, Cruciplacolithus edwardsii, Prinsius dimorphosus, Cruciplacolithus tenuis, Chiasmolithus danicus, Prinsius martinii* and *Chiasmolithus bidens.*

Cruciplacolithus primus is a rare species, and large forms of this species were not observed. *Prinsius petalosus, Ellipsolithus macellus* and *Chias-*

molithus consuetus known from the Danian in the Tethys are absent.

The fact that the presence of the *Prinsius dimorphosus* Zone could not be established at any locality may be due either to a hiatus, or to the wide spacing of the samples in several sections. It is just as likely that the zonal characteristics cannot be recognized for ecological reasons.

The Danian in its type region does not extent beyond the upper part of the *Cruciplacolithus tenuis* Zone as defined in the present paper. The Selandian corresponds to the uppermost part of the *Cruciplacolithus tenuis* and the *Ellipsolithus macellus* Zones.

Previous investigations

Species of calcareous nannofossils of the Danish Danian and of the Selandian have been listed by Perch-Nielsen (1969a, b) and Edwards (1973a).

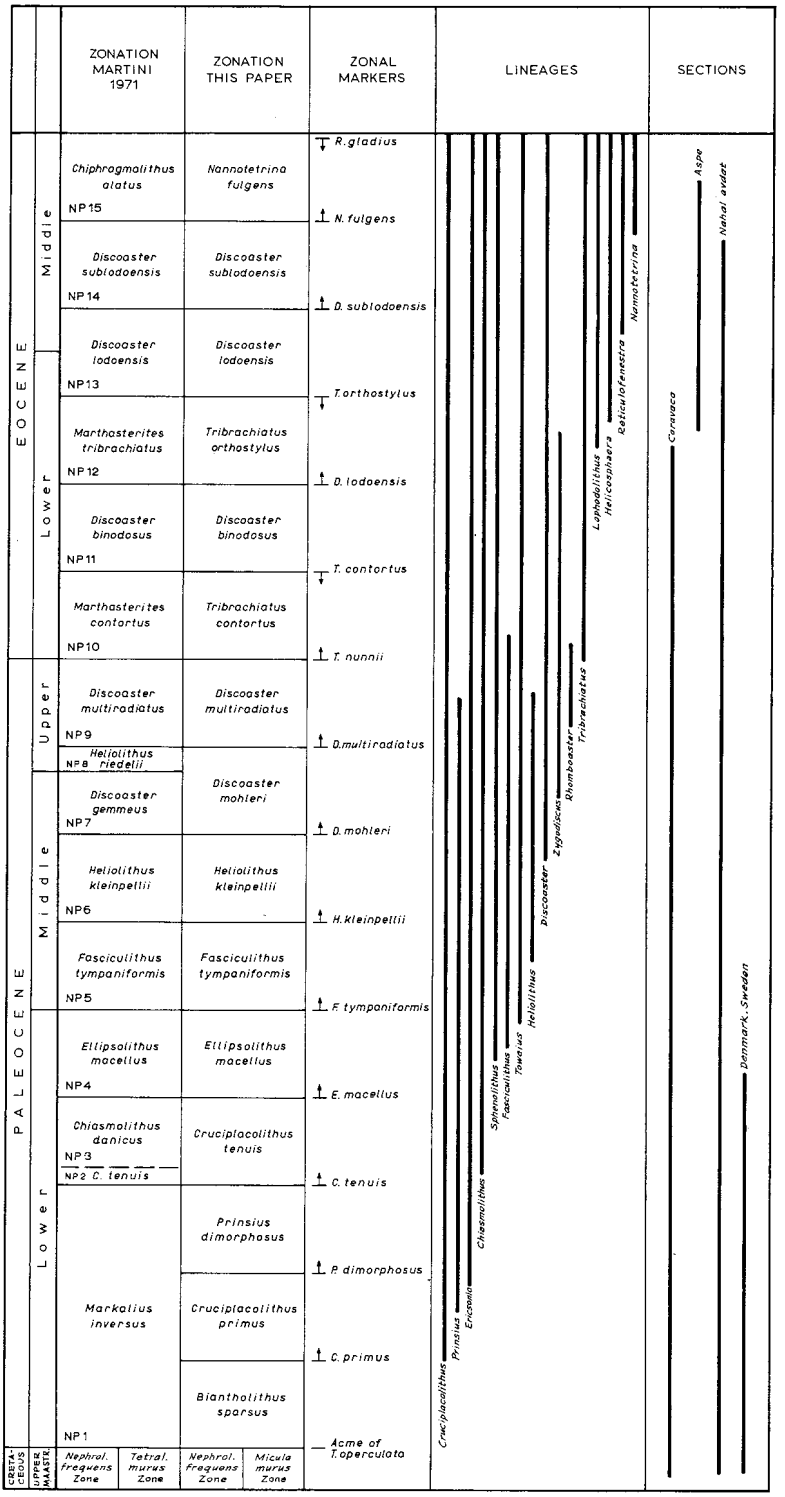

Fig. 28 Chart showing a comparison between Martini's zonation and the zonation used in this report, and the extension of the sections and the lineages described in this report.

Chapter IV

BIOZONATION

Many zonations and partial zonations have been published for the Cenozoic during the last 20 years. Zonal systems currently in use are those of Martini (1971) and of Bukry (1971c, 1973, 1975). These schemes are very similar, but Martini's zonation is based on outcrop sections, while in the scheme of Bukry the data were derived mainly from deep sea drillings.

As in most other nannofossil zonations, the units of Martini and Bukry are interval zones, based on the entry or exit of single species of which neither the origin nor the relationships with other species are known. Such a zone becomes hard to recognize if the marker species is not found.

Biozones based on species of which the position in some phylogenetic lineage is known are more easily recognizable, especially when several contemporaneous lineages can be used. Since most of the markers used by Martini appeared to form part of a lineage, the zonation given below (fig. 28) largely corresponds to that of Martini.

A weakness in Martini's scheme is his use of last occurrences of species to define zonal boundaries; several zones in the Lower Eocene are defined in this way. Calcareous nannofossils are easily reworked, which means that this type of boundary is highly undesirable. Bukry, therefore, based his zones in this interval (almost all of which have the same name as Martini's zones) on entries of species. Unfortunately several of these species are ill defined and/or rare.

We have chosen to follow the zonal scheme of Martini for two reasons: (a) the introduction of a new schema in which several names are the same as in other schemes would only lead to confusion, (b) the chance that a new zonation will be used is thought to be slight; most authors will probably continue to refer to the "sophisticated" NP numbers.

For each zone the lineage segments which may increase the recognizability of the zone are given below. For (frequencies of) species typical for the zone the reader is referred to Martini (1971) and Bukry (1971, 1975).

As the Uppermost Maastrichtian was considered as well, the discussion of the zonation begins with the uppermost zone of the Cretaceous.

Micula murus Zone Bukry and Bramlette, 1970, emend. Romein, 1977

Definition: Interval zone from the entry of *Micula murus* to the mass occur-

rence (or increased frequency) of *Braarudosphaera bigelowii* and/or *Thoracosphaera operculata.*

Remarks: Bukry and Bramlette used the extinction of most Cretaceous calcareous nannofossils to define the upper boundary of their zone. In most sections covering the Cretaceous/Tertiary boundary interval, and especially in closely sampled, continuous sections there is, however, no such level; generally, typical Cretaceous species disappear gradually from the record in the Lower Tertiary. It is not yet known whether these species crossed the boundary or whether their presence is the result of reworking. In our opinion the second possibility seems the most likely one, as nannofossils can easily be reworked, owing to their small size.

From the literature it is known (Worsley and Martini, 1970; Worsley, 1974) that *Micula murus* was probably restricted to tropical regions. In boreal regions the *Nephrolithus frequens* Zone is the highest zone in the Maastrichtian. This zone was introduced by Cepek and Hay (1969) and defined as "the interval from the first occurrence of *N. frequens* to the level of extinction of most Cretaceous species". The definition of the upper boundary of this zone is emended here in the same way as the upper boundary of the *M. murus* Zone. The order of entry of *N. frequens* and *M. murus* is still under discussion.

Age: Late Maastrichtian.

Biantholithus sparsus Zone Perch-Nielsen, 1971, emend. this paper

Definition: Interval zone from the massive occurrence or increased frequency of *Braarudosphaera bigolowii* and/or *Thoracosphaera operculata* to the entry of *Cruciplacolithus primus.*

Remarks: Mohler and Hay (1967) introduced the *Markalius astroporus* Zone as the lowest zone in the Tertiary. They defined the lower boundary of the zone by the first occurrence of *M. astroporus.* Investigations by Perch-Nielsen (1969b) of assemblages from Danish localities of Maastrichtian and Danian age, however, indicated that *M. astroporus* already occurs in Maastrichtian sediments. She nevertheless retained the *M. astroporus* Zone as the lowermost Danian zone, but she based the lower boundary of the zone on the entry of *Biantholithus sparsus.* In 1971, Perch-Nielsen introduced the *B. sparsus* Zone to replace the *M. astroporus* Zone (= *Markalius inversus* Zone, NP 1, of Martini, 1971).

In the present paper the definitions of both the lower and the upper boundary of the *B. sparsus* Zone are changed. The lower boundary of the zone is placed at the massive occurrence or increased frequency of *Braarudosphaera bigelowii* and/or *Thoracosphaera operculata* as *Biantholithus sparsus*

is a rare species in most sections. The upper boundary of the zone, originally placed by Mohler and Hay at the entry of *Cruciplacolithus tenuis* is lowered to the first occurrence of *Cruciplacolithus primus.*

The floras in this partial range zone are dominated by the long-ranging species *B. bigelowii* and/or *T. operculata.* Species which certainly have their first occurrence in this zone are: *Biantholithus sparsus* at the base, *Braarudosphaera alta* nov. sp., *Biscutum parvulum* nov. sp. and *Neocrepidolithus fossus* (Romein) nov. comb. The rest of the assemblages consists of species which continue from the Cretaceous. Because of their persistent presence in Tertiary assemblages the following species are suspected to have survived the Cretaceous/Tertiary "boundary event": *Braarudosphaera bigelowii, Thoracosphaera operculata, Thoracosphaera saxea, Markalius astroporus, Cyclagelosphaera reinhardtii, Biscutum castrorum, Octolithus multiplus* (Perch-Nielsen) nov. comb., *Micula decussata, Neocrepidolithus neocrassus* (Perch-Nielsen) nov. comb. and *Goniolithus fluckigeri.*

The *Biantholithus sparsus* Zone corresponds to the lower part of the *Markalius inversus* Zone (NP 1) of Martini.

Reference locality: Section Caravaca, Barranco del Gredero, samples SP561–564. The zone has a thickness of 50 cm at this locality.

Distribution: Caravaca: SP561–564; Nahal Avdat: IR54, 55; Stevns Klint: DN35, 36; Dania: DN43–45; Kjølby Gaard: DN49–51.

Age: Early Paleocene.

Cruciplacolithus primus Zone Romein, this paper

Definition: Interval zone from the entry of *Cruciplacolithus primus* to the first occurrence of *Prinsius dimorphosus.*

Remarks: The base of this zone is defined by the appearance of the first representative of the *Cruciplacolithus* lineage. Within the zone the maximum length of the zonal marker increases from 4 μ at the base to 9 μ at the top. *Cruciplacolithus edwardsii* nov. sp. and *Ericsonia cava* are seen to develop from *C. primus* in the upper part of the zone. In the same interval *Prinsius petalosus* (Ellis and Lohman) nov. comb., the first representative of the *Prinsius* lineage, enters the assemblages. *Placozygus sigmoides,* an important species for the correlation of the Scandinavian sections, also has its first occurrence in this zone. The zone is equivalent to the middle part of the *Markalius inversus* Zone (NP 1) of Martini.

Reference locality: Section Caravaca, Barranco del Gredero, samples SP565–576. At this locality the zone has a thickness of 8 m.

Distribution: Caravaca: SP565–576; Nahal Avdat: IR56–59; Stevns Klint:

DN37–39; Dania: DN46, 47; Kjølby Gaard: DN52; Boesdal: DN60–66; Bulbjerg: DN54–59; Limhamn: S132–134.
Age: Early Paleocene.

Prinsius dimorphosus Zone Romein, this paper

Definition: Interval zone from the first occurrence of *Prinsius dimorphosus* type 1 to the entry of *Cruciplacolithus tenuis.*
Remarks: The marker for the base of this zone developed from *Prinsius petalosus* in the time interval corresponding to the uppermost part of the underlying zone. Type 1 of the marker dominates the associations in the lower part of the zone, and it is supposed to develop into *Prinsius dimorphosus* type 2 in the upper part.

The angle of rotation of the bars in *Cruciplacolithus edwardsii* increases in progressively higher associations from this zone.

More circular forms of *Ericsonia cava,* and forms intermediate between *C. primus* and *C. tenuis* occur in the upper part of the zone. The first representatives of the genus *Neochiastozygus* (*N. denticulatus* and *N. modestus*) also appear in the upper part of the zone. This zone corresponds to the upper part of the *Markalius inversus* Zone (NP 1) of Martini.
Reference locality: Section Caravaca, Barranco del Gredero, samples SP577–600. At this locality the zone has a thickness of 22.5 m.
Distribution: Caravaca: SP577–600; Nahal Avdat: IR60–66. The presence of this zone could not be established in the Scandinavian sections.
Age: Early Paleocene.

Cruciplacolithus tenuis Zone Mohler and Hay, 1967, emend. this paper.

Definition: Interval zone from the appearance of *Cruciplacolithus tenuis* to the first occurrence of *Ellipsolithus macellus.*
Remarks: Our investigation of the holotype of *Cruciplacolithus tenuis* showed that Stradner's illustration of this specimen is incomplete. The *figure* warrants the determination *Cruciplacolithus primus,* but the *specimen* is clearly different, which means that *C. tenuis* must be retained as a separate species (see chapter on taxonomy). As a consequence of the different concepts of *C. tenuis* in the literature, the base of our *C. tenuis* Zone is probably higher than that given by most other authors.

The zone was introduced by Mohler and Hay as the interval from the entry of *C. tenuis* to the first occurrence of *F. tympaniformis.* In the type locality at Pont Labau (S.W. France), sample Gan 782 was chosen as the most representative sample, but the (reversed) illustrations of *C. tenuis* are

from specimens from the *F. tympaniformis* Zone.

Martini (1971) lowered the upper boundary of the zone to the first occurrence of *Chiasmolithus danicus,* and inserted the *Ellipsolithus macellus* Zone (NP4) in between the *C. danicus* Zone (NP3) and the *F. tympaniformis* Zone (NP5). Thus, Martini's *C. tenuis* Zone probably corresponds to the lower part of the *C. tenuis* Zone at Pont Labau. As *C. danicus* is not present in this section (Hay and Mohler's *C. danicus* warrants the determinations *C. consuetus* and *C. californicus*) or in the Caravaca and Nahal Avdat sections, the upper boundary of our *C. tenuis* Zone is drawn at the first occurrence of *E. macellus*.

In this zone *Chiasmolithus danicus* is seen to evolve from late forms of *Cruciplacolithus edwardsii*. Other species appearing in this zone and belonging to one or other of the lineages are *Ericsonia subpertusa* which developed from circular forms of *E. cava,* and *Prinsius martinii* which evolved from *P. dimorphosus* type 2.

Reference locality: Section Caravaca, Barranco del Gredero, samples SP601–605. In this section the zone has a thickness of 21 m.

Distribution: Caravaca: SP601–605; Nahal Avdat: IR67–75; Fakse: DN67–71; Bredstrup Klint: DN72–76; Klintholm: DN78–80; Limhamn: S135, 136.

Age: Early Paleocene.

Ellipsolithus macellus Zone Martini, 1971

Definition: Interval zone from the entry of *Ellipsolithus macellus* to the appearance of *Fasciculithus tympaniformis*.

Remarks: There are no evolutionary events which would give a better definition for the base of this zone.

Cruciplacolithus latipons nov. sp. and *Chiasmolithus consuetus* both developed from *Cruciplacolithus primus* during the time-span of this zone, the former species in the early part, the latter in the later part.

Ericsonia eopelagica evolved from *Ericsonia cava* in the course of the early part of the zone.

Chiasmolithus bidens which descends from *Chiasmolithus danicus* and *Prinsius bisulcus* which developed from *P. martinii,* enter the record in the upper part of the zone.

The earliest representatives of the *Sphenolithus* lineage and of the *Fasciculithus* lineage are found in the upper part of the zone.

Age: Early Paleocene.

Fasciculithus tympaniformis Zone Mohler and Hay, 1967

Definition: Interval zone from the appearance of *Fasciculithus tympaniformis* to the first occurrence of *Heliolithus kleinpellii*.
Remarks: The first radiation of *Fasciculithus* is found in the *E. macellus* and *F. tympaniformis* Zones, but *F. tympaniformis* is the only species which has a range that extends beyond the upper boundary of the zone.

Heliolithus elegans (Roth) nov. comb., the ancestor of *Heliolithus cantabriae* and of the *Discoaster* group 1 developed from *Fasciculithus bitectus* nov. sp. in the course of this zone.

The first representative of the genus *Toweius, T. pertusus* is derived from *Prinsius bisulcus* in the lower part of the zone.
Age: Middle Paleocene.

Heliolithus kleinpellii Zone Mohler and Hay, 1967

Definition: Interval zone from the entry of *Heliolithus kleinpellii* to the first occurrence of *Discoaster mohleri*.
Remarks: *H. kleinpellii* is the final species in the *Heliolithus* lineage, which shows a trend towards reduction in the thickness of all cycles present. The earliest *Discoaster* species, *Discoaster bramlettei* (Bukry and Percival) nov. comb., appears in the upper part of this zone; it descends from *Heliolithus elegans*.
Age: Middle Paleocene.

Discoaster mohleri Zone Hay, 1964, emend. this paper

Definition: Interval zone from the appearance of *Discoaster mohleri* to the entry of *Discoaster multiradiatus*.
Remarks: Bukry and Percival (1971) changed Hay's *Discoaster gemmeus* Zone to *Discoaster mohleri* Zone for taxonomical reasons.

Here the *Discoaster mohleri* Zone is given a wider scope than Hay originally intended. This author placed the upper boundary of his zone at the appearance of *Heliolithus riedelii*.

In most sections, however, this species is lacking; it seems to have had a limited geographical distribution. In the present zonation the name *D. mohleri* Zone is used for the combined *D. mohleri* Zone and *Heliolithus riedelii* Zone (Bramlette and Sullivan, 1961). The latter zone was made to correspond to the interval from the first occurrence of *H. riedelii* to the entry of *Discoaster multiradiatus*.

As a substitute for the latter zone Bukry (1973) introduced the *Discoaster nobilis* Zone, which should be more or less equivalent with the *H. riedelii*

Zone. In our sections we found that *D. nobilis* appears at the same level as *D. multiradiatus,* which makes Bukry's zone less useful.

D. mohleri is a descendant of *Discoaster bramlettei,* found in the upper part of the *H. kleinpellii* Zone, and in turn is found to be ancestral to the group of *Discoaster* species which show no interference in cross-polarized light.

The first representative of the genus *Zygodiscus* s.s. appears in the *D. mohleri* Zone. This species, *Zygodiscus clausus* nov. sp., is ancestral to *Z. adamas* which appears in this zone as well.

Ericsonia universa is seen to follow from *E. robusta* in the upper part of the zone.

Age: Late Paleocene.

Discoaster multiradiatus Zone Bramlette and Sullivan, 1961

Definition: Interval zone from the entry of *Discoaster multiradiatus* to the appearance of *Tribrachiatus nunnii* (Brönnimann and Stradner) nov. comb.

Remarks: The nominate species is found to have developed from *Heliolithus megastypus* (Bramlette and Sullivan) nov. comb. in the upper part of the preceding zone. It is the earliest representative of a group of *Discoaster* species which do show interference in cross-polarized light. The mean number of rays in *D. multiradiatus* decreases in this zone and the next higher zone.

The genus *Rhomboaster* appears in the lower part of the zone with *Rhomboaster intermedia* nov. sp.; radiation in this genus is observed in the upper part of the zone. The earliest representative of the related genus *Tribrachiatus, T. spineus* (Shafik and Stradner) nov. comb., appears in the upper part of the zone.

In *Fasciculithus* there is a second radiation in this zone.

Age: Late Paleocene.

Tribrachiatus contortus Zone Hay, 1964

Definition: Interval zone from the first occurrence of *Tribrachiatus nunnii* (Brönnimann and Stradner) nov. comb. to the last occurrence of *Tribrachiatus contortus.*

Remarks: The *Tribrachiatus nunnii-T. contortus-T. orthostylus* lineage seems to allow for a detailed biostratigraphical subdivision, but unfortunately the former two species have a limited geographical distribution.

The Paleocene/Eocene boundary is generally placed at the base of this zone (Martini, 1971; Perch-Nielsen, 1975). If *T. nunnii* is absent from the

associations, this boundary is hard to recognize. Bukry (1975) therefore placed the boundary at the appearance level of *Discoaster diastypus,* which is somewhat higher in the *T. contortus* Zone.

The mean number of rays in *D. multiradiatus* in this zone is lower than 21 in our assemblages.

The upper boundary of this zone is hard te recognize when *T. contortus* is absent, as is the case in the Caravaca section; here the boundary is placed above the appearance of *T. orthostylus* and below the entry of *Discoaster barbadiensis,* on the basis of evidence from the Nahal Avdat section.
Age: Early Eocene.

Discoaster binodosus Zone Mohler and Hay, 1967

Definition: Interval zone from the last occurrence of *Tribrachiatus contortus* to the entry of *Discoaster lodoensis.*
Remarks: In this partial range zone the earliest *Discoaster* species with free, ornamented arms are found; probably they are a further development from *D. ornatus.*

In the group of *Discoaster* species with lack interference, *Discoaster barbadiensis* evolves from *D. multiradiatus.*

Discoaster pacificus, which belongs to the *D. diastypus* lineage, evolves from *D. diastypus* in the range of this zone.
Age: Early Eocene.

Tribrachiatus orthostylus Zone Brönnimann and Stradner, 1960

Definition: Interval zone from the first occurrence of *Discoaster lodoensis* to the last occurrence of *Tribrachiatus orthostylus.*
Remarks: The name of this partial range zone was changed by Proto Decima et al. (1975) from *Marthasterites tribrachiatus* Zone to *Tribrachiatus orthostylus* Zone for taxonomical reasons.

Discoaster kuepperi developed from *Discoaster robustus* in the time interval corresponding to the lower part of this zone. A differentiation of *Discoaster* species with free, ornamented arms is found in the upper part of the zone. *Helicosphaera* is thought to have evolved from *Zygodiscus,* via *Lophodolithus* in the course of this zone.
Age: Early Eocene.

Discoaster lodoensis Zone Brönnimann and Stradner, 1960

Definition: Interval zone from the exit of *Tribrachiatus orthostylus* to the appearance of *Discoaster sublodoensis.*

Remarks: Transitional forms between *D. lodoensis* and *D. sublodoensis* occur in the upper part of this partial range zone. The first species of *Reticulofenestra, Reticulofenestra dictyoda* probably evolved from *Toweius occultatus* in the same interval.
Age: Late Early Eocene – Early Middle Eocene.

Discoaster sublodoensis Zone Hay, 1964

Definition: Interval zone from the entry of *Discoaster sublodoensis* to the appearance of *Nannotetrina fulgens.*
Remarks: *Nannotetrina cristata,* the oldest species of the genus which evolved from *Micula decussata*, is found in the upper part of this zone.
Age: Middle Eocene.

Nannotetrina fulgens Zone Hay, 1967, emend. Martini, 1971

Definition: Interval zone from the appearance of *Nannotetrina fulgens* to the last occurrence of *Rhabdosphaera gladius.*
Remarks: The name of this zone was changed by Proto Decima et al. (1975) from *Chiphragmalithus alatus* Zone to *N. fulgens* Zone for taxonomical reasons.

Only the lower, and possibly the middle, part of this zone correspond to the uppermost part of our Aspe section.

Sphenolithus obtusus and *S. furcatolithoides* are seen to develop from *S. radians* in the lower part of this zone.
Age: Middle Eocene.

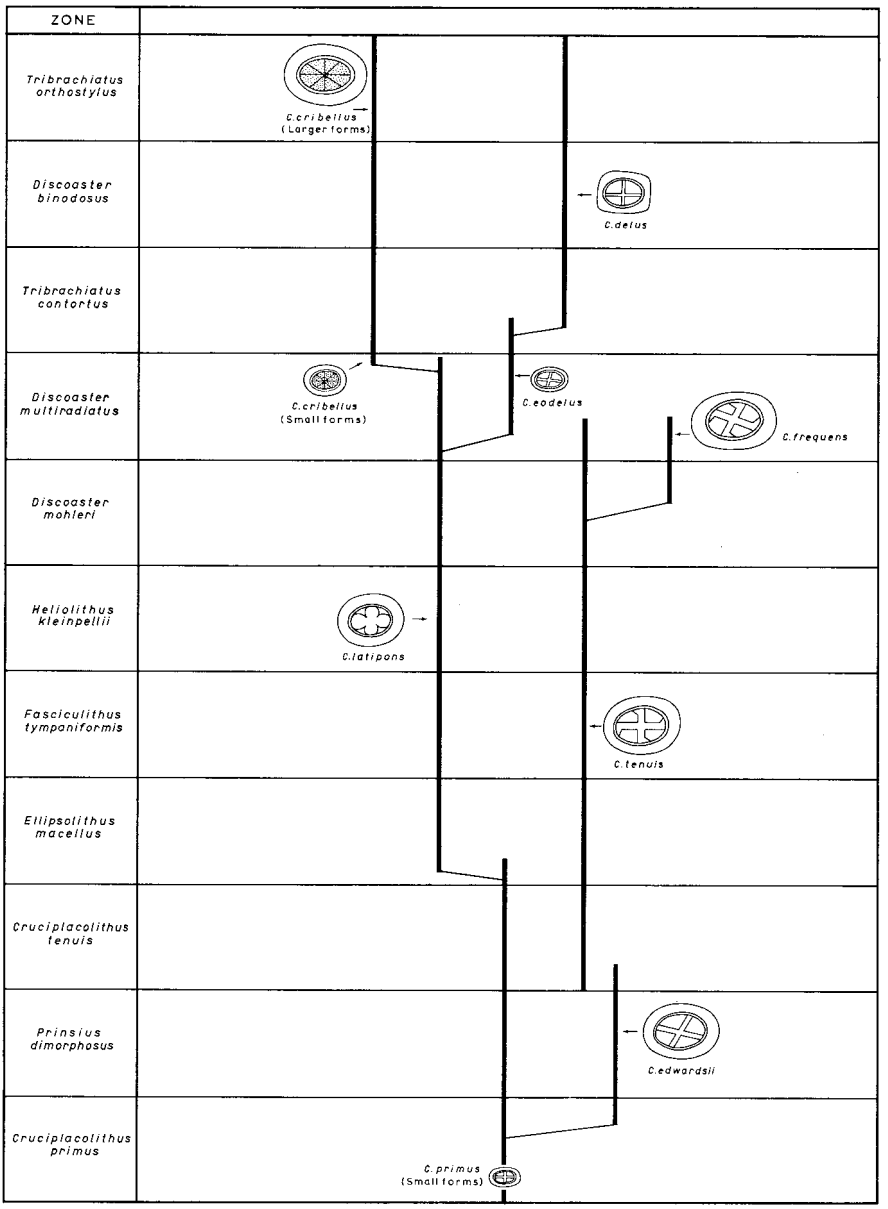

Fig. 29 Lineages in the genus *Cruciplacolithus*.

Chapter V

THE LINEAGES

The relationships, trends, morphoclines and lineages (or, better, lines of descent; see Chapter II) suggested in this chapter are based primarily on observations in the L.M., using the method described in Chapter I. The indispensable information about the ultrastructure of the species was obtained by S.E.M. investigations, and from S.E.M. and T.E.M. micrographs available in the literature.

Most of the information given below results from our own observations of the tropical assemblages found in the thick and continuous sediment series of Caravaca, Aspe and Nahal Avdat.

Lineages are described in the following families (arranged in the order of appearance of the first representative of each family): 1. the Coccolithaceae, 2. the Noëlaerhabdaceae, 3. the Sphenolithaceae, 4. the Fasciculithaceae, 5. the Heliolithaceae, 6. the Discoasteraceae, 7. the Zygodiscaceae. Finally, lineages are presented, which comprise the genera *Micula, Rhomboaster, Tribrachiatus* and *Nannotetrina* (8).

For the description of the genera and species considered hereafter, the reader is referred to Chapter VI.

LINEAGES IN THE COCCOLITHACEAE

1.a. Lineages in the genus *Cruciplacolithus* (fig. 29)

1.a.1. Morphoclines in *Cruciplacolithus primus* s.l.

As already indicated by its name, this species is the first, true representative of the genus. The earliest forms are very small (3–5 μ), have a narrow central area and a fragile central cross. The number of elements in the narrow margin varies from 25 to 30. The central cross is in line with the axes of the ellipse.

In progressively higher assemblages from the *C. primus* Zone, the maximum size of the specimens increases to 9 μ (figs. 30, 31). These larger forms show a wider margin with up to 66 elements, and a larger central area, but the central cross is still aligned with the axes of the ellipse.

Somewhat above the level of first occurrence of forms larger than 9 μ (in the upper part of the *C. primus* Zone), we started to find specimens in which

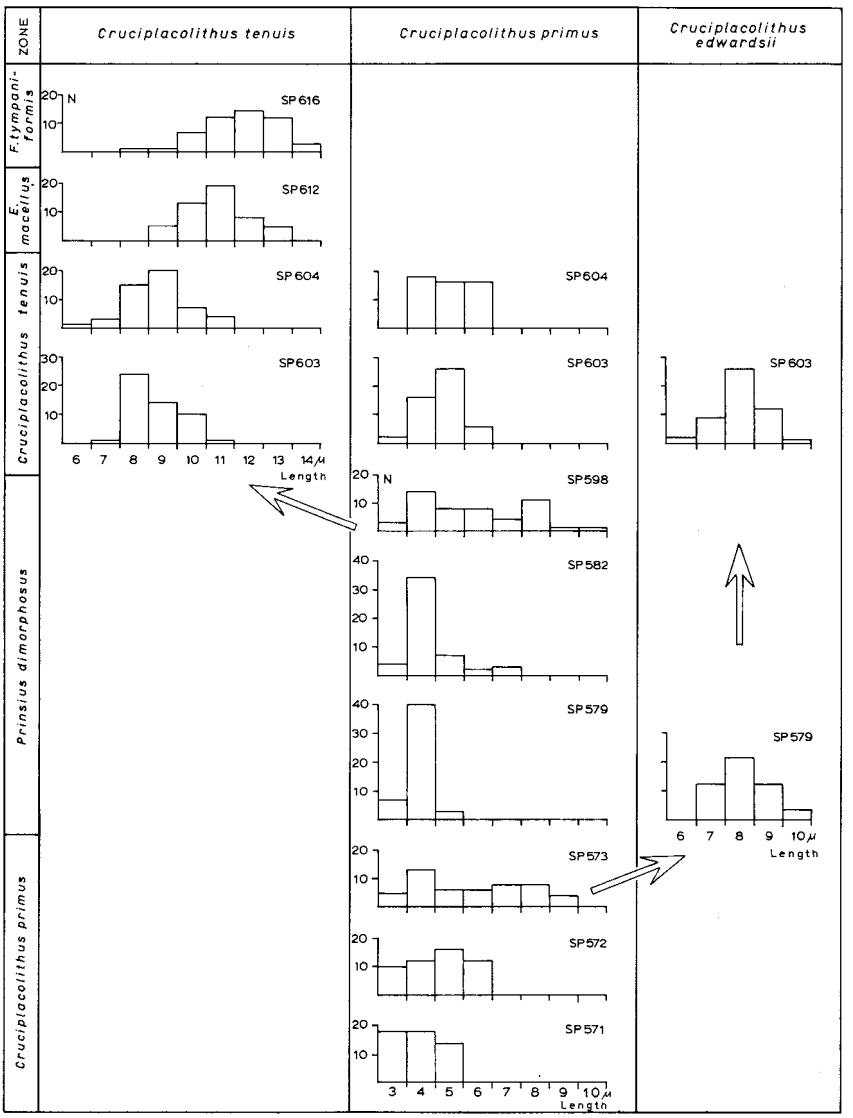

Fig. 30 Histograms showing the lenght distributions of assemblages (N = 50) of *C. primus*, *C. edwardsii* and *C. tenuis* in the *C. primus* to *F. tympaniformis* zonal interval in the Caravaca section.

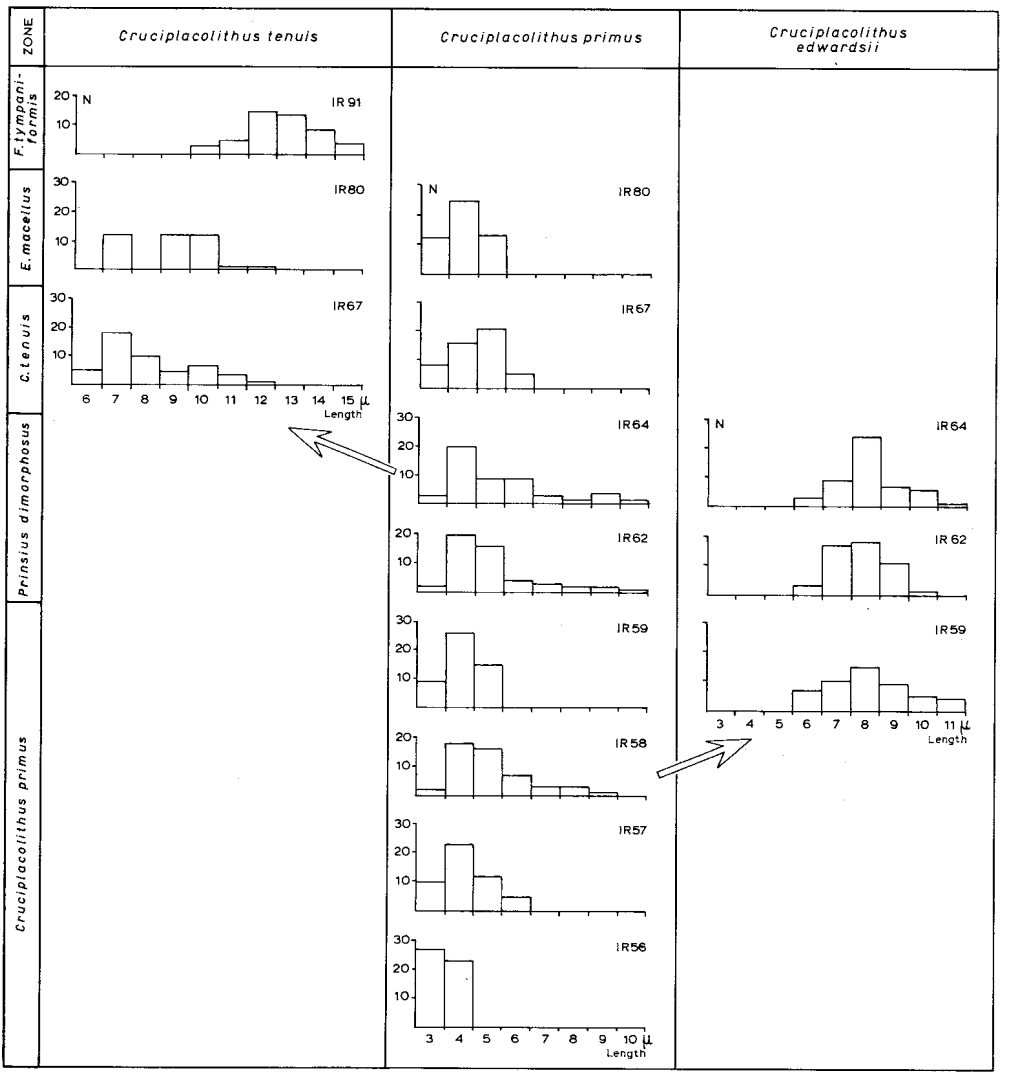

Fig. 31 Histograms showing the length distribution of assemblages (N = 50) of *C. primus*, *C. edwardsii* and *C. tenuis* in the *C. primus* to *F. tympaniformis* zonal interval in the Nahal Avdat section.

the Y_1-bars were no longer parallel to the Y-axis. The size of these specimens ranges from 6 to 10 μ. Such forms have been assigned to *Cruciplacolithus edwardsii* nov. sp.

After the branching off of *C. edwardsii*, *C. primus* continues its range in the assemblages, but only in smaller forms (3–5 μ). In the uppermost part

of the *C. primus* Zone and in the *P. dimorphosus* Zone the maximum length of specimens of *C. primus* increases again, until finally forms of 10 μ are found. In these larger forms, several elements at the tips of the bars show an optical orientation and a form, which differ from the other elements in the bars. Somewhat higher, small triangular protuberances (so-called feet) appear which invariably point counter-clockwise in distal view. The forms with such feet have been assigned to *Cruciplacolithus tenuis.*

After the branching off of *C. tenuis, C. primus* continues to be present in the assemblages, but again in smaller forms only (3–6 μ). The species begins to decrease in numbers in the *C. tenuis* Zone and it becomes rare in the *E. macellus* Zone.

In the latter zone *C. primus* is seen to give rise to *Chiasmolithus consuetus* (fig. 37); the species is probably also ancestral to *Cruciplacolithus latipons,* which appears in the same zone.

1.a.2. The morphocline in *Cruciplacolithus edwardsii*

In early forms of this species in the *C. primus* Zone, only the Y_1-bars make an angle with the Y-axis. The rotation from the Y-axis is in clockwise direction in distal view. In somewhat younger assemblages the X_1-bars make an angle with the X-axis as well, again in clockwise direction. In order to get an impression of the changes in this species we carried out a biometric study in which the following parameters were measured (fig. 32): (1) the angle between the X_1-bars and the X-axis ($\angle XX_1$), (2) the angle between the Y_1-bars and the Y-axis ($\angle YY_1$).

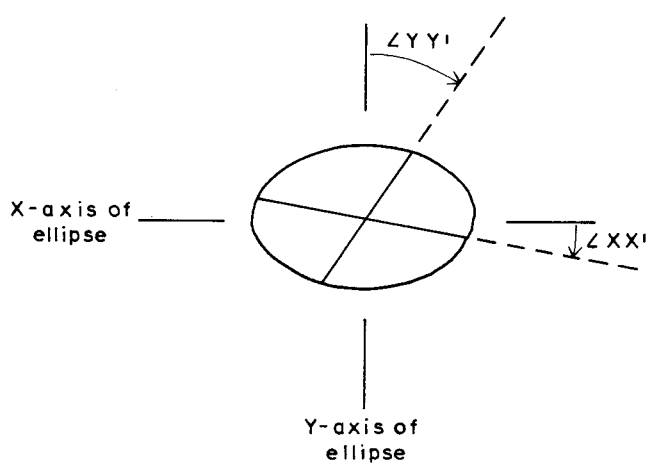

Fig. 32 Parameters measured in *Cruciplacolithus edwardsii.*

In our study we used L.M. observations on fixed mounts in cross-polarized light. Thirty specimens were measured in each of the samples used for this comparison. Some selection was inevitable as only well preserved specimens which were lying flat could be used for measuring.

For specimens lying with the distal side upwards the working procedure for measuring the angles of rotation consists of the following steps: (1) rotation of the object table until the X-axis of the specimen is parallel to the X-cross-hair, (2) reading of the scale → X, (3) anti-clockwise rotation of the table until the X_1-bars are parallel to the X-cross-hair, (4) reading of the scale → Y; X-Y gives the angle XX_1; (5) further anti-clockwise rotation of the table until the Y_1-bars are parallel to the Y-cross-hair, (6) reading of the scale → Z; X-Z gives the angle YY_1; $\angle XX_1 + 90 - YY_1$ gives the angle X_1Y_1. For specimens lying with the proximal side upwards, the table was rotated in the opposite direction.

As the interval containing *C. edwardsii* is thickest in the Caravaca section the measurements were first performed on a set of 7 samples from this Spanish locality. The results are given in figure 33. The following conclusions can be drawn: (1) the mean angle of rotation of the bars increases in progressively younger assemblages, (2) the mean angle of rotation of the Y_1-bars is invariably higher than that of the X_1-bars, (3) the mean angle X_1Y_1 is smaller than 90°.

In order to check this conclusion the same measurements were performed on a set of 3 samples from the corresponding stratigraphic interval in the Nahal Avdat section. The results of these measurements are given in figure 34. From this figure it can be concluded that the same trend occurs in this section.

In both the Caravaca and the Nahal Avdat sections, the species disappears rather suddenly from the record. Near the disappearance level, in the lower part of the *C. tenuis* Zone, the bars are no longer straight, but in distal view they are slightly curved clockwise. In cross-polarized light and with the gypsum plate the bars begin to show a patchy colour distribution. These youngest forms of *C. edwardsii* are probably transitional to *Chiasmolithus danicus,* but typical specimens of the latter species do not occur in sections in the Tethys realm.

1.a.3. The morphocline in *Cruciplacolithus tenuis* (figs. 28, 30, 31)

In the *C. tenuis* to *F. tympaniformis* zonal interval, the maximum length of specimens of *C. tenuis* increases from 11 μ to 14 μ in the Caravaca section, and from 12 μ to 15 μ in the Nahal Avdat section. Above the *F. tympaniformis* Zone the maximum length measured was 18 μ, but the frequency

of the species decreases. In the *D. mohleri* Zone forms begin to occur in which the bars make an angle with the axes of the ellipse, in clockwise direction in distal view. These forms have been assigned to *Cruciplacolithus frequens* (Perch-Nielsen) nov. comb. The bars in this species remain normal to each other, and the angle of rotation never exceeds 15°. Both *C. tenuis* and *C. frequens* disappear in the *D. multiradiatus* Zone.

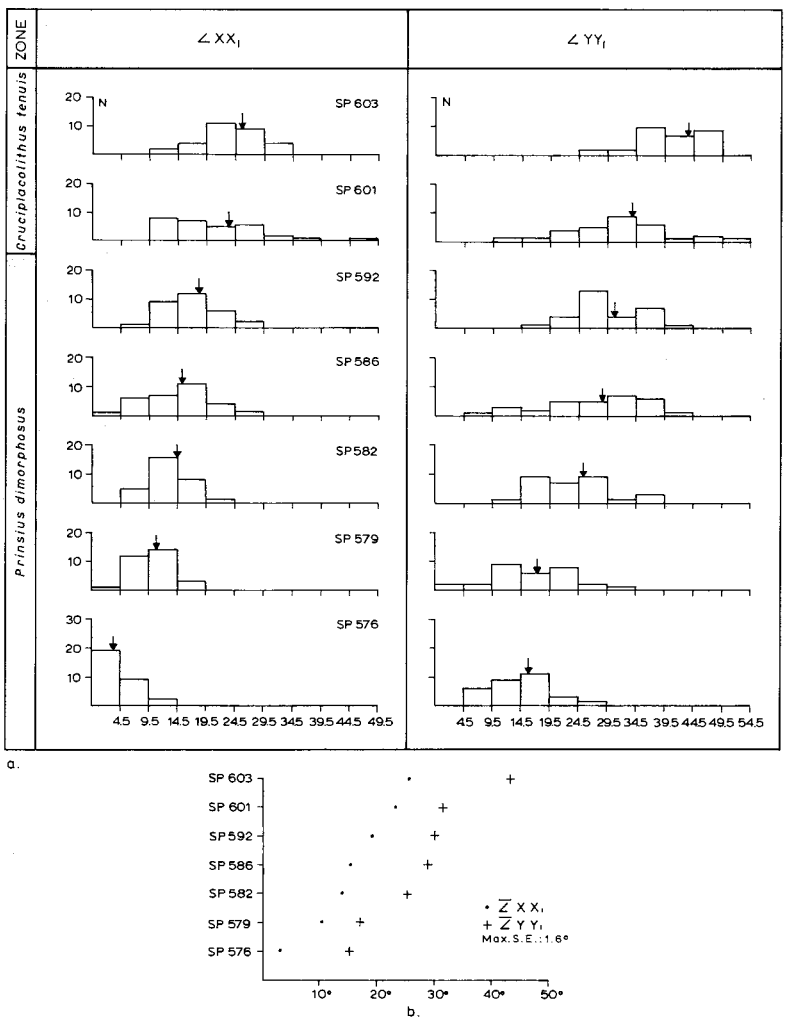

Fig. 33 The angles XX_1 and YY_1 in assemblages (N = 30) of *Cruciplacolithus edwardsii* from the Caravaca section. a. Histograms, b. Mean values.

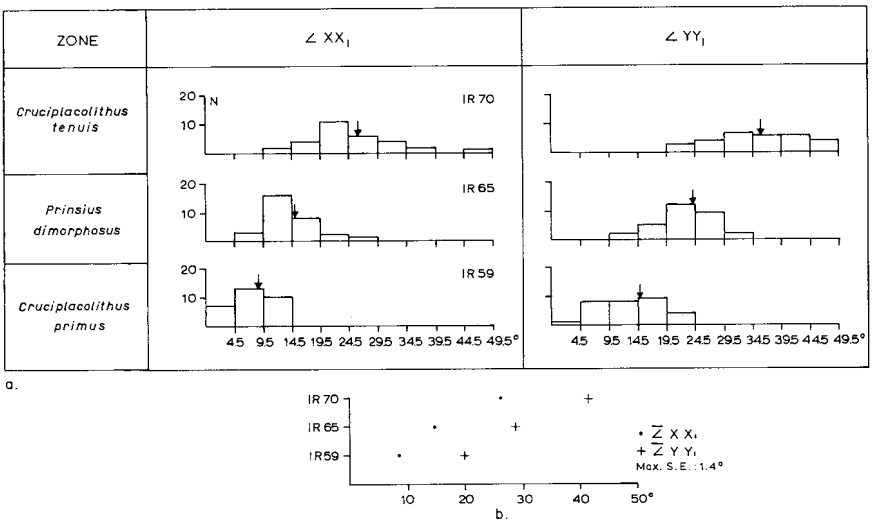

Fig. 34 The angles XX_1 and YY_1 in assemblages (N = 30) of *Cruciplacolithus edwardsii* from the Nahal Avdat section. a. Histograms, b. Mean values.

1.a.4. Relationships between *Cruciplacolithus latipons* nov. sp., *Cruciplacolithus cribellus* (Bramlette and Sullivan) nov. comb. and *Cruciplacolithus eodelus* (Bukry and Percival) nov. comb. (fig. 28)

Cruciplacolithus latipons starts its range in the *E. macellus* Zone. The species is thought to have developed from *C. primus*. The main transformation is seen in the increase in the width of the bars, which become blade-like. The species is rare in the *E. macellus* Zone and occurs sporadically in the *F. tympaniformis* to *D. multiradiatus* Zonal interval.

Cruciplacolithus latipons is thought to be ancestral to *C. cribellus*, which appears in the *D. multiradiatus* Zone. The development towards *C. cribellus* includes the following steps: (1) further lateral growth of the bars, so that the central area becomes completely closed. All bars must have grown to the same extent because there are diagonal sutures in the central plate of *C. cribellus*, (2) perforation of the central plate.

Also *C. eodelus* is considered to have developed from the exceedingly rare *C. latipons*. This species also appears in the *D. multiradiatus* Zone. It is thought that in this development the bars became reduced to narrow structures, which are no longer parallel to the axes of the ellipse but which make

a small angle with them in clockwise direction (in distal view). Simultaneously the wall became narrower and its inner margin steeper.

Cruciplacolithus delus is seen to evolve from *C. eodelus* in the course of the *T. contortus* Zone by gradually acquiring a more quadrangular outline and a stronger vaulting of the coccolith.

1.a.5. Changes in *Cruciplacolithus* in the sections in Scandinavia

C. primus is the first representative of the genus in the Scandinavian sections as well. In this region the species remains small in the *C. primus* Zone, and *C. edwardsii* does not occur in this zone as it does in the Tethys sections. The gradual transition from *C. primus* to *C. tenuis* was not found either; the latter species enters the assemblages rather suddenly.

The specimens of *C. edwardsii* found in the lower part of the *C. tenuis* Zone are comparable with the youngest forms found in Spain and Israel; i.e. they seem to be forms which are transitional between *C. edwardsii* and *Chiasmolithus danicus*. Somewhat higher in the Scandinavian *C. tenuis* Zone the first typical specimens of *Chiasmolithus danicus* are found, which are characterized by strongly curved, rather wide bars.

1.a.6. The origin of the genus *Cruciplacolithus*

C. primus might have evolved from *Cruciplacolithus? inseadus* in the course of the *B. sparsus* Zone in that the tangential bars in the central area completely disappeared. This species in turn might have developed from representatives of the Cretaceous genus *Sollasites*. Notwithstanding a persistent search, we could find no trace of *Cruciplacolithus? inseadus* in our assemblages.

1.b. Lineages in the genus *Ericsonia* (fig. 35)

The first representative of this genus is *Ericsonia cava,* which appears just below the boundary between the *C. primus* and *P. dimorphosus* Zones. These early forms are small (3–5 μ) and have a narrow, open central area. They are clearly seen to evolve from small forms of *C. primus* in that the central cross becomes reduced. In the *P. dimorphosus – E. macellus* zonal interval the maximum length increases to about 7 μ, but the frequency decreases after reaching a peak in the *P. dimorphosus* Zone of the Tethys sections.

E. eopelagica, which appears in the *E. macellus* Zone, probably developed from *E. cava,* but we did not observe the transition. This development re-

quired no more than an increase in the relative width of the margin and a change to a less steep outward slope of the shields.

E. cava is also ancestral to *E. subpertusa*. In the upper part of the *P. dimorphosus* Zone we found variants of *E. cava* with a more circular outline. The number of these circular forms increases in progressively younger assemblages. In these forms the following gradual changes take place: (1) the wall

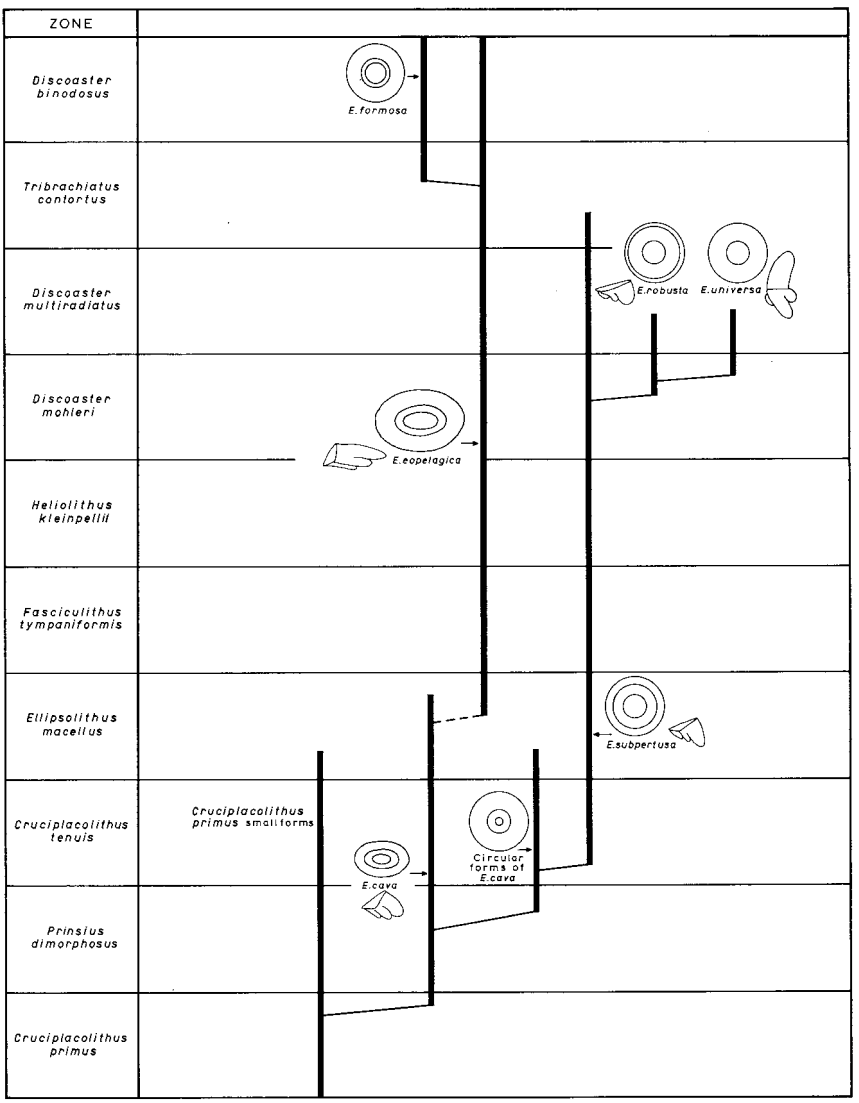

Fig. 35 Lineages in the genus *Ericsonia*.

gradually shifts to a more distal position with regard to the shields; in the end the outer margin of the wall projects beyond the outer margin of the proximal shield. This projection can be observed best in the light microscope ("focus effect", see Chapter VI), (2) the outward slope of the shields becomes steeper, (3) the sutures in the wall, which are counter-clockwise oblique in earlier forms, become hook-shaped; i.e., near the inner margin of the wall they are oblique clockwise, but in the middle of the wall they bend in the opposite direction (fig. 36). The circular forms that show this hooked type of sutures, steeply sloping shields and the "focus effect" of the wall have been assigned to the species *E. subpertusa.*

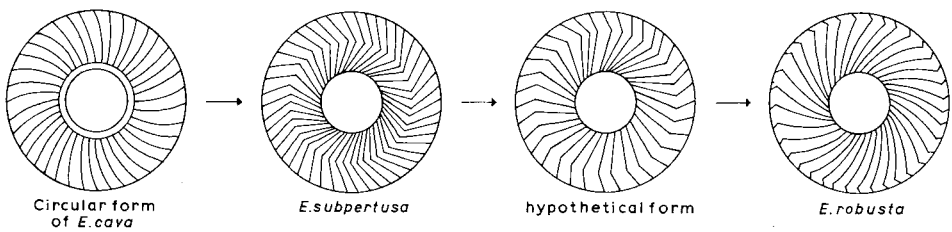

Fig. 36 Changes in the orientation of the sutures in the wall in the development of *E. robusta* from circular forms of *E. cava.*

The ratio between the width of the margin and the diameter of the central opening is highly variable in *E. subpertusa*; it varies from 2 to about 0.5.

E. robusta is seen to develop from *E. subpertusa* in the course of the *D. mohleri* Zone by the following structural changes: (1) an increase in the width of the wall, (2) a further lateral shift of the wall, to such an extent that it almost completely covers the distal shield, (3) an enlargement of the clockwise oblique parts of the hook-shaped sutures, to such an extent that almost the entire suture becomes straight and oblique clockwise.

E. robusta is in turn ancestral to *E. universa,* which also appears in the *D. mohleri* Zone. This change includes an increase in the height of the outer margin of the wall, and a proximal elongation of the proximal cycle of the distal shield.

The change from an elliptical outline to a circular form is repeated in the *T. contortus* Zone. In this zone individuals in the assemblages of *Ericsonia eopelagica* develop a circular outline that is characteristic of *Ericsonia formosa.* This species and *E. eopelagica* form an important part of the Eocene floras.

1.c. Lineages in the genus *Chiasmolithus* (fig. 37)

Lineages in this genus have been described by Gartner (1970), who divided the genus into two groups on the basis of the construction of the bars. For a further subdivision of these two groups the shape of the bars has been taken into account. The relations suggested below largely conform to those proposed by Gartner; a different opinion is expressed about the origin of the two groups however.

1.c.1. Lineages in group 1 (forms with non-split bars)

The earliest representative of this group is *Chiasmolithus consuetus,* which appears in the *E. macellus* Zone. The species evolved from *Cruciplacolithus primus* in the course of the lower part of this zone. Intermediate forms between both species have been found only in the Caravaca section. At first, *C. primus* forms are found in which the bars are still aligned with the axes of the ellipse but in which the margin is *Chiasmolithus*-like. Somewhat higher in the section the central cross of these forms begins to rotate clockwise in distal view. The angle of rotation increases rapidly to forms in which the angles XX_1 and YY_1 are about 45°. During (and after) this rotation the bars remain normal to each other.

The early forms of *C. consuetus* are relatively small (3–8 μ), but the maximum size increases in younger assemblages. In the *D. multiradiatus* Zone the first specimens larger than 12 μ appear; they have been assigned to *C. californicus.* In higher zones the gradation between *C. consuetus* and *C. californicus* disappears. The latter species gradually disappears from the assemblages in the *D. sublodoensis* Zone, but *C. consuetus* ranges well into the *N. fulgens* Zone. In the course of this zone, *C. titus* evolved from *C. consuetus* by developing a strong bend of the X_1-bars, clockwise in distal view.

1.c.2. Lineages in group 2 (forms with split bars)

Chiasmolithus bidens is the earliest representative of this group. In the Caravaca and Nahal Avdat sections the species enters suddenly in the *E. macellus* Zone, but in the sections in Scandinavia we found intermediates between *C. danicus* and *C. bidens* in the same zone. *C. bidens* probably evolved from *C. danicus* in boreal waters and migrated afterwards to warmer waters. In Spain and Israel the first occurrence of *C. bidens* coincides approximately with that of *C. consuetus*; the latter species has not been found in Scandinavia. The distribution of *C. consuetus* thus seems to have been restricted to more tropical waters.

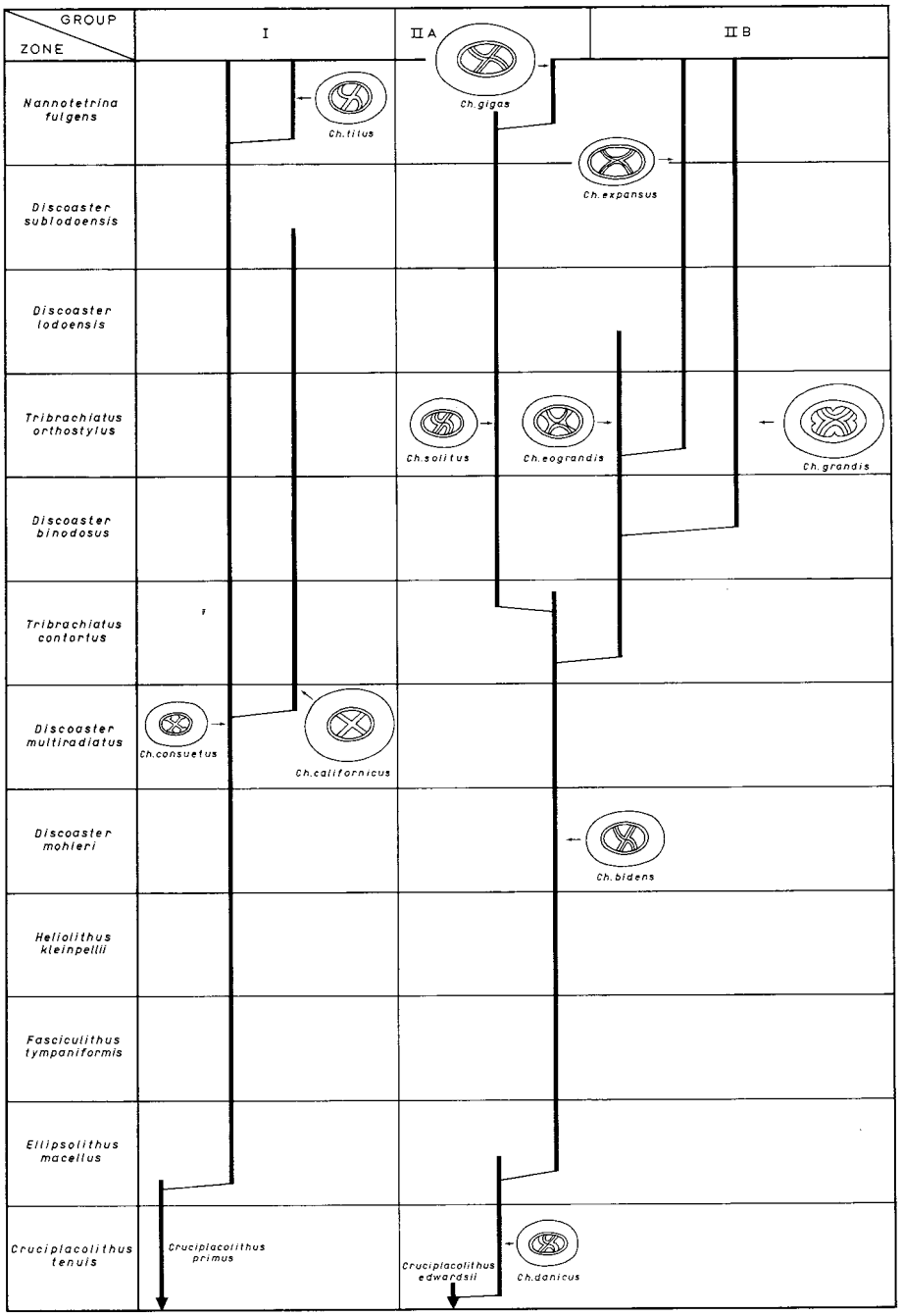

Fig. 37 Lineages in the genus *Chiasmolithus*.

The descendants of *C. danicus* can be divided into the following two groups on the basis of the shape of the bars:

Group 1; as in *C. danicus,* the Y_1-bars are straight and the X_1-bars are curved (clockwise in distal view) in the species of this group, wich are *C. bidens, C. solitus* and *C. gigas. C. solitus* is thought to have evolved from *C. bidens* in the course of the *T. contortus* Zone; *C. solitus* is in turn thought to be ancestral to *C. gigas,* which appears in the *N. fulgens* Zone.

Group 2; in the species belonging to this group both the X_1-bars and the Y_1-bars are strongly curved; the former clockwise in distal view, the latter in the opposite direction. The oldest species showing this type of bars is *C. eograndis,* which is considered to have developed from *C. bidens* in the *T. contortus* Zone. *C. eograndis* is considered to be ancestral to *C. grandis,* which appears in the *D. binodosus* Zone, and to *C. expansus,* which enters the record in the *T. orthostylus* Zone.

LINEAGES IN THE NOËLAERHABDACEAE (fig. 38)

2.a. Lineages in the genus *Prinsius*

Prinsius petalosus (Ellis and Lohman) nov. comb. is considered to be the earliest representative of the genus. The species was found only in the Caravaca section, where it enters the assemblages in the *C. primus* Zone. After the species has reached its maximum frequency in the upper part of this zone, variants begin to occur in which the distal crown of petaloid elements is almost completely reduced. These forms are considered to be transitional between *P. petalosus* and *P. dimorphosus* type 1. In addition to this reduction the following steps are presumed to have occurred in the evolution to *P. dimorphosus* type 1: (a) an increase in the size of the coccoliths (from about 1 μ to 3 μ), (b) a decrease in the number of coccoliths in the sphere (from 45 to 10), (c) a change in the outline of the coccolith, namely from elliptical to circular.

Prinsius dimorphosus type 1 shows only a single centro-distal cycle; this cycle is considered to be homologous with the basal parts of the distal crown in *P. petalosus.*

P. dimorphosus type 2 evolved from *P. dimorphosus* type 1, probably in the course of the *P. dimorphosus* Zone. In this type there are two, superposed centro-distal cycles. The lower cycle is probably a distal continuation of the proximal shield, inserted between the distal shield and the upper centro-distal cycle. Specimens of type 2 generally have a somewhat more elliptical outline than those of type 1. The presence of specimens of type 2 could be

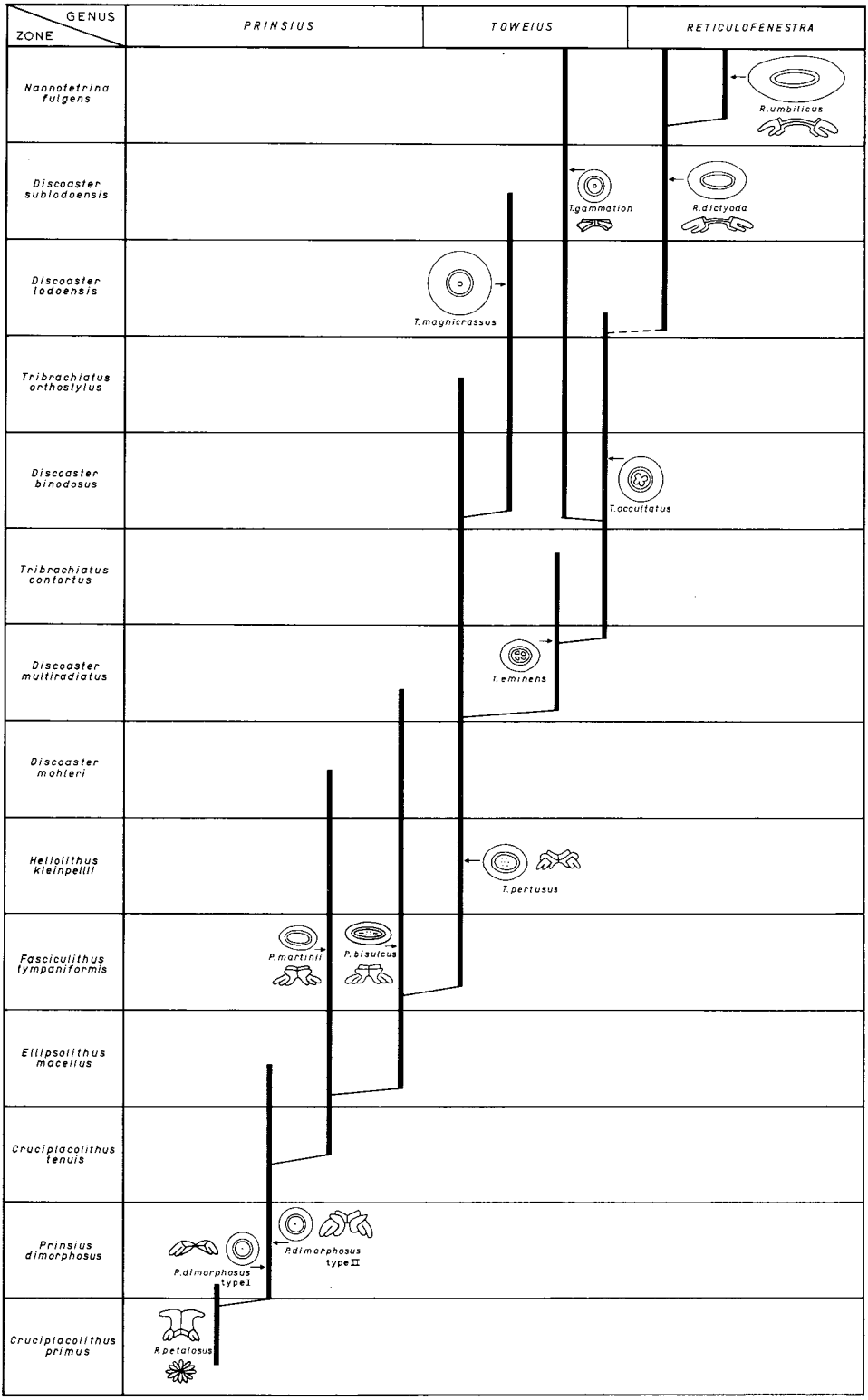

Fig. 38 Lineages in the family Noëlaerhabdaceae.

established with certainty only in the Scandinavian sections. Both types are known to occur on the same coccosphere (Perch-Nielsen, 1969a).

The elliptical *Prinsius martinii* is seen to develop from *P. dimorphosus* type 2 in the course of the *C. tenuis* Zone, during which the following changes took place: (a) an increase in the number of elements in the margin and in the lower centro-distal cycle, i.e. from 13 to about 30, (b) a change from a predominantly circular outline to a predominantly elliptical outline, (c) a more regular arrangement of the elements in the lower centro-distal cycle.

Prinsius bisulcus shows a higher number of elements in the margin and in the lower centro-distal cycle than *P. martinii,* from which it is seen to develop in the course of the *E. macellus* Zone. The elements near the poles in the upper centro-distal cycle became more regularly arranged; two sutures along the X-axis are formed. The centro-distal cycles became pierced by a small number of pores. Early forms of *P. bisulcus* are small and subelliptical to elliptical; they have a small number of pores. Later forms are larger, more distinctly elliptical and have more pores.

2.b. Lineages in the genus *Toweius*

Toweius pertusus (Sullivan) nov. comb., the first species in *Toweius,* is seen to develop from early forms of *P. bisulcus*; it appears in the lower part of the *F. tympaniformis* Zone. The following changes are observed in the transition from *Prinsius* to *Toweius*: (a) a further increase in the number of elements in the margin, in the lower centro-distal cycle, and especially in the upper centro-distal cycle, (b) a more regular arrangement of the elements in the upper centro-distal cycle, and an increase in the thickness of this cycle, (c) coalescing of the elements of the proximal shield in such a way that a proximal central plate is formed; this plate is closely pressed against the upper centro-distal cycle, (d) an increase in the number of pores in the central area. These pores pierce both the proximal plate and the upper centro-distal cycle.

The maximum size of the coccoliths of *T. pertusus* increases in the *F. tympaniformis* to *D. multiradiatus* zonal interval. The number of pores increases in this interval from about 6 to a maximum of 24. This trend towards the formation of a more open central area is apparent in several descendants of *T. pertusus.*

In *T. eminens* s.l., which appears in the *D. multiradiatus* Zone, groups of pores coalesce to form a small number (4 to 7) of larger openings. In *T. occultatus,* which is thought to have developed from *T. eminens* s.l. in the course of the upper part of the *D. multiradiatus* Zone, the bars be-

tween these larger openings disappear, so that a single, large central opening is formed.

The largest and thickest species in the genus is *T. magnicrassus* (Bukry) nov. comb., which is thought to have developed from *T. pertusus* in the course of the *D. binodosus* Zone. The central area in this species was probably closed by a reticule.

Toweius gammation (Bramlette and Sullivan) nov. comb., which appears in the *D. binodosus* Zone, evolved from *T. occultatus*. In intermediate forms the central opening gradually becomes smaller. In addition there is a complete reduction of the proximal cycle of the distal shield and of the upper centro-distal cycle.

2.c. Lineages in the genus *Reticulofenestra*

Only two species of this genus occur in our material. The oldest species is *Reticulofenestra dictyoda,* which appears in the *D. lodoensis* Zone. It descends either from *Toweius occultatus* or from *Toweius pertusus,* although specimens of the latter species have not been observed at such a high level in our sections.

The following essential changes in morphology took place in the development from *Toweius* to *Reticulofenestra*: (a) the disappearance of a separate lower centro-distal cycle; the course of the sutures in the inner margin of the upper cycle of the distal shield indicates that in *Reticulofenestra* the lower centro-distal cycle fused with the distal shield; (b) thinning of the upper centro-distal cycle, and an increase in the number of pores in this cycle and in the central part of the proximal shield, resulting in a finely perforated, central reticule; (c) an increase in the distance between the upper and lower cycles of the distal shield, and an increase in the degree of imbrication of the elements in the upper cycle of this shield.

In the *D. lodoensis* and *D. sublodoensis* Zones the maximum size of *Reticulofenestra dictyoda* increases from 5 μ to 10 μ. In the *N. fulgens* Zone the first variants larger than 10.5 μ were observed. These forms have been assigned to *R. umbilicus*. The diameter of the central area and the width of the marginal part of the centro-distal cycle are highly variable in this species.

LINEAGES IN THE SPHENOLITHACEAE

3.a. Lineages in the genus *Sphenolithus* (fig. 39)

The first representative of this genus, *S. primus,* appears in the *E. macellus* Zone. Early forms are rather small (4 μ), but the height and the diameter

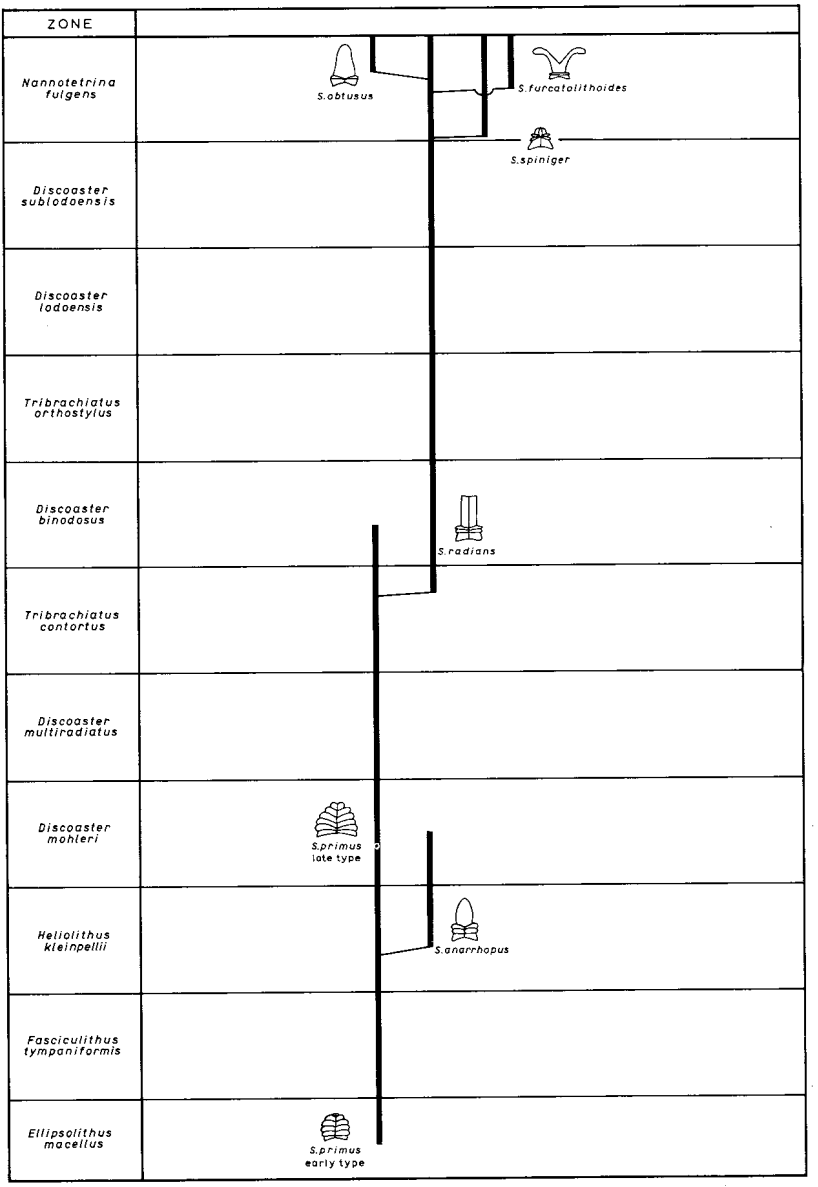

Fig. 39 Lineages in the genus *Sphenolithus*.

increase to about 8 μ in the *H. kleinpellii* Zone. The first species seen to develop from *S. primus* is *S. anarrhopus,* in the course of the *H. kleinpellii* Zone. As in almost all later, direct and indirect descendants of *S. primus,* the column remains unchanged, but the morphology of the cone alters: one of the topmost elements in the cone becomes enlarged to a blade-like spine, while the total number of superposed cycles in the cone decreases to two or three.

In *S. radians,* which is thought to have developed from *S. primus* in the course of the *T. contortus* Zone, four of the topmost elements in the cone are enlarged to a centro-distal spine. There are two or three superposed cycles in the basal part of the cone.

S. spiniger is observed to develop from *S. radians* in the course of the *N. fulgens* Zone. Both species show the same construction, but in the former the hight of the cone has become smaller than that of the column.

Another descendant of *S. radians,* seen to develop in this interval, is *S. obtusus.* In this species the number of cycles in the lower part of the cone is reduced to only one. This cycle has probably coalesced with the column, which would explain the obtuse angle formed by the extinction lines.

S. furcatolithoides also shows a single cycle in the lower part of the cone. This species enters the record in the *N. fulgens* Zone, and is seen to develop from *S. radians.* The number of large elements in the cone is reduced to two in this species.

LINEAGES IN THE FASCICULITHACEAE

4.a. Lineages in the genus *Fasciculithus* (fig. 40)

The oldest species in this genus is the large and robust *F. magnus,* which first occurs in the *E. macellus* Zone. The larger part of the thick column shows radially arranged elements; in a thin, upper slice, however, the sutures are anti-clockwise oblique. This different orientation of the elements is probably the result of torsion. The central body is relatively small.

A first radiation in the genus occurred in the course of the *E. macellus* and *F. tympaniformis* Zones. All species in this interval have a central body.

F. magnus is thought to be ancestral to both *F. magnicordis* nov. sp. and *F. ulii,* which appear in the *E. macellus* Zone. In the former descendant the central body became relatively larger than in *F. magnus,* but in *F. ulii* it became reduced.

Like *F. magnus, F. ulii* shows an upper slice with anti-clockwise oblique sutures, but in the latter species this slice is surmounted by a distal cycle of

clockwise imbricating elements (dome).

In *F. janii* the column shows a well differentiated "upper slice" which surrounds the dome.

In *F. bitectus* nov. sp. this dome is relatively flat and covers a distinct, separate cycle of elements (median cycle) which is considered homologous with the "upper slice" of the column of *F. ulii*.

In *F. billii* the dome is relatively low; a well-differentiated "upper slice" is not present in the column.

In *F. tympaniformis* there is no clear distinction between a column and a dome; in our opinion these units coalesced in the development from *F. ulii*. A central body is present in early forms, but it disappears in the upper part of the *F. tympaniformis* Zone.

A second period of radiation in the genus occurred in the course of the

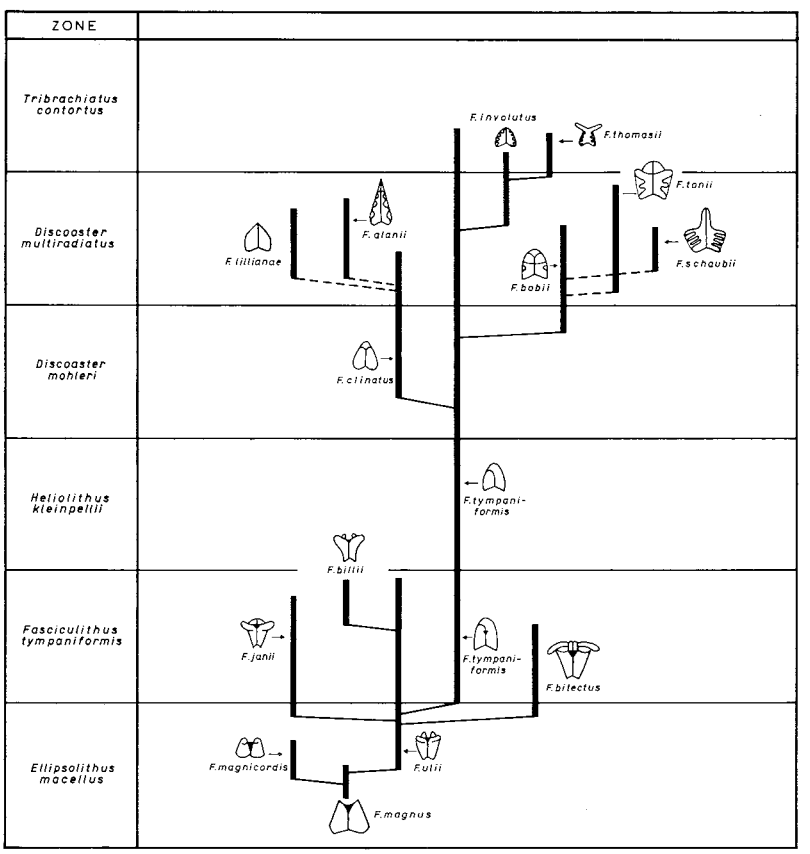

Fig. 40 Lineages in the genus *Fasciculithus*.

D. mohleri and *D. multiradiatus* Zones. The species which evolved in in this time span can be roughly subdivided into three groups; *F. tympaniformis* is ancestral to all three.

The species in the first group are medium-sized and have a more or less triangular outline in side view. The oldest species in this group is *F. clinatus*, which is seen to develop from *F. tympaniformis* by a gradual change in its outline in the course of the *D. mohleri* Zone.

F. alanii and *F. lillianae* most probably descend from *F. clinatus*. In the former species the column shows fenestrae, and the cone is relatively high; in the latter species the cone has disappeared, and there are fewer elements in the column.

The species in the second group are large and have a parallel-sided or proximally tapering column. The sturdy *F. bobii* is considered to have evolved from *F. tympaniformis* in the course of the upper part of the *D. mohleri* Zone. It shows a single, distal row of fenestrae. Both *F. tonii* and *F. schaubii* probably developed from *F. bobii* in the course of the *D. multiradiatus* Zone. In the former species the number of rows of fenestrae has increased to two or three; in the latter species the maximum number of rows is four.

The species in the third and youngest group, which developed from *F. tympaniformis*, are relatively small and have a star-like outline in proximal or distal view. *F. involutus*, which appears in the *D. multiradiatus* Zone, is the first representative of this group. Its cone is low and the column shows regularly arranged fenestrae. In *F. thomasii*, which is seen to develop from *F. involutus* in the time span corresponding to the upper part of the *D. multiradiatus* Zone, the cone is transformed into a distally flaring cycle, and the fenestrae become smaller.

LINEAGES IN THE HELIOLITHACEAE

5.a. Lineages in the genus *Heliolithus* (fig. 41)

Heliolithus elegans (Roth) nov. comb. is considered to be the first representative of the genus. The species appears in the *F. tympaniformis* Zone. In our opinion the species evolved from *Fasciculithus bitectus* nov. sp. The most essential transformation in this development is the change in the orientation of the elements in the column: instead of being radially orientated they become arranged tangentially, and are oblique anti-clockwise in distal view. As a result the sutures in the column acquire the same orientation as those in the median cycle and in the distal cycle (= dome in *Fasciculi-*

thus). In addition the diameter of the median cycle increases, so that it becomes visible in distal or proximal view.

The following trends can be observed in the *H. elegans* – *H. cantabriae* – *H. kleinpellii* morphocline: (a) a decrease in the height of the column, (b) an increase in the diameter of the distal cycle, (c) the formation of a central channel (opening).

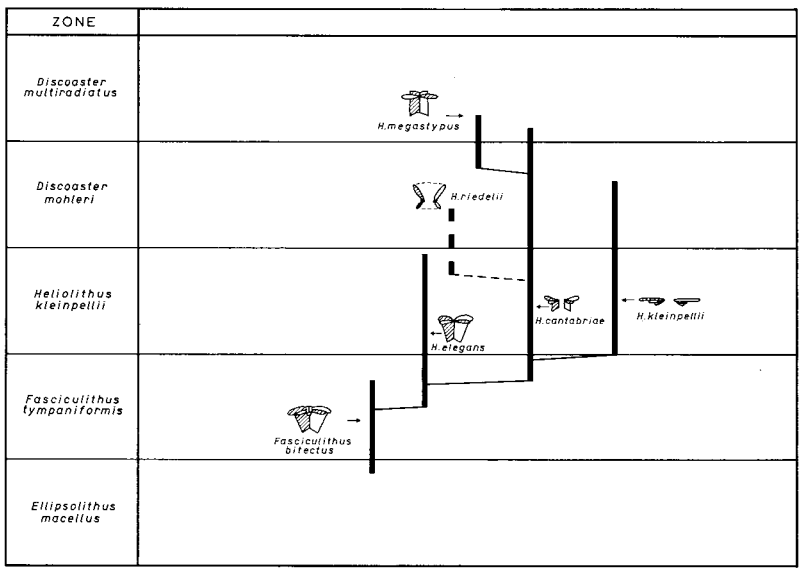

Fig. 41 Lineages in the genus *Heliolithus*.

H. megastypus (Bramlette and Sullivan) nov. comb. evolved from *H. cantabriae* in the course of the *D. mohleri* Zone. In this development the median cycle becomes considerably wider than the column, while the distal cycle is reduced.

LINEAGES IN THE DISCOASTERACEAE

6.a. Lineages in *Discoaster* group 1 (species without a regular extinction cross, fig. 42)

Discoaster bramlettei (Bukry and Percival) nov. comb., the first representative of this group of *Discoaster* is seen to evolve from *Heliolithus elegans* (Bukry) nov. comb. in the time span corresponding to the upper part of the *H. kleinpellii* Zone. In this change from *Heliolithus* to *Discoaster* the following transformations took place (fig. 43): (a) reduction of the column and a

change in position of its most distal part with regard to the other cycles, (b) reduction of the distal cycle, and (c) an increase in the diameter of the median cycle.

D. bramlettei shows a large variation in the structure of the centre; there are forms with remnants of the column and the distal cycle, and the centre may be open or closed. In somewhat later forms the number of elements

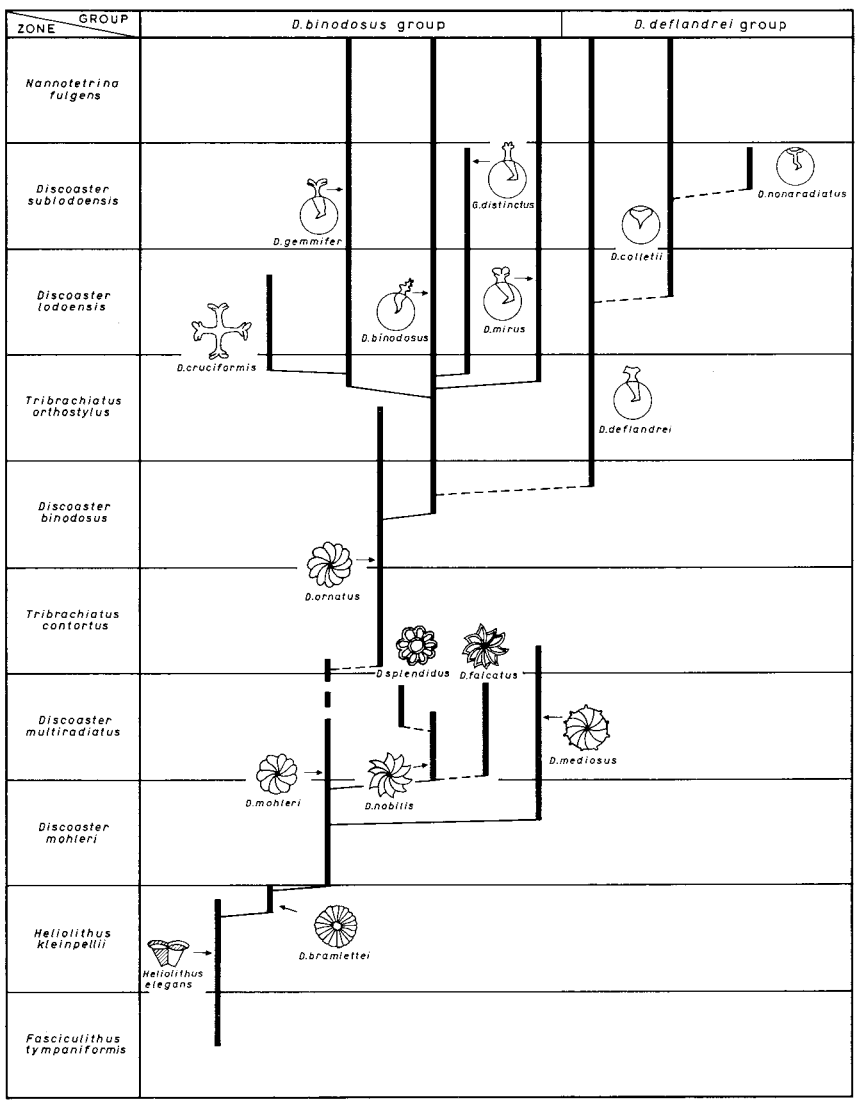

Fig. 42 Lineages in the genus *Discoaster* (Group 1, species without a regular extinction cross).

decreases; they are transitional to *D. mohleri.*

In *D. mohleri, D. nobilis* and *D. mediosus* the outer parts of the rays become free. In *D. nobilis* these parts are curved counter-clockwise in distal view, while they are radial in *D. mediosus.*

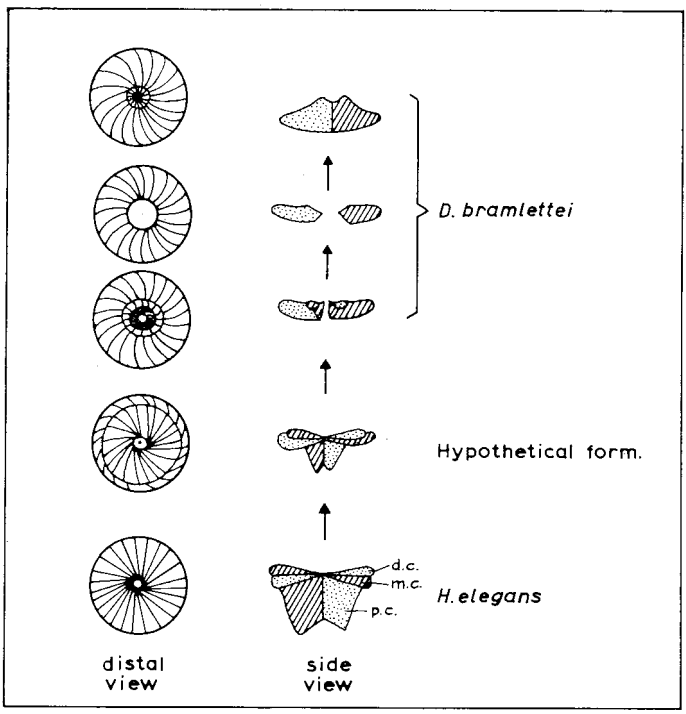

Fig. 43 The transition from *Heliolithus elegans* to *Discoaster bramlettei.*

D. falcatus and the closely related *D. splendidus* probably evolved from *D. nobilis.* These thin species have a short range in the *D. multiradiatus* Zone. The thin species in the other group of *Discoaster* occur in the same stratigraphic interval.

D. ornatus, which appears in the *T. contortus* Zone, differs from *D. mohleri* only in its narrow interradial incisions, but the origin of *D. ornatus* poses a problem. The species in considered to have evolved from *D. mohleri,* but no overlap in ranges was observed in our sections.

D. ornatus is thought to be ancestral to two other groups of *Discoaster* found in the Eocene, the *D. binodosus* group and the *D. deflandrei* group. In the former the arms show a terminal bifurcation with a sharp angle between

both tips, and each arm has at least one set of paired, lateral nodes.

In *D. binodosus,* which starts its range in the zone named after this species, the arms are relatively long and the nodes are situated close to the central disc or near the middle of the arms. In *D. gemmifer, D. cruciformis, D. mirus* and *D. distinctus,* which appear in the *T. orthostylus* Zone, the nodes have shifted to a more terminal position. They coalesced with the bifurcated tips of the arms in the first three species.

In the species belonging to the *D. deflandrei* group the arms also bifurcate, but the terminal angle is obtuse. The arms are not ornamented. *D. deflandrei,* the oldest species in this group, is thought to have evolved from *D. binodosus* in the course of the *D. binodosus* Zone. *D. deflandrei* is in turn considered to be ancestral to *D. colletii,* which appears in the *D. lodoensis* Zone. The rare *D. nonaradiatus* is probably closely related to *D. colletii.*

6.b. Lineages in *Discoaster* group 2 (species which show a regular extinction cross, fig. 44)

The ancestor of this group is *Heliolithus megastypus. D. multiradiatus,* the oldest species in the group, is seen to evolve from *H. megastypus* in the course of the upper part of the *D. mohleri* Zone. In this transition the changes in morphology are the same as those enumerated for the transition from *H. elegans* to *D. bramlettei*: reduction of the column, reduction of the distal cycle, increase in diameter of the median cycle, and rearrangement of these structures.

The variation in the early representatives of *D. multiradiatus* is comparable to the variation in the early forms of *D. bramlettei*; again there are variants with remnants of the distal cycle and of the column, and the centre may be open or closed. In the small *D. lenticularis,* which starts its range in the *D. multiradiatus* Zone, the distal cycle is retained in a reduced form.

The closely related thin species, *D. perpolithus* and *D. elegans,* evolved in the later part of the *D. multiradiatus* Zone from variants of *D. multiradiatus* with a proximal stem. This stem is formed by an enlargement of the central parts of the elements, in proximal direction; it is not homologous with the column in *Heliolithus.*

The Eocene descendants of *D. multiradiatus* can be divided into the *D. diastypus* group and the *D. barbadiensis* group.

The species in the former group show both a proximal and a distal cone (or stem). In the lineage *D. diastypus – D. pacificus – D. lodoensis – D. sublodoensis* the following trends have been observed: (a) a decrease in the number of rays (arms) from about 15 to 5 and, (b) a decrease in the diameter and height of the proximal and distal cones (stems).

The species in the *D. barbadiensis* group show only the proximal cone (or stem). In the lineage *D. barbadiensis* – *D. robustus* – *D. kuepperi* the maximum number of rays decreases from 18 to 12, and the diameter of the proximal side of the proximal stem (or cone) increases.

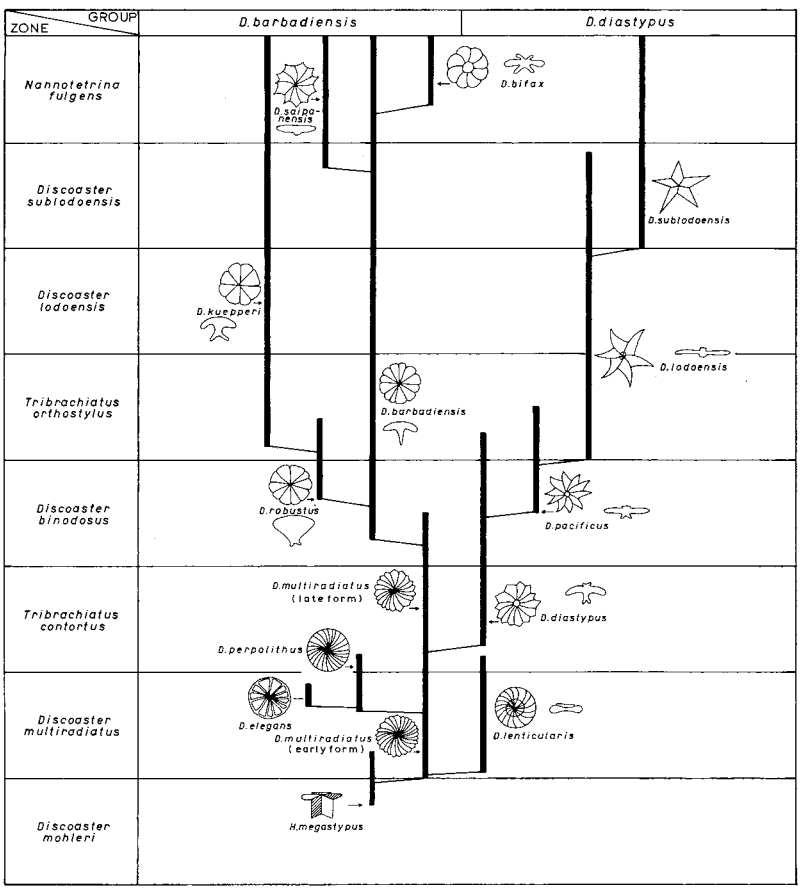

Fig. 44 Lineages in the genus *Discoaster* (Group 2, species with a regular extinction cross).

In the time equivalent of the *D. binodosus* Zone, *D. barbadiensis* is seen to evolve from late forms of *D. multiradiatus* with a proximal stem. This species is considered ancestral to *D. saipanensis* which appears in the *D. sublodoensis* Zone, and to *D. bifax* which enters the record in the *N. fulgens* Zone.

6.c. The morphocline in *D. multiradiatus*

The investigation of the assemblages with *D. multiradiatus* gave the impression that the number of rays in this species decreases in progressively younger assemblages, a change already suggested by Moshkovitz (1967). In order to test this hypothesis and to establish a possible relation with the diameter of the nannoliths, 30 specimens were measured and the number of rays counted in each of 8 samples from the Caravaca section and in 10 samples from Nahal Avdat. The numerical results are given in figures 45 and 46. From these figures the following, rough conclusions can be drawn: (a) the mean number of rays decreases in progressively younger assemblages, (b) the mean number of rays is generally more than 21 below the boundary between the *D. multiradiatus* and *T. contortus* Zones; less than 21 above

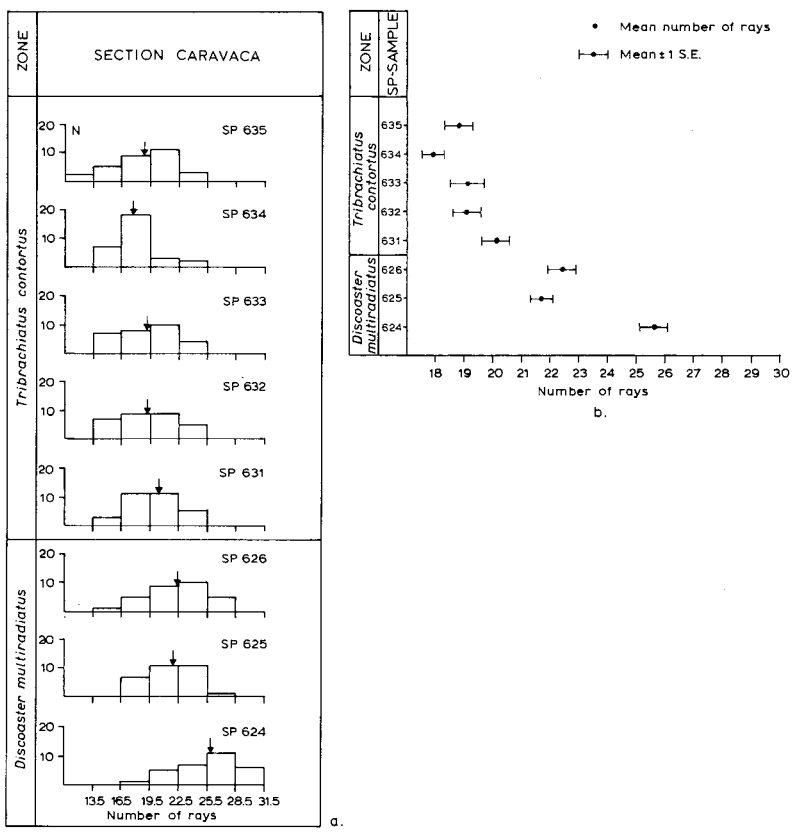

Fig. 45 The number of rays in assemblages (N = 30) of *Discoaster multiradiatus* in the *D. multiradiatus*- and *T. contortus* Zones in the Caravaca section. a. Histograms, b. Means.

this boundary. No positive or negative correlation could be shown between the number of rays and the diameter of the nannoliths. The diameter varies from 9 to 17 μ in the investigated samples.

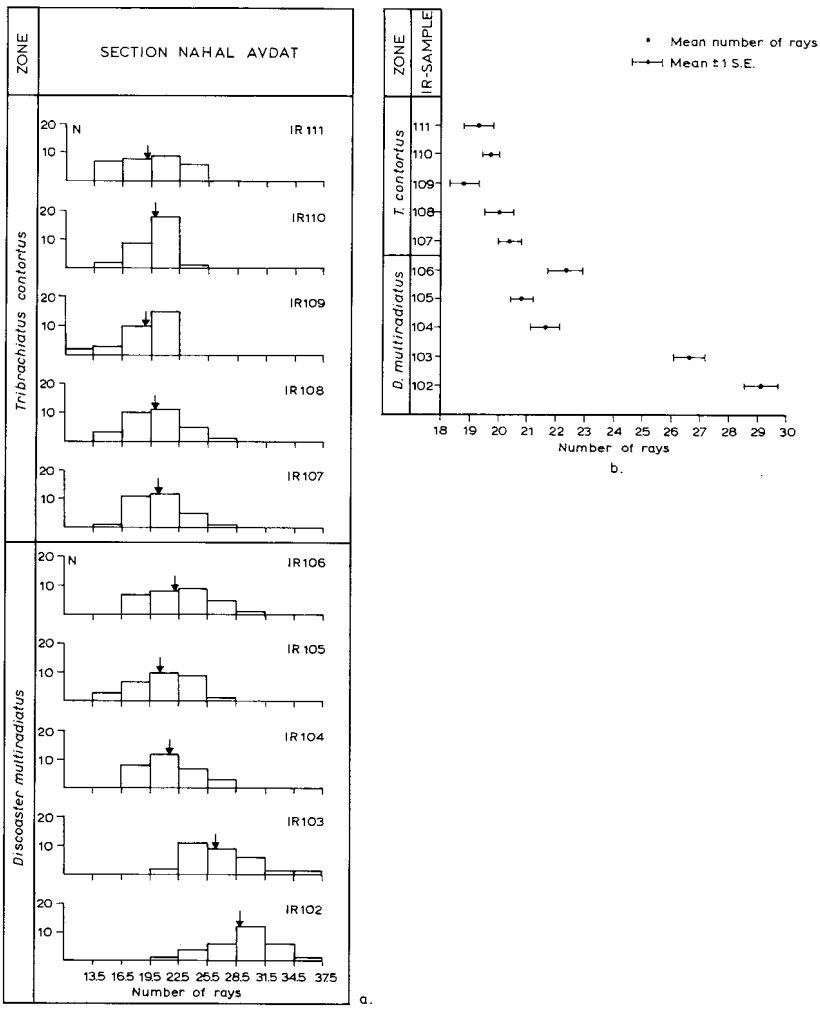

Fig. 46 The number of rays in assemblages (N = 30) of *Discoaster multiradiatus* in the *D. multiradiatus*- and *T. contortus* Zones in the Nahal Avdat section. a. Histograms, b. Means.

In addition two samples from the section near Pont Labau (S.W. France) were incorporated in this study. Hay and Mohler (1967) assigned both these samples (827 and 873) to the *D. multiradiatus* Zone. The mean number of rays is 23.2 in sample 827, and 17.9 in sample 837 (see fig. 47). As the last

figure is far below 21 this sample was suspected to belong to the *T. contortus* Zone. After a long search this assignment was confirmed by the discovery of two specimens of *T. nunnii,* which ranges from the lower boundary of the *T. contortus* Zone upwards.

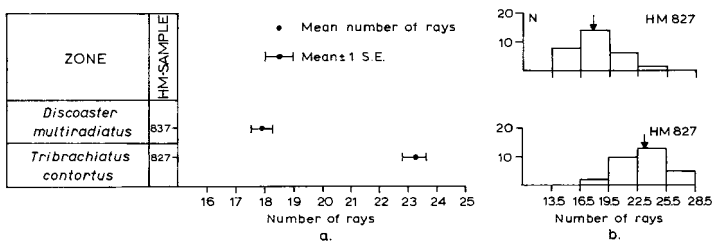

Fig. 47 The number of rays in two assemblages (N = 30) of *Discoaster multiradiatus* from the section at Pont Labau. a. Means, b. Histograms.

LINEAGES IN THE ZYGODISCACEAE (fig. 48)

7.a. Lineages in the genus *Zygodiscus*

Zygodiscus clausus nov. sp. is the first representative of the genus *Zygodiscus.* The species enters the record in the *D. mohleri* Zone. Early specimens show a closed central plate and a relatively wide bar. This bar makes a small angle in clockwise direction with the X-axis of the coccolith in distal view. In these early forms the bar is homogenous, and in the centre it can hardly be differentiated from the central plate. In somewhat later forms the bar is well differentiated and has rotated in a clockwise direction, in such a way that it makes a small angle in counter-clockwise direction with the Y-axis. The ultrastructure of the bar has also changed: the optical behaviour on one side of the axis differs from that on the other side.

Z. adamas is seen to evolve from late forms of *Z. clausus* in the course of the *D. mohleri* Zone. The most drastic change in this development is a torsion of both longitudinal halves of the bar, which results in a diamond-shaped, compact cross-structure in *Z. adamas.* Simultaneously with this process the central plate opens at each side of the central structure. In early specimens of *Z. adamas* the central cross is broad and the openings are small. In later forms the cross is narrower and the openings are larger. At the periphery the central plate bends in a distal direction to form a low margin.

Z. plectopons is seen to evolve from *Z. adamas* towards the end of the *D. mohleri* Zone. In *Z. plectopons* the openings at each side of the narrow,

central cross increase in size to such an extent that only a narrow strip of the central plate is left. The margin is considerably higher than in *Z. adamas*; it is also wider, probably because of the presence of a rim. The narrow, central cross-bar makes a small angle with the Y-axis in anti-clockwise direction in distal view. It is connected to the central plate along a V-shaped suture. In the early, smaller specimens the crossed ultra-structure of the bar-like, central cross is still recognizable in cross-polarized light; in later forms the central structure consists of two parallel laths, separated by a median suture.

Z. plectopons is thought to be ancestral to *Lophodolithus nascens.*

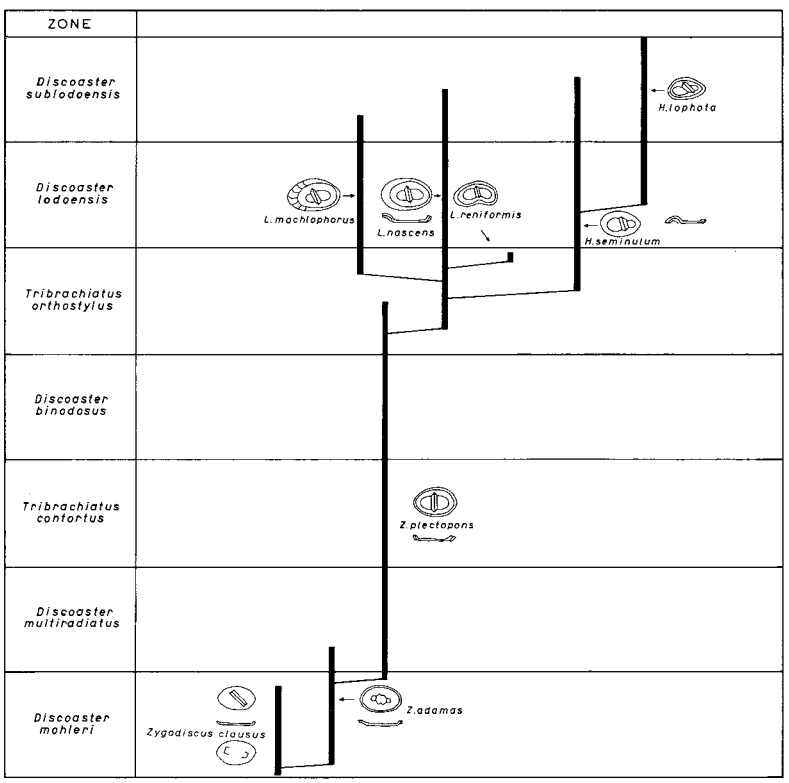

Fig. 48 Lineages in the family Zygodiscaceae.

7.b. Lineages in the genus *Lophodolithus*

In our opinion the following two structural changes took place in the development from *Z. plectopons* to *L. nascens* in the course of the *T. orthostylus* Zone: (a) an increase in the height of the margin at one pole, (b)

the formation of a flange, which is widest at the side where the margin is highest. *L. mochlophorus* and *L. reniformis* are connected with *L. nascens* in the *T. orthostylus* Zone; in the former species a crenulation of the flange developed, in the latter there was a change in the outline.

L. nascens is considered to be the ancestor of *Helicosphaera seminulum,* which makes its appearance in the upper part of the *T. orthostylus* Zone. The essential change in this development is a bend of the margin and of the flange in proximal direction. As a result of this curvature the wall becomes evenly concavo-convex, while the elements of the rim are orientated in a helicoidal way.

7.c. Lineages in the genus *Helicosphaera*

Only two species belonging to *Helicosphaera* occur in the investigated interval. *H. lophota* is seen to evolve from *H. seminulum* in the course of the *D. lodoensis* Zone by an anti-clockwise rotation of the central bar.

For later lineages in the genus, the reader is referred to Haq (1973b).

THE *MICULA – RHOMBOASTER – TRIBRACHIATUS* LINEAGE (fig. 49)

8.a. Introduction

In our opinion the frequent occurrence of species of the Cretaceous genus *Micula* in the Paleocene and Lower Eocene is not due to reworking. It it thought that at least *M. decussata* survived the massive extinction at the end of the Cretaceous.

Similarities in construction suggest that this species is ancestral to the genera *Rhomboaster* and *Nannotetrina.*

8.b. The *Micula-Rhomboaster* lineage

In the lower part of the *D. multiradiatus* Zone nannoliths were found with a rhombohedral outline. They consist of several calcite units. This *Rhomboaster intermedia* nov. sp. it considered transitional between *M. decussata* (which is cube-shaped and composed of at least 8 elements) and *Rhomboaster bitrifida* nov. sp. (which has the basic shape of a rhombohedron, and which is composed of a single calcite unit).

In *Rhomboaster intermedia* six of the twelve edges are thickened: the 3–2, 3–4 and 3–3a edges, and the 1a–1, 1a–2a and 1a–4a edges. *Rhomboaster bitrifida* originated from *R. intermedia* in the course of the *D. multiradiatus* Zone. This development included the following changes: (a)

fusion of the elements to a single, homogenous calcite unit, (b) depression of the faces and edges, and (c) "reduction" of the corners 3 and 1a, and "prolongation" of the other six corners.

In *R. calcitrapa,* which is seen to evolve from *R. bitrifida,* these six corners are elongated even further, so that spine-like protrusions are formed.

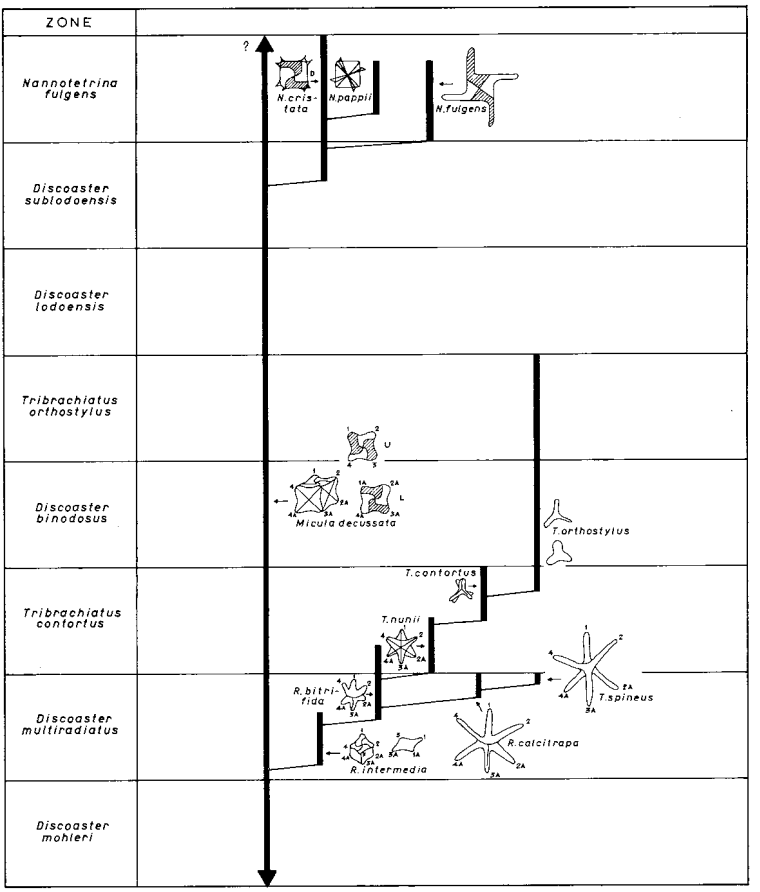

Fig. 49 The *Micula-Rhomboaster-Tribrachiatus* lineage and the *Micula-Nannotetrina* lineage.

8.c. The *Rhomboaster-Tribrachiatus* lineage

A basic change in construction occurred in the development of the genus *Tribrachiatus* from *Rhomboaster*: the two superposed, arrow-head-like structures in *Rhomboaster* are transformed into two superposed, triradiate structures in *Tribrachiatus.* The former corners 4, 2 and 3a form the upper triradiate structure, the corners 1, 2a and 4a the lower one.

The oldest species of *Tribrachiatus* is *T. spineus*, which probably evolved from *R. calcitrapa* in the later part of the *D. multiradiatus* Zone. *T. nunnii*, the index species for the lower boundary of the *T. contortus* Zone is thought to have evolved from *R. bitrifida*.

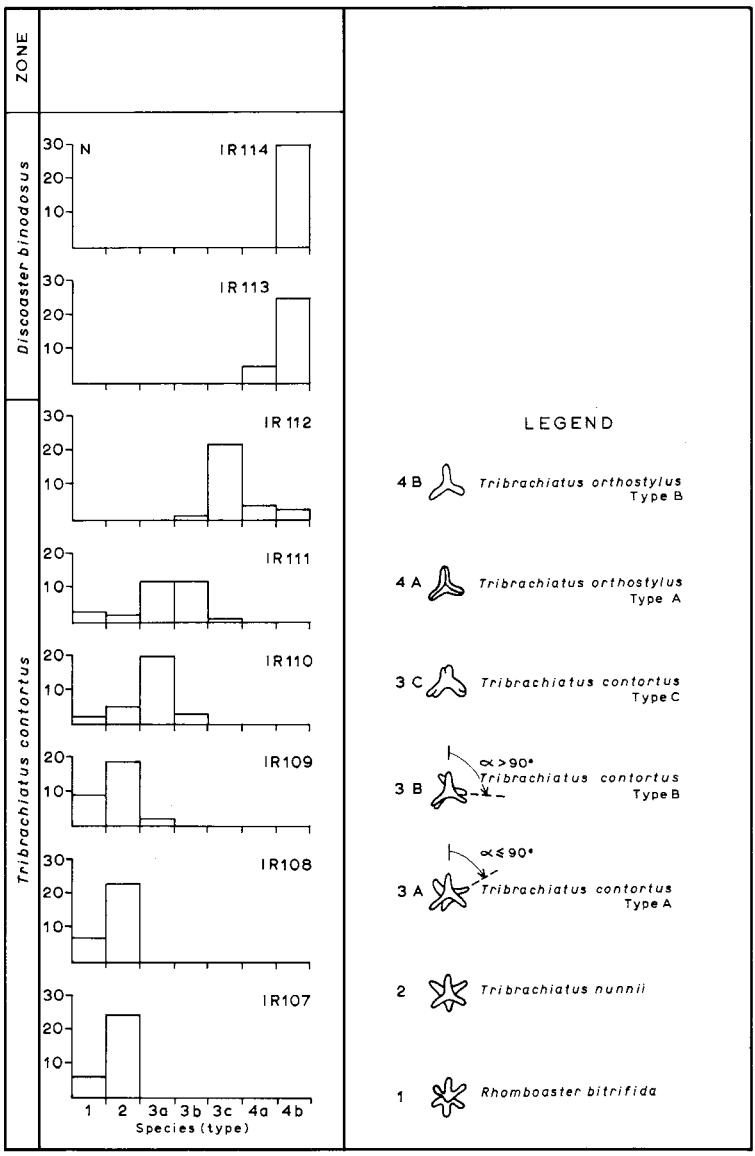

Fig. 50 Histograms (N = 30) showing the replacement in time of members of the *Rhomboaster — Tribrachiatus* lineage in the Nahal Avdat section.

8.d. The *Tribrachiatus* morphocline

In the *T. nunnii* – *T. contortus* – *T. orthostylus* morphocline the upper triradiate structure rotates with respect to the lower one; the total angle of rotation is 60°. The relative direction of this rotation can be deduced with the aid of the slightly curved ridges on the arms; if the upper structure is considered fixed, the rotation is clockwise. The upper and lower triradiate structures become fused in a late stage of the rotation.

The first specimens of *T. orthostylus* occur in the uppermost part of the *T. contortus* Zone. From the histograms of fig. 50 it can be concluded that the species in this morphocline gradually replace each other.

8.e. Origin of the genus *Nannotetrina* and relations in this genus (fig. 49)

The oldest species of *Nannotetrina* is *N. cristata*, which appears in the *D. sublodoensis* Zone. When a specimen of this species is looked at from the closed, smooth side, the sutures appear slightly curved counter-clockwise. In cross-polarized light, and with the gypsum plate, the second and fourth quadrants are blue, and the others are yellow. The only other species which shows a similar pattern of sutures and colours is *Micula decussata,* in proximal or distal view and at a low focus level. Because of this similarity *M. decussata* is considered to be ancestral to *Nannotetrina.*

N. cristata thus corresponds basically to one half of a specimen of *M. decussata*; arbitrarily the smooth, closed side is considered distal.

N. fulgens is seen to evolve from *N. cristata* by an increase in the length of the sides of the base in clockwise direction, so that spine-like projections are formed. In certain variants of this species the sides of the base are reduced, which results in four-rayed forms (= *Nannotetrina alata*).

N. pappii is observed to follow from *N. cristata* by a clockwise rotation of the bars and the sutures, in distal view. The species starts its range in the *N. fulgens* Zone.

Chapter VI

TAXONOMY

All species encountered in the investigated sections are discussed in this chapter. For most genera the form and orientation of the extinction cross as well as the colour distribution are given. The patterns are based on observations in a Leitz Orthoplan light microscope, which gives the real image (not the inverted one, as is the case in some other L.M. types). The position of the polarizers, and the orientation of the gypsum plate, as well as the position of the n_α and the n_γ in this plate are given in fig. 4.

All descriptions refer to a standard orientation of the fossils with respect to the polarization directions; unless otherwise stated these descriptions refer to the distal side of the specimens. As a rule the convex side of a coccolith is considered to be the distal side. The longer axis in elliptical coccoliths is called X-axis, the shorter, Y-axis. Most descriptive terms are taken over from Hay et al. (1966), Hay and Mohler (1967) and from the recommendations of the "Round Table on Calcareous Nannofossils" (Farinacci, 1971), but for several genera new descriptive terms are defined.

Calcareous nannofossils are here regarded as plant remains, and consequently the rules of the I.C.B.N. are followed. Use was made of the "Annotated Indexes and Bibliographies" of Loeblich and Tappan (1966–1973), and the "Catalogue of Calcareous Nannofossils" (Farinacci, 1969–1974). The families, genera and species are dealt with in time order for an easier review of the assumed lineages; an alphabetical index is given on page 180. All samples, holotypes and paratypoids are stored in the micropaleontological collection of the Utrecht State University.

Kingdom PLANTAE Linné, 1753

Division HAPTOPHYTA v. d. Hoek, 1978

Class HAPTOPHYCEAE Christensen, 1962

Ordo COCCOLITHOPHORALES Schiller, 1926

Family BRAARUDOSPHAERACEAE Deflandre, 1947

Remarks: Nannoliths composed of five elements and showing a five-fold symmetry belong to this family. The division in genera is based on characteristics of the outer margin of the elements.

Genus **Braarudosphaera** Deflandre, 1947

Type species: *Pontosphaera bigelowi* Deflandre, 1947
Remarks: This genus is restricted to nannoliths with five outward curving or trapezoidal elements.

Braarudosphaera bigelowii (Gran and Braarud) Deflandre

Pontosphaera bigelowi Gran and Braarud, 1935, p. 338, fig. 67.
Braarudosphaera bigelowi (Gran and Braarud) Deflandre, 1947, p. 439, textfigs. 1–5; Haq, 1971, p. 41, pl. 11, figs. 3, 4.
For further references see Haq, 1971a.

Remarks: The pentaliths of this well-known and easily identifiable species show a considerable variation in size. Complete pentagondodekahedrals were only found in the *B. sparsus* Zone in the Caravaca section.
Dimensions: diameter: 5–15 μ.
Distribution: Spain: *B. sparsus* Zone – *D. sublodoensis* Zone; Israel: *T. orthostylus* Zone – *D. sublodoensis* Zone; Scandinavia: *B. sparsus* Zone – *C. tenuis* Zone.

Braarudosphaera alta nov. sp.
(pl. 2, fig. 3; pl. 9, figs. 2, 3)

Braarudosphaera aff. *B. discula* Bramlette and Riedel, 1954, Romein, 1977, p. 269, pl. 1, figs. 2a-c.

Derivation of name: From altus (lat.), high.
Description: This species of *Braarudosphaera* has a high, slightly tapering, cylindrical body, composed of many parallel layers. Specimens show a rounded to circular outline in distal or proximal view, and a square to rectangular outline in side view.
Differential diagnosis: The species resembles *Braarudosphaera discula* Bramlette and Riedel in proximal or distal view, but the latter species consists of only one layer of elements. *Micrantholithus procerus* Bukry and Bramlette has a subelliptical outline in side view, and the elements show indentations. The species might be confused (in side views) with species of *Nannoconus*; these, however, show a helicoid arrangement of the elements.
Dimensions: height: 8–12 μ, diameter: 8–10 μ.
Holotype: T 360, pl. 2, fig. 3, sample SP566. *C. primus* Zone.
Type locality: Barranco del Gredero.
Stratum: Jorquera Formation Member B.
Age: Early Paleocene.
Paratypoids: T364a, b, pl. 9, figs. 2, 3, sample SP566.
Distribution: Spain: *B. sparsus* Zone, *C. primus* Zone.

Genus **Micrantholithus** Deflandre, 1954

Type species: *Micrantholithus flos* Deflandre, 1950

Micrantholithus attenuatus Bramlette and Sullivan

Micrantholithus attenuatus Bramlette and Sullivan, 1961, p. 154, pl. 8, figs. 8, 9–11.

Remarks: Only isolated, V-shaped elements of this species have been found.
Dimensions: length: 10–12 μ.
Distribution: Spain: *T. orthostylus* Zone – *D. sublodoensis* Zone.

Micrantholithus crenulatus Bramlette and Sullivan

Micrantholithus crenulatus Bramlette and Sullivan, 1961, p. 155, pl. 9, figs. 3, 4; Sullivan, 1964, p. 189, pl. 8, figs. 5–7; Sullivan, 1965, p. 39, pl. 8, fig. 6.

Remarks: This pentalith is composed of triangular elements with a crenulated outer margin. The Lower Cretaceous *Micrantholithus hoschulzii* (Reinhardt) Thierstein shows the same outline and composition, but this species has not been reported from the Upper Cretaceous and the Lower Tertiary so far.
Dimensions: diameter: 10–12 μ.
Distribution: Spain: *D. lodoensis* Zone – *N. fulgens* Zone; Israel *D. lodoensis* Zone – *D. sublodoensis* Zone.

Micrantholithus flos Deflandre

Micrantholithus flos Deflandre, 1950, p. 1157, textfigs. 8–11; Deflandre and Fert, 1954, p. 166, pl. 13, figs. 10, 11; textfigs. 113, 114; Bramlette and Sullivan, 1961, p. 155, pl. 9, fig. 8.

Remarks: The triangular elements of this pentalith are concave marginally, and their sides are thickened.
Dimensions: diameter 12–13 μ.
Distribution: Spain: *T. orthostylus* Zone – *D. sublodoensis* Zone.

Family BISCUTACEAE Black, 1971

Genus **Biscutum** Black, 1959

Type species: *Biscutum testudinarium* Black, 1959
Remarks: Black defined this genus as a group of imperforate coccoliths composed of more than one layer of elements, which are closely appressed. We now know too that the species are elliptical, that the elements at the

poles of the ellipse (both in the distal and in the proximal shield) are larger than the other elements, and that the extinction lines in the wall are dextrogyre.

Biscutum castrorum Black
(pl. 1, figs. 2, 3)

Biscutum castrorum Black, 1959, p. 326, pl. 10, fig. 2; Perch-Nielsen, 1968, p. 79, text-fig. 40; pl. 28, figs. 1–5.
Coccolithus sp. B Edwards, 1967, pl. 1, figs. 10, 13.
Biscutum aff. *B. castrorum* Black, Perch-Nielsen, 1969b, p. 57, pl. 3, fig. 1.
Conococcolithus panis Edwards, 1973, p. 73, figs. 2–21.

Remarks: The shields of this long-elliptical species are composed of 18–27 elements. The elements of the distal shield slope outwards for most of their length; near the central area they slope inwards. The sutures are subradial. The elements of the proximal shield extend into and close the proximal central area. Distally, this area is filled in with a single cycle of centrally sloping, triangular elements.

B. castrorum differs from *Biscutum constants* (Gorka) Black, 1959 not only in its larger size and in the higher number of elements, but also in the different construction of the proximal central area: in *B. constans* the proximal parts of the elements in the distal central area cycle extend into the proximal central area (see Noël, 1970, pl. 33, figs. 1–10).
Dimensions: length: 5–7 μ.
Distribution: Israel: *B. sparsus* Zone, *C. primus* Zone; Scandinavia: *B. sparsus* Zone – *E. macellus* Zone.

Biscutum parvulum nov. sp.
(pl. 1, fig. 10; pl. 2, figs. 1, 2)

Biscutum sp. Romein, 1977, p. 270, pl. 1, figs. 4a, b.

Derivation of name: From parvulus (lat.), small.
Description: The distal shield of this very small, elliptical coccolith is composed of about 16 elements, separated by subradial, sometimes notched sutures. The central area is closed by two rows of triangular elements, one on each side of the longer axis of the ellipse. Each row consists of about eight elements, sloping down to this axis. The spherical coccospheres are composed of about 16 coccoliths. Unfortunately, our attempts to obtain good photographs of the proximal side failed.
Differential diagnosis: *B. constans* (Gorka) is larger than *B. parvulum* (5–7 μ) and has ovoid coccospheres. *B. castrorum* shows a higher number of elements (18–27).

Dimensions: length of coccolith: 2–3 μ; diameter of sphere: 5 μ.
Holotype: T 359a, pl. 2, fig. 1, sample SP566, *C. primus* Zone.
Type locality: Barranco del Gredero.
Stratum: Jorquera Formation, Member B.
Age: Early Paleocene.
Paratypoid: T 359b, pl. 2, fig. 2, from sample SP566.
Distribution: Spain: *B. sparsus* Zone, *C. primus* Zone; Israel: *B. sparsus* Zone, *C. primus* Zone.

Family ELLIPSAGELOSPHAERACEAE Noël, 1965

Genus **Cyclagelosphaera** Noël, 1965

Type species: *Cyclagelosphaera margereli* Noël, 1965
Remarks: This genus includes circular coccoliths, which are composed of a distal shield with anti-clockwise oblique sutures, a monocyclic proximal shield the elements of which almost reach the centre, and a central area which is closed distally by one or two cycles of elements.

Cyclagelosphaera reinhardtii (Perch-Nielsen) Romein, 1977

Tergestiella barnesae (Black) Reinhardt, 1966, partim, p. 15, pl. 1, figs. 2a, b; pl. 12, fig. 2; pl. 23, fig. 6; text-figs. 2a, b, c; non pl. 2, figs. 1a, b.
Markalius reinhardtii Perch-Nielsen, 1968, p. 76, pl. 23, figs. 6–8; text-fig. 38; Perch-Nielsen, 1969b, p. 63, pl. 3, figs. 2–4; pl. 7, figs. 13, 14.
Cyclagelosphaera reinhardtii (Perch-Nielsen) Romein, 1977, p. 274.

Remarks: In distal view and between crossed nicols, the central area shows strongly dextrogyre extinction lines; on the shields these lines widen to radial, dark zones. The species can easily be differentiated from *Markalius astroporus* (Stradner): in cross-polarized light the shields of *C. reinhardtii* are bright, while they are faintly illuminated in *M. astroporus*; when the gypsum plate is inserted, the blue and yellow zones in the shields in *C. reinhardtii* continue in the central area, while they alternate in *M. astroporus*.
Dimensions: diameter: 5–8 μ.
Distribution: Spain: *B. sparsus* Zone – *D. multiradiatus* Zone; Israel: *B. sparsus* Zone – *E. macellus* Zone; Scandinavia: *B. sparsus* Zone – *E. macellus* Zone.

Genus **Markalius** Bramlette and Martini, 1964

Type species: *Cyclococcolithus leptoporus* Murray and Blackman var. *inversus* Deflandre and Fert, 1954.

Remarks: Bramlette and Martini introduced this genus for circular coccoliths composed of two closely appressed, monocyclic shields and a central "plug" of elements; the sutures of the distal shield should be strongly oblique clockwise in distal view. Perch-Nielsen (1965) emended the genus in such a way that two more species could be included in the otherwise monotypic genus (*M. reinhardtii* and *M. circumradiatus*). These species, however, show anticlockwise oblique sutures in distal view, and a high, central cycle of elements, which is typical for species of *Cyclagelosphaera*.

Markalius astroporus (Stradner) Hay and Mohler (pl. 1, fig. 7)

Cyclococcolithus astroporus Stradner, in Gohrbandt, 1963, p. 75, pl. 9, figs. 5–7; text-figs. 2a, b, 3.
Markalius inversus (Deflandre) Bramlette and Martini, 1964, partim, p. 302, pl. 2, figs. 4–9, non pl. 7, fig. 2a; Martini, 1964, p. 49, pl. 6, figs. 9, 10; Perch-Nielsen, 1968, p. 72, pl. 24, figs. 1–8; pl. 25, fig. 1; text-fig. 35.
Markalius astroporus (Stradner) Hay and Mohler, 1967, p. 1528, pl. 196, figs. 32–35; pl. 198, figs. 2, 6; Shafik and Stradner, 1971, p. 84, pl. 3, figs. 3, 4.
Markalius nielsenae Shumenko, 1976, p. 28, pl. 5, figs. 5, 6.

Remarks: Specimens show variation not only in the number of elements (18–36), but also in the size and the shape of the central area. The ratio between the total diameter and the diameter of the central area varies from 4 to 2; the area may be open or closed.

M. astroporus and *M. nielsenae* are placed in synonomy because the discriminatory feature (the presence of one cycle or two cycles in the central area) is beyond the resolution power of the L.M.

In distal view and in cross-polarized light, the central area shows strongly dextrogyre extinction lines. These become vague in the distal shield where they bend in the opposite direction. In the same view but at a lower focus, the proximal shield shows a vague, dextrogyre extinction figure.
Dimensions: diameter: 5–9 μ.
Distribution: Spain: *B. sparsus* Zone – *D. mohleri* Zone; Israel: *B. sparsus* Zone – *C. tenuis* Zone; Scandinavia: *B. sparsus* Zone – *E. macellus* Zone.

Genus **Cruciplacolithus** Hay and Mohler, 1967

Type species: *Heliorthus tenuis* Stradner, 1961
Synonym: *Campylosphaera*
Description:

Shape: The species in this genus are (sub)elliptical in plane view and concavo-convex in side view.

Construction: The species are constructed with a wide or narrow, com-

posite margin, surrounding a central area which is bridged by a central cross-structure parallel, or almost parallel to the axes of the ellipse.

Margin: The margin is composed of three cycles of elements: an inward sloping wall, surrounded by an outward sloping, composite distal shield, which lies upon a proximal shield, which also slopes outwards.

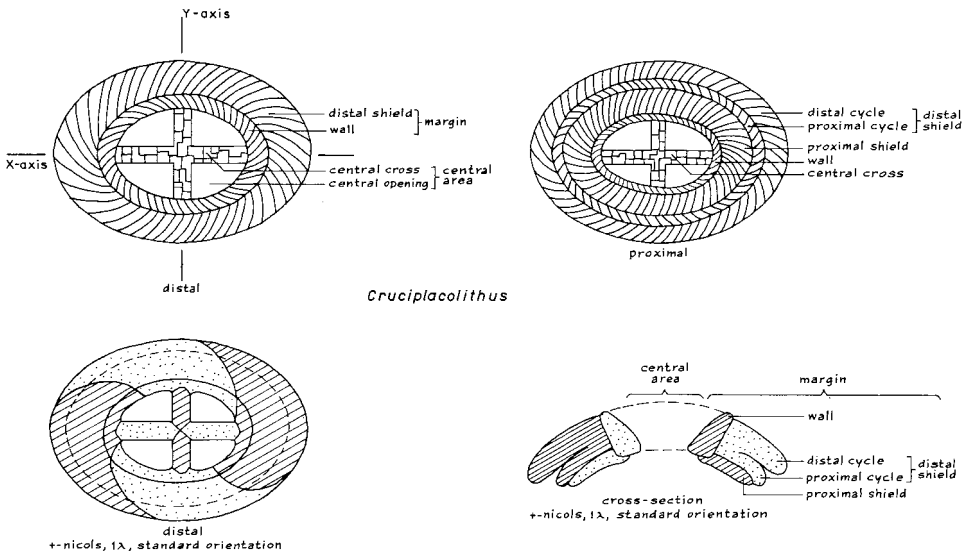

Wall: In distal view this cycle shows anti-clockwise imbricating elements, separated by anti-clockwise oblique sutures. In proximal view, the outer strip of the wall is covered by the inner strip of the proximal shield. The inner strip of the wall shows anti-clockwise oblique sutures in this view.

Distal shield: This shield is composed of a distal cycle and a narrower proximal cycle. These cycles are free-standing over most of their width, but they fuse near the wall. The proximal cycle is closely appressed with the proximal shield.

In distal view the distal cycle shows clockwise imbricating elements, separated by clockwise oblique sutures.

In proximal view the elements of the proximal cycle show anti-clockwise imbrication and anti-clockwise oblique sutures in the strip which is not covered by the proximal shield.

Proximal shield: This shield is somewhat narrower than the proximal cycle of the distal shield. In proximal view it shows clockwise imbricating elements, separated by clockwise oblique sutures.

Central structure: This structure has the form of a cross. The four bars

are generally straight, normal to and bisecting each other. The cross is attached to the lower distal side of the wall. It is composed of calcite plates stacked one on top of the other. The bars in the direction of the X-axis are called the X_1-bars, those in the direction of the Y-axis the Y_1-bars.

Specific criteria: The species are based on (a) the degree of vaulting of the coccolith, and (b) the form and orientation of the central cross.

Standard orientations:

Distal view: Convex side upwards; X-axis of the coccolith parallel to the X-cross-hair.

Side view: X-axis of the coccolith parallel to the X-cross-hair; convex side of the coccolith pointing to the positive direction of the Y-cross-hair.

Extinction lines: These lines are sharpest in the wall and in the proximal shield, and they are vague in the distal shield. The lines are laevogyre in distal view. In the standard orientation for distal view, imaginary lines connecting the extinction lines in opposite quadrants in the wall form an angle of about 20° with the Y-axis and of a few degrees with the X-axis, both in anti-clockwise direction.

Colour distribution: In the standard orientation for distal view the sectors enclosed by the extinction lines in the margin, along the X-axis, are blue, the others yellow. In the same orientation the Y_1-bars are blue, the others yellow.

In the standard orientation for side view the left cross-section of the distal shield and the right cross-sections of the wall and the proximal shield are blue; the other sections are yellow.

Differential diagnosis: In the closely related genus *Chiasmolithus,* the wall lies in a more distal position with respect to the distal shield than in *Cruciplacolithus.* In our opinion the position of this cycle is a better diagnostic feature than the position of the central cross. The construction of the margin in *Ericsonia* is basically the same as in *Cruciplacolithus,* but in the former genus the central area is open.

Cruciplacolithus primus Perch-Nielsen s.l.

Coccolithus helis Stradner. Bramlette and Martini, 1964, partim, p. 298, pl. 1, figs. 10–12, non pl. 7, figs. 5, 6; Martini, 1964, p. 48, pl. 6, figs. 5, 6; Moshkovitz, 1967, p. 148, pl. 2, fig. 1; pl. 5, fig. 11.

Non *Coccolithus helis* Stradner, in Gohrbandt, 1963, p. 74, pl. 8, fig. 16; pl. 9, figs. 1, 2; Edwards, 1966, text-figs. 9, 12; Radomski, 1968, p. 600, pl. 45, figs. 17, 18.

Cruciplacolithus primus Perch-Nielsen, 1977, p. 746, pl. 17, figs. 7, 8; pl. 50, figs. 11, 12.

Cruciplacolithus aff. *C. tenuis* (Stradner) Hay and Mohler, Romein, 1977, p. 271, pl. 1, fig. 6.

Remarks: Perch-Nielsen introduced this name for small forms of *Cruciplaco-*

lithus, which have a simple cross-structure without feet, which is orientated along the axes of the ellipse. The name is used here in a wider sense to include forms which share the characteristics of the cross-structure but which have larger dimensions. The number of elements in the margin varies from 25 to 66.
Dimensions: length: 3–10 μ.
Distribution: Spain: *C. primus* Zone – *E. macellus* Zone; Israel: *C. primus* Zone – *E. macellus* Zone; Scandinavia: *C. primus* Zone, *C. tenuis* Zone.

Cruciplacolithus edwardsii nov. sp.
(pl. 2, figs. 7, 8; pl. 9, figs. 9, 10)

Coccolithus helis Stradner, Edwards, 1966, text-fig. 9, 12.
Chiasmolithus helis (Stradner) Locker, 1968, pl. 1, figs. 3, 4.
Cruciplacolithus tenuis (Stradner) Hay and Mohler, Roth, 1973, pl. 13, fig. 2; pl. 17, fig. 1.

Description: This species of *Cruciplacolithus* is characterized by a central cross, the bars of which make an angle in clockwise direction with the axes of the ellipse in distal view. The angles XX_1 and YY_1 are generally smaller in earlier forms of this species than in later ones (see chapter IV). The number of elements in the margin is about 60.
Remarks: In a strict sense these forms should be assigned to the genus *Chiasmolithus*. Here they are placed in *Cruciplacolithus* since especially the earlier forms still have a typical *Cruciplacolithus*-like margin.
Differential diagnosis: The species differs from *Chiasmolithus consuetus* in having longer bars, which are not normal to each other, and from *Chiasmolithus danicus* in having non-curved, more slender bars.
Dimensions: length: 6–10 μ.
Holotype: T361, pl. 2, fig. 7, from sample SP590, *P. dimorphosus* Zone.
Type locality: Barranco del Gredero.
Stratum: Jorquera Formation, Member B.
Age: Early Paleocene.
Paratypoids: T 362, pl. 2, fig. 8; T 366a, b, pl. 9, figs. 9, 10, sample SP590.
Distribution: Spain: *C. primus* Zone – *C. tenuis* Zone; Israel: *C. primus* Zone – *C. tenuis* Zone; Scandinavia: *C. primus* Zone – *C. tenuis* Zone.

Cruciplacolithus tenuis (Stradner) Hay and Mohler

Heliorthus tenuis Stradner, 1961, p. 84, text-figs. 64, 65.
Coccolithus helis Stradner, in Gohrbandt, 1963, p. 74, pl. 8, fig. 16; pl. 9, figs. 1, 2 (all proximal views and not distal ones as indicated by Gartner, or mirror images).
Cruciplacolithus tenuis (Stradner) Hay and Mohler, 1967; Hay and Mohler, 1967, p. 1527, pl. 196, figs. 29–31 (proximal views and not distal ones as indicated by Hay and Mohler, or mirror images);

pl. 198, figs. 1, 17; Perch-Nielsen, 1972, pl. 4; Haq and Lohmann, 1976, pl. 3, figs. 3, 4.
Cruciplacolithus notus Perch-Nielsen, 1977, p. 746, pl. 17, fig. 4; pl. 50, fig. 2.

Remarks: As in *C. primus*, the bars of the central cross are aligned with the major axes of the ellipse. In *C. tenuis,* however, the tips of the bars show triangular protrusions (feet). These feet always point anti-clockwise in distal view. In the standard orientation for distal view the optical behaviour of a foot is opposite to that of the adjacent bar.

Our investigation of the holotype of *H. tenuis* from Haidhof (kindly provided by Dr. Stradner) revealed that this specimen has feet. However, in his drawing of the holotype Stradner did not indicate their presence.
Dimensions: length: 7–14 μ.
Distribution: Spain: *C. tenuis* Zone – *D. mohleri* Zone; Israel: *C. tenuis* Zone – *D. multiradiatus* Zone; Scandinavia: *C. tenuis* Zone, *E. macellus* Zone.

Cruciplacolithus latipons nov. sp.
(pl. 9, figs. 7, 8)

Derivation of name: from latus (lat.), broad, and pons (lat.), bridge.
Description: The relatively wide margin of this rather flat species is composed of about 40 elements. The wall is narrow with respect to the distal shield. The small central opening is almost closed by the central cross structure, which is aligned with the major axes of the ellipse.

In cross-polarized light, the shields and the cross structure show a low birefringence, but the wall is bright. The bars show small black dots (which probably indicates the presence of pores) and a vague median extinction line.
Differential diagnosis: The species differs from *C. primus* in the wider bars, and from *C. tenuis* in the absence of feet. *C. eodelus* has more slender bars, and shows a stronger distal vaulting.
Dimensions: length: 5–8 μ.
Holotype: T 365a, pl. 9, fig. 7, from sample SP614, *F. tympaniformis* Zone.
Type locality: Barrenco del Gredero.
Stratum: Jorquera Formation, Member C.
Age: Middle Paleocene.
Paratypoid: T 365b, pl. 9, fig. 8, sample SP614.
Distribution: Spain: *E. macellus* Zone – *D. multiradiatus* Zone; Israel: *E. macellus* Zone.

Cruciplacolithus frequens (Perch-Nielsen) nov. comb.
(pl. 9, fig. 6)

Chiasmolithus frequens Perch-Nielsen, 1977, p. 746, pl. 18, figs. 2, 4; pl. 19, figs. 1, 3, 5; pl. 50, fig. 5, 6.

Remarks: The bars of the central cross have feet, which point counter-clockwise in distal view, as in *C. tenuis*. The species differ in the orientation of the cross: in *C. frequens* it makes an angle of up to 15° with the axes of the ellipse in anti-clockwise direction in distal view.

The number of elements in the margin varies from 50 to 66. The coccoliths are assigned to the genus *Cruciplacolithus* because of the *Cruciplacolithus*-like construction of the margin.
Dimensions: length: 12–14 μ.
Distribution: Spain: *D. mohleri* Zone – *D. multiradiatus* Zone; Israel: *D. multiradiatus* Zone.

Cruciplacolithus eodelus (Bukry and Percival) nov. comb.

Campylosphaera eodela Bukry and Percival, 1971, p. 125, pl. 1, figs. 1–4.

Remarks: This species differs from *C. delus* (Bramlette and Sullivan) nov. comb. in the lower number of elements in the margin, in its smaller size and in its more elliptical outline. Transitional forms between both species occur frequently in the *T. contortus* Zone.
Dimensions: length: 6–10 μ.
Distribution: Spain: *D. multiradiatus* Zone – *T. contortus* Zone; Israel: *T. contortus* Zone.

Cruciplacolithus cribellus (Bramlette and Sullivan) nov. comb.

Coccolithites cribellum Bramlette and Sullivan, 1961, p. 151, pl. 7, figs. 5, 6.
Coccolithus cribellum (Bramlette and Sullivan) Sullivan, 1964, p. 181, pl. 3, fig. 5; Sullivan, 1965, p. 31, pl. 3, figs. 1–4; Stradner, 1969, p. 412, pl. 85, figs. 5–8.
Ericsonia cf. *E. cribella* (Bramlette and Sullivan) Perch-Nielsen, 1972, p. 1020, pl. 4, fig. 6.

Remarks: The margin of this species is composed of 27 to 45 elements. The central area is closed by a perforated plate, consisting of four sub-plates joined along the diagonals. The circular pores (6–18) are arranged in such a way that "bridges" are formed along the main axes of the ellipse. The number of pores is lower, and the diameter of the central area is smaller in earlier forms than in later ones. In most specimens, however, the pores are obscured by overgrowth.

In the standard orientation for distal view, and with the gypsum plate, a

sector shaped like an egg-timer along the X-axis, bordered by the diagonals and the wall, is blue, the other sectors in the central area are yellow.

C. cribellus might be a junior synonym of *Discolithus fenestratus* Deflandre and Fert, 1954; in our opinion, however, the T.E.M. micrograph of the holotype of the latter species is of too bad a quality to place the species in synonomy.

Dimensions: length: 6–14 μ.

Distribution: Spain: *D. multiradiatus* Zone – *N. fulgens* Zone; Israel: *D. binodosus* Zone – *D. sublodoensis* Zone.

Cruciplacolithus delus (Bramlette and Sullivan) Perch-Nielsen

Coccolithus delus Bramlette and Sullivan, 1961, p. 151, pl. 7, figs. 1, 2; Sullivan, 1964, p. 180, pl. 1, figs. 8, 9.

Cyathosphaera crux (Deflandre) Hay and Towe, 1961, p. 507, pl. 2, fig. 1.

Coccolithus delus (Bramlette and Sullivan) Perch-Nielsen, 1967, p. 22, pl. 1, figs. 1–3.

Campylosphaera dela (Bramlette and Sullivan) Hay and Mohler, 1967, p. 1531, pl. 198, fig. 14; Stradner, 1969, p. 414, pl. 85, figs. 1–4.

Cruciplacolithus delus (Bramlette and Sullivan) Perch-Nielsen, 1971d, p. 22, pl. 13, figs. 7, 8; Perch-Nielsen, 1972, pl. 4, fig. 2; Haq and Lohmann, 1976, pl. 9, fig. 3.

Remarks: This species is easily distinguished from others in the genus by its subquadrangular outline, and strong distal vaulting. The margin is composed of 50–70 elements. The slender bars are normal to each other and make a small angle with the axes of the ellipse in clockwise direction in distal view.

The extinction lines in the wall show an irregular pattern, probably because of the steepness of the wall. With the gypsum plate, the second and fourth quadrants of the wall, and the Y_1-bars are blue.

Dimensions: length: 8–12 μ.

Distribution: Spain: *T. contortus* Zone – *N. fulgens* Zone; Israel: *T. contortus* Zone – *D. sublodoensis* Zone.

Genus **Ericsonia** Black, 1964

Type species: *Ericsonia occidentalis* Black 1964

Introduction

In 1964 Black introduced the genus *Ericsonia* for "circular or elliptical coccoliths with a well-defined central opening, surrounded by three or more apparently concentric rings of granules, which are differently orientated in adjacent rings". The holotype of the type species was depicted in proximal view, and probably the generic definition refers only to the proximal side. The holotype, a tracing of which is given above, shows the following three cycles: 1. an outer cycle with subradial sutures, 2. a median cycle with

counter-clockwise oblique sutures; the elements imbricate anti-clockwise, 3. an inner cycle showing clockwise imbricating elements, separated by clockwise oblique sutures.

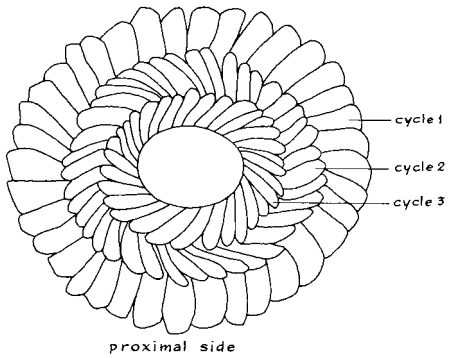

Tracing of *E. occidentalis* Black

It is assumed here that cycle 1 represents the proximal side of the distal shield. As for the other cycles two possibilities exist: (a). cycle 2 represents the proximal shield, and cycle 3 the proximal side of the wall, or (b). cycle 2 represents the (rather wide) proximal cycle of the distal shield, and cycle 3 the proximal shield. In this case the wall should have disappeared. The latter interpretation seems to be the most likely one, as the other species assigned to *Ericsonia* by Black (*E. alternans, E. ovalis*) show four cycles, the innermost one of which is the proximal side of the wall. If this interpretation is true, *Ericsonia* differs from *Coccolithus* by the presence of a well differentiated proximal cycle of the distal shield, which projects beyond the proximal shield.

Strictly speaking, *Ericsonia* is a junior synonym of *Coccolithus*. The type species *C. pelagicus* (lectotype, designated by Braarud et al., 1964) shows three cycles in proximal view: distal shield, proximal shield and wall. It seems justifiable, however, to retain the name *Ericsonia* for a group of Paleocene and Eocene coccoliths, which have a well differentiated proximal cycle of the distal shield.

In addition, we prefer to avoid the "loaded" name *Coccolithus* Schwarz, 1894, of which the type species *C. oceanicus* Schwarz, 1894 was proposed "for all the forms hitherto described, recent and fossil, and for which the clays from the Lias of the Dorset coast were designated as the type locality (Braarud et al., 1964)".

Description:

Shape: The species in this genus are subelliptical or circular in plan view and concavo-convex in side view.

Construction: The species are composed of a wide or narrow, high or low, composite margin, surrounding an open central area. The margin shows basically the same construction as in *Cruciplacolithus*.
Specific criteria: The species are based on the outline of the coccolith and on the relative position, form and height of the wall.
Standard orientations: See under *Cruciplacolithus*.
Extinction lines: In elliptical species the extinction pattern is the same as in *Cruciplacolithus*. In circular species imaginary lines connecting the gyres in opposite quadrants make an angle of about 20° with the polarization directions, anti-clockwise in distal view.
Colour patterns: In elliptical species the colour pattern is the same as in *Cruciplacolithus*. In circular species the second and the fourth quadrants are blue, the other two are yellow.
Differential diagnosis: The difference between *Ericsonia* and *Coccolithus* was already indicated in the introduction. The genus differs from *Cruciplacolithus* and *Chiasmolithus* in the open central area.

Ericsonia cava (Hay and Mohler) Perch-Nielsen
(pl. 2, fig. 4, 5)

Coccolithus sp. *Martini*, 1964, p. 49, pl. 6, figs. 7, 8; pl. 7, figs. 9, 10.
Coccolithus cavus Hay and Mohler, 1967, p. 1524, pl. 196, figs. 1–3; pl. 197, figs. 5, 7, 10, 12; Perch-Nielsen, 1969a, p. 322, pl. 33, figs. 3–6; Roth, 1973, p. 729, pl. 14, figs. 1, 2, 4, 5.
Ericsonia cava (Hay and Mohler) Perch-Nielsen, 1969b, p. 61, pl. 2, figs. 7, 8.

Remarks: The wall and the shields of this elliptical to subcircular species are composed of 30 to 46 elements. Distally, the wall overlaps the inner strip of the distal shield.
E. cava can be distinguished from *E. eopelagica* by its steeper distal shield, the overlap of the wall on the distal shield, and by its smaller size.
Dimensions: length: 3–7 μ.
Distribution: Spain: *C. primus* Zone – *E. macellus* Zone; Israel: *P. dimorphosus* Zone – *C. tenuis* Zone; Scandinavia: *C. tenuis* Zone – *E. macellus* Zone.

Ericsonia subpertusa Hay and Mohler
(pl. 2, fig. 6)

Markalius inversus (Deflandre) Bramlette and Martini, 1964, partim, p. 302, pl. 7, figs. 2a, b, non pl. 2, figs. 4–9.
Ericsonia subpertusa Hay and Mohler, 1967, p. 1531, pl. 198, figs. 11, 15, 18; pl. 199, figs. 1–3; Roth, 1973, p. 730, pl. 12, fig. 5; Haq and Lohmann, 1976, pl. 1, figs. 7, 8; Perch-Nielsen, 1977, pl. 16, fig. 3.

Ericsonia aff. *E. subpertusa* Hay and Mohler, Perch-Nielsen, 1969a, partim, p. 325, text-fig. 4, non text-fig. 3.
Ericsonia? subpertusa Hay and Mohler, Perch-Nielsen, 1969b, p. 62, pl. 2, figs. 1, 2.

Remarks: The number of elements in the margin of this species varies from 36 to 50. The distal shield shows a steep outward slope. The inner, distal side of this shield is covered by the elements of the gently inward sloping wall. This wall is composed of strongly clockwise imbricating, plate-like elements. The sutures are oblique clockwise near the centre, and bend in the opposite direction at about half their length. The opposite direction of the sutures in the wall and the distal shield produce a characteristic herringbone pattern in the L.M.

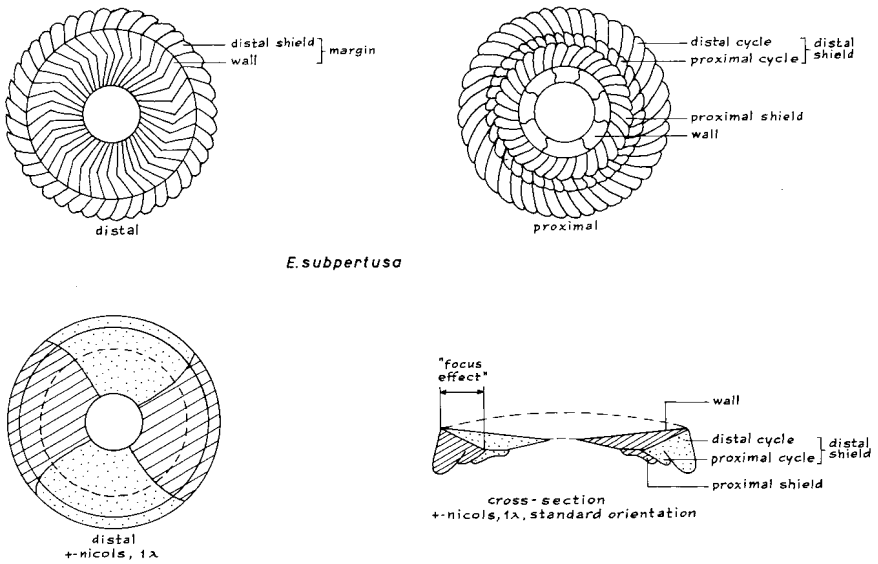

Another typical feature of the species is the "focus effect" in cross-polarized light. As in all other species in the genus, the wall and the proximal shield are bright. When the species is observed from the distal side, and if the focus is raised, the outer margin of the bright zone does not remain in the same place as in all other species of *Ericsonia,* but shifts outwards. This is a reflection of the fact that the outer margin of the wall projects beyond that of the proximal shield.
Dimensions: diameter: 4–9 μ.
Distribution: Spain: *C. tenuis* Zone – *D. multiradiatus* Zone; Israel: *C. tenuis* Zone – *T. contortus* Zone; Scandinavia: *C. tenuis* Zone, *E. macellus* Zone.

Ericsonia eopelagica (Bramlette and Riedel) nov. comb.

Tremalithus eopelagicus Bramlette and Riedel, 1954, p. 392, pl. 38, figs. 2a, b.
Coccolithus eopelagicus (Bramlette and Riedel) Bramlette and Sullivan, 1961, p. 141; Hay, Mohler and Wade, 1966, p. 385, pl. 1, fig. 1; Haq and Lohmann, 1976, pl. 8, figs. 10–12; pl. 13, figs. 3, 4.
Coccolithus crassus Bramlette and Sullivan, 1961, p. 139, pl. 1, figs. 4a-d; Sullivan, 1964, p. 180, pl. 3, figs. 4a, b.
Coccolithus sarsiae Black, 1962, p. 125, pl. 8, fig. 2; pl. 9, figs. 2–6.
Coccolithus muiri Black, 1964, p. 309, pl. 50, figs. 5, 6.
Ericsonia ovalis Black, 1964, p. 312, pl. 52, figs. 3, 4; Haq, 1968, p. 21, pl. 1, figs. 4–9; pl. 2, figs. 1–4; pl. 4, figs. 1, 2; Edwards, 1972, pl. 6, figs. 5, 6.
Ericsonia occidentalis Black, 1964, p. 311, pl. 52, figs. 1, 2.
Coccolithus lithos Hay, Mohler and Wade, 1966, p. 385, pl. 1, figs. 6–9.
Ericsonia insolita Perch-Nielsen, 1971, p. 13, pl. 1, fig. 1; pl. 7, figs. 4, 6; pl. 61, figs. 14, 15.
Coccolithus pelagicus (Wallich) Schiller. Wise and Wind, 1977, pl. 9, figs. 5, 6.

Remarks: Bramlette and Riedel introduced this species for large sized coccoliths (16–20 μ) which have a high number of elements in their margin (up to 60). The name is used here in a wider sense to include similarly constructed Paleocene coccoliths which have a smaller size and a lower number of elements (28–46).
Dimensions: length: 5–20 μ.
Distribution: Spain: *E. macellus* Zone – *N. fulgens* Zone; Israel: *E. macellus* Zone – *D. sublodoensis* Zone; Scandinavia: *E. macellus* Zone.

Ericsonia robusta (Bramlette and Sullivan) Perch-Nielsen

Cyclolithus? robustus Bramlette and Sullivan, 1961, p. 141, pl. 2, fig. 7.
Heliolithus sp. Wind and Wise, 1977, partim, p. 296, pl. 14, figs. 4–6, non pl. 13, figs. 5, 6.
Heliolithus sp. Wind and Wise, 1977, p. 296, pl. 13, figs. 3, 4; pl. 14, figs. 7–10.
Ericsonia cf. *E. robusta* (Bramlette and Sullivan) Perch-Nielsen, Perch-Nielsen, 1977, partim, pl. 16, figs. 1, 4, 5, non pl. 16, fig. 6.
Non *Ericsonia robusta* (Bramlette and Sullivan) Perch-Nielsen, 1977, p. 774, pl. 16, figs. 2, 7.

Remarks: The wall and the shields of this circular species are composed of 50 to 60 elements. The slightly inward sloping wall covers the distal shield almost completely. The wall shows hook-shaped sutures, which are oblique *clockwise* for their larger part. The subvertical distal shield shows slightly clockwise oblique sutures.

In proximal view the following cycles can be observed (from the centre outwards):
(a) the inner strip of the wall, with anti-clockwise oblique sutures,
(b) the proximal shield with clockwise oblique sutures,
(c) the proximal cycle of the distal shield with anti-clockwise oblique sutures,
(d) the proximal side of the distal cycle of the distal shield, with anti-clockwise oblique sutures,

(e) (in oblique proximal view) the outer strip of the wall, with anti-clockwise oblique sutures.

The ratio between the diameter of the central opening and the width of the margin varies from 5 to 1.

In the standard orientation for distal view, imaginary lines connecting the dextrogyre extinction lines make an angle of about 30° with the polarization directions in clockwise direction. With the gypsum plate, the second and the fourth quadrants are blue.

The species differs from *E. subpertusa* in the more distal position of the wall and in the opposite direction of the larger part of the sutures in this wall.

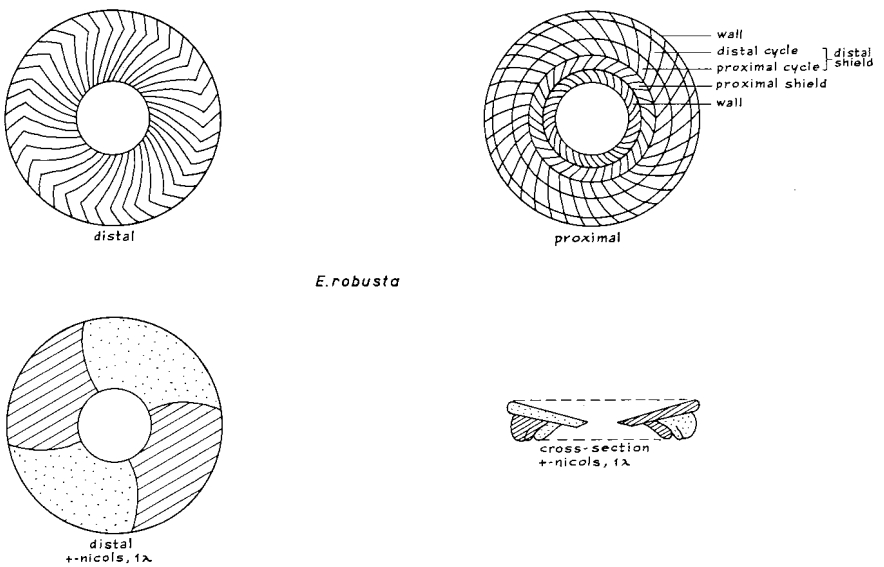

In their illustrations of the distal side of *Heliolithus* sp. (pl. 14, figs. 5, 6) and of *Heliolithus* sp. A (pl. 14, figs. 7, 8), Wind and Wise depicted the proximal side of *E. robusta.*

Dimensions: diameter: 8–12 μ.

Distribution: Spain: *D. multiradiatus* Zone; Israel: *D. mohleri* Zone – *D. multiradiatus* Zone.

Ericsonia universa (Wind and Wise) nov. comb.
(pl. 10, fig. 14)

Heliolithus sp. Wind and Wise, 1977, partim, p. 296, pl. 13, figs. 5, 6, non pl. 14, figs. 4–6.
Heliolithus universus Wind and Wise, 1977, p. 296, pl. 12, figs. 1–6; pl. 13, figs. 1, 2; pl. 14, figs. 1–3.

Remarks: The high, distally flaring wall is characteristic of this species, which has 40 to 60 elements in its margin. The sutures in the wall are oblique clockwise. The distal shield can be observed in oblique distal view: its elements imbricate counter-clockwise, and they are separated by clockwise oblique sutures.

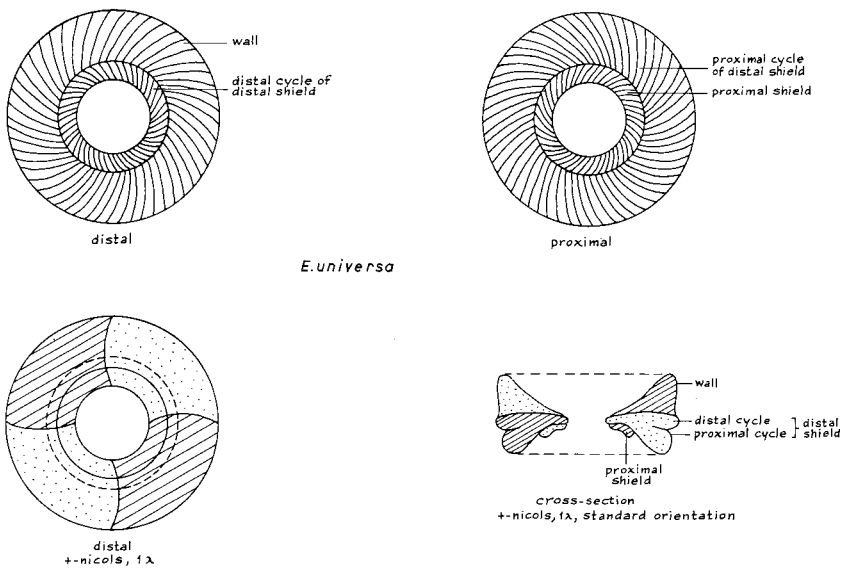

In proximal view the following cycles can be seen (from the centre outwards):

(a) the relatively narrow proximal shield with clockwise oblique sutures,
(b) the wide, somewhat flaring, proximal cycle of the distal shield with counter-clockwise oblique sutures.

The height of the wall is variable, and intermediate forms between this species and *E. robusta* occur in the *D. mohleri* Zone.

The extinction and colour patterns are the same as in *E. robusta.*

In their illustrations of this species (as *H. universus*), Wind and Wise depicted the *proximal* side in pl. 14, figs. 2, 3.

Dimensions: diameter: 8–16 μ.

Distribution: Spain: *D. multiradiatus* Zone; Israel: *D. mohleri* Zone – *D. multiradiatus* Zone.

Ericsonia pacificana (Bukry) nov. comb.

Coccolithus? sp. Radomski, 1968, p. 568, pl. 46, figs. 3, 4.
Striatococcolithus pacificanus Bukry, 1971b, p. 323, pl. 7, figs. 3–8.

Remarks: In proximal view this narrow elliptical species shows a configuration which is typical for *Ericsonia,* but in distal view a different construction can be observed. The species has no wall. Instead the distal shield slopes steeply inwards near the narrow, elliptical opening (as in *M. astroporus*). Near the centre the sutures are oblique clockwise; at about one third of their length they bend in the opposite direction. The number of elements in the margin varies from 38 to 45.

Since the extinction and colour patterns are comparable to those in *Ericsonia,* the species is transferred to this genus.

Dimensions: length: 8–14 μ.

Distribution: Spain: *T. contortus* Zone – *N. fulgens* Zone; Israel: *D. binodosus* Zone – *D. sublodoensis* Zone.

Ericsonia formosa (Kamptner) nov. comb.

Cyathosphaera diaphragma Hay and Towe, 1962, partim, p. 510, pl. 6, figs. 2, 5, non pl. 6, figs. 1, 3, 4, 6.

Cyclococcolithus formosus Kamptner, 1963, p. 163, pl. 2, fig. 8; Reinhardt, 1967, p. 209, pl. 1, figs. 3, 4, 7, 8; pl. 6, figs. 3, 6; text-fig. 11; Haq and Lohmann, 1976, pl. 8, fig. 7; pl. 1, fig. 12.

Coccolithus lusitanicus Black, 1964, p. 308, pl. 50, figs. 1, 2.

Ericsonia alternans Black, 1964, p. 312, pl. 50, fig. 4; Perch-Nielsen, 1971, p. 11, pl. 1, figs. 9–11; Edwards and Perch-Nielsen, 1975, pl. 11, fig. 11.

Cyclococcolithus lusitanicus (Black) Hay, Mohler and Wade, 1966, p. 390, pl. 7, figs. 3–6; Bramlette and Wilcoxon, 1967, p. 103, pl. 3, figs. 16, 17.

Cyclococcolithus orbis Gartner and Smith, 1967, p. 4, pl. 4, figs. 1–3.

Cyclococcolithina formosa (Kamptner) Wilcoxon, 1970, p. 82; Gartner, 1971, p. 109; Edwards, 1973a, pl. 7, figs. 1–5.

Cyclococcolithina lusitanica (Black) Wilcoxon, 1970, p. 82.

Coccolithus formosus (Kamptner) Wise, 1973, p. 593, pl. 4, figs. 1–6.

Remarks: This circular to subcircular species of *Ericsonia* shows 40 to 50 elements in each of its margin cycles. It differs from *E. eopelagica* only in its more circular outline. The distal edges of the wall and the distal shield lie at the same level, while in *E.subpertusa* the wall is superposed on the distal shield. Intermediate forms between *E. eopelagica* and *E. formosa* occur in the *T. contortus* Zone.

Dimensions: diameter: 6–11 μ.

Distribution: Spain: *T. contortus* Zone – *N. fulgens* Zone; Israel: *D. binodosus* Zone – *D. sublodoensis* Zone.

Genus Chiasmolithus Hay, Mohler and Wade, 1966

Type species: *Tremalithus oamaruensis* Deflandre, 1954

Description:

Shape: The species in this genus are subelliptical in plane view and con-

cavo-convex in side view.

Construction: The species are constructed with a wide or narrow, composite margin, which surrounds an open central area spanned by a central cross-structure.

Margin: As in *Cruciplacolithus* the margin is composed of a composite distal shield, a wall and a proximal shield with an equal number of elements. The directions of imbrication, and the directions of the sutures in the different cycles are also the same as in *Cruciplacolithus*. In *Chiasmolithus,* however, the wall lies in a more distal position with respect to the shields, and generally it slopes more steeply inwards than in *Cruciplacolithus*.

In some species the wall shows triangular projections into the central area (teeth).

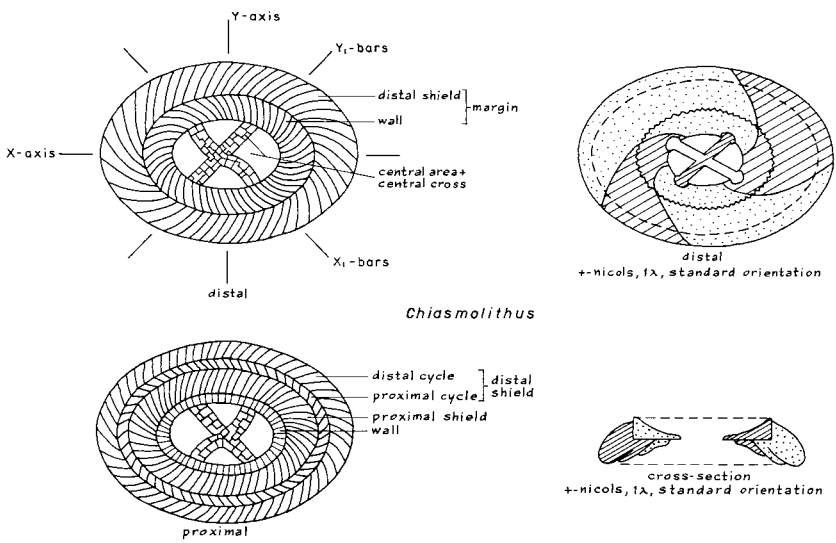

Central area: The central area is spanned by a distally vaulting, modified X- or H-shaped cross-structure. The bars of this structure are never parallel to the axes of the ellipse. They are attached to the lower distal side of the wall. The bars in the direction of the X-axis are called X_1-bars, those in the direction of the Y-axis, Y_1-bars. On the basis of the construction of the bars two groups can be distinguished (Gartner, 1970):

Group 1: The cross-bars are composed of tabular calcite elements stacked one on the top of the other. In cross-polarized light the bars react as homogeneous units.

Group 2: Distally, the bars are organized in a different way than proximally: distally they show lath-like elements, parallel to the axis of the bar;

proximally the elements are perpendicular to, and interfinger with each other along this axis. In cross-polarized light the bars show an extinction line along the axis, which gives them a split appearance.

Species of this group may show a minutely perforated plate in the interareas between the bars.

Standard orientations and extinction lines: See under *Cruciplacolithus*.

Colour distribution: The distribution of the blue and yellow sectors in the margin is the same as in *Cruciplacolithus*. In the species belonging to group 1 the colours of the bars are the same as in *Cruciplacolithus*; in group 2 they are opposite on either side of the median extinction line.

Differential diagnosis: *Chiasmolithus* differs from *Cruciplacolithus* in the more distal position of the wall with respect to the shields; in addition the bars of the central cross are never aligned with the major axes of the ellipse.

Chiasmolithus danicus (Brotzen) Bramlette and Martini (pl. 3, fig. 1)

Cribrosphaerella danica Brotzen, 1959, p. 25, text-fig. 9/1–8.

Coccolithus danicus (Brotzen) Bramlette and Martini, 1964, p. 298, pl. 1, figs. 15, 16; Martini, 1964, p. 48, pl. 6, figs. 3, 4.

Chiasmolithus danicus (Brotzen) Hay and Mohler, 1967a, p. 1526, (non pl. 196, figs. 16, 21, 22; pl. 198, figs. 8, 12, 13); Gartner, 1970, p. 942, pl. 10; Perch-Nielsen, 1972, pl. 4, figs. 3, 5; Haq and Lohmann, 1976, pl. 3, figs. 5–7.

Non *Chiasmolithus danicus* (Brotzen) Hay and Mohler, Roth, 1973, p. 732, pl. 13, figs. 3–5.

Remarks: Each cycle in the margin is composed of 50 to 60 elements. The bars of the central cross are wide and sturdy, so that they almost close the central area. The Y_1-bars are strongly curved clockwise in distal view, in such a way that the central parts are subparallel to the X-axis of the ellipse. The angle XX_1 varies from 23° to 39°; the angle YY_1, from 16° to 38° (clockwise in distal view).

The bars are composed of plate-like and lath-like elements, both distally and proximally; in cross-polarized light they display a pattern which is intermediate between that of species of group 1 and group 2.

Dimensions: length: 9–12 μ.

Distribution: Scandinavia: *C. tenuis* Zone – *E. macellus* Zone.

GROUP 1

Chiasmolithus consuetus (Bramlette and Sullivan) Hay and Mohler

Coccolithus consuetus Bramlette and Sullivan, 1961, p. 139, pl. 1, figs. 2a-c; Stradner, in Gohrbandt, 1963, p. 74, pl. 8, figs. 10–13.

Chiasmolithus consuetus (Bramlette and Sullivan) Hay and Mohler, 1967, partim, p. 1526, pl. 198, fig. 16, non pl. 196, figs. 23–25; Gartner, 1970, p. 942, fig. 9; Perch-Nielsen, 1977, pl. 19, figs. 2, 4, 6.

Chiasmolithus bidens (Bramlette and Sullivan) Hay and Mohler, 1967a, partim, p. 1526, pl. 196, figs. 14, 15, 17, non pl. 197, figs. 4, 9, 14.

Chiasmolithus danicus (Bramlette and Sullivan) Hay and Mohler, 1967a, partim, p. 1526, pl. 198, figs. 12, 13, non pl. 196, figs. 16, 21, 22; pl. 198, fig. 8.

Remarks: The wall and the shields of this species are each composed of 44 to 50 elements. The line along which the wall and the distal shield meet has a characteristic serrated appearance in the L.M. The ratio between the width of the distal shield and the width of the wall varies from 2 to 3.

The bars of the central cross seem to be straight and perpendicular to each other in the L.M. S.E.M. micrographs, however, reveal that the X_1-bars are slightly curved and that they are somewhat off-set in the centre, in anti-clockwise direction. The bars form an angle with the main axes of the ellipse in clockwise direction; this angle varies from 20° to 55° (generally about 45°), and it is not dependent on size or stratigraphic level.

Early specimens are small, but sizes increase in higher stratigraphic levels.
Dimensions: length: 5–12 μ.
Distribution: Spain: *E. macellus* Zone – *N. fulgens* Zone; Israel: *E. macellus* Zone – *D. sublodoensis* Zone.

Chiasmolithus californicus (Sullivan) Hay and Mohler

Coccolithus aff. *C. gigas* Bramlette and Sullivan, 1961, p. 140, pl. 1, figs. 7a-d.

Coccolithus californicus Sullivan, 1964, p. 180, pl. 2, figs. 3, 4.

Chiasmolithus californicus (Sullivan) Hay and Mohler, 1967a, p. 1527, pl. 196, figs. 18–20; pl. 198, fig. 5; Gartner, 1970, p. 941, fig. 8; Haq and Lohmann, 1976, pl. 9, fig. 7; pl. 3, fig. 9.

Chiasmolithus danicus (Brotzen) Hay and Mohler, 1967a, partim, p. 1526, pl. 196, figs. 16, 21, 22, non pl. 198, figs. 8, 12, 13.

Remarks: *C. californicus* shows the same construction as *C. consuetus*; the species differ only in their size (*C. californicus* has about 60 elements in its margin cycles). The angles XX_1 and YY_1 vary over the same range as in *C. consuetus*.
Dimensions: length: 13–17 μ.
Distribution: Spain: *T. contortus* Zone – *D. sublodoensis* Zone; Israel: *D. multiradiatus* Zone – *T. orthostylus* Zone.

Chiasmolithus titus Gartner

Chiasmolithus titus Gartner, 1970, p. 945, fig. 17.

Remarks: This species is very similar to *C. consuetus*, but it differs in the

markedly dextrogyre-curved X_1-bars. As a consequence of this curvature the bars are almost parallel to the Y_1-bars. The species differs from *C. solitus* in the non-split character of the bars.
Dimensions: length: 7–9 μ.
Distribution: Spain: *N. fulgens* Zone.

GROUP 2

Chiasmolithus bidens (Bramlette and Sullivan) Hay and Mohler

Coccolithus bidens Bramlette and Sullivan, 1961, p. 139, pl. 1, fig. 1; Stradner, in Gohrbandt, 1963, p. 72, pl. 8, figs. 1, 2; Sullivan, 1964, p. 180, pl. 1, fig. 10.
Chiasmolithus bidens (Bramlette and Sullivan) Hay and Mohler, 1967a, partim, p. 1526, pl. 197, figs. 4, 9, 14, non pl. 196, figs. 14, 15, 17; Gartner, 1970, p. 941, pl. 7; Edwards, 1973a, pl. 5, figs. 5, 6; Perch-Nielsen, 1977, pl. 18, figs. 5, 6.
Chiasmolithus consuetus (Bramlette and Sullivan) Hay and Mohler, 1967a, partim, p. 1526, pl. 196, figs. 23, 24, 25, non pl. 198, fig. 16.
Chiasmolithus solitus (Bramlette and Sullivan) Locker, 1968, pl. 1, figs. 5, 6.
Chiasmolithus eograndis Perch-Nielsen, Haq and Lohmann, 1976, pl. 9, fig. 11.
Chiasmolithus cf. *C. eograndis* Perch-Nielsen, Wise and Wind, 1977, pl. 9, figs. 2, 3.

Remarks: The wall and the shields are each composed of 51 to 75 elements. In the central cross-structure the Y_1-bars are in an even line, but the X_1-bars are centrally off-set, anti-clockwise, in distal view. The angles XX_1 and YY_1 vary from 40° to 50° in clockwise direction. In well preserved specimens the inter-areas between the bars are closed by perforated plates.

The species owes its name to two tooth-like projections of the wall into the central area. These teeth are placed symmetrically with respect to the X-axis. In early populations of the species the teeth are absent; in progressively later populations, which are generally composed of somewhat larger forms, small indentations, and later, teeth occur.
Dimensions: length: 6–13 μ.
Distribution: Spain: *E. macellus* Zone – *D. multiradiatus* Zone; Israel: *E. macellus* Zone – *T. contortus* Zone; Scandinavia: *E. macellus* Zone.

Chiasmolithus eograndis Perch-Nielsen
(pl. 3, fig. 2)

Chiasmolithus eograndis Perch-Nielsen, 1971d, p. 16, pl. 10, figs. 5, 6; pl. 13, figs. 1–4; pl. 60, figs. 17, 18; Edwards and Perch-Nielsen, 1975, pl. 6, figs. 6, 10, 14, 15; pl. 7, figs. 4, 7.

Remarks: The wall and the shields of this species are constructed of 60–100 elements each. In typical specimens the more or less H-shaped central structure has wide bars, which almost close the central area. The species may

be hard to differentiate from *C. bidens* and *C. grandis*. S.E.M. micrographs have revealed the presence of perforated plates in the interareas.
Dimensions: length: 11–13 μ.
Distribution: Spain: *T. contortus* Zone – *D. lodoensis* Zone; Israel: *D. binodosus* Zone – *T. orthostylus* Zone.

Chiasmolithus solitus (Bramlette and Sullivan) Locker

Coccolithus solitus Bramlette and Sullivan, 1961, p. 140, pl. 2, fig. 4; Sullivan, 1964, p. 181, pl. 1, fig. 13.
Chiasmolithus solitus (Bramlette and Sullivan) Locker, 1968, p. 221, pl. 1, figs. 5, 6; Gartner, 1970, p. 945, fig. 16; Perch-Nielsen, 1971d, p. 21, pl. 11, fig. 1; pl. 12, figs. 1–5; pl. 13, fig. 5; pl. 14, fig. 11; pl. 60, figs. 19, 20.

Remarks: The rather high wall and the relatively narrow shields are composed of 46 to 60 elements each. The Y_1-bars are straight and make an angle with the Y-axis in clockwise direction in distal view. The X_1-bars are curved dextrogyre.

In cross-polarized light the wall is very bright, and the shields are only faintly illuminated.
Dimensions: length: 12 μ.
Distribution: Spain: *D. lodoensis* Zone – *N. fulgens* Zone; Israel: *T. contortus* Zone – *D. sublodoensis* Zone.

Chiasmolithus grandis (Bramlette and Riedel) Radomski

Coccolithus grandis Bramlette and Riedel, 1954, p. 391, pl. 38, fig. 1; Deflandre, in Deflandre and Fert, 1954, p. 152, text-fig. 48; Bramlette and Sullivan, 1961, p. 140, pl. 2, figs. 1–3.
Chiasmolithus grandis (Bramlette and Riedel) Radomski, 1968, p. 560, pl. 44, figs. 3, 4; Gartner, 1970, p. 944, figs. 11/3; 14; Perch-Nielsen, 1971d, p. 18, pl. 9, figs. 1, 2; pl. 10, fig. 4; pl. 60, figs. 1, 2.

Remarks: This large species of *Chiasmolithus* has 80 to 100 elements in its high, steeply inward sloping wall and in its relatively narrow shields. Characteristic is the presence of four teeth; imaginary lines connecting these teeth in opposite quadrants, make a small angle with the main axes of the ellipse, anti-clockwise in distal view.

The X_1-bars are curved dextrogyre, the Y_1-bars laevogyre, in distal view.
Dimensions: length: 16–24 μ.
Distribution: Spain: *T. orthostylus* Zone – *N. fulgens* Zone; Israel: *D. binodosus* Zone – *D. sublodoensis* Zone.

Chiasmolithus expansus (Bramlette and Sullivan) Gartner

Coccolithus expansus Bramlette and Sullivan, 1961, p. 139, pl. 1, fig. 5; Sullivan, 1965, p. 32, pl. 2, fig. 5; Hay, Mohler and Wade, 1966, p. 366.
Chiasmolithus expansus (Bramlette and Sullivan) Gartner, 1970, p. 943, fig. 11/1, 2; Perch-Nielsen, 1971d, p. 17, pl. 9, fig. 3; pl. 10, figs. 1–3; pl. 11, fig. 5; pl. 60, figs. 9, 10.

Remarks: The high wall and the relatively narrow shields are each composed of a large number of elements (60–80). The slender, strongly distally arching bars of the central structure are curved in such a way that the central part is more or less parallel to the X-axis of the ellipse. The species differs from *C. grandis*, mainly in the absence of teeth; as a consequence, overgrown specimens are hard to differentiate from *C. grandis*.
Dimensions: length: 15–20 μ.
Distribution: Spain: *T. orthostylus* Zone – *N. fulgens* Zone; Israel: *T. orthostylus* Zone – *D. sublodoensis* Zone.

Chiasmolithus gigas (Bramlette and Sullivan) Gartner

Coccolithus gigas Bramlette and Sullivan, 1961, p. 140, pl. 1, fig. 7; Sullivan, 1965, p. 32, pl. 2, fig. 6.
Chiasmolithus gigas (Bramlette and Sullivan) Gartner, 1970, p. 943, figs. 12, 13/1a-c.

Remarks: This large species has about 50 elements in its wall and in its wide shields. The curved bars in the relatively small central area make a small angle with the main axes of the ellipse in clockwise direction, in distal view.
Dimensions: length: 20–24 μ.
Distribution: Spain: *N. fulgens* Zone.

Family AHMUELLERELLACEAE Reinhardt, 1965 emend. Hoffmann, 1970

Genus Placozygus Hoffmann, 1970

Type species: *Glaukolithus fibuliformis* Reinhardt, 1964

Placozygus sigmoides (Bramlette and Sullivan) nov. comb. (pl. 1, fig. 8)

Zygodiscus sigmoides Bramlette and Sullivan, 1961, p. 149, pl. 4, figs. 11a-e; Bramlette and Martini, 1964, p. 303, pl. 4, figs. 4, 5; Perch-Nielsen, 1969b, p. 65, pl. 5, figs. 1–3; Haq and Lohmann, 1976, pl. 3, figs. 1, 2; Wise and Wind, 1977, p. 309, pl. 43, figs. 5, 6.
Zygodiscus simplex Bramlette and Sullivan, 1961, p. 151, pl. 6, figs. 19–22; Hay and Mohler, 1967a, partim, p. 1532, pl. 200, figs. 2, 3, 5, non pl. 199, figs. 11, 15, 22; pl. 200, fig. 6; pl. 201, fig. 3.
Zygodiscus adamas Bramlette and Sullivan, Stradner, in Gohrbandt, 1963, p. 76, pl. 9, figs. 13, 14.

Remarks: The margin of this species is composed of a low wall, surmounted

by a high rim. The wall consists of plate-like, non imbricating elements; the rim of strongly inclined, clockwise imbricating elements.

The basal part of the distally arching bar is also formed by non imbricating plate-like elements. The distal part consists of two bundles of rod-like elements, which meet in the centre. Each bundle makes a small angle with the Y-axis, in anti-clockwise direction; this produces the sigmoid pattern of the bar in the L.M.

The central spine is composed of helicoidally arranged, short, lath-like elements. In most of our specimens the spine has broken off.

Typical specimens of the species are relatively flat, they show large openings at each side of the bar, and their length varies from 7 to 9 μ. In the Paleocene, variants occur, which are thicker, which have a wider wall and rim, and smaller openings. Their length varies from 12 to 14 μ. The species is transferred to the genus *Placozygus* because of the construction of the bar and the margin. The extinction lines in the margin are dextrogyre in distal view.

Dimensions: length 7–14 μ.

Distribution: Spain: *C. primus* Zone – *T. contortus* Zone; Israel: *C. primus* Zone – *T. contortus* Zone; Scandinavia: *C. primus* Zone – *E. macellus* Zone.

Family NOËLAERHABDACEAE Jerković, 1970

Remarks: The type genus of the family Prinsiaceae (Hay and Mohler, 1967) was designated by Edwards (1973b); the name Noëlaerhabdaceae, introduced by Jerković, 1970 for this group of coccoliths has, however, priority.

Genus **Prinsius** Hay and Mohler, 1967

Type species: *Coccolithus bisulcus* Stradner, 1963

Description:

Shape: The species in this genus are subelliptical to circular in plane view, and concavo-convex in side view.

Construction: The species have a relatively wide, composite margin, which surrounds a fully or partly closed central area.

Margin: The margin is composed of a thick, composite distal shield and a thin proximal shield. Both shields slope outwards, and are constructed of an equal number of elements.

Distal shield: This shield consists of a thick distal cycle and a somewhat smaller and thinner proximal cycle. The cycles are free-standing over most of their width, but they coalesce near the central area. The distal cycle shows slightly clockwise imbricating elements, separated by subradial to

slightly clockwise oblique sutures.

In proximal view, the sutures are subradial in both cycles.

Proximal shield: This shield is smaller than, and closely appressed with, the proximal cycle of the distal shield. The sutures are subradial in proximal view. The longish, wedge-shaped elements bend in distal direction near the central area; somewhat higher up they bend again, now in centro-lateral direction to close the central area.

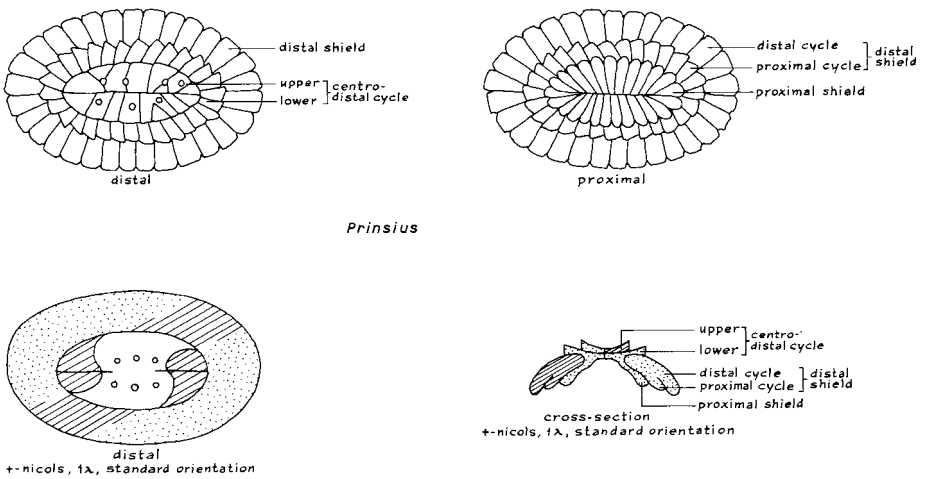

Central area: The central area is closed by two, partly superposed cycles of elements: an upper centro-distal cycle and a lower one.

Lower centro-distal cycle: This cycle has a serrated outline. It covers the inner edge of the distal shield, and it slopes outwards to the upper, central part of the proximal shield. The central part of this cycle is covered by the upper centro-distal cycle. The sutures between the elements are strongly oblique clockwise in distal view. The number of elements equals that in the shields.

Upper centro-distal cycle: This gently inwards sloping cycle has a somewhat smaller diameter than the lower one. It is composed of irregularly shaped elements, which close or almost close the central area. Proximally the cycle is in contact with the central part of the proximal shield. The number of elements in the cycle is generally lower than in the other cycle.

Specific criteria: The species are based on the outline and on the construction of the central area.

Standard orientations

Distal view: Convex side of coccolith upwards; X-axis parallel to the X-cross-hair.

Side view: X-axis parallel to the X-cross-hair; convex side pointing to the positive direction of the Y-cross-hair.
Extinction lines: The lines are most distinct in the central area, and vague in the shields. In the central area they are strongly dextrogyre in distal view. In circular species the lines are straight in the central part of the central area; they make a small angle with the polarization directions, anti-clockwise in distal view.
Colour patterns: In the standard orientation for distal view, the sectors in the central area enclosed by the extinction lines, along the X-axis are blue; the others are yellow.

In the standard orientation for side view, the left cross-section of the distal shield and the right cross-section of the upper centro-distal cycle are blue; the other sections are yellow.
Differential diagnosis: *Prinsius* differs from the closely related *Toweius* in the essentially closed central area and in the irregular arrangement of the elements in the upper centro-distal cycle.

Prinsius petalosus (Ellis and Lohman) nov. comb.

Toweius petalosus Ellis and Lohman, 1973, p. 107, pl. 1, figs. 1–11; Romein, 1977, p. 275, pl. 2, figs. 5a-c.

Remarks: The shields of this extremely small species are composed of 9 to 17 elements. The distal central area is filled in by a crown of petaloid elements, which are separated by anti-clockwise oblique sutures in distal view.

The species is transferred to the genus *Prinsius* because of its small size, the low number of elements in the shields, and its behaviour in cross-polarized light.

In the uppermost part of the *C. primus* Zone, specimens with reduced crowns occur; they are considered as transitional forms between *P. petalosus* and *P. dimorphosus* type 1.
Dimensions: length of coccolith: 1–2 μ; diameter of coccosphere: 6–8 μ.
Distribution: Spain: *C. primus* Zone – *P. dimorphosus* Zone.

Prinsius dimorphosus (Perch-Nielsen) Perch-Nielsen
(pl. 3, figs. 3–6)

Coccospheres, in Bramlette and Martini, 1964, p. 320, pl. 1, figs. 19, 20.
Vollständiges Gehaus, Martini, 1964, p. 52, pl. 7, figs. 5, 6.
Fossil coccosphere, in Black, 1965, p. 132, fig. 3.
Biscutum? dimorphosum Perch-Nielsen, 1969a, p. 318, pl. 32, figs. 1–3a, 4; text-fig. 1; Perch-Nielsen, 1969b, p. 57, pl. 4, figs. 6–12.
Biscutum dimorphosum Perch-Nielsen, Perch-Nielsen, 1972, pl. 8, fig. 2.
Prinsius dimorphosus (Perch-Nielsen) Perch-Nielsen, 1977, p. 794, pl. 30, figs. 10–13.

Remarks: As already indicated by its name, two types of coccoliths can be distinguished in this species; both types were found to occur on the same coccosphere (Perch-Nielsen, 1969a, text-fig. 1).

Specimens of type 1 have a circular outline. They show 9 to 11 elements in their shields and central area. When viewed from the distal side, the sutures in the distal shield have the form of a modified Z; they are slightly oblique clockwise for most of their length, but they bend in the opposite direction near the central area. Thus a kind of peg-in-hole connection exists between the elements. The distal central area, except for a small central pore, is closed by a cycle of triangular elements.

In proximal view three cycles are visible: the distal cycle of the distal shield, the proximal cycle of the distal shield, and the proximal shield. The latter two cycles are closely appressed.

The elements of the proximal shield are widest near the outer margin of the coccolith, and they narrow towards the centre, where they bend in distal direction. The elements extend to the inner edge of the distal shield; their distal terminations can be observed in distal views of specimens in which the distal central area elements have disappeared (pl. 3, fig. 4). The elements of the proximal shield may form a grill-like structure in the proximal central area.

Dimensions: diameter: 2–3 μ.

Distribution: Spain: *P. dimorphosus* Zone – *C. tenuis* Zone; Israel: *P. dimorphosus* Zone – *E. macellus* Zone; Scandinavia: *C. tenuis* Zone – *E. macellus* Zone.

Specimens of *P. dimorphosus* type 2 differ from those of type 1 in having a more elliptical outline, a higher number of elements in their shields (11–13), and in the presence of *two* superposed cycles of elements in the distal central area (upper an lower centro-distal cycle). The elements of the proximal shield form a grill-like structure in the centre.

Dimensions: length: 2–3 μ.

Distribution: Scandinavia: *C. tenuis* Zone, *E. macellus* Zone.

Prinsius martinii (Perch-Nielsen) Haq
(pl. 3, figs. 7, 8)

Ericsonia? martinii Perch-Nielsen, 1969a, p. 324, pl. 32, figs. 3b, 5–7; text-fig. 2; Perch-Nielsen, 1969b, p. 61, pl. 4, figs. 13, 14.

Prinsius martinii (Perch-Nielsen) Haq, 1971a, partim, p. 18, pl. 5, figs. 2, 3, 5, 10, non pl. 5, fig. 1; Edwards, 1973b, p. 86, fig. 83; Haq and Lohmann, 1976, pl. 1, fig. 5; pl. 14, figs. 1, 2; Perch-Nielsen, 1977, pl. 30, fig. 3.

Remarks: This elliptical species differs from *P. dimorphosus* type 2 in the

higher number of elements in the shields (25–32), and in its larger dimensions. The central area is distally closed by the irregularly arranged elements of the upper centro-distal cycle, and proximally by the central part of the proximal shield.

Dimensions: length: 4–5 μ.

Distribution: Spain: *C. tenuis* Zone – *D. mohleri* Zone; Israel: *C. tenuis* Zone – *D. mohleri* Zone; Scandinavia: *C. tenuis* Zone – *E. macellus* Zone.

Prinsius bisulcus (Stradner) Hay and Mohler

Coccolithus bisulcus Stradner, in Gohrbandt, 1963, p. 72, pl. 8, figs. 3–6; text-fig. 3.
Prinsius bisulcus (Stradner) Hay and Mohler, 1967, p. 1529, pl. 196, figs. 10–13; pl. 197, fig. 6; Roth, 1973, p. 732, pl. 17, fig. 2; Wise and Wind, 1977, pl. 6, figs. 3–6.

Remarks: In the L.M., in normal light, the species is characterized by the presence of darker lines along the X-axis, one at each pole of the central area. S.E.M. micrographs indicate that these lines represent fissures between the elements in the upper centro-distal cycle. The fissures probably coincide with sutures in the underlying proximal shield.

Up to six pores are present in the central area and are arranged along the sutures in the upper centro-distal cycle. These pores are thought to correspond to openings in the proximal shield.

The shields and the lower centro-distal cycle are composed of 35–40 elements.

Dimensions: length: 6–10 μ.

Distribution: Spain: *E. macellus* Zone – *D. multiradiatus* Zone; Israel: *E. macellus* Zone – *D. mohleri* Zone; Scandinavia: *E. macellus* Zone.

Genus **Toweius** Hay and Mohler, 1967

Type species: *Toweius craticulus* Hay and Mohler, 1967

Description:

Shape: The species are elliptical, subcircular or circular in plane view, and concavo-convex in side view.

Construction: The species are composed of a relatively wide, composite margin, and two modified, partly superposed cycles of elements in the central area.

Margin: The margin is composed of a thick, composite distal shield and a thin proximal shield. Both shields slope outwards and consist of an equal number of elements.

Distal shield: This shield consists of a thick distal cycle and a thinner and smaller proximal cycle, which are free-standing over most of their width but

which coalesce near the central area.

The elements of the distal cycle imbricate clockwise in distal view; the sutures are subradial to slightly oblique anti-clockwise.

In proximal view the sutures in the distal cycle are oblique anti-clockwise, and those in the proximal cycle clockwise.

Proximal shield: This shield is closely appressed with the proximal cycle of the distal shield. The shield bends in distal direction near the central area, and somewhat higher up it takes part in the formation of a perforated central plate. The sutures are oblique anti-clockwise in proximal view.

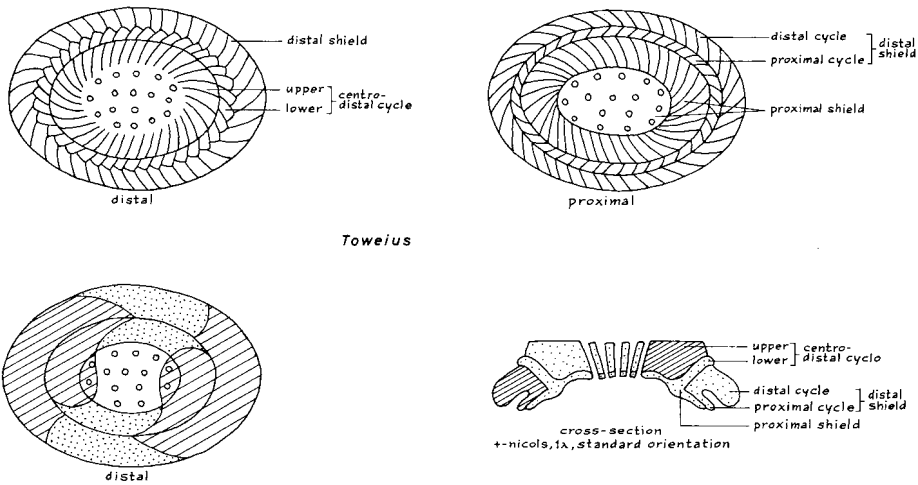

Central area: As stated above, the proximal side of the central area is closed by the proximal shield. Distally, the area is closed by an upper and a lower centro-distal cycle. The number of elements in these cycles equals that in the shield.

Lower centro-distal cycle: This cycle slopes steeply inwards; probably it fuses with the proximal shield in the centre. The cycle has a serrated outline and covers the inner margin of the distal shield. The lath-like elements in the cycle are separated by strongly clockwise oblique sutures. The larger part of this cycle is covered by the upper centro-distal cycle.

Upper centro-distal cycle: The surface of this thick cycle slopes gently inwards, but the sides are steep. Internally, the elements imbricate anti-clockwise; more distally the elements bend and become imbricated clockwise. At the surface of the cyle the sutures are slightly oblique clockwise. The cycle may be pierced by pores or openings. At its base, the cycle is closely appressed with the proximal shield.

Specific criteria: The species are based on the size of the coccolith, the number and form of the openings in the central area, and the number of centro-distal cycles.

Standard orientations

Distal view: X-axis parallel to the X-cross-hair; concave side of coccolith downwards.

Side view: X-axis parallel to the X-cross-hair; convex side in the positive direction of the Y-cross-hair.

Extinction lines: The lines are sharper in the central area than in the shields. In the former area they are strongly dextrogyre, in the latter laevogyre. In circular species the lines in the central area form an angle of about 20° with the polarization directions, counter clockwise, in distal view.

Colour patterns: In the standard orientation for distal view, the sectors in the central area enclosed by the extinction lines, and along the X-axis, are blue; the other sectors are yellow.

In the standard orientation for side view the left cross-section of the distal shield, and the right cross-section of the upper centro-distal cycle are blue, the other sections are yellow.

Differential diagnosis: The genus differs from the closely related genus *Prinsius* in the thicker, and more regularly constructed upper centro-distal cycle. It also differs from the closely related genera *Reticulofenestra, Cribrocentrum* and *Dictyococcites* in the arrangement of the pores in the central area, in the presence of two centro-distal cycles (the other genera have only one cycle), and in the smaller degree of imbrication of the elements in the upper cycle of the distal shield.

Toweius pertusus (Sullivan) nov. comb.
(pl. 3, fig. 9)

Coccolithus pertusus Sullivan, 1965, p. 32, pl. 3, figs. 5, 6.

Toweius craticulus Hay and Mohler, 1967, p. 1530, pl. 196, figs. 7–9; pl. 197, figs. 2, 3; Edwards and Perch-Nielsen, 1975, pl. 3, figs. 3, 6, 8, 9; pl. 8, fig. 2; Haq and Lohmann, 1976, pl. 1, figs. 9–11; Perch-Nielsen, 1977, pl. 30, fig. 4.

Toweius helianthus (Hay and Towe) Hay and Mohler, 1967, p. 1530, pl. 197, fig. 8.

Toweius sp. Perch-Nielsen, 1971, p. 32, pl. 8, figs. 1–4, 7; Perch-Nielsen, 1972, pl. 7, figs. 1, 2; Perch-Nielsen, 1977, pl. 30, figs. 5, 8, 9.

Ericsonia robusta (Bramlette and Sullivan) Edwards and Perch-Nielsen, 1975, pl. 8, fig. 2.

Remarks: The pores in the thick, upper centro-distal cycle of this elliptical to oval species are arranged in a single or double cycle. Their number varies from 6 in early populations to 24 in later ones. Early specimens show furrows along the X-axis; they are transitional between *T. pertusus* and *P. bisulcus*.

Dimensions: length (diameter): 4–9 μ.
Distribution: Spain: *F. tympaniformis* Zone – *T. orthostylus* Zone; Israel: *E. macellus* Zone – *D. binodosus* Zone.

Toweius eminens (Bramlette and Sullivan) Gartner s.l. (pl. 4, fig. 1)

Coccolithus eminens Bramlette and Sullivan, 1961, p. 139, pl. 1, fig. 3; Radomski, 1968, p. 564, pl. 45, figs. 7, 8.
Cruciplacolithus eminens (Bramlette and Sullivan) Hay and Mohler, 1967, partim, p. 1527, pl. 196, figs. 26–28, non pl. 198, figs. 9, 10.
Toweius eminens (Bramlette and Sullivan) Gartner, 1971, p. 114, pl. 5, figs. 4–6; Haq and Lohmann, 1976, pl. 4, fig. 1; Wise and Wind, 1977, p. 296, pl. 5, figs. 1–3.
Toweius tovae Perch-Nielsen, 1971c, p. 359, pl. 13, figs. 1–3, 5; pl. 14, figs. 8, 9; Wise and Wind, 1977, p. 296, pl. 5, fig. 6; pl. 6, fig. 1.

Remarks: The species is characterized by the presence of 4 to 7 large, radially arranged, triangular openings in the upper centro-distal cycle. Perch-Nielsen (1971c) separated forms with 6 or 7 openings from *T. eminens* (with 4 openings), giving them the name *T. tovae*. In our opinion, the variation in the number of openings represents intraspecific variation.

Intermediate forms between this species and *T. pertusus* occur frequently in the *D. mohleri* Zone.
Dimensions: length (diameter): 6–8 μ.
Distribution: Spain: *D. mohleri* Zone – *T. contortus* Zone; Israel: *D. mohleri* Zone – *T. contortus* Zone.

Toweius occultatus (Locker) Perch-Nielsen

Coccolithus occultatus Locker, 1967, p. 764, pl. 1, fig. 5; pl. 2, figs. 9, 10.
Toweius occultatus (Locker) Perch-Nielsen, 1971a, p. 32, pl. 17, figs. 1, 2, 4, 7; pl. 18, fig. 6.
Toweius callosus Perch-Nielsen, 1971a, p. 31, pl. 17, figs. 3, 5, 6; pl. 18, fig. 5; pl. 61, figs. 32, 33; Edwards and Perch-Nielsen, 1975, pl. 3, fig. 12; pl. 6, fig. 9.
Toweius cf. *T. occultatus* (Locker) Perch-Nielsen, Edwards and Perch-Nielsen, 1975, pl. 3, fig. 13.

Remarks: The upper centro-distal cycle of this species shows a variable degree of reduction: forms with two to four, inwards projecting remnants of this cycle occur, as well as forms with a large or small, smooth and circular opening.

Forms, intermediate between this species and *T. eminens* occur frequently in the *D. multiradiatus* Zone.
Dimensions: diameter: 6–8 μ.
Distribution: Spain: *T. contortus* Zone – *D. lodoensis* Zone; Israel: *D. multiradiatus* Zone – *D. lodoensis* Zone.

Toweius gammation (Bramlette and Sullivan) nov. comb.
(pl. 4, figs. 4, 5)

Coccolithites gammation Bramlette and Sullivan, 1961, p. 152, pl. 7, figs. 7, 14.
Cyclococcolithus gammation (Bramlette and Sullivan) Sullivan, 1964, p. 181, pl. 3, fig. 7.
Markalius sp. Wise and Constans, 1977, pl. 1, figs. 3, 4.

Remarks: The lower centro-distal cycle and the shields are each composed of 41 to 60 elements. This circular species differs from all others in the genus in the absence of both the upper centro-distal cycle, and the proximal cycle of the distal shield. The elements of the proximal shield may or may not close the central area. The forms have been assigned to *Toweius* because of the extinction pattern. Intermediate forms between this species and *T. occultatus* have been observed in the *D. binodosus* Zone.
Dimensions: diameter: 5–8 μ.
Distribution: Spain: *D. binodosus* Zone – *N. fulgens* Zone; Israel: *D. binodosus* Zone – *D. sublodoensis* Zone.

Toweius magnicrassus (Bukry) nov. comb.
(pl. 4, figs. 2, 3)

Coccolithus magnicrassus Bukry, 1971, p. 309, pl. 2, figs. 1–5.

Remarks: This large and robust, elliptical to subcircular species has 55–80 elements in each of its cycles. The upper centro-distal cycle surrounds an irregular to smooth elliptical central opening. The presence of a reticule in this opening is suspected, but T.E.M. or S.E.M. micrographs of well-preserved specimens are not yet available. The species differs from *T. occultatus* in its larger size and in the relatively wider shields. The species was transferred to *Toweius* because of its construction and extinction pattern.
Dimensions: length (diameter): 10–16 μ.
Distribution: Spain: *T. orthostylus* Zone – *D. sublodoensis* Zone; Israel: *D. binodosus* Zone – *D. sublodoensis* Zone.

Genus **Reticulofenestra** Hay, Mohler and Wade, 1966

Type species: *Reticulofenestra caucasica* Hay, Mohler and Wade, 1966
Description:

Shape: The species are subelliptical in plane view, and concavo-convex in side view.

Construction: The coccoliths in this genus have a relatively wide margin and a central area closed by a narrow, inner cycle of elements and by a central reticule.

Margin: The slightly outwards sloping margin is composed of a composite distal shield and a smaller proximal shield. The number of elements is the same in both shields.

Distal shield: This shield is constructed of a thick distal cycle and a thinner proximal cycle. The cyles are free, and widely spaced over most of their width, but they fuse near the central area. In distal view the distal cycle shows strongly clockwise imbricating elements, separated by slightly counter-clockwise oblique sutures.

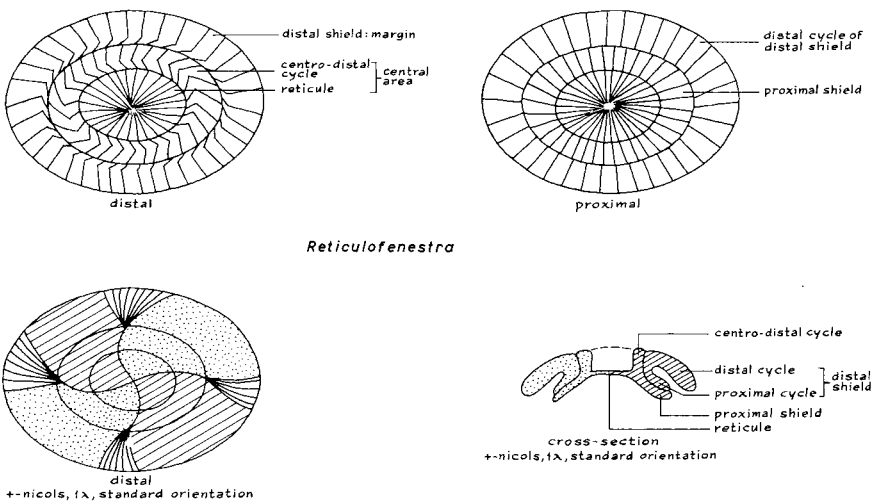

Proximal shield: This shield is slightly wider than, and closely appressed with the proximal cycle of the distal shield. In proximal view the sutures are slightly oblique anti-clockwise.

As in *Prinsius* and *Toweius* the elements bend in distal direction near the central area, and, somewhat higher up, in centro-lateral direction to take part in the formation of the central reticule.

Central area: This area is concave in distal view. It is filled in with a single centro-distal cycle, which forms the central reticule.

Centro-distal cycle: This rather narrow cycle is composed of strongly anti-clockwise imbricating elements. The sutures are slightly oblique clockwise. At the base of the cycle the elements bend towards the centre, where they form the reticule.

Central reticule: Each element of the centro-distal cycle forms a thin and long lath which extends to the centre of the coccolith. The narrowly spaced laths are connected by very small and short transverse laths.

Specific criteria: The species are based on the size of the coccolith, on the relative proportions of margin and central area, and on characteristics of the margin.
Standard orientations: See under *Toweius*.
Extinction lines: The extinction lines are sharpest in the central area. Here they are strongly dextrogyre in distal view. The central parts of the lines are straight, and they form an angle of about 20° in anti-clockwise direction with the polarization directions in distal view. In the margin the lines widen to V-like sectors.
Colour patterns: In the standard orientation for distal view the sectors lying along the X-axis and enclosed by the extinction lines in the central area are blue. The other sectors are yellow.

In the standard orientation for side view the right cross-section of the distal shield, the proximal shield and the centro-distal cycle are blue; the other sectors are yellow.
Differential diagnosis: See under *Toweius*.

Reticulofenestra dictyoda (Deflandre and Fert) Stradner (pl. 4, fig. 6)

Discolithus dictyodus Deflandre and Fert, 1954, p. 140, partim, text-fig. 15, non text-fig. 16.
Cyclococcolithus dictyodus (Deflandre and Fert) Hay and Towe, 1962, p. 503, pl. 5, fig. 4; pl. 7, fig. 1.
Coccolithus marismontium Black, 1964, p. 309, pl. 51, figs. 1–4; pl. 52, fig. 3.
Non *Reticulofenestra dictyoda* (Deflandre and Fert) Stradner, in Stradner and Edwards, 1968, p. 19, pl. 12–14; pl. 22, fig. 4; text-fig. 2c.
Reticulofenestra dictyoda (Deflandre and Fert) Stradner, Perch-Nielsen, 1971d, p. 30, pl. 25, figs. 1–3; Perch-Nielsen, 1977, pl. 30, fig. 2.
Toweius callosus Perch-Nielsen, 1971d, partim, p. 31, pl. 61, figs. 32, 33, non pl. 17, figs. 3, 5, 6; pl. 18, fig. 5.

Remarks: The shields and the centro-distal cycle of this elliptical to sub-elliptical species are composed of 40 to 60 elements. The relatively small central area is closed by a reticule. The sutures in the distal shield are strongly oblique clockwise from the central area to about the middle of the shield, but then they bend in subradial direction. Intermediate forms between this species and *R. umbilicus* occur in the *N. fulgens* Zone.
Dimensions: length: 5–13 μ.
Distribution: Spain: *D. lodoensis* Zone – *N. fulgens* Zone; Israel: *D. lodoensis* Zone – *D. sublodoensis* Zone.

Reticulofenestra umbilicus (Levin) Martini and Ritzkowski

Coccolithus umbilicus Levin, 1965, p. 265, pl. 41, fig. 2; Gartner and Smith, 1967, p. 3, pl. 1, figs. 3, 4; pl. 2, figs. 1–3.

Coccolithus cf. *C. placomorphus* (Kamptner) Reinhardt, 1966, p. 21, pl. 22, figs. 29, 30; pl. 20, fig. 3.
Coccolithus pelycomorphus Reinhardt, 1966, p. 515, pl. 1, figs. 2, 6; text-fig. 5; Reinhardt, 1967, p. 206, pl. 1, figs. 10, 11, 14; pl. 5, fig. 10; pl. 7, fig. 4; text-fig. 6.
Apertapetra samodurovi Hay, Mohler and Wade, 1966, partim, p. 388, pl. 6, figs. 1–3, non pl. 6, figs. 4–7.
Reticulofenestra caucasica Hay, Mohler and Wade, 1966, partim, p. 386, pl. 2, fig. 5; pl. 3, figs. 1, 2; pl. 4, figs. 1, 2, non pl. 2, figs. 6–8; Perch-Nielsen, 1967, p. 26, pl. 1, figs. 9–11.
Non *Reticulofenestra caucasica* Hay, Mohler and Wade, Levin and Joerger, 1967, p. 168, pl. 2, fig. 2.
Reticulofenestra placomorpha (Kamptner) Stradner, Haq, 1968, p. 29, pl. 3, fig. 3; Stradner and Edwards, 1968, partim, p. 22, pl. 19, 20, 22–24; pl. 25, figs. 1, 2, non pl. 21.
Reticulofenestra umbilica (levin) Martini and Ritzkowski, 1968, p. 137; Perch-Nielsen, 1971d, p. 30, pl. 21, fig. 7; pl. 23, figs. 1, 2; pl. 24, figs. 1–3.

Remarks: The wide shields and the narrow centro-distal cycle of this large, elliptical species are each composed of about 100 elements. The inner strip of the distal shield which has anti-clockwise oblique sutures is relatively narrow. The relative proportions of the margin and the central area vary widely.
Dimensions: length: 11–21 μ.
Distribution: Spain: *N. fulgens* Zone.

Family ZYGODISCACEAE Hay and Mohler, 1967

Genus **Zygodiscus** Bramlette and Sullivan, 1961

Type species: *Zygodiscus adamas* Bramlette and Sullivan, 1961
Introduction:

This genus was introduced by Bramlette and Sullivan for "coccoliths with an elliptical rim, a transverse bar with more than one segment of different calcite orientation, and some vestige, at least, of a basal plate". The type species, *Z. adamas* is a Tertiary species, but since 1961 many Jurassic and Cretaceous species have been assigned to the genus. Although these species fulfil the minimum requirements for the genus, they differ considerably from the type species in their ultrastructure. The description of the genus given below pertains only to the Tertiary representatives of the genus.
Description:

Shape: The species are elliptical in plane view, and slightly concavo-convex in side view.

Construction: The species are composed of a high or low, composite margin, a complex bar along the Y-axis, and a wide or narrow central plate.

Margin: The distally flaring margin is composed of an inner cycle (wall) and an outer one (rim). The wall is a continuation of the central plate; it is composed of elements which imbricate clockwise in distal view. The ele-

ments of the rim imbricate in the opposite direction in the same view.

Bar: This structure is basically composed of two laths, which cross in the centre. The bar makes a small angle with the Y-axis, counter-clockwise in distal view.

Central plate: This plate either closes the central area or it surrounds the openings at each side of the bar. The plate probably consists of radially orientated elements (electron micrographs could not be found in the literature).

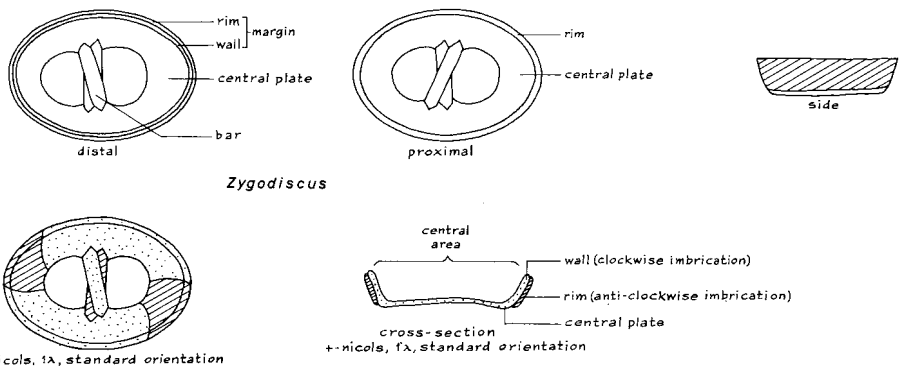

Specific criteria: The species are based on the shape of the bar and on the size of the openings in the central plate.

Standard orientations

Distal view: Convex side upwards; X-axis parallel to the X-cross-hair.

Side view: X-axis parallel to the X-cross-hair; convex side pointing in the positive direction of the Y-cross-hair.

Extinction lines: The lines are sharpest in the central plate. They are dextrogyre in distal view. One line is almost parallel to the X-axis, the other makes an angle with the Y-axis, anti-clockwise in distal view.

Colour patterns: In the standard orientation for distal view, the smaller sectors enclosed by the extinction lines are blue, the others are yellow. In the standard orientation for side view, the cross-sections of the rim are blue; the other sections are yellow.

Differential diagnosis: *Zygodiscus* differs from the closely related genus *Lophodolithus* in the absence of a flange. Species of *Pontosphaera* show a similar extinction and colour pattern, but they lack a complex bar.

Zygodiscus clausus nov. sp.
(pl. 10, figs. 3, 4)

Derivation of name: From claudere (lat.): to close.

Description: The species is composed of a closed, elliptical plate, which is somewhat thickened marginally, and a wide, bar-like central structure. This bar is well differentiated from the plate only at its poles; centrally it seems to be continuous with the plate. In early specimens the bar makes a small angle with the X-axis in clockwise direction; in later specimens the angle increases to such an extent that the bar makes a small angle with the Y-axis in anti-clockwise direction.
Differential diagnosis: This species differs from all others in the genus by its closed central area.
Dimensions: length: 10–13 μ.
Holotype: T 369a, pl. 10, fig. 3 from sample SP619, *D. mohleri* Zone.
Type locality: Barranco del Gredero.
Stratum: Jorquera Formation, Member C.
Age: Middle Paleocene.
Paratypoid: T 369b, pl. 10, fig. 4, sample SP619.
Distribution: Spain: *D. mohleri* Zone.

Zygodiscus adamas Bramlette and Sullivan
(pl. 10, fig. 5)

Zygodiscus adamas Bramlette and Sullivan, 1961, p. 148, pl. 4, figs. 9, 10; Sullivan, 1964, p. 186, pl. 6, figs. 4–6; Hay and Mohler, 1967a, p. 1532, pl. 198, figs. 3, 4, 7; pl. 199, figs. 8–10.
Non *Zygodiscus adamas* Bramlette and Sullivan, Stradner, in Gohrbandt, 1963, p. 76, pl. 9, figs. 13, 14.

Remarks: The diamond-shaped central cross-structure is characteristic of the species. The structure consists of an upper and a lower lath, which cross in the centre. The upper lath makes an angle of about 40° with the Y-axis in anti-clockwise direction; the lower lath forms about the same angle with this axis in the opposite direction. This construction can best be observed in cross-polarized light; in the standard orientation for distal view, and with the gypsum plate, the upper lath is yellow, and the tips of the lower one are blue.

In early specimens the openings at each side of the central structure are small, and the marginal ridge is low. In later forms the openings are wider, and the ridge is higher.
Dimensions: length: 10–13 μ.
Distribution: Spain: *D. mohleri* Zone, *D. multiradiatus* Zone.

Zygodiscus plectopons Bramlette and Sullivan
(pl. 10, fig. 6)

Zygodiscus plectopons Bramlette and Sullivan, 1961, p. 148, pl. 4, fig. 12; Sullivan, 1964, p. 187, pl. 5, fig. 8; Sullivan, 1965, p. 38, pl. 6, fig. 7.

Zygodiscus aff. *Z. plectopons* Bramlette and Sullivan, 1961, p. 158, pl. 4, fig. 13.
Zygodiscus herlyni Sullivan, 1964, p. 168, pl. 6, figs. 1–3.

Remarks: The plate-openings at each side of the bar are larger in later forms than in earlier ones. At its edge the plate curves in distal direction to form a wall. In later specimens the wall is thickened, probably by an outer cycle of elements (rim).
Dimensions: length: 8–14 μ.
Distribution: Spain: *D. mohleri* Zone – *T. orthostylus* Zone; Israel: *T. contortus* Zone – *T. orthostylus* Zone.

Genus **Neochiastozygus** Perch-Nielsen, 1971

Type species: *Neochiastozygus perfectus* Perch-Nielsen, 1971
Description:

Shape: The species have the form of shallow baskets, which are elliptical in plane view. The smaller, slightly concave side is considered to be proximal.

Construction: The species are composed of a relatively narrow, composite margin, and a central cross-structure that bridges the open central area along the Y-axis.

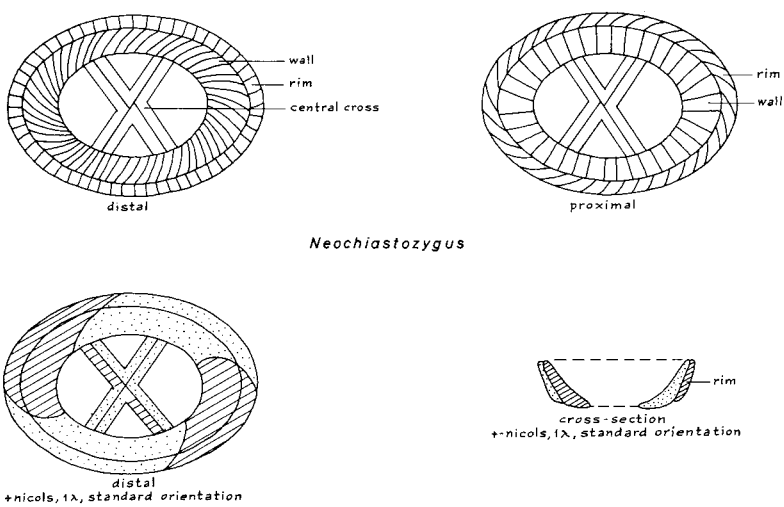

Margin: This structure consists of an inner cycle of elements (wall) and an outer one (rim). These cycles are closely appressed, and they show an equal number of elements.

Wall: The elements in the inwards sloping wall show a strong, clockwise imbrication in distal view. The elements are widest at the base and taper in

distal direction. In proximal view the sutures between the elements are subradial.

Rim: The rim which also slopes inwards is generally narrower than the wall. In most species it is composed of lath-like elements, which strongly imbricate counter-clockwise in distal view. The rim does not extend in proximal direction as far as the wall.

Central structure: The structure generally has the form of an X. It is attached to the lower distal side of the wall. Generally, each bar of the X is composed of two laths, parallel to the axis of the bar.

Specific criteria: The species are based on (a) the relative proportions of the wall and the rim, (b) the construction of the rim, (c) the shape, construction and orientation of the cross-structure.

Standard orientations:

Distal view: X-axis parallel to the X-cross-hair; widest side of the margin upwards.

Side view: X-axis parallel to the X-cross-hair; widest side of the margin in the positive direction of the Y-cross-hair.

Extinction lines: The extinction lines can best be observed in the wall. Here they are dextrogyre in distal view. The bars of the cross-structure show a median extinction line, which gives them a split appearance.

Colour patterns: In the standard orientation for distal view the wall-sectors lying along the X-axis and enclosed by the extinction lines are blue; the other sectors in the wall are yellow.

In the same orientation, the bars which make an angle with the Y-axis in anti-clockwise direction are evenly blue, the others are yellow.

In the standard orientation for side view, the left cross-section of the wall, and the right cross-section of the rim are blue; the other sections are yellow.

Differential diagnosis: In *Neococcolithes,* the margin consists of only a single cycle of elements, and the cross-bars have a non-split appearance in cross-polarized light.

Neochiastozygus denticulatus (Perch-Nielsen) Perch-Nielsen

Heliorthus? denticulatus Perch-Nielsen, 1969b, p. 62, pl. 5, fig. 5.
Neochiastozygus denticulatus (Perch-Nielsen) Perch-Nielsen, 1971b, p. 60, pl. 6, fig. 7; pl. 7, figs. 10–12.

Remarks: The orientation of the rather wide cross-bars make this species easily recognizable: in distal view the bars make a small angle with the axes of the ellipse in counter-clockwise direction.

Dimensions: length: 5–6 μ.

Distribution: Spain: *P. dimorphosus* Zone – *C. tenuis* Zone; Israel: *P. dimorphosus* Zone – *C. tenuis* Zone; Scandinavia: *C. tenuis* Zone.

Neochiastozygus modestus Perch-Nielsen

Neochiastozygus modestus Perch-Nielsen, 1971b, p. 62, pl. 5, figs. 5–8; pl. 7, figs. 22, 23; Perch-Nielsen, 1977, pl. 38, fig. 11; pl. 39, figs. 1, 3, 4, 6, 9; pl. 40, figs. 7–10.

Remarks: Distally, the wall and the rim are about the same height. The wall is somewhat wider than the rim. Each bar of the central cross is composed of two laths, parallel to the axis of the bar.
Dimensions: length: 4–6 μ.
Distribution: Spain: *P. dimorphosus* Zone – *F. tympaniformis* Zone; Israel: *C. tenuis* Zone – *F. tympaniformis* Zone.

Neochiastozygus saepes Perch-Nielsen

Heliorthus? distentus (Bramlette and Sullivan) Perch-Nielsen, 1969b, p. 63, pl. 5, fig. 9.
Neochiastozygus saepes Perch-Nielsen, 1971b, p. 64, pl. 6, figs. 3–6; pl. 7, figs. 7–9.

Remarks: Typical specimens have a serrated, subelliptical outline in plane view. The wall is low and narrow; the rim is high and wide and is composed of elements separated by subvertical sutures. The relatively narrow central area is spanned by an X-like cross-structure.
Dimensions: length: 6–8 μ.
Distribution: Spain: *C. tenuis* Zone; Israel: *C. tenuis* Zone.

Neochiastozygus aff. N. saepes Perch-Nielsen

Zygolithus concinnus Martini, Stradner, 1963, partim, pl. 4, fig. 8a, non pl. 4, fig. 8b.

Remarks: These forms have a paperclip-like outline in plane view. The wall and the rim are about the same width, but the rim is higher. The rim consists of block-like elements, separated by subvertical sutures. The cross-bars form a wide X.
Dimensions: length: 5–7 μ.
Distribution: Spain: *C. tenuis* Zone, *E. macellus* Zone; Israel: *C. tenuis* Zone, *E. macellus* Zone.

Neochiastozygus imbriei Haq and Lohmann

Neochiastozygus imbriei Haq and Lohmann, 1976, p. 183, pl. 4, fig. 3; Perch-Nielsen, 1977, pl. 38, figs. 5, 9; pl. 49, figs. 20, 21.

Remarks: This long-elliptical species has a low, narrow wall and a high rim.

The latter is composed of lath-like elements, separated by subvertical sutures. In typical specimens, the narrow bars make a small angle with the X-axis. Forms that are intermediate between this species and *Neochiastozygus* aff. *N. saepes* occur in the *C. tenuis* Zone.

N. imbriei differs from *N. denticulatus* in its narrower cross-bars, which all make a high angle with the Y-axis.

Dimensions: length: 5–7 μ.

Distribution: Spain: *C. tenuis* Zone; Israel: *C. tenuis* Zone.

Neochiastozygus perfectus Perch-Nielsen

Neochiastozygus perfectus Perch-Nielsen, 1971b, p. 63, pl. 6, figs. 1, 2; pl. 7, figs. 24, 25; Perch-Nielsen, 1977, pl. 38, figs. 6, 10, 12.

Remarks: Distally, the rim is higher and narrower than the wall. In the L.M. this feature can best be observed in cross-polarized light, and with the gypsum plate. Typical specimens have a slender X-like cross-structure, composed of bars which are slightly thickened near the wall.

Dimensions: length: 7–9 μ.

Distribution: Scandinavia: *C. tenuis* Zone, *E. macellus* Zone.

Neochiastozygus distentus (Bramlette and Sullivan) Perch-Nielsen

Zygolithus distentus Bramlette and Sullivan, 1961, p. 150, pl. 6, figs. 4–7.

Non *Zygolithus distentus* Bramlette and Sullivan, Stradner, 1963, p. 77, pl. 10, figs. 4, 5.

Non *Heliorthus distentus* (Bramlette and Sullivan) Perch-Nielsen, 1969b, p. 63, pl. 5, fig. 9.

Neochiastozygus distentus (Bramlette and Sullivan) Perch-Nielsen, 1971b, p. 61, pl. 4, figs. 1–4; pl. 7, figs. 1–3; Perch-Nielsen, 1977, pl. 38, figs. 3, 4, 8; pl. 39, figs. 2, 5, 8; pl. 40, figs. 1–3.

Remarks: The species has a wide wall and a narrow rim. Characteristic for the species are the wide bars of the central cross; specimens occur in which the bars close the central area.

Dimensions: length: 7–10 μ.

Distribution: Spain: *F. tympaniformis* Zone – *T. contortus* Zone; Israel: *F. tympaniformis* Zone – *T. contortus* Zone.

Neochiastozygus concinnus (Martini) Perch-Nielsen

Zygolithus concinnus Martini, 1961, p. 18, pl. 3, fig. 35; pl. 5, fig. 54; Bramlette and Martini, 1964, p. 304, pl. 4, figs. 13, 14; pl. 7, fig. 3.

Zygolithus chiastus Martini, Bramlette and Sullivan, 1961, p. 149, partim, pl. 6, fig. 1, non pl. 6, figs. 2, 3.

Zygolithus distentus Bramlette and Sullivan, Stradner, 1963, p. 77, pl. 10, figs. 4, 5.

Heliorthus concinnus (Martini) Hay and Mohler, 1967a, p. 1533, pl. 199, figs. 16–18; pl. 201, figs. 6, 7, 10; Perch-Nielsen, 1969b, p. 62, pl. 5, figs. 6–8.

Neochiastozygus concinnus (Martini) Perch-Nielsen, 1971b, p. 59, pl. 4, fig. 6; pl. 7, figs. 4–6.

Remarks: In this species the cross-structure has the form of a narrow X. In typical specimens the bars are slender and somewhat thickened near the wall. In the L.M. a more or less rectangular structure can be observed in the centre of the cross. The wall and the rim can be well differentiated in cross-polarized light.
Dimensions: length: 7–10 μ.
Distribution: Spain: *F. tympaniformis* Zone – *T. contortus* Zone; Israel: *T. contortus* Zone.

Neochiastozygus junctus (Bramlette and Sullivan) Perch-Nielsen

Zygolithus junctus Bramlette and Sullivan, 1961, p. 150, pl. 6, fig. 11; Sullivan, 1964, p. 187, pl. 7, fig. 15.
Heliorthus junctus (Bramlette and Sullivan) Hay and Mohler, 1967a, p. 1533; Stradner, 1969, p. 418, pl. 87, figs. 9–12.
Neochiastozygus junctus (Bramlette and Sullivan) Perch-Nielsen, 1971b, p. 61, pl. 4, figs. 7, 8; pl. 7, figs. 18, 19; Edwards and Perch-Nielsen, 1975, pl. 1, fig. 9.

Remarks: The wall of this species, the largest species of *Neochiastozygus,* is wide but the rim is narrow. In addition to its large size, the species is characterized by the small angle which the bars of the cross make with the Y-axis. The bar-elements are orientated normal to the bar-axes. In cross-polarized light the bars have a split appearance.
Dimensions: length: 11–13 μ.
Distribution: Spain: *F. tympaniformis* Zone – *D. multiradiatus* Zone; Israel: *D. mohleri* Zone.

Genus **Neococcolithes** Sujkowski, 1931

Type species: *Neococcolithes lososnensis* Sujkowski, 1931
Description:

Shape: The species are narrow elliptical in plane view, and have the form of a truncated cone in side view; the side with the smaller diameter is considered to be proximal.

Construction: The species are composed of a distally flaring margin and an X- or H-shaped central structure, which spans the open central area along the Y-axis.

Margin: The margin consists of a low wall, superposed by a high rim. These cycles have an equal number of elements.

Wall: This very thin cycle has a triangular cross-section. The sutures are radial in proximal view.

Rim: This high cycle is constructed of anti-clockwise imbricating, lath-like elements.

Central structure: The structure consists of several homogeneous calcite blocks.
Specific criteria: The species are differentiated on the basis of the outline of the coccolith and the shape of the central structure.
Standard orientations:

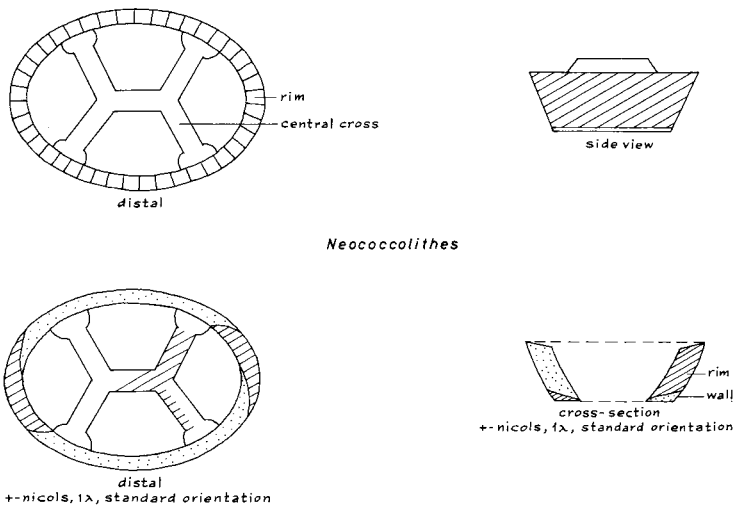

Distal view: X-axis parallel to the X-cross-hair; widest side of the coccolith turned upwards.

Proximal view: X-axis parallel to the X-cross-hair; widest side pointing in the positive direction of the Y-cross-hair.

Extinction lines: These lines can be observed only in the margin; they are strongly dextrogyre in distal view.

Colour patterns: In the standard orientation for distal view, the smaller sectors in the margin which are enclosed by the extinction lines are blue; the other sectors are yellow.

In the central structure the colours are vague; the right half of the structure is bluish, the other half yellowish in the standard orientation for distal view.

In the standard orientation for side view, the right cross-section of the rim is blue, the other is yellow; the colours in the wall are probably reversed.

Differential diagnosis: *Neococcolithes* differs from *Neochiastozygus* in the construction of the central structure and in the composition of the margin, the latter containing two superposed cycles instead of two enclosing ones.

Neococcolithes protenus (Bramlette and Sullivan) Hay and Mohler

Zygolithus protenus Bramlette and Sullivan, 1961, p. 150, pl. 6, fig. 15.
Chiphragmalithus protenus (Bramlette and Sullivan) Sullivan, 1964, p. 179, pl. 1, fig. 1.
Neococcolithes protenus (Bramlette and Sullivan) Hay and Mohler, 1967, p. 1533, pl. 199, figs. 19–21; pl. 201, fig. 9; Edwards and Perch-Nielsen, 1975, pl. 1, fig. 11; pl. 3, fig. 11; pl. 6, figs. 7, 8; pl. 8, fig. 6; pl. 9, fig. 4.
Non *Neococcolithes protenus* (Bramlette and Sullivan) Hay and Mohler, Perch-Nielsen, 1969b, p. 64, pl. 5, fig. 4.

Remarks: Typical specimens show a narrow margin and a slender, X-shaped cross-structure. Variants with a somewhat wider margin and central cross occur in the *T. orthostylus* Zone; they are pobably transitional to *N. dubius*.
Dimensions: length: 5–7 μ.
Distribution: Spain: *D. multiradiatus* Zone – *D. sublodoensis* Zone; Israel: *T. contortus* Zone – *T. orthostylus* Zone.

Neococcolithes dubius (Deflandre) Black

Zygolithus dubius Deflandre, in Deflandre and Fert, 1954, p. 149, text-figs. 43, 44, 68; Perch-Nielsen, 1967, p. 28, pl. 5, figs. 13, 14.
Chiphragmalithus dubius (Deflandre) Sullivan, 1964, p. 179, pl. 1, fig. 2.
Neococcolithes dubius (Deflandre) Black, 1967, p. 143; Perch-Nielsen, 1977, pl. 27, fig. 6.
Zygolithus pediculatus Perch-Nielsen, 1967, p. 29, pl. 5, figs. 8–11.
Zygolithus pyramidus Perch-Nielsen, 1967, p. 29, pl. 5, figs. 1–5.
Neococcolithes pediculatus (Perch-Nielsen) Perch-Nielsen, 1971d, p. 48, pl. 40, figs. 4–6; pl. 42, figs. 16–18.
Neococcolithes pyramidus (Perch-Nielsen) Perch-Nielsen, 1971d, p. 48, pl. 42, fig. 13.

Remarks: In this relatively high species the H-shaped central structure is higher than the margin. The central part of the structure makes a small angle in clockwise direction with the X-axis in distal view. Specimens with a thickened margin and/or a thickened central structure are regarded as variants, not as separate species.
Dimensions: length: 7–9 μ.
Distribution: Spain: *T. orthostylus* Zone – *N. fulgens* Zone; Israel: *T. orthostylus* Zone – *D. sublodoensis* Zone.

Neococcolithes minutus (Perch-Nielsen) Perch-Nielsen

Zygolithus minutus Perch-Nielsen, 1967, p. 28, pl. 5, figs. 6, 7.
Neococcolithes minutus (Perch-Nielsen) Perch-Nielsen, 1971, p. 47, pl. 42, figs. 1–4.

Remarks: This species differs from *N. dubius* only in its more narrow elliptical outline.
Dimensions: length: 6–8 μ.
Distribution: Spain: *D. sublodoensis* Zone, *N. fulgens* Zone.

Genus **Lophodolithus** Deflandre, 1954

Type species: *Lophodolithus mochlophorus* Deflandre, 1954

Description:

Shape: The species have an ovoid or kidney-shaped outline in plane view and a wedge-shaped outline in distal view. The widest side of the specimens is considered to be distal.

Construction: The species are composed of a margin (which forms a narrow central plate proximally, and a flange distally) and a complex bar.

Margin: The distally flaring margin is composed of an inner cycle (wall) and an outer one (rim).

Wall: This cycle is a continuation of the central plate in distal direction. It is constructed of lath-like elements, which imbricate clockwise in distal view.

Rim: The base of this cycle lies somewhat above the level of the central plate. The cycle is composed of lath-like elements which imbricate counter-clockwise in distal view.

Flange: This structure is a continuation of the wall and the rim in outward-lateral direction. In distal view the sutures in the distal flange cycle are slightly oblique clockwise; the sutures in the proximal cycle are oblique clockwise in proximal view.

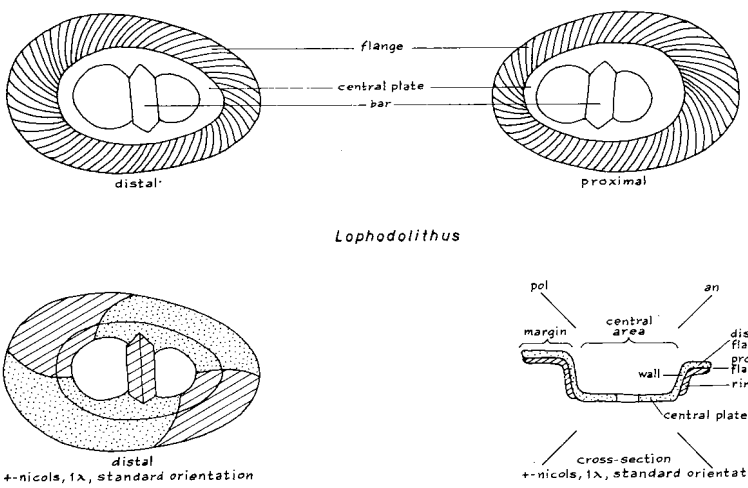

Central area: The open central area is surrounded by a narrow strip of the central plate, which consists of radially arranged elements. The central area is bridged along the Y-axis by a complex bar, which divides the area into two subcircular openings of unequal size. The bar shows an axial suture and is connected to the central plate along a V-shaped suture.

The margin is highest and the flange is widest at the side with the larger opening in the central area.

Specific criteria: The species are distinguished on the basis of the outline of the coccolith in plane view and according to the shape of the flange.

Standard orientations:

Distal view: X-axis parallel to the X-cross-hair in such a way that the highest part of the margin (or the widest side of the flange) is on the left, and the widest side of the coccolith turned upwards.

Side view: X-axis forming an angle of 45° in clockwise direction with the X-cross-hair in such a way that the normal to the distal side points to the right.

Extinction lines: These lines are sharper in the central plate than in the margin. They are dextrogyre in distal view. In the standard orientation for distal view, one line makes a small angle with the X-axis in clockwise direction; the other makes a somewhat larger angle in counter-clockwise direction with the Y-axis.

Colour patterns: In the standard orientation for distal view, the smaller sectors enclosed by the extinction lines are blue; the other sectors are yellow. In the standard orientation for side view, the central plate, the wall and the distal flange cycle are yellow; the rim and the proximal flange cycle are blue.

Differential diagnosis: *Lophodolithus* differs from the closely related *Zygodiscus* in the presence of a flange. The differences between this genus and *Pontosphaera* are given under *Pontosphaera.*

Lophodolithus nascens Bramlette and Sullivan
(pl. 8, fig. 4)

Lophodolithus nascens Bramlette and Sullivan, 1961, p. 145, pl. 4, figs. 7, 8; Perch-Nielsen, 1971, p. 41, pl. 37, figs. 1–4.

Lophodolithus cf. *L. nascens* Bramlette and Sullivan, Perch-Nielsen, 1977, pl. 27, fig. 7; pl. 28, fig. 5.

Remarks: The composite bar makes a small angle with the Y-axis in counter-clockwise direction in distal view. The width of the flange is variable. Intermediate forms between this species and *Z. plectopons* were observed in the *T. orthostylus* Zone.

Dimensions: length: 8–14 μ.

Distribution: Spain: *T. orthostylus* Zone – *D. sublodoensis* Zone; Israel: *T. orthostylus* Zone – *D. sublodoensis* Zone.

Lophodolithus mochlophorus Deflandre

Lophodolithus mochlophorus Deflandre, 1954, p. 147, pl. 12, figs. 20–23; Bramlette and Sullivan, 1961, p. 145, pl. 4, fig. 6; Perch-Nielsen, 1971d, p. 40, pl. 38, fig. 1; Wise and Constans, 1976, pl. 3, fig. 1.

Remarks: This species has a flange along its total periphery. In the standard orientation for distal view, the margin is higher, and the flange at the left pole is wider than in *L. nascens.*

The flange is crenulated where it is widest.

Dimensions: length: 17–19 μ.

Distribution: Spain: *T. orthostylus* Zone – *D. sublodoensis* Zone; Israel: *D. sublodoensis* Zone.

Lophodolithus reniformis Bramlette and Sullivan

Lophodolithus reniformis Bramlette and Sullivan, 1961, p. 135, pl. 4, fig. 5; Perch-Nielsen, 1971d, p. 41, pl. 38, figs. 2, 3.

Remarks: This species differs from *L. nascens* in its kidney-shaped outline. This shape is mainly the result of the unequal width of the flange.

Dimensions: length: 8–11 μ.

Distribution: *T. orthostylus* Zone; Israel: *T. orthostylus* Zone.

Genus Helicosphaera Kamptner, 1954

Type species: *Coccolithus carteri* (Wallich) Kamptner, 1941

Introduction: In the present paper the opinion of Jafar and Martini (1975) about the name of this genus is shared: their re-examination of the original description of the (extant) "*Coccosphaera*" *carteri* Wallich, 1877, gave strong evidence that *Helicopontosphaera* Hay and Mohler, 1967 is a junior synonym of *Helicosphaera.*

Description:

Shape: The species have an elliptical or ovoid outline in plane view, and they are convaco-convex in side view. The convex side is considered distal.

Construction: The species are composed of a composite, concavo-convex margin which spirals counter-clockwise in distal view, a narrow central plate, and a central bar.

Margin: This complicated structure consists of a distal cycle (wall) and a proximal cycle (rim), which are closely appressed.

Wall: This cycle is a continuation of the central plate. It shows strongly clockwise imbricating elements in distal view. The sutures are subradial in this view.

Rim: The base of this cycle lies at a somewhat higher level than the base of the central plate. The cycle spirals counter-clockwise in distal view, in such a way that it overlaps itself over a short interval. The sutures are oblique clockwise in proximal view.

Central plate: This plate is very narrow and lines the central openings. It

is composed of a single cycle of radially orientated elements. The sutures are radial in both proximal and distal view.

Central bar: This structure shows an axial suture. It is connected to the central plate along a V-like suture. The bar invariably makes an angle in counter-clockwise direction with the Y-axis in distal view.

The margin is wider and more strongly curved at one pole than at the other.

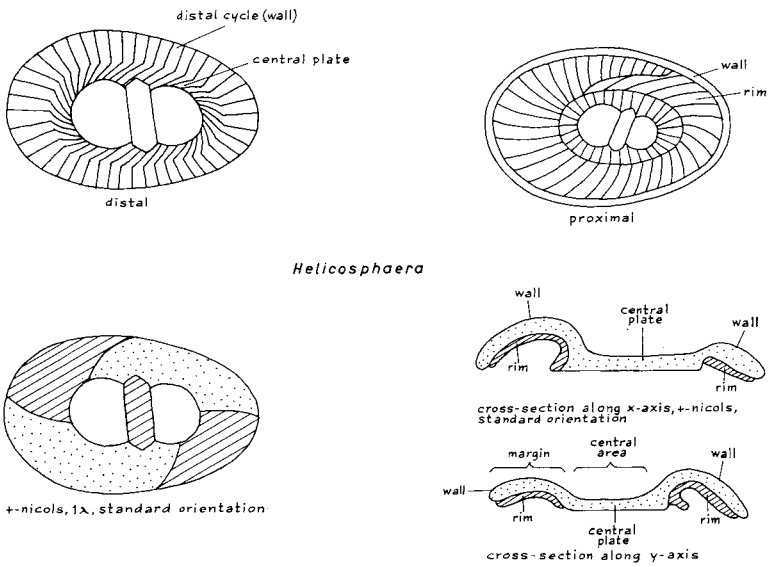

Specific criteria: Criteria for distinguishing species are the outline of the coccoliths in plane view and the composition of the central area.

Standard orientations:

Distal view: Convex side of the margin upwards; X-axis parallel to the X-cross-hair in such a way that the pole where the margin is widest points to the left.

Side view: X-axis parallel to the X-cross-hair as described above; convex side of the coccolith pointing in the positive direction of the Y-crosshair.

Extinction lines: In the standard orientation for distal view, the lines are dextrogyre. The position of the lines is comparable to their position in *Lophodolithus* and *Zygodiscus*.

Colour patterns: In the standard orientation for distal view the smaller sectors enclosed by the extinction lines are blue; the other sectors are yellow. In the standard orientation for side view, the cross-section of the rim are blue, and the sections of the central plate and the wall are yellow.

Differential diagnosis: *Helicosphaera* differs from *Zygodiscus* and *Lophodolithus* in its concavo-convex margin.

Helicosphaera seminulum Bramlette and Sullivan

Helicosphaera seminulum seminulum Bramlette and Sullivan, 1961, p. 144, pl. 4, figs. 1, 2; Perch-Nielsen, 1967, p. 25, pl. 3, figs. 4, 5.
Helicosphaera seminulum Bramlette and Sullivan, Hay and Towe, 1962, p. 512, pl. 1, figs. 1, 3, 5.
Non *Helicosphaera seminulum* Bramlette and Sullivan, Stradner and Edwards, 1968, p. 38, pl. 39, 40.
Helicopontosphaera seminulum (Bramlette and Sullivan) Stradner, 1969, p. 419, pl. 87, figs. 19, 20; Perch-Nielsen, 1971d, p. 44, pl. 34, fig. 4; pl. 35, figs. 1, 2, 5, 6; pl. 37, figs. 6; Haq, 1973b, p. 46, pl. 1, fig. 4; pl. 3, figs. 7, 8; Wise and Constans, 1976, pl. 1, fig. 1.

Remarks: The species has a smooth, ovoid outline in plane view. The open central area is transversely spanned by a bar, in such a way that a large opening is formed at the left side and a smaller one at the right side (in standard orientation).

Intermediate forms between this species and *H. lophota,* in which the bar makes a high angle with the Y-axis, occur in the *D. lodoensis* Zone.
Dimensions: length: 10–13 μ.
Distribution: Spain: *T. orthostylus* Zone – *N. fulgens* Zone; Israel: *T. orthostylus* Zone – *D. sublodoensis* Zone.

Helicosphaera lophota Bramlette and Sullivan

Helicosphaera seminulum lophota Bramlette and Sullivan, 1961, p. 144, pl. 4, figs. 3, 4; Perch-Nielsen, 1967, p. 25, pl. 3, figs. 1–3.
Helicosphaera seminulum Bramlette and Sullivan, Stradner and Edwards, 1968, p. 38, pl. 39, 40.
Helicopontosphaera lophota (Bramlette and Sullivan) Perch-Nielsen, 1971d, p. 43, pl. 34, figs. 1, 2; pl. 36, figs. 1, 2; Haq, 1973b, p. 40, pl. 1, figs. 1–3; pl. 3, figs. 9, 10; Wise and Constans, 1976, pl. 4, fig. 2.

Remarks: The species differs from *H. seminulum* in the orientation of the central bar: it makes a small angle with the X-axis in clockwise direction in distal view. As a consequence the openings at each side of the bar are long and narrow.
Dimensions: length: 10–15 μ.
Distribution: Spain: *D. lodoensis* Zone – *N. fulgens* Zone; Israel: *D. lodoensis* Zone – *D. sublodoensis* Zone.

Family SPHENOLITHACEAE Vekshina, 1959

Genus **Sphenolithus** Deflandre, 1952

Type species: *Sphenolithus radians* Deflandre, 1952

Description:

Shape: The species have the form of a dome or cone with a concave base. The pointed or convex side is considered distal, the concave side proximal.

Construction: The species are composed of a relatively low, basal column, superposed by a cone, which may be differentiated into one or more basal cycles and a centro-distal spine.

Column: The column has the form of a truncated cone with a flat top and a concave base. It is composed of 9 to 13 radially arranged elements, which have a triangular cross-section. The sutures are subradial in proximal view.

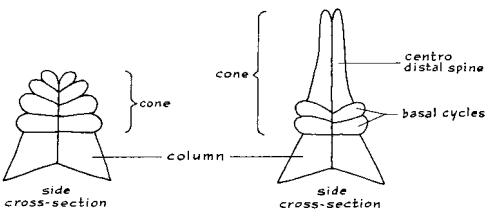

Sphenolithus

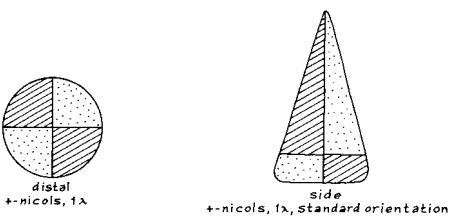

Cone: The composition of this structure is rather variable. Basically it consists of one or more superposed cycles of wedge-shaped, radially arranged elements. The diameter of these cycles and the number of elements in them decrease upwards in the nannolith.

Specific criteria: The species are distinguished according to features such as the form and construction of the cone, the relative proportions of the column and the cone, and the angle between the extinction lines in side view.

Standard orientations:

Distal view: Pointed or convex side upwards; concave side downwards.

Side view: Convex or pointed side in the positive direction of the Y-cross-hair; base parallel to the X-cross-hair.
Extinction lines: In the standard orientation for distal view, the lines are parallel to the polarization directions, and they bisect in the centre of the nannolith. In the standard orientation for side view, two lines can be observed: (a) a median line, which is straight in most species, and (b) a line between the column and the cone. The latter line is straight, and perpendicular to the median line, or it is irregular and not normal to the median line.
Colour patterns: In the standard orientation for distal view, the second and the fourth quadrant are blue, the others are yellow.

In the standard orientation for side view, the right half of the column and the left half of the cone are blue; the other halves are yellow.
Differential diagnosis: *Sphenolithus* can easily be distinguished from *Fasciculithus* in the L.M. by the opposite colour distribution in the standard orientation for side view.

Sphenolithus primus Perch-Nielsen

Sphenolithus primus Perch-Nielsen, 1971c, p. 357, pl. 11, fig. 4; pl. 12, figs. 4, 5, 7–12; pl. 14, figs. 22–24; Perch-Nielsen, 1972, pl. 16, fig. 10.
Sphenolithus sp. Perch-Nielsen, 1971c, p. 359, pl. 11, figs. 1–3, 5, 6.

Remarks: The low column of this beehive-shaped species is composed of 7 to 11 elements. The cone is somewhat higher than the dome; it consists of three to four superposed cycles of radially arranged, irregular elements. The number of elements in these cycles decreases in distal direction.
Dimensions: diameter: 5–7 μ., height: 4–8 μ.
Distribution: Spain: *E. macellus* Zone – *D. binodosus* Zone; Israel: *E. macellus* Zone – *D. binodosus* Zone.

Sphenolithus anarrhopus Bukry and Bramlette

Sphenolithus anarrhopus Bukry and Bramlette, 1969, p. 140, pl. 3, figs. 5–8.
Sphenolithus sp. 1 Perch-Nielsen, 1971c, p. 358, pl. 12, figs. 1, 6.
Sphenolithus sp. 2 Perch-Nielsen, 1971c, p. 359, pl. 12, figs. 2, 3.
Sphenolithus cf. *S. radians* Deflandre, Haq, 1971a, p. 34, pl. 10, fig. 9.

Remarks: The species differs from *S. primus* in the further distal projection of one of the elements in the centre of the cone. In the standard orientation for side view, the median extinction line bifurcates to the left and to the right in the cone.
Dimensions: diameter: 4–6 μ., height: 5–7 μ.
Distribution: Spain: *H. kleinpellii* Zone, *D. mohleri* Zone; Israel: *D. mohleri* Zone.

Sphenolithus radians Deflandre
(pl. 7, fig. 9)

Sphenolithus radians Deflandre, in Grassé, 1952, p. 466, fig. 343, J-K; fig. 363, A-G; Perch-Nielsen, 1971d, p. 53, pl. 47, figs. 1–9; pl. 48, figs. 1–7; Perch-Nielsen, 1977, pl. 31, fig. 8.

Remarks: The low column is composed of 7 to 11 elements. The basal part of the cone consists of 2 to 4 cycles of basically wedge-shaped elements. The upper part of the cone is formed of about four, radially arranged, blade-like elements. In early specimens these blades are not as high as in later ones.
Dimensions: diameter: 4–6 μ., height: 6–10 μ.
Distribution: Spain: *T. contortus* Zone – *N. fulgens* Zone; Israel: *T. contortus* Zone – *D. sublodoensis* Zone.

Sphenolithus spiniger Bukry

Sphenolithus spiniger Bukry, 1971, p. 321, pl. 6, figs. 10–12; pl. 7, figs. 1, 2; Perch–nielsen, 1977, pl. 31, figs. 6, 7 (?).

Remarks: In this species the column is higher than the cone. The lower part of the cone shows two superposed cycles of radially arranged wedges; these surround three or four subvertical, short, central blades. Specimens have an equilateral-triangular outline in side view.
Dimensions: diameter: 4–5 μ., height: 4–7 μ.
Distribution: Spain: *N. fulgens* Zone.

Sphenolithus furcatolithoides Locker

Sphenolithus furcatolithoides Locker, 1967, p. 363, pl. 1, figs. 14–16; text-figs. 7, 8; Perch-Nielsen, 1971d, p. 53, pl. 49, figs. 1–4; Perch-Nielsen, 1977, pl. 31, figs. 2–5.

Remarks: The species has a low column. The cone is composed of a low basal cycle, and two high, blade-like central elements, which are joined at their base, but which diverge distally. In our material the free, outwards bending parts are generally broken off.
Dimensions: height: 5–8 μ.
Distribution: Spain: *N. fulgens* Zone.

Sphenolithus obtusus Bukry

Sphenolithus obtusus Bukry, 1971, p. 321, pl. 6, figs. 1–9; Perch-Nielsen, 1977, pl. 31, fig. 1.

Remarks: The species is composed of a low column and a high cone. The basal cycle of the cone is very thin and hardly observable in the L.M. The distal part seems to be composed of four blades, which are normal to each

other. The species owes its name to the obtuse angle formed by the extinction lines between the column and the cone in side view.
Dimensions: height: 6–12 μ.
Distribution: Spain: *N. fulgens* Zone.

Family FASCICULITHACEAE Hay and Mohler, 1967

Genus **Fasciculithus** Bramlette and Sullivan, 1961

Type species: *Fasciculithus involutus* Bramlette and Sullivan, 1961
Description:

Shape: The species have the form of a massive cylinder. One side of the cylinder is pointed or convex; the other side shows a conical depression. The latter side is considered to be proximal, the other distal. The species show radial symmetry.

Construction: Most species are composed of a high or a low column, superposed by a high or low cone.

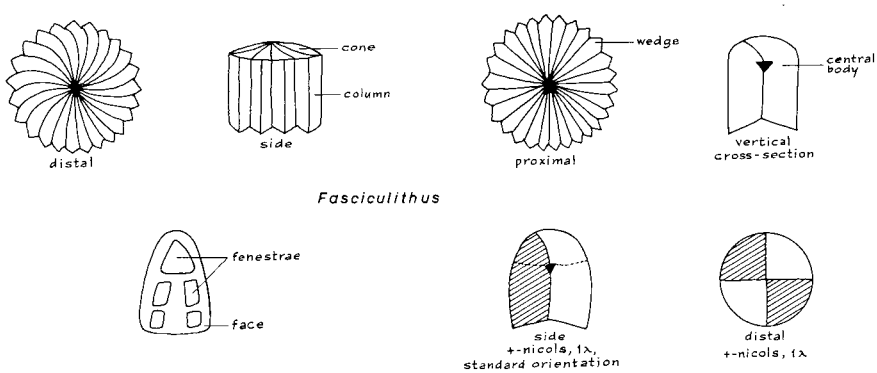

Column: This structure consists of radially arranged, high, wedge-shaped elements. The outer surface of each wedge shows a median ridge over the total height, which gives the column a rosette-like outline in plane view. All wedges have the same length, or groups of longer and shorter ones alternate. In the latter case the species have a star-like outline in plane view, and on the sides of the column slightly concave, larger *faces* are formed. In these faces smaller or larger holes may occur, which are here called *fenestrae*. A common configuration of these fenestrae is given above. Distally the column is slightly concave.

Many species show a conical or diamond-shaped body in the distal centre of the column. This *central body* can only be observed in side view in the

L.M.; it is dark in cross-polarized light.

Cone: This structure may have the form of a cone, a dome or a spine. It is composed of clockwise imbricating (or spiralling) elements. Generally, their number is lower than the number in the column. The sutures are laevogyre in distal view.

Specific criteria: The species are based on the morphology and the composition of the column and the cone.

Standard orientations:

Distal view: Cone upwards, concave side of column downwards.

Side view: Cone pointing in the positive direction of the Y-cross-hair, base of the column parallel to the X-cross-hair.

Extinction lines: In the standard orientation for distal view, the lines are parallel to the cross-hairs, and bisect each other in the centre of the nannolith.

In the standard orientation for side view, a straight median extinction line can be observed in the column and the cone. In some species the line is curved in the cone.

Colour patterns: In the standard orientation for distal view, the second and the fourth quadrant are blue; the others are yellow.

In the standard orientation for side view, the left half of the nannolith is blue, the other half is yellow.

Differential diagnosis: In the L.M., and in plane view, *Fasciculithus* can easily be distinguished from the closely related *Heliolithus* with the aid of the extinction lines; the angle between the lines and the cross-hairs is 0° in *Fasciculithus*, while it is about 20° in *Heliolithus*.

Fasciculithus magnus Bukry and Percival
(pl. 9, fig. 14)

Fasciculithus magnus Bukry and Percival, 1971, p. 131, pl. 4, figs. 9–12; Perch-Nielsen, 1977, pl. 11, figs. 4–12, pl. 49, figs. 10, 16, 22.

Remarks: This large species is composed of a column and a central body only; a well-defined cone is absent. The column consists of 25–35 wedges with a smooth outer surface. The base of the column is slightly concave; at the distal side a deep, conical depression is present. The sutures are radial in proximal view, but in distal view they are oblique counter-clockwise.

The central body, lying at the base of the distal depression, shows an equilateral-triangular cross-section in side view. In the same view, vague incisions can be observed in the inner, upper part of the column.

Dimensions: diameter: 10–12 μ., height: 10–15 μ.

Distribution: Spain: *E. macellus* Zone; Israel: *E. macellus* Zone.

Fasciculithus magnicordis nov. sp.
(pl. 9, figs. 12, 13)

Derivation of name: from magnus (lat.), large, and cors (lat.), heart.
Description: This species is composed of a distally tapering column and a central body. The column consists of 20 to 30 wedges with a smooth outer surface. The proximal side of the column is flat to slightly concave; the distal side is concave. The sutures are slightly oblique anti-clockwise in distal view; in proximal view they are radial.

The central body is relatively large, and it extends from the distal depression to, or almost to the proximal side. In the L.M. the body shows a cut-diamond-like cross-section in side view. In the same view, a vague incision can be observed in the upper, inner part of the column.
Differential diagnosis: *F. magnicordis* can be distinguished from the closely related *F. magnus* by its smaller size, and by its relatively larger central body.
Dimensions: height: 6–8 μ., diameter: 8–10 μ.
Holotype: T 367a, pl. 9, fig. 12, from sample SP609, *E. macellus* Zone.
Type locality: Barranco del Gredero.
Stratum: Jorquera Formation, Member C.
Age: Early Paleocene.
Paratypoid: T 367b, pl. 9, fig. 13, sample SP609.
Distribution: Spain: *E. macellus* Zone.

Fasciculithus ulii Perch-Nielsen
(pl. 4, fig. 7)

Fasciculithus ulii Perch-Nielsen, 1971c, p. 350, pl. 2, figs. 1–4; pl. 14, figs. 17, 18; Perch-Nielsen, 1977, pl. 10, figs. 18–20; pl. 11, figs. 1–3; pl. 49, figs. 23–25.
Fasciculithus cf. *F. ulii* Perch-Nielsen, Roth, 1973, partim, p. 734, pl. 16, fig. 2, non pl. 16, fig. 1.

Remarks: The column and the relatively low cone are composed of 20 to 30 elements. The column has an irregular outer surface. The cone surrounds a depression, at the base of which the central body lies. This body shows an equilateral cross-section in side view. In the same view, vague incisions can be observed in the inner, uppermost part of the column.
Dimensions: diameter: 5–7 μ., height: 5–10 μ.
Distribution: Spain: *E. macellus* Zone, *F. tympaniformis* Zone; Israel: *E. macellus* Zone, *F. tympaniformis* Zone.

Fasciculithus bitectus nov. sp.
(pl. 9, fig. 15)

Derivation of name: "with two roofs" (lat.).

Description: The column of this species consists of 20 to 30 elements with smooth outer surfaces. It tapers slightly in proximal direction, and it shows a conical basal depression. The central body has a triangular cross-section in side view; it is larger in earlier specimens than in later ones.

The cone extends both in distal and lateral direction; it extends to, or almost to the margin of the column. The cone is covered by a convex, centrally depressed, distal cycle of elements. The sutures in this cycle are oblique anti-clockwise in distal view. The diameter of this cycle is larger than that of the column and the cone.

Differential diagnosis: The species differs from *F. janii* in the presence of a distal cycle. It can be distinguished from species of *Heliolithus* by the orientation of the extinction lines in distal or proximal view: in *F. bitectus* they are parallel to the polarization directions, while they make an angle with these in *Heliolithus*.

Dimensions: diameter: 6–8 μ., height: 7–8 μ.

Holotype: T 368a, pl. 9, fig. 15, from sample IR85, *E. macellus* Zone.

Type locality: Nahal Avdat.

Stratum: Taqiye Formation, Lower Marl Member.

Age: Early Paleocene.

Distribution: Spain: *E. macellus* Zone – *F. tympaniformis* Zone; Israel: *E. macellus* Zone – *F. tympaniformis* Zone.

Fasciculithus janii Perch-Nielsen
(pl. 5, fig. 1)

Fasciculithus janii Perch-Nielsen, 1971, p. 352, pl. 5, figs. 1–4; pl. 14, figs. 37–39; Perch-Nielsen, 1977, pl. 12, figs. 2–5, 8–18; pl. 49, fig. 26.

Remarks: The column and the cone are composed of 20 to 30 elements. The column forms an upwards and outwards flaring, distal edge, with anti-clockwise imbricating elements. In the L.M., and in side view, vague incisions can be observed, running inwards from the junction of the edge and the column.

The cone is dome-shaped, and consists of slightly clockwise imbricating elements. The central body shows a triangular cross-section in side view.

F. janii differs from *F. ulii* in the presence of a flaring edge and in the larger diameter of the cone.

Dimensions: diamater: 5–7 μ., height: 6–9 μ.

Distribution: Spain: *F. tympaniformis* Zone; Israel: *E. macellus* Zone, *F. tympaniformis* Zone.

Fasciculithus tympaniformis Hay and Mohler

Fasciculithus tympaniformis Hay and Mohler, in Hay et al., 1967, p. 447, pl. 8, figs. 1–5; pl. 9, figs. 1–5; Perch-Nielsen, 1971c, p. 349, pl. 1, figs. 1–5; Edwards and Perch-Nielsen, 1975, pl. 1, figs. 2–8; pl. 5, figs. 1–3.

Fasciculithus involutus Bramlette and Sullivan, Wind and Wise, 1977, p. 295, pl. 14, fig. 12; pl. 15, figs. 1–6; pl. 16, figs. 1–6; Perch-Nielsen, 1977, pl. 10, figs. 22, 23.

Remarks: The column of this species is composed of 16 to 30 elements with a smooth outer surface. The column is parallel-sided, or it tapers slightly in distal direction.

The low cone consists of clockwise imbricating elements, separated by laevogyre sutures. The number of elements is equal to, or lower than that in the column.

The small central body has a trapezoidal cross-section in side view. It was observed only in early populations of the species.

In typical specimens the median extinction line bends to the left distally in the standard orientation for side view.

Dimensions: diameter: 5–8 μ., height: 6–9 μ.

Distribution: Spain: *F. tympaniformis* Zone – *T. contortus* Zone; Israel: *F. tympaniformis* Zone – *T. contortus* Zone.

Fasciculithus billii Perch-Nielsen

Fasciculithus billii Perch-Nielsen, 1971c, p. 352, pl. 4, fig. 11; pl. 5, figs. 5–10; pl. 14, figs. 31–33.

Remarks: The column and the cone of this species show 20 to 30 elements. The column is parallel-sided, but it has deep furrows.

The cone projects slightly beyond the upper edge of the column.

The central body has a subquadrangular outline in side view. *F. billii* differs from *F. ulii* in its low cone; intermediate forms occur frequently in the *F. tympaniformis* Zone.

Dimensions: diameter: 5–8 μ., height: 5–8 μ.

Distribution: Spain: *F. tympaniformis* Zone; Israel: *F. tympaniformis* Zone.

Fasciculithus clinatus Bukry

Fasciculithus clinatus Bukry, 1971b, p. 318, pl. 4, figs. 8, 9.

Remarks: *F. clinatus* differs from *F. tympaniformis* in its strongly distally tapering sides; typical specimens show an almost triangular outline in side view. In the standard orientation for side view the median extinction line curves to the left or to the right, distally, or it bifurcates to form a V-like pattern.

Intermediate forms between *F. tympaniformis* and *F. clinatus* were observed in the *D. mohleri* Zone.
Dimensions: diameter: 5–6 μ., height: 5–7 μ.
Distribution: Spain: *D. mohleri* Zone, *D. multiradiatus* Zone; Israel: *D. mohleri* Zone, *D. multiradiatus* Zone.

Fasciculithus bobii Perch-Nielsen

Fasciculithus bobii Perch-Nielsen, 1971c, p. 351, pl. 1, fig. 6; pl. 3, figs. 1–6; pl. 14, figs. 34–36.

Remarks: The parallel-sided column of this rare species consists of 20 to 30 wedges. A single cycle of larger fenestrae occurs in the upper part of the column. Each fenestra extends over one or two wedges. The cone is composed of a low number of laevogyre ridges.
Dimensions: diameter: 8–10 μ., height: 8–10 μ.
Distribution: Spain: *D. multiradiatus* Zone; Israel: *D. mohleri* Zone, *D. multiradiatus* Zone.

Fasciculithus tonii Perch-Nielsen

Fasciculithus tonii Perch-Nielsen, 1971c, p. 354, pl. 7, fig. 4; pl. 14, figs. 15, 16.
Fasciculithus mitreus Gartner, 1971, partim, p. 109, pl. 3, figs. 1, 2, 3a, b, non pl. 3, fig. 4.

Remarks: The column of this large, mitre-shaped species is built up of 20 to 30 wedges of unequal length. Groups of longer elements alternate with shorter ones, resulting in a star-like outline in plane view. The column shows two to three superposed cycles of large fenestrae; each fenestra extends over several wedges. The high and wide cone consists of 10 to 15 elements, which spiral clockwise in distal view.
Dimensions: diameter: 12–17 μ., height: 14–17 μ.
Distribution: Spain: *D. multiradiatus* Zone; Israel: *D. multiradiatus* Zone.

Fasciculithus lillianae Perch-Nielsen
(pl. 5, fig. 3)

Fasciculithus lillianae Perch-Nielsen, 1971c, partim, p. 353, pl. 6, fig. 1; pl. 14, figs. 40–42, non pl. 6, fig. 3.

Remarks: This species consists only of a column. This column shows 8 to 12, wide wedges with a smooth outer surface, which twist distally in clockwise direction.
Dimensions: diameter: 6–10 μ., height: 7–11 μ.
Distribution: Spain: *D. multiradiatus* Zone; Israel: *D. multiradiatus* Zone.

Fasciculithus alanii Perch-Nielsen

Fasciculithus alanii Perch-Nielsen, 1971c, p. 355, pl. 7, figs. 1–3; pl. 9, fig. 4; pl. 14, figs. 13, 14.
Fasciculithus lillianae Perch-Nielsen, 1971c, partim, p. 353, pl. 6, fig. 3, non pl. 6, fig. 1; pl. 14, figs. 40–42.

Remarks: The species is easily recognized by its high conical outline. The column, composed of 10 to 15 wedges, has a star-like outline in plane view. The sides of the column show 5 to 7 faces, each with two rows of two to three superposed, smaller fenestrae at the base, and a larger fenestra at the top.

The high cone consists of 10 to 15, clockwise spiralling elements. Intermediate forms between this species and *F. lillianae* occur frequently in the *D. multiradiatus* Zone.

Dimensions: diameter: 6–8 μ., height: 7–9 μ.

Distribution: Spain: *D. multiradiatus* Zone; Israel: *D. multiradiatus* Zone.

Fasciculithus schaubii Hay and Mohler
(pl. 5, fig. 2)

Fasciculithus schaubii Hay and Mohler, 1967a, p. 1536, pl. 203, figs. 2, 4, 7, 10; pl. 204, figs. 1–3, 5–7; Perch-Nielsen, 1971c, p. 354, pl. 7, fig. 6; pl. 9, fig. 1; pl. 14, figs. 25–27; Haq and Lohmann, 1976, pl. 4, figs. 11, 12.
Fasciculithus richardii Perch-Nielsen, 1971c, p. 355, pl. 8, figs. 1–6.
Fasciculithus? sp. Edwards and Perch-Nielsen, 1975, pl. 8, fig. 7.

Remarks: The parallel-sided column of this species has a star-like outline in plane view. Each of the four to six faces on the column show two vertical rows of 3 to 4 fenestrae at the base, and a larger fenestra at the top, over the total width of the underlying rows. The column is composed of 12 to 16 wedge-like elements; etched specimens (pl. 5, fig. 2) indicate that the wedges are built up of a large number of layers, parallel to the base of the nannolith.

F. richardii is considered as a variant of *F. schaubii* which has a low number of elements.

Dimensions: diameter: 8–12 μ., height: 9–13 μ.

Distribution: Spain: *D. multiradiatus* Zone; Israel: *D. multiradiatus* Zone.

Fasciculithus involutus Bramlette and Sullivan
(pl. 5, figs. 4, 5)

Fasciculithus involutus Bramlette and Sullivan, 1961, partim, p. 164, pl. 14, figs. 1–3, non pl. 14, figs. 4, 5; Hay and Mohler, 1967a, p. 1537, pl. 203, figs. 1, 3, 6, 9; pl. 204, figs. 4, 8, 9; Perch-Nielsen, 1971c, p. 351, pl. 4, figs. 1–10; pl. 7, fig. 5; pl. 14, figs. 28–30.
Non *Fasciculithus involutus* Bramlette and Sullivan, Stradner, in Gohrbandt, 1963; p. 79, pl. 10, figs. 14, 15.

Non *Fasciculithus involutus* Bramlette and Sullivan, Wind and Wise, 1977, p. 295, pl. 14, fig. 12; pl. 15, figs. 1–6; pl. 16, figs. 1–6.

Remarks: The parallel-sided to slightly distally tapering column shows 7 to 9 faces. Each face displays two vertical rows of three, smaller fenestrae, superposed by a large, distal fenestra.

The low cone shows clockwise imbricating elements.

Wind and Wise pointed out that the holotype of this species might be an etched specimen of *F. tympaniformis*. In our opinion, however, it is not: *F. involutus* has a star-like outline in plane view, while even strongly etched specimens of *F. tympaniformis* have a circular outline in this view. In addition *F. involutus* is smaller, it has a more restricted stratigraphic range, and the fenestrae are more regularly arranged.

Dimensions: diameter: 5–6 μ., height: 5–6 μ.

Distribution: Spain: *D. multiradiatus* Zone.

Fasciculithus thomasii Perch-Nielsen

Fasciculithus thomasii Perch-Nielsen, 1971, p. 353, pl. 6, figs. 5, 6; pl. 9, fig. 3.

Remarks: The strongly distally tapering column is composed of 16 to 20 elements which differ in length; as a result the base has a star-like outline in proximal view. The configuration of the fenestrae in the 6 to 7 faces is basically the same as in *F. involutus,* but the fenestrae are smaller.

The cone is modified to a plate-like structure, which is concave in distal direction. This deviating type of cone gives the specimens an egg-timer-like outline in side view.

Dimensions: diameter: 5–6 μ., height: 5–6 μ.

Distribution: Spain: *D. multiradiatus* Zone, *T. contortus* Zone.

Family HELIOLITHACEAE Hay and Mohler, 1967

Genus **Heliolithus** Bramlette and Sullivan, 1961

Type species: *Heliolithus riedelii* Bramlette and Sullivan, 1961

Description:

Shape: The shape of the species in this genus is rather variable; the species may be mushroom-, egg-timer- or disc-shaped. They are invariably circular in plane view, and they show radial symmetry. The widest side of the nannolith is considered to be distal.

Construction: The species are composed of three superposed cycles of elements, which differ in diameter and thickness. The cycles may or may not close the centre.

These cycles are: a distal cycle, a median cycle and a column, all with the same number of elements.

Column: This cycle has the form of a high or low, parallel-sided, or distally somewhat tapering cylinder. Generally, the diameter of the cylinder is larger than the height. Proximally, it shows a cone-like depression, distally it is convex. Its elements are tangentially arranged. The sutures are oblique anti-clockwise in distal view.

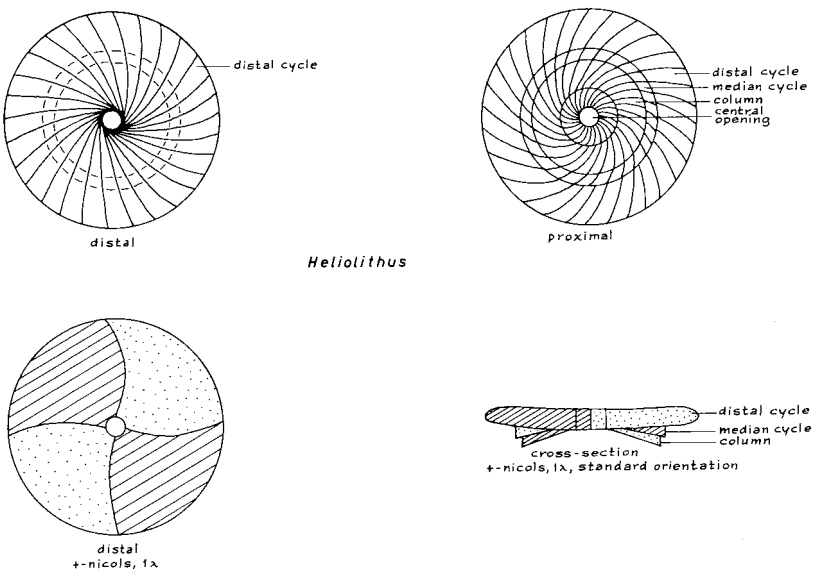

Median cycle: The diameter of this cycle is slightly larger than that of the column. The cycle has the form af a thin disc. The sutures are oblique anti-clockwise in distal view.

Distal cycle: This cycle projects beyond the other two. It has the form of a disc or of a distally opening, truncated cone. The lath-like or wedge-like elements are marginally pointed. The sutures are oblique anti-clockwise in distal view.

Specific criteria: The species are distinguished according to the relative proportions of the cycles and on their orientation.

Standard orientations:

Distal view: Side with the largest diameter turned upwards.

Side view: Distal cycle parallel to the X-cross-hair; axis of the column parallel to the Y-cross-hair.

Extinction lines: In the standard orientation for distal view,. the lines are

laevogyre. The lines are straight over most of their length, and curve marginally. The straight parts make an angle of about 20° with the polarization directions in clockwise direction, in distal view.

In the standard orientation for side view a straight, median extinction line can be observed.

Colour patterns: In the standard orientation for distal view, the larger parts of the second and fourth quadrants are blue; the other sectors are yellow.

In the standard orientation for side view, the left half of the column, the left half of the distal cycle and the right half of the median cycle are blue; the other halves are yellow.

Heliolithus elegans (Roth) nov. comb.
(pl. 5, fig. 6)

Bomolithus elegans Roth, 1973, p. 734, pl. 15, figs. 1–4, 5 (?), 6; Perch-Nielsen, 1977, pl. 12, fig. 1.

Remarks: The species was transferred to the genus *Heliolithus* because it is composed of three superposed cycles, and because of its behaviour in cross-polarized light.

The cycles show 25 to 40 elements. Diagnostic features for this species are the high, proximally flaring (or parallel sided) column, and the well differentiated median cycle with elements which imbricate anti-clockwise in proximal view. The centre may be open or closed.

Dimensions: diameter: 7–11 μ., height: 7–9 μ.

Distribution: Israel: *F. tympaniformis* Zone, *H. kleinpellii* Zone.

Heliolithus cantabriae Perch-Nielsen

Heliolithus cantabriae Perch-Nielsen, 1971b, p. 55, pl. 2, figs. 1, 3, 5, 7; pl. 7, figs. 33–36; Perch-Nielsen, 1977, pl. 3, figs. 9, 13, 17.

Fasciculithus rotundus Haq and Lohmann, 1976, p. 182, pl. 4, figs. 8, 9.

Remarks: The species differs from *H. kleinpellii* in its higher column, its narrower central canal, and the relatively smaller diameter of the distal cycle. The latter cycle is flat or concave in distal direction.

Dimensions: diameter: 8–14 μ., height: 7–11 μ.

Distribution: Spain: *H. kleinpellii* Zone – *D. multiradiatus* Zone; Israel: *F. tympaniformis* Zone – *D. mohleri* Zone.

Heliolithus kleinpellii Sullivan

Heliolithus aff. *H. kleinpellii* Bramlette and Sullivan, Bramlette and Sullivan, 1961, p. 164, pl. 14, fig. 12.

Heliolithus kleinpellii Sullivan, 1964, p. 193, pl. 12, fig. 5; Hay and Mohler, 1967, p. 1531, pl. 199, figs. 4–7; pl. 200, figs. 1, 4; Perch-Nielsen, 1971c, p. 54, pl. 2, figs. 2, 4, 6; pl. 7, figs. 26, 27.

Remarks: The cycles of this species show 29 to 50 elements. The parallel-sided column is wide and low; the centre is open.

The median cycle is about the same height as the column, but the diameter is somewhat larger. The cycles are connected along a sawtooth-like suture.

The distal cycle is almost flat and projects far beyond the lower cycles. The centre of this cycle may be open or closed.

Dimensions: diameter: 11–15 μ., height: 4–5 μ.

Distribution: Spain: *H. kleinpellii* Zone, *D. mohleri* Zone, Israel: *H. kleinpellii* Zone, *D. mohleri* Zone.

Heliolithus megastypus (Bramlette and Sullivan) nov. comb.
(pl. 5, figs. 7, 8)

Discoasteroides megastypus Bramlette and Sullivan, 1961, p. 163, pl. 13, figs. 14, 15; Perch-Nielsen, 1971c, pl. 1, fig. 6; Perch-Nielsen, 1977, pl. 10, figs. 6, 7–16.

Discoasteroides megastypus (?) Bramlette and Sullivan, Perch-Nielsen, 1977, pl. 13, fig. 14.

Remarks: The species is composed of a high column, a wide median cycle and a very reduced distal cycle. Each cycle has 26 to 35 elements. The closed column is parallel-sided or tapers slightly in proximal direction. Its top is conical and its base shows a conical depression. The central ridges on the elements continue in the conical top. The sutures are radial to slightly oblique clockwise in proximal view.

The median cycle projects far beyond the column. The cycle is centrally depressed at both sides. The sutures are radial in proximal view, but they are slightly oblique anti-clockwise in distal view.

The distal cycle, if present, is verty thin; the sutures are subradial in distal view.

All previous authors have assigned this species to the genus *Discoasteroides* because of the presence of a "heliolithic" stem. In the type species of this genus (*Discoasteroides kuepperi*), however, this stem is formed by a proximal elongation of the rays and is not a separate structure as in *H. megastypus*.

Specimens with a completely or almost completely reduced column and/or distal cycle occur frequently in the upper part of the *D. mohleri* Zone and in the lower part of the *D. multiradiatus* Zone; they are transitional between *H. megastypus* and *D. multiradiatus*.

Dimensions: diameter: 7–11 μ., height: 5–8 μ.

Distribution: Spain: *D. mohleri* Zone – *D. multiradiatus* Zone; Israel: *D. mohleri* Zone, *D. multiradiatus* Zone.

Family DISCOASTERACEAE Vekshina, 1959

Genus **Discoaster** Tan Sin Hok, 1927

Type species: *Discoaster pentaradiatus* Tan Sin Hok, 1927
Description:

Shape: The species are star-shaped or rosette-like in plane view. In side view they are biconvex, biconcave, concavo-convex or plano-convex. All species show radial symmetry.

Construction: The species are basically constructed of radially arranged, wedge-shaped elements. The sutures are straight or slightly dextrogyre on one side of the asterolith (facies inferior) and laevogyre on the other side (facies superior). When the elements are simple and joined over most of their length, they are called rays; when they are free-standing over most of their length and ornamented they are called arms.

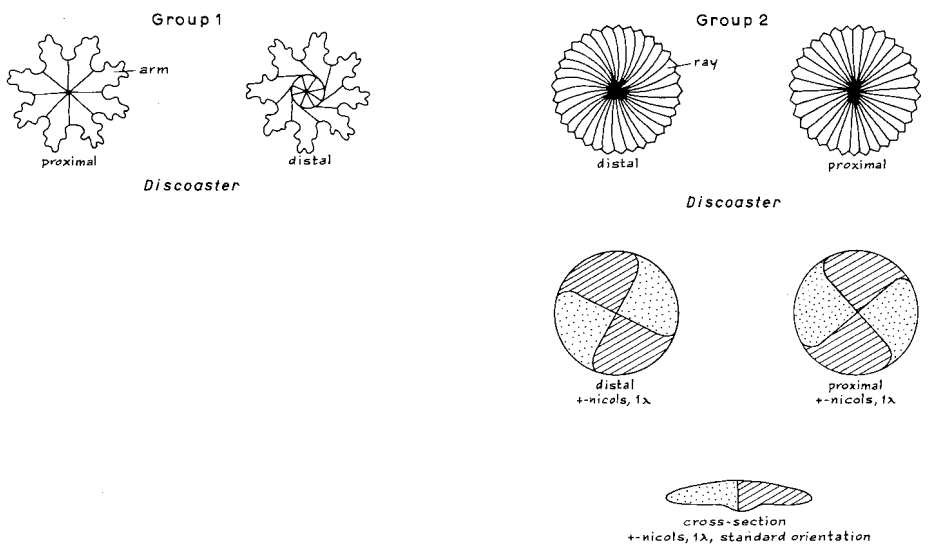

Specific criteria: The species are differentiated on the basis of the shape and the number of the arms/rays and the form of the central disc.
Obervations in cross-polarized light: In plane view, *Discoaster* species show a low birefringence between crossed nicols. On the basis of the extinction

pattern two groups of species can be distinguished in the genus:

Group 1: the asteroliths do not show a regular extinction cross; asteroliths with ornamented arms belong to this group.

Group 2: the species show a regular extinction cross. The extinction lines are sharpest when the focus is raised somewhat above the asterolith, if the side with laevogyre sutures is lying upwards (or lowered if the other side lies upwards).

The lines are normal to each other and bisect in the centre of the asterolith. They are straight over the larger part of their length. When the side with laevogyre sutures lies upwards the lines make an angle of about 20° in clockwise direction with the polarization directions. In this orientation the lines are laevogyre marginally. In the closely related genus *Heliolithus* the side of the nannolith showing this orientation of the lines is considered to be distal; it seems reasonable therefore to consider the side of an asterolith where the sutures are laevogyre as the distal side, regardless whether it is concave or convex. Asteroliths in which the elements are joined over most of their length belong to this group.

Standard orientations:

Distal view: Side with laevogyre sutures turned upwards.

Side view: Distal side in the positive direction of the Y-cross-hair; longer axis of the asterolith parallel to the X-cross-hair.

Colour patterns: Regular extinction patterns can be observed only in asteroliths of group 2. In distal view, the larger part of the second and the fourth quadrant is blue; the other quadrants are yellow. In the standard orientation for side view, the right half of the asterolith is blue, the other half is yellow.

Differential diagnosis: *Discoaster* differs from all other genera, which have radial symmetry in the low birefringence in cross-polarized light.

GROUP 1

Discoaster bramlettei (Bukry and Percival) nov. comb.

Discoasteroides bramlettei Bukry and Percival, 1971, p. 129, pl. 3, figs. 10–12; Perch-Nielsen, 1977, pl. 13, figs. 6, 7.

Markalius variabilis Perch-Nielsen, 1977, p. 747, pl. 13, figs. 11, 12, 15, 16, 18–20; pl. 50, figs. 15–20.

Remarks: Early specimens of this species show characteristics of the genus *Heliolithus*, while later types show a morphology which is more typical for *Discoaster*. In distal view the following cycles can be discerned: (a) a wide outer cycle of elements separated by counter-clockwise oblique sutures (= distal side of median cycle in *Heliolithus*), (b) a middle cycle of elements

with anti-clockwise oblique to subradial sutures (= distal side of the distal cycle in *Heliolithus*), (c) an inner cycle of elements separated by anti-clockwise oblique to hook-shaped sutures (= distal side of column in *Heliolithus*).

In proximal view one can observe (a) a wide outer cycle of elements separated by subradial sutures (= proximal side of median cycle in *Heliolithus*), (b) a narrow, central cycle with subradial sutures (= proximal side of column in *Heliolithus*).

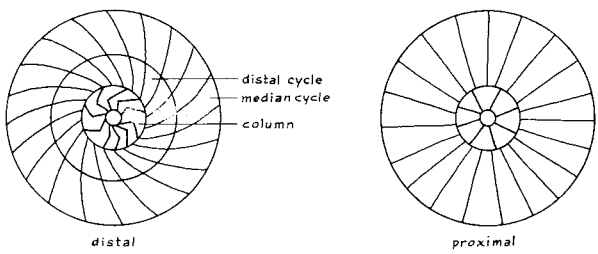

Discoaster bramlettei

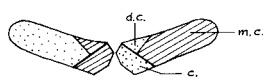

cross-section
+-nicols, 1λ, standard orientation

The centre may be open or closed, and one or more of the central cycles may be absent. The number of elements in the outer cycle decreases rapidly from more than 20 in early forms to 11–16 in late forms.

In cross-polarized light, only the central cycles show high interference colours.

Dimensions: diameter: 8–11 μ.

Distribution: Israel: *H. kleinpellii* Zone, *D. mohleri* Zone.

Discoaster mohleri Bukry and Percival
(pl. 5, fig. 9)

Discoaster gemmeus Stradner, Hay and Mohler, 1967a, p. 1538, pl. 204, figs. 19–21; pl. 205, figs. 1–3; pl. 206, figs. 3, 5, 6, 8; Haq, 1971a, p. 37, pl. 12, fig. 5; pl. 13, figs. 1, 3; pl. 14, fig. 1.

Discoaster mohleri Bukry and Percival, 1971, p. 128, pl. 3, figs. 3–5; Haq and Lohmann, 1976, pl. 2, figs. 1, 2.

Remarks: This biconvex species shows 9 to 19 rays, which are joined through most of their length. Typical specimens have rounded tips. The rays are axially highest, and the sutures between them are deeply incised. The rays

of opposite quadrants may be connected centrally. Transitional forms between this species and *D. nobilis* occur frequently in the *D. mohleri* Zone.
Dimensions: diameter: 5–12 μ.
Distribution: Spain: *D. mohleri* Zone, *D. multiradiatus* Zone; Israel: *D. mohleri* Zone, *D. multiradiatus* Zone.

Discoaster mediosus Bramlette and Sullivan

Discoaster mediosus Bramlette and Sullivan, 1961, p. 161, pl. 12, figs. 7, 8; Hay and Mohler, 1967a, p. 1539, pl. 204, figs. 17, 18; pl. 206, fig. 2; Wind and Wise, 1977, pl. 17, fig. 7.

Remarks: The diameter of the central disc is relatively large. The free-standing parts of the rays are parallel-sided and smooth, or they taper outward and are irregular. The tips of the rays are rounded. The number of rays varies from 7 to 12, and a proximal and/or distal knob may be present.
Dimensions: diameter: 10–15 μ.
Distribution: Spain: *D. multiradiatus* Zone – *T. contortus* Zone; Israel: *D. mohleri* Zone – *T. contortus* Zone.

Discoaster nobilis Martini

Discoaster nobilis Martini, 1961, p. 11, pl. 2, fig. 23; pl. 5, fig. 51; Hay and Mohler, 1967a, p. 1538, pl. 204, fig. 16; pl. 205, figs. 6, 9; Haq and Lohmann, 1976, pl. 2, fig. 7.

Remarks: The tips of the 8 to 13 rays of this biconvex species are pointed. The extent to which the rays are joined is highly variable. The tips of the rays may point in clockwise, anti-clockwise or radial direction. The sutures at the distal side are curved (laevogyre) or hook-shaped. Near the centre of the disc the elements may be somewhat raised at one side or at both sides, thus forming a low central cone.
Dimensions: diameter: 6–20 μ.
Distribution: Spain: *D. multiradiatus* Zone; Israel: *D. multiradiatus* Zone.

Discoaster falcatus Bramlette and Sullivan

Discoaster falcatus Bramlette and Sullivan, 1961, p. 159, pl. 11, figs. 14, 15; Haq, 1969, p. 8, pl. 5, fig. 2; text-fig. 2.
Discoaster limbatus Bramlette and Sullivan, 1961, p. 160, pl. 12, fig. 3; Haq and Lohmann, 1976, pl. 2, fig. 10.

Remarks: This rare species shows 6 to 10, thin rays with pointed tips. The right margin of each ray shows a thickening in distal view. These ridges are curved laevogyre in distal view. They continue into the centre, where they are connected by a circular ridge. Thus a low knob is formed.

Bramlette and Sullivan separated *D. limbatus* from *D. falcatus* on the basis of the irregular outline of the outer parts of the rays of the former species. In our material, however, it was observed that the outline depends on the focus level: at a high focus and in distal view the outline appears to be smooth; at a lower focus level the outline is irregular.
Dimensions: diameter: 8–20 μ.
Distribution: Spain: *D. multiradiatus* Zone.

Discoaster splendidus Martini

Discoaster splendidus Martini, 1960, p. 80, pl. 10, figs. 25, 26, 29; Martini, 1961, p. 11, pl. 2, fig. 21.
Discoaster helianthus Bramlette and Sullivan, 1961, p. 160, pl. 11, fig. 18; Haq and Lohmann, 1976, pl. 2, fig. 12; Wind and Wise, 1977, pl. 17, fig. 6.

Remarks: The 8 to 15 rays of this rare species are joined along most of their length, and they show pointed tips. The thin faces of the rays are thickened marginally. These ridges unite in the centre, where they are connected by a circular ridge. Thus a low knob is formed, which is higher and wider at the distal side than at the proximal side of the asterolith. Transitional forms between this species and *D. falcatus* occur in the *D. multiradiatus* Zone.
Dimensions: diameter: 9–11 μ.
Distribution: Spain: *D. multiradiatus* Zone.

Discoaster araneus Bukry
(pl. 6, figs. 7, 8)

Rhomboaster calcitrapa Gartner, 1971, partim, p. 114, pl. 4, fig. 2, non pl. 4, figs. 3–6.
Discoaster araneus Bukry, 1971, p. 45, pl. 2, fig. 1–3.

Remarks: The 7–10 rays are joined along 1/2 to 1/3 of their length. They are of unequal length, do not necessarily lie in the same plane and the angles between them are variable.

In distal view the slender, outward tapering rays are straight or they are curved laevo- or dextrogyre. A rather high stem with irregular outline is present in the centre of the proximal side. The convex distal side shows hook-shaped sutures.
Dimensions: diameter: 11–20 μ.
Distribution: Caravaca: *D. multiradiatus* Zone.

Discoaster ornatus Stradner

Discoaster ornatus Stradner, 1958, p. 188, fig. 38; Stradner and Papp, 1961, p. 64, pl. 2, figs. 1–6; text-fig. 8/2.

Remarks: The 5 to 10 rays are joined along about half their length. The free parts are rounded or they have an angular outline. The rays are highest axially, and the sutures are deeply incised; narrow U-like incisions occur in the interradial areas. The sutures at the distal side are curved or hook-shaped.
Dimensions: diameter: 6–15 μ.
Distribution: Spain: *T. contortus* Zone – *T. orthostylus* Zone; Israel: *T. contortus* Zone, *D. binodosus* Zone.

Discoaster binodosus Martini
(pl. 7, fig. 2)

Discoaster binodosus Martini, 1958, p. 361, pl. 4, figs. 18, 19; Bramlette and Sullivan, 1961, p. 158, pl. 11, fig. 1; Stradner and Papp, 1961, p. 66, pl. 4, figs. 1–7; pl. 5, figs. 1–6; text-fig. 8/4.
Discoaster binodosus binodosus Martini, 1958, p. 362, pl. 4, fig. 18; Perch-Nielsen, 1971, p. 61, pl. 52, fig. 6.
Discoaster binodosus hirundinus Martini, 1958, p. 362, pl. 4, fig. 19; Perch-Nielsen, 1971, p. 62, pl. 52, fig. 7.
Non *Discoaster binodosus hirundinus* Martini, Perch-Nielsen, 1967, p. 30, pl. 7, figs. 1–4.

Remarks: The shape of the 7 to 9 arms of this species is highly variable: the arms are long or short, they are parallel-sided or taper outwards, and they have or do not have a terminal bifurcation. The rounded interradial incisions and the presence of at least one set of paired nodes are, however, characteristic of this species.
Dimensions: diameter: 8–17 μ.
Distribution: Spain: *T. orthosylus* Zone – *N. fulgens* Zone: Israel: *D. binodosus* Zone – *D. lodoensis* Zone.

Discoaster deflandrei Bramlette and Riedel

Discoaster deflandrei Bramlette and Riedel, 1954, p. 399, pl. 39, fig. 6; text-fig. 1; Bramlette and Sullivan, 1961, p. 158, pl. 11, fig. 4; Stradner and Papp, 1961, p. 71, pl. 10, figs. 1–6; text-fig. 8/7.

Remarks: Specimens show 5 to 8 robust arms with an angular outline. The bifurcating tips of the arms form an obtuse angle. The interradial incisions are subcircular. Overgrown specimens of *D. gemmifer*, *D. mirus* and *D. binodosus* may be very similar to this species.
Dimensions: diameter: 7–8 μ.
Distribution: Spain: *T. orthostylus* Zone – *N. fulgens* Zone; Israel: *D. binodosus* Zone – *T. orthostylus* Zone.

Discoaster mirus Deflandre

Discoaster mirus Deflandre, in Grassé, 1952, p. 465, fig. 362; Martini, 1961, p. 12, pl. 3, fig. 24; Stradner and Papp, 1961, p. 68, pl. 6, figs. 1–6; pl. 7, figs. 1–5; text-figs. 8/5, 24/7.

Remarks: Specimens show 5 to 10, relatively short, robust arms. The arms bifurcate in such a way that two lobes are formed, which enclose a sharp angle. Each pair of lobes shows a pair of small nodes at its base. In specimens with a high number of arms the nodes of adjacent arms almost touch each other and nearly close the angular to rounded interradial incisions.
Dimensions: diameter: 11–18 μ.
Distribution: Spain: *D. sublodoensis* Zone – *N. fulgens* Zone; Israel: *T. orthostylus* Zone – *D. lodoensis* Zone.

Discoaster gemmifer Stradner

Discoaster distinctus Martini, Stradner, 1959, p. 1086, fig. 20.
Discoaster gemmifer Stradner, 1961, p. 86, fig. 83; Stradner and Papp, 1961, partim, p. 69, pl. 8, figs. 3–10; pl. 9, figs. 1–5; pl. 24, figs. 4–6; text-fig. 8/6, non pl. 8, figs. 1, 2; Perch-Nielsen, 1971d, p. 63, pl. 53, figs. 3, 4.

Remarks: The number of arms in this species varies from 6 to 8. The tips of the bifurcating arms form an angle of about 90°. The terminal pair of nodes is separated from the tips of the arms by short incisions; specimens in which these incisions are not well developed are very similar to *D. deflandrei.*

The arms are generally somewhat longer in later specimens than in earlier ones.
Dimensions: diameter: 12–17 μ.
Distribution: Spain: *D. lodoensis* Zone – *N. fulgens* Zone; Israel: *T. orthostylus* Zone – *D. sublodoensis* Zone.

Discoaster distinctus Martini

Discoaster nov. sp. Martini, 1959, p. 363, pl. 4, fig. 17.
Discoaster distinctus Martini, 1960, p. 395, pl. 6; Bramlette and Sullivan, 1961, p. 159, pl. 11, figs. 11–13; Stradner and Papp, 1961, p. 72, pl. 11, fig. 1; text-fig. 8/8.
Non *Discoaster distinctus* Martini, Stradner, 1959, p. 1086, fig. 20; Stradner 1959, p. 484, figs. 33–39.

Remarks: The specimens show 5 to 8, terminally incised arms. Each arm has paired lateral nodes just below the lowest point of the incision. The species differs from *D. binodosus* in the more terminal position of the nodes.
Dimensions: diameter: 10–13 μ.
Distribution: Spain: *T. orthostylus* Zone – *D. sublodoensis* Zone.

Discoaster cruciformis Martini

Discoaster cruciformis Martini, 1958, p. 357, pl. 2, fig. 9; Bramlette and Sullivan, 1961, p. 158, pl. 11, fig. 5; Perch-Nielsen, 1972, pl. 13, fig. 3.
Discoaster gemmifer Stradner. Stradner and Papp, 1961, partim, p. 69, pl. 8, figs. 1, 2, non pl. 8, figs. 3–10; pl. 9, figs. 1–5; pl. 24, figs. 4–6; text-fig. 8/6.

Remarks: This species is easily recognized by its four, strongly concavo-convex, marginally bifurcating or blunt arms.
Dimensions: diameter: 10–12 μ.
Distribution: Israel: *T. orthostylus* Zone – *D. lodoensis* Zone.

Discoaster colletii Parejas

Discoaster colletii Parejas, in Bersier, 1939, p. 237, figs. 18, 21; Stradner, 1959, p. 478, figs. 30–32; Stradner and Papp, 1961, p. 78, pl. 13, figs. 1–6; text-figs. 8/15, 24/8.

Remarks: The 5 to 7, almost wedge-shaped rays are separated by very narrow and deep interradial incisions. Marginally the rays are slightly concave.
Dimensions: diameter: 8–13 μ.
Distribution: Spain: *D. lodoensis* Zone – *N. fulgens* Zone; Israel: *D. lodoensis* Zone.

Discoaster nonaradiatus Klumpp

Discoaster nonaradiatus Klumpp, 1953, p. 383, text-fig. 3/5; Bramlette and Sullivan, 1961, p. 162, pl. 12, fig. 13; Stradner and Papp, 1961, p. 74, pl. 1, fig. 3; text-fig. 8/10.

Remarks: The few specimens found of this species show 7 or 8 arms. They are slender and bifurcate marginally into two simple branches, which form a large, obtuse angle.
Dimensions: diameter: 10 μ.
Distribution: Spain: *D. sublodoensis* Zone.

GROUP 2

Discoaster multiradiatus Bramlette and Riedel
(pl. 6, figs. 1–3)

Discoaster multiradiatus Bramlette and Riedel, 1954, p. 396, pl. 38, fig. 10; Bramlette and Sullivan, 1961, p. 161, pl. 12, fig. 10; Haq and Lohmann, 1976, pl. 2, figs. 3–6.
Discoaster aff. *D. multiradiatus* Bramlette and Riedel, Perch-Nielsen, 1972, pl. 14, fig. 5.

Remarks: This easily recognizable, biconvex species of *Discoaster* has the form of a rosette. It is composed of 16 to 35 rays, pointed marginally, which

are joined along most of their length. The composition of the proximal and distal central area is rather variable in early specimens. The following configurations were observed in the proximal central area: (a) The sutures between the rays are straight and continue into the very centre, (b) The elements in the centre are separated by slightly dextrogyre sutures. In cross-polarized light the centre is bright and shows dextrogyre extinction lines in proximal view. This deviating central cycle is interpreted as a remnant of the column in *Heliolithus*, (c) The rays are centrally enlarged in proximal direction, forming a short stem. The sutures in this stem are oblique clockwise.

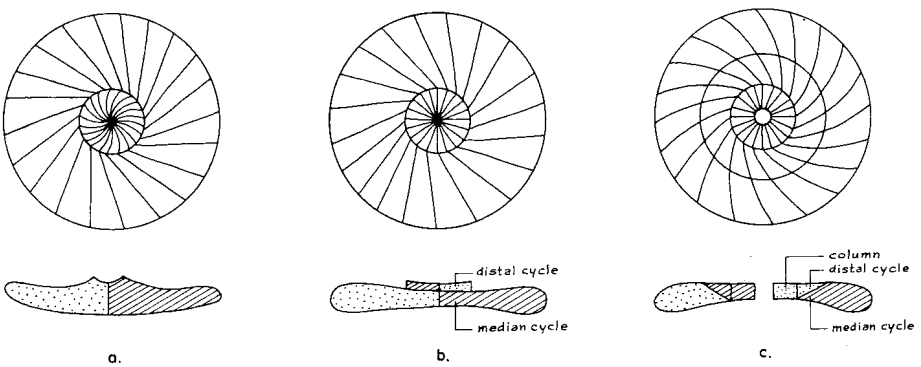

Variation in the configuration of the distal side of *D.multiradiatus*

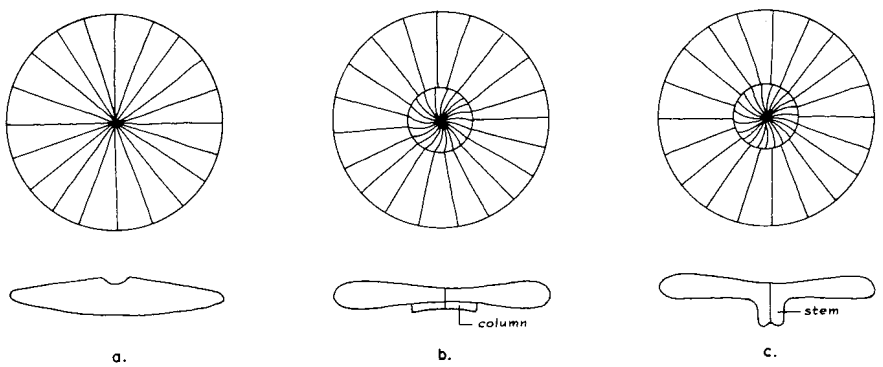

Variation in the configuration of the proximal side of *D.multiradiatus*

In the distal central area: (a) the rays slightly imbricate clockwise near the depressed centre; the sutures change their direction from slightly oblique anti-clockwise to the opposite direction, (b) the centre shows a thin, distal cycle of elements, separated by radial sutures. This cycle is interpreted as a remnant of the distal cycle in *Heliolithus*, (c) the centre shows two con-

centric cycles which may or may not close the area. These cycles are interpreted as remnants of the (extended) column and the distal cycle in *Heliolithus*. This type of centre is bright in cross-polarized light; the extinction lines are laevogyre in distal view.

The mean number of rays is higher in earlier populations of this species than in later ones.

Dimensions: diameter: 8–22 μ.

Distribution: Spain: *D. multiradiatus* Zone – *D. binodosus* Zone; Israel: *D. multiradiatus* Zone – *D. binodosus* Zone.

Discoaster lenticularis Bramlette and Sullivan

Discoaster lenticularis Bramlette and Sullivan, 1961, p. 160, pl. 12, figs. 1, 2; Sullivan, 1964, p. 191, pl. 11, fig. 1; Sullivan, 1965, p. 42, pl. 10, fig. 10; Radomski, 1968; p. 582, pl. 48, fig. 1.
Discoaster multiradiatus Bramlette and Riedel, Edwards, 1973, pl. 14, fig. 6.
Discoaster sp. Edwards and Perch-Nielsen, 1975, pl. 4, fig. 3.

Remarks: This rather small, centrally slightly depressed, biconvex species is composed of a wide disc superposed by a small, central cycle of elements. The distal cycle shows the same number of elements (18–27) as the disc; the sutures are radial.

Dimensions: diameter: 5–8 μ.

Distribution: Spain: *D. multiradiatus* Zone – *T. contortus* Zone; Israel: *D. multiradiatus* Zone.

Discoaster perpolitus Martini
(pl. 6, fig. 4)

Discoaster perpolitus Martini, 1961, p. 9, pl. 2, fig. 20; pl. 5, fig. 50; Sullivan, 1965, p. 43, pl. 10, fig. 12.
Discoaster multiradiatus Bramlette and Riedel var., Bramlette and Sullivan, 1961, p. 162, pl. 12, fig. 11.
Discoaster aff. *D. multiradiatus* Bramlette and Riedel, Perch-Nielsen, 1972, pl. 14, fig. 5.
Discoaster elegans Bramlette and Sullivan, Perch-Nielsen, 1972, pl. 14, fig. 6.

Remarks: The species shows the same composition as, and is closely related to *D. multiradiatus*; it differs only in having more delicate rays, which show concentric ridges and thickened borders.

The species can be distinguished from *D. elegans* by its higher number of elements and by the absence of a distal stem.

Dimensions: diameter: 9–19 μ.

Distribution: Spain: *D. multiradiatus* Zone.

Discoaster elegans Bramlette and Sullivan

Discoaster elegans Bramlette and Sullivan, 1961, p. 159, pl. 11, figs. 14, 15; Sullivan, 1964, p. 190, pl. 10, figs. 5, 6.
Non *Discoaster elegans* Bramlette and Sullivan, Perch-Nielsen, 1972, pl. 14, fig. 6.

Remarks: The 15 to 17 thin rays are thickened marginally, and they may show concentric ridges. A slender stem is present in the centre of the concave, distal side.
Dimensions: 11–15 μ.
Distribution: Spain: *D. multiradiatus* Zone.

Discoaster diastypus Bramlette and Sullivan

Discoaster diastypus Bramlette and Sullivan, 1961, p. 159, pl. 11, figs. 6–8; Perch-Nielsen, 1971d, p. 62, pl. 51, figs. 8, 10.
Discoaster aff. *D. diastypus* Bramlette and Sullivan, Bramlette and Sullivan, 1961, p. 159, pl. 11, figs. 9, 10.
Discoaster spp. 2, 3 Perch-Nielsen, 1972, pl. 14, figs. 1, 2.

Remarks: This species is easily recognized by the presence of a central stem at both sides of the disc. This stem is higher and wider at the proximal side than at the other side.

The proximal stem consists of a low number of elements separated by dextrogyre sutures in proximal view.

The distal stem is composed of the same number of elements as the disc (12–17), and it shows dextrogyre sutures in distal view.

The rounded or pointed tips of the rays point in a clockwise, radial or anti-clockwise direction.
Dimensions: diameter: 15–22 μ.
Distribution: Spain: *T. contortus* Zone – *T. orthostylus* Zone; Israel: *T. contortus* Zone – *T. orthostylus* Zone.

Discoaster barbadiensis Tan Sin Hok
(pl. 7, fig. 1)

"Kalkerdige Krystaldrusen" Ehrenberg, 1854, p. 155, pl. 24, fig. 67; pl. 25, figs. 13–15.
"Crystalloids of the Chalk" Jukes-Browne and Harrison, 1892, p. 178, text-figs. 4–6.
Discoaster barbadiensis Tan Sin Hok, 1927, p. 119; Bramlette and Riedel, 1954, p. 398, pl. 39, fig. 5; Bramlette and Sullivan, 1961, p. 158, pl. 11, fig. 2; Perch-Nielsen, 1971, p. 61, pl. 51, fig. 5.

Remarks: The 11 to 18, marginally rounded or pointed rays are joined along almost their total length. The rays in the centre of the proximal side bend in proximal direction to form a high, proximally concave stem. The sutures in the stem are dextrogyre in proximal view.

Dimensions: diameter: 9–11 μ.
Distribution: Spain: *D. binodosus* Zone – *N. fulgens* Zone; Israel: *D. binodosus* Zone – *D. sublodoensis* Zone.

Discoaster robustus Haq

Discoaster robustus Haq, 1969, p. 12, fig. 7; text-fig. 1c.

Remarks: The species is typified by its almost flat distal side and conical proximal side, which gives the specimens a triangular outline in side view. The 8 to 15 pointed or rounded rays are joined throughout their length.
Dimensions: diameter: 10–12 μ.
Distribution: Spain: *D. binodosus* Zone – *T. orthostylus* Zone; Israel: *D. binodosus* Zone – *T. orthostylus* Zone.

Discoaster pacificus Haq

Discoaster pacificus Haq, 1969, p. 11, pl. 4, figs. 4–7; text-fig. 3.

Remarks: Specimens of this species show 8 or 9 rays, which are joined along about half their length. The free parts of the rays have a dextrogyre curvature in distal view. In this view the left side of each ray shows a thickening. Centrally, the rays form a low distal and a somewhat higher proximal stem. In the distal stem the sutures are subradial; in the proximal stem they are dextrogyre in proximal view.

The species differs from the closely related *D. diastypus* in the lower number of rays and the shorter proximal stem, and differs from the also related *D. lodoensis* in the higher number of rays and the higher and wider stems.
Dimensions: diameter: 16–22 μ.
Distribution: Israel: *D. binodosus* Zone – *T. orthostylus* Zone.

Discoaster lodoensis Bramlette and Riedel

Discoaster lodoensis Bramlette and Riedel, 1954, p. 398, pl. 39, fig. 3; Bramlette and Sullivan, 1961, p. 161, pl. 12, figs. 4, 5; Stradner and Papp, 1961, p. 92, pl. 25, 26; text-figs. 9/3, 24/9; Perch-Nielsen, 1971d, p. 64, pl. 52, fig. 2.

Remarks: In typical specimens the 5 to 7, pointed, in distal view dextrogyre rays are free along most of their length. The left side of each ray is thickened in distal view. The distal knob shows radial sutures, the proximal one, dextrogyre sutures in proximal view. The length of the rays is highly variable.
Dimensions: diameter: 16–26 μ.

Distribution: Spain: *T. orthostylus* Zone – *D. sublodoensis* Zone; Israel: *T. orthostylus* Zone – *D. sublodoensis* Zone.

Discoaster kuepperi Stradner

Discoaster kuepperi Stradner, 1959, p. 478, figs. 17, 21; Stradner and Papp, 1961, p. 93, pl. 27, figs. 1–6; text-figs. 9/6, 9/16; Perch-Nielsen, 1971, p. 64, pl. 51, figs. 6, 7, 9, 11, 12; Perch-Nielsen, 1972, pl. 13, figs. 5, 6.

Discoasteroides kuepperi (Stradner) Bramlette and Sullivan, 1961, p. 163, pl. 13, figs. 16–19; Sullivan, 1964, p. 192, pl. 12, fig. 1, 2.

Non *Discoasteroides kuepperi* (Stradner) Bramlette and Sullivan, Hay and Towe, 1962, p. 515, pl. 10, fig. 1.

Remarks: The 8 to 12, marginally rounded or pointed rays are joined along almost their total length. Near the centre of the proximal side the rays extend in proximal and sideward direction to form a proximal cone. This cone shows dextrogyre sutures in proximal view. The height and the width of the cone are highly variable.

Dimensions: diameter: 8–14 μ.

Distribution: Spain: *T. orthostylus* Zone – *D. sublodoensis* Zone; Israel: *T. orthostylus* Zone – *D. sublodoensis* Zone.

Discoaster wemmelensis Achuthan and Stradner

Discoaster wemmelensis Achuthan and Stradner, 1967, p.5, pl. 4, figs. 3, 4; text-fig. 2; Perch-Nielsen, 1971, p. 65, pl. 2, figs. 1, 2; pl. 53, figs. 5, 6; Perch-Nielsen, 1977, pl. 14, fig. 6.

Remarks: This asterolith is composed of two superposed cycles of elements; the distal cycle is wider and thicker than the proximal one. The cycles have an equal number of elements (20–25). The elements are joined throughout their length. The sutures are subradial on both sides of the asterolith.

The species closely resembles *D. lenticularis*, but in the latter species the widest cyle is the proximal one.

Dimensions: diameter: 5–8 μ.

Distribution: Spain: *D. lodoensis* Zone – *N. fulgens* Zone; Israel: *D. lodoensis* Zone – *D. sublodoensis* Zone.

Discoaster sublodoensis Bramlette and Sullivan

Discoaster sublodoensis Bramlette and Sullivan, 1961, p. 162, pl. 12, fig. 6; Sullivan, 1965, p. 43, pl. 10, fig. 11; Perch-Nielsen, 1977, pl. 14, figs. 11, 12.

? *Discoaster quinarius* (Ehrenberg) Bersier, Stradner and Papp, 1961, p. 89, pl. 22, figs. 1–4, 8; text-fig. 9/4.

Remarks: The 5 to 6, sharply pointed, straight rays are joined along about

half their length. In typical specimens the sides of the rays are slightly concave.
Dimensions: diameter: 8–13 μ.
Distribution: Spain: *D. sublodoensis* Zone – *N. fulgens* Zone; Israel: *D. sublodoensis* Zone.

Discoaster saipanensis Bramlette and Riedel

Discoaster saipanensis Bramlette and Riedel, 1954, p. 398, pl. 39, fig. 4; Stradner and Papp, 1961, p. 90, pl. 22, figs. 5–7, 9; text-fig. 9/5; Perch-Nielsen, 1971, p. 65, pl. 51, fig. 4; pl. 52, fig. 4.

Remarks: The 7 to 9 rays of this concavo-convex species are joined along about two-thirds of their length. In typical specimens the sides of the straight radiating, sharply pointed rays are slightly concave. A low stem is generally present in the centre of the concave, proximal side.

Intermediate forms between this species and *D. barbadiensis* were observed in the *D. sublodoensis* Zone.
Dimensions: diameter: 8–11 μ.
Distribution: Spain: *D. sublodoensis* Zone – *N. fulgens* Zone.

Discoaster bifax Bukry

Discoaster bifax Bukry, 1971b, p. 313, pl. 3, figs. 6–11; Perch-Nielsen, 1977, pl. 14, figs. 2, 8, 9.

Remarks: The 13 to 19 rays of this concavo-convex species are joined throughout their length and are rounded marginally. In the centre of the convex, distal side the rays bend in distal and sideward direction to form an open cone, the diameter of which is about one-third of the total diameter. The centre of the concave proximal side shows a narrow and short stem.

The sutures are subradial in both distal and proximal view.
Dimensions: diameter: 7–9 μ.
Distribution: Spain: *N. fulgens* Zone.

Family RHABDOSPHAERACEAE Lemmermann, 1908

Genus Rhabdosphaera Haeckel, 1894

Type species: *Rhabdosphaera claviger* Murray and Blackman, 1898
Description:

Shape: The species have the form of a modified nail. The pointed side is considered distal.

Construction: The species are composed of a relatively high, central process and a low, composite base.

Central process: This hollow structure consists of helicoidally arranged, lath-like elements. Near its base the structure may be thickened (collar).

Base: The subcircular base shows one or more concentric cycles of elements surrounding a central opening which is in line with the central channel in the central process.

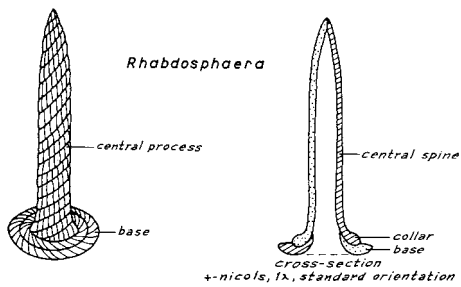

Specific criteria: The species are differentiated on the basis of the shape of the central process and the presence or absence of a collar.

Standard orientation: The specimens are generally observed in side view: base parallel to the X-cross-hair; central process pointing in the positive direction of the Y-cross-hair.

Colour distribution: In the standard orientation for side view the right cross-section of the central process and the collar, and the left cross-section of the base are blue; the other sections are yellow.

Rhabdosphaera sp.

Rhabdosphaera sp. Bramlette and Sullivan, 1961, p. 148, pl. 5, fig. 18.

Remarks: This species of *Rhabdosphaera* is characterized by its parallel-sided, truncated central process, which is somewhat constricted in the lower part. The species can be differentiated from *R. truncata* by its single, and simple basal plate.

Dimensions: height: 10 μ.

Distribution: Spain: *D. multiradiatus* Zone.

Rhabdosphaera perlonga (Deflandre) Bramlette and Sullivan

Rhabdolithus perlongus Deflandre, in Deflandre and Fert, 1954, p. 158, pl. 12, figs. 34, 35; text-fig. 86.

Rhabdolithus pinguis Deflandre, in Deflandre and Fert, 1954, p. 158, pl. 12, figs. 26, 27.

Rhabdosphaera perlonga (Deflandre) Bramlette and Sullivan, 1961, p. 146, pl. 5, fig. 7; Sullivan, 1965, p. 36, pl. 7, fig. 7.

Rhabdosphaera cf. *R. pinguis* Deflandre, Stradner, 1969, p. 415, pl. 89, figs. 13–15.

Remarks: The distally somewhat inflated process and the simple base typify this species.
Dimensions: height: 15–17 μ.
Distribution: Spain: *T. orthostylus* Zone; Israel: *T. orthostylus* Zone.

Rhabdosphaera crebra (Deflandre) Bramlette and Sullivan

Rhabdolithus creber Deflandre, in Deflandre and Fert, 1954, p. 157, pl. 12, figs. 31–33; text-figs. 81, 82.
Rhabdosphaera crebra (Deflandre) Bramlette and Sullivan, 1961, p. 146, pl. 5, figs. 4, 5.
Blackites creber (Deflandre) Stradner, in Stradner and Edwards, 1968, p. 29; Stradner, 1969, p. 415, pl. 89, figs. 4, 5.

Remarks: The relatively short central process tapers to a pointed tip and shows a distinct collar.
Dimensions: height: 8–11 μ.
Distribution: Spain: *T. orthostylus* Zone – *D. lodoensis* Zone; Israel: *T. orthostylus* Zone – *D. lodoensis* Zone.

Rhabdosphaera scabrosa (Deflandre) Bramlette and Sullivan

Rhabdolithus scabrosus Deflandre, in Deflandre and Fert, 1954, p. 158, pl. 12, fig. 30; text-fig. 85.
Rhabdosphaera scabrosa (Deflandre) Bramlette and Sullivan, 1961, p. 147, pl. 5, fig. 11; Sullivan, 1965, p. 37, pl. 7, fig. 6.

Remarks: The relatively high central process shows a uniform taper in distal direction. The single basal plate may be rather wide.
Dimensions: height: 16–21 μ.
Distribution: Spain: *T. orthostylus* Zone – *D. sublodoensis* Zone; Israel: *D. lodoensis* Zone – *D. sublodoensis* Zone.

Rhabdosphaera truncata Bramlette and Sullivan

Rhabdosphaera truncata Bramlette and Sullivan, 1961, p. 147, pl. 5, fig. 15; Sullivan, 1965, p. 37, pl. 7, fig. 1; Stradner, 1969, p. 415, pl. 89, figs. 6–8.

Remarks: The parallel-sided, truncated central process has a distinct collar.
Dimensions: height: 11 μ.
Distribution: Spain: *T. orthostylus* Zone.

Rhabdosphaera inflata Bramlette and Sullivan

Rhabdosphaera inflata Bramlette and Sullivan, 1961, p. 146, pl. 5, figs. 4, 5.
Rhabdolithus inflatus (Bramlette and Sullivan) Perch-Nielsen, 1977, p. 804, pl. 37, figs. 9, 10.

Remarks: This easily recognizable species shows an inflated, rugose central

process and a simple base. Early specimens are less inflated than later ones.
Dimensions: height: 13–23 μ.
Distribution: Spain: *D. sublodoensis* Zone; Israel: *D. sublodoensis* Zone.

Family PONTOSPHAERACEAE Lemmermann, 1908

Genus **Pontosphaera** Lohmann, 1902

Type species: *Pontosphaera syracusana* Lohmann, 1902
Synonyms: *Discolithus, Discolithina, Transversopontis, Koczyia.*
Description:

Shape: The species have the form of a slightly concavo-convex elliptical plate, which may or may not have a high or low margin. The convex side is considered to be distal.

Construction: The species in this genus are composed of a proximal (or outer) cycle of elements and a distal (or inner) cycle. These cycles are closely appressed. The following three groups of species can be distinguished in the genus:

Group 1. The species in this group have the form of a concavo-convex, elliptical plate, which may be somewhat thickened at the periphery. The plate is composed of a distal plate cycle and a proximal one.

Distal plate cycle: The elements in this cycle are lath-shaped; they are parallel to the elliptical periphery.

Proximal plate cycle: In this cycle the elements have a lath-like or wedge-like outline. They are perpendicular to the periphery. In the centre the elements meet along a line connecting the foci of the ellipse.

Group 2. The species in this group differ from those in the foregoing one in the presence of a high or low margin, which flares in distal direction. The margin is formed by a distal continuation of the plate cycles. The inner cycle of the margin is called the *wall,* the outer cycle the *rim*. The wall is thicker than the rim.

Wall: The lath-like elements of the distal plate cycle continue in the wall, where they are arranged in a helicoidal way. The imbrication of the laths is clockwise in distal view. Several species show regularly spaced, inward projecting structures (called *struts*) at the inner side of the wall.

Rim: The relatively thin rim is composed of lath-like elements which imbricate anti-clockwise in distal view.

Group 3. The species in this group differ from those in group 2 in the presence of a narrow or wide distal *flange.* This structure is formed by a bend in the wall and the rim in lateral, outward direction. Generally, the

distal flange cycle projects further outwards than the proximal cycle. The distal flange cycle shows counter-clockwise oblique sutures in distal view; in the proximal cycle the sutures are oblique anti-clockwise in proximal view.

Specific criteria: The species are distinguished on the basis of the presence or absence of a margin and a flange, on the shape and the size of openings in the central plate and on the presence or absence of struts.

Central openings: The openings in the central plate lie along the X-axis. Four types of openings can be distinguished: 2 slits; 2 smaller openings; 2 larger openings; and 1 larger, elliptical opening. At least one of these types of openings occurs in each species group.

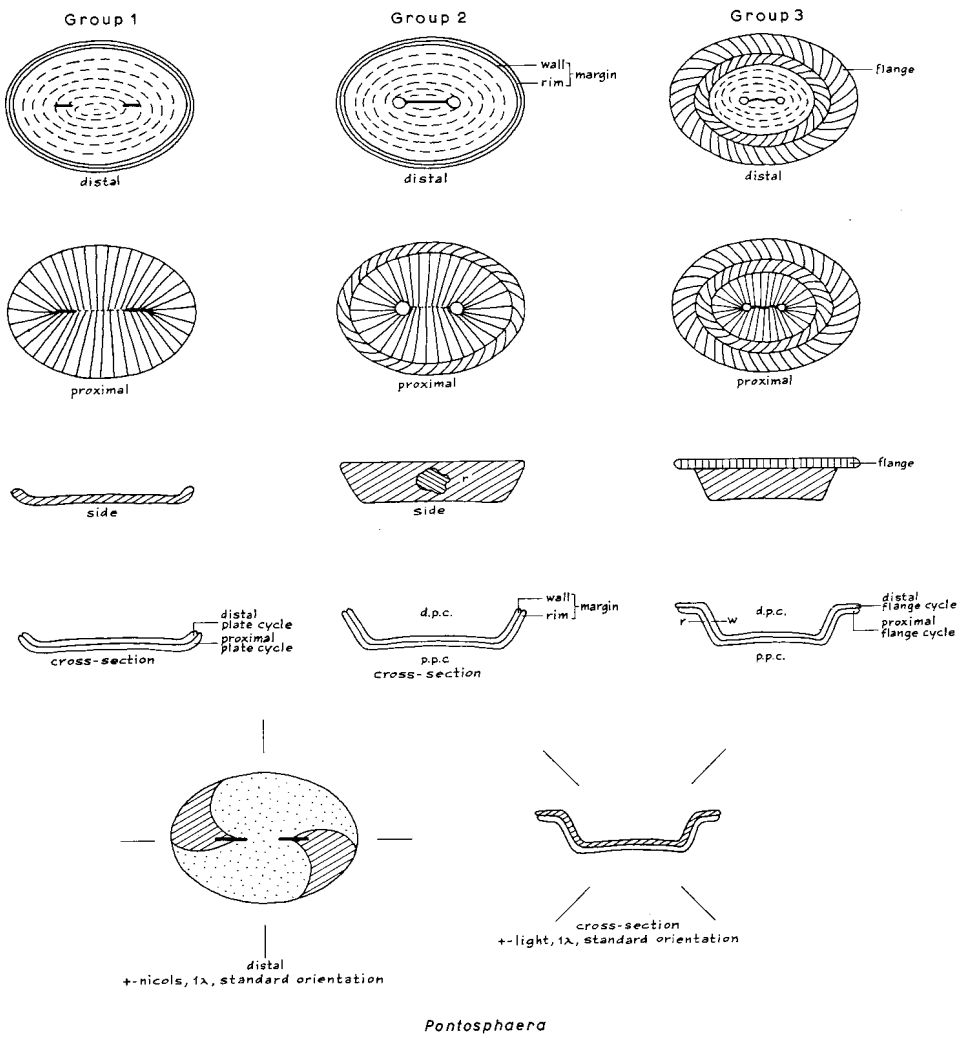

Pontosphaera

Standard orientations:

Distal view: Convex side (side with the margin) upwards; X-axis parallel to the X-cross-hair.

Side view: X-axis making an angle of 45° with the X-cross-hair in anti-clockwise direction, the normal to the distal side making the same angle with this cross-hair in clockwise direction.

Extinction lines: These lines are sharper in the central plate than in the margin and in the flange. They are dextrogyre in distal view.

Colour distribution: In the standard orientation for distal view the smaller sectors enclosed by the extinction lines are blue; the other sectors are yellow. In the standard orientation for side view the wall, the distal cycle of the flange and part of the distal plate cycle are blue; the other cycles are yellow.

Differential diagnosis: The species of group 3 may be confused with species of *Lophodolithus,* particularly because the extinction lines in this genus are also dextrogyre. The genera can be distinguished by the presence of a complex bar in *Lophodolithus,* and, if this has disappeared, by the uneven height of the flange.

GROUP 1

Pontosphaera plana (Bramlette and Sullivan) Haq

Discolithus planus Bramlette and Sullivan, 1961, p. 143, pl. 3, fig. 7.
Discolithina plana (Bramlette and Sullivan) Levin, 1965, p. 266, pl. 41, fig. 9; Perch-Nielsen, 1971, p. 35, pl. 29, fig. 4.
Pontosphaera plana (Bramlette and Sullivan) Haq, 1971a, p. 22, pl. 10, fig. 1; pl. 12, fig. 6.

Remarks: The sometimes rather thick central plate shows two slits along the X-axis. The species differs from *D. versa* in the absence of a marginal ridge.
Dimensions: length: 9–12 μ.
Distribution: Spain: *T. orthostylus* Zone – *N. fulgens* Zone; Israel: *D. binodosus* Zone – *D. sublodoensis* Zone.

Pontosphaera versa (Bramlette and Sullivan) nov. comb.

Discolithus versus Bramlette and Sullivan, 1961, p. 144, pl. 3, fig. 16.
Discolithina cf. *D. versa* (Bramlette and Sullivan) Levin and Joerger, 1967, p. 168, pl. 2, fig. 11.

Remarks: The central plate shows two slits along the X-axis and a thickened margin.
Dimensions: length: 8–14 μ.
Distribution: Spain: *T. orthostylus* Zone – *N. fulgens* Zone.

Pontosphaera multipora (Kamptner) Roth

Discolithus multiporus Kamptner, 1948, p. 5, pl. 1, fig. 9; Stradner and Adamiker, 1966, p. 340, pl. 2, fig. 1.
Discolithus vigintiforatus Kamptner, 1948, p. 5, pl. 1, fig. 8.
Discolithus lineatus Deflandre, in Deflandre and Fert, 1954, p. 137, pl. 10, figs. 17, 18; text-fig. 50.
Discolithus distinctus Bramlette and Sullivan, 1961, p. 141, pl. 2, figs. 8, 9.
Discolithina multipora (Kamptner) Martini, 1965, p. 400; Haq, 1968; p. 36, pl. 6, figs. 4–9; Perch-Nielsen, 1971, p. 34, pl. 26, figs. 1–5.
Discolithina confossa Hay, Mohler and Wade, 1966, p. 391, pl. 9, figs. 1–9.
Pontosphaera vadosa Hay, Mohler and Wade, 1966, partim, p. 391, pl. 8, fig. 4, non pl. 8, figs. 1–3.
Discolithina distincta (Bramlette and Sullivan) Levin and Joerger, 1967, p. 166, pl. 1, figs. 14, 15.
Discolithina aff. *D. distincta* (Bramlette and Sullivan) Levin and Joerger, Gartner and Smith, 1967, p. 5, pl. 6, figs. 4–6.
Discolithina cribraria Perch-Nielsen, 1967, p. 25, pl. 2, figs. 1–3.
Discolithina cf. *D. punctosa* (Bramlette and Sullivan) Perch-Nielsen, 1967, p. 25, pl. 2, figs. 4, 5.
Pontosphaera multipora (Kamptner) Roth, 1970, p. 860; Wise and Constans, 1976, pl. 2, fig. 3; Proto Decima et al., 1975, p. 50, pl. 5, fig. 24.

Remarks: The central plate shows two slits along the X-axis and two or three concentric rows of pores. These pores lie on the sutures of the proximal plate cycle. Their number varies from 14 to 36. The thickened margin is wider in later specimens than in earlier ones.
Dimensions: length: 9–15 μ.
Distribution: Spain: *T. orthostylus* Zone – *D. sublodoensis* Zone; Israel: *T. orthostylus* Zone – *N. fulgens* Zone.

Pontosphaera duocava (Bramlette and Sullivan) nov. comb.

Discolithus duocavus Bramlette and Sullivan, 1961, p. 141, pl. 2, fig. 11; Sullivan, 1964, p. 182, pl. 4, fig. 5.
Discolithina duocava (Bramlette and Sullivan) Perch-Nielsen, 1971d, p. 34, pl. 29, fig. 5.
Discolithus ocellatus Bramlette and Sullivan, 1961, p. 142, pl. 3, fig. 2.
Discolithina ocellata (Bramlette and Sullivan) Perch-Nielsen, 1971d, p. 34, pl. 29, fig. 6.

Remarks: The central plate shows two smaller or larger openings along the X-axis. The openings may or may not be connected by a furrow. *P. duocava* should have larger openings than *D. ocellata*; the species are here placed in synonomy because the differences in the size of the openings are regarded as intraspecific variation.
Dimensions: length: 8–12 μ.
Distribution: Spain: *T. orthostylus* Zone – *D. sublodoensis* Zone; Israel: *T. orthostylus* Zone – *D. sublodoensis* Zone.

Pontosphaera pulchra (Deflandre) nov. comb. (pl. 8, fig. 2)

Discolithus pulcher Deflandre, in Deflandre and Fert, 1954, p. 143, pl. 12, figs. 17, 18; Bramlette and Sullivan, 1961, p. 143, pl. 3, fig. 8.
Helicosphaera sp. Hay and Towe, 1962, p. 512, pl. 1, figs. 4, 6.
Transversopontis obliquipons (Deflandre) Hay, Mohler and Wade, 1966, p. 391, pl. 8, fig. 5.
Transversopontis pulcher (Deflandre) Hay, Mohler and Wade, 1966, p. 391; Perch-Nielsen, 1967, partim, p. 27, pl. 3, figs. 9–11, non pl. 11, fig. 1; Perch-Nielsen, 1971d, p. 39, pl. 28, fig. 6; pl. 31, figs. 2, 3; pl. 32, figs. 5, 6.
Transversopontis pseudopulcher Perch-Nielsen, 1967, p. 27, pl. 4, figs. 11, 12; Perch-Nielsen, 1971d, p. 39, pl. 31, figs. 1, 5, 6; pl. 32, figs. 1–4.
Discolithus rectipons Haq, 1968, partim, p. 39, pl. 7, figs. 7–9, non pl. 11, fig. 1.

Remarks: The central plate contains two large openings separated by a central bridge parallel to the Y-axis. The high margin is supported by about 20 struts. The central furrow connecting the openings may or may not be parallel to the X-axis.
Dimensions: length: 8–12 μ.
Distribution: Spain: *T. orthostylus* Zone – *N. fulgens* Zone; Israel: *D. binodosus* Zone – *D. sublodoensis* Zone.

Pontosphaera prava (Locker) nov. comb.

Transversopontis prava Locker, 1967, p. 761, pl. 1, fig. 1; pl. 2, figs. 1, 15; Perch-Nielsen, 1971, p. 38, pl. 33, figs. 1, 2, 4–6.
Discolithina pulchra (Deflandre) Levin, Edwards, 1973, pl. 8, fig. 5.

Remarks: This rare species can be distinguished from *P. pulcheroides* by the shape and the composition of the central bridge. The bridge is slender, oblique and slightly curved. The slightly oblique central furrow divides the bridge into two halves, which are somewhat off-set at the furrow.
Dimensions: length: 11–13 μ.
Distribution: Israel: *D. binodosus* Zone – *D. sublodoensis* Zone.

Pontosphaera pectinata (Bramlette and Sullivan) Proto Decima et al.

Discolithus pectinatus Bramlette and Sullivan, 1961, p. 142, pl. 3, figs. 4, 5.
Discolithina pectinata (Bramlette and Sullivan) Levin; 1965, p. 266; Perch-Nielsen, 1967, p. 25, pl. 2, figs. 10–12; Perch-Nielsen, 1971d, p. 35, pl. 26, fig. 6.
Pontosphaera pectinata (Bramlette and Sullivan) Proto Decima et al., 1975, p. 50, pl. 5, fig. 23.

Remarks: The raised margin of this species is supported by about 20 slender struts. The central plate shows two slits in the foci of the ellipse.

Dimensions: length: 10–12 μ.
Distribution: Israel: *D. binodosus* Zone – *D. sublodoensis* Zone.

Pontosphaera exilis (Bramlette and Sullivan) nov. comb.

Discolithus exilis Bramlette and Sullivan, 1961, p. 142, pl. 2, fig. 10.
Transversopontis exilis (Bramlette and Sullivan) Perch-Nielsen, 1971d, p. 38, pl. 27, figs. 3, 5, 6; pl. 31, fig. 4.

Remarks: This species in characterized by two large openings in the central plate and a high margin. The diameter of the openings is larger than the width of the bridge. Specimens may show a short central furrow.
Dimensions: length: 12–14 μ.
Distribution: Israel: *T. orthostylus* Zone – *D. sublodoensis* Zone.

Pontosphaera pulcheroides (Sullivan) nov. comb.

Discolithus aff. *D. pulcher* Deflandre, Bramlette and Sullivan, 1961, p. 143, pl. 3, figs. 9, 10.
Discolithus pulcheroides Sullivan, 1964, p. 183, pl. 4, fig. 7.
Discolithina pulchra (Deflandre) Levin, 1965, p. 266, pl. 41, fig. 6.
Discolithina pulcheroides (Sullivan) Levin and Joerger, 1967, p. 167, pl. 2, fig. 8; Haq, 1968, p. 38, pl. 7, figs. 1–3; Stradner and Edwards, 1968, p. 38, pl. 38, figs. 6–10.
Discolithina cf. *D. pulcheroides* (Sullivan) Levin and Joerger, Gartner and Smith, 1967, p. 4, pl. 6, figs. 1–3.
Transversopontis obliquipons (Deflandre) Hay, Mohler and Wade, Perch-Nielsen, 1967, p. 27, pl. 3, figs. 6–8.
Transversopontis pulcheroides (Sullivan) Perch-Nielsen, 1971, p. 40, pl. 33, figs. 3, 7.

Remarks: This species differs from *P. pulchra* only in the low angle which the bridge makes with the Y-axis. In *P. obliquipons* this angle is considerably larger.
Dimensions: length: 10–12 μ.
Distribution: Spain: *T. orthostylus* Zone – *N. fulgens* Zone; Israel: *T. orthostylus* Zone – *D. sublodoensis* Zone.

Pontosphaera bicaveata (Perch-Nielsen) nov. comb.

Discolithina bicaveata Perch-Nielsen, 1967, p. 23, pl. 4, figs. 8–10; Perch-Nielsen, 1971, p. 33, pl. 27, fig. 7.

Remarks: The species has a high margin and two circular openings in the central plate. The diameter of the central bridge is smaller than that of the openings. The species differs from *P. duocava* in its higher margin, and from *P. exilis* in the smaller diameter of the openings.
Dimensions: length: 10–12 μ.
Distribution: Israel: *T. orthostylus* Zone – *D. lodoensis* Zone.

Pontosphaera obliquipons (Deflandre) nov. comb.

Discolithus obliquipons Deflandre, in Deflandre and Fert, 1954, p. 139, pl. 11, figs. 1, 2; text-fig. 53.
Zygolithus cf. *Z. obliquipons* Deflandre, Stradner, 1964, p. 135, fig. 19.
Discolithina obliquipons (Deflandre) Stradner, Stradner and Edwards, 1968, p. 37, pl. 36, 37, 38, figs. 1–5; Haq, 1968, p. 38, pl. 7, figs. 4–6; pl. 11, fig. 2.
Transversopontis obliquipons (Deflandre) Hay, Mohler and Wade, Perch-Nielsen, 1971d, p. 38, pl. 30, fig. 5.
Non *Transversopontis obliquipons* (Deflandre) Hay, Mohler and Wade, 1966, p. 391, pl. 8, fig. 5; Perch-Nielsen, 1967, p. 27, pl. 3, figs. 6–8.

Remarks: This rare species of *Pontosphaera* is characterized by the strongly oblique bridge between the narrow openings in the central plate. The species differs from *P. pulcheroides* in the absence of struts and in the higher angle between the Y-axis and the bridge.
Dimensions: length: 6–10 μ.
Distribution: Spain: *D. lodoensis* Zone – *D. sublodoensis* Zone.

Pontosphaera scissura (Perch-Nielsen) nov. comb.

Discolithina scissura Perch-Nielsen, 1971d, p. 36, pl. 27, figs. 2, 4; pl. 61, figs. 4, 5.

Remarks: This rare species shows a high margin and one continuous slit (or two shorter ones) in the central plate along the X-axis.
Dimensions: length: 13–16 μ.
Distribution: Spain: *N. fulgens* Zone.

GROUP 3

Pontosphaera fimbriata (Bramlette and Sullivan) nov. comb.

Discolithus fimbriatus Bramlette and Sullivan, 1961, p. 142, pl. 3, fig. 1.
Syracosphaera fimbriata (Bramlette and Sullivan) Bukry and Bramlette, 1969, p. 141.
Koczyia fimbriata (Bramlette and Sullivan) Perch-Nielsen, 1971, p. 37, pl. 27, fig. 1; pl. 29, figs. 1, 2.

Remarks: The central plate shows two medium-sized openings connected by a central furrow.
Dimensions: length: 13–18 μ
Distribution: Spain: *T. orthostylus* Zone – *D. sublodoensis* Zone; Israel: *D. lodoensis* Zone – *D. sublodoensis* Zone.

Pontosphaera labrosa (Bukry and Bramlette) Perch-Nielsen

Reticulofenestra caucasica Hay, Mohler and Wade, 1966, partim, p. 368, pl. 2, figs. 6–8, non pl. 2, fig. 5; pl. 3, figs. 1, 2; pl. 4, figs. 1, 2.
Syracosphaera labrosa Bukry and Bramlette, 1969, p. 141, pl. 3, figs. 15–17.
Pontosphaera labrosa (Bukry and Bramlette) Perch-Nielsen, 1977, p. 789, pl. 27, fig. 5.

Remarks: This rare species has a high, distally flaring margin and a relatively narrow flange. It differs from *P. fimbriata* in the presence of a single, large opening in the central plate.
Dimensions: length: 14–16 μ.
Distribution: Israel: *D. lodoensis* Zone.

Pontosphaera excelsa (Perch-Nielsen) Perch-Nielsen

Koczyia excelsa Perch-Nielsen, 1971, p. 37, pl. 28, figs. 1–5; pl. 60, fig. 16.
Pontosphaera excelsa (Perch-Nielsen) Perch-Nielsen, 1977, p. 789, pl. 27, figs. 2, 3.

Remarks: The margin is supported by about 20 struts. The central plate shows a medium-sized central opening.
Dimensions: length: 11–13 μ.
Distribution: Israel: *D. sublodoensis* Zone.

Pontosphaera formosa (Bukry and Bramlette) nov. comb.

Syracosphaera formosa Bukry and Bramlette, 1969, p. 140, pl. 3, figs. 12–14.

Remarks: The wide flange shows about 30 units in cross-polarized light. These units are probably the result of crenulation (as in *L. mochlophorus*). The central plate shows a large opening. The species differs from *P. labrosa* in the distinctly wider and crenulated (?) flange.
Dimensions: length: 14–17 μ.
Distribution: Spain: *N. fulgens* Zone.

Genera INCERTAE SEDIS

Genus **Thoracosphaera** Kamptner, 1927

Type species: *Syracosphaera heimi* Lohmann, 1920
Remarks: This genus was introduced by Kamptner for hollow, globular bodies composed of many calcareous elements. He designated *T. pelagica* as the type species, which is the same form described by Lohmann (1920) as *Syracosphaera heimi*. The systematic position of thoracosphaerids has always been a problem. Kamptner regarded them as coccolithophorids but stated that this assignment could be proved only by study of the living material. Other authors, therefore, classed these forms under genera incertae sedis. Fütterer (1976) assigned *T. heimi* to the calcareous dinoflagellates because of the large resemblance between this form and the spherical cysts of calciodinellid forms with an apical archeopyle. He also considered most of the fossil *Thoracosphaera* species to be calcareous dinoflagellate cysts.

Although we are also inclined to assign the thoracosphaerids to the calcareous dinoflagellates, these forms are still grouped here under genera incertae sedis, as long as biology has not given evidence of the dinoflagellate nature of the extant *T. heimi*.

Thoracosphaera operculata Bramlette and Martini
(pl. 1, fig. 1)

Thoracosphaera deflandrei Kamptner, Stradner, 1961, p. 84, text-fig. 74; Hay and Mohler, 1967a, p. 1534, pl. 203, fig. 8; Haq, 1971, p. 50, pl. 9, figs. 10, 11; pl. 14, fig. 8.
Thoracosphaera operculata Bramlette and Martini, 1964, p. 305, pl. 5, figs. 3–7; Perch-Nielsen, 1969a, p. 330, pl.34, fig. 9.
Thoracosphaera sp. Perch-Nielsen, 1969b, p. 65, pl. 2, figs. 13, 14.
Thoracosphaera sp. 3 Perch-Nielsen, 1971d, p. 55, pl. 50, fig. 1.

Remarks: Characteristic features of this species are: the spherical test composed of very small lath-like elements and the presence of a circular opening covered by a lid (operculum).

The proximal margin of the operculum is reinforced by a single cycle of larger elements. The number of elements in the operculum seems to be higher in later specimens than in earlier ones.
Dimensions: diameter of sphere: 15–20 μ., diameter of operculum: 5–6 μ.
Distribution: Spain: *B. sparsus* Zone – *T. contortus* Zone; Israel: *B. sparsus* Zone – *T. contortus* Zone; Scandinavia: *B. sparsus* Zone – *E. macellus* Zone.

Thoracosphaera saxea Stradner

Thoracosphaera saxea Stradner, 1961, p. 84, text-fig. 71; Stradner, in Gohrbandt, 1963, p. 78, pl. 10, fig. 8; Hay and Mohler, 1967a, p. 1534, pl. 203, fig. 5.
Thoracosphaera cf. *T. imperforata* Kamptner, Bramlette and Martini, 1964, p. 305, pl. 5, figs. 1, 2.
Thoracosphaera cf. *T. deflandrei* Kamptner, Moshkovitz, 1967, p. 154, pl. 5, fig. 8.
Thoracosphaera cf. *T. operculata* Bramlette and Martini, Edwards, 1973, pl. 15, fig. 6.
Thoracosphaera deflandrei Kamptner. Haq and Lohmann, 1976, pl. 3, fig. 10.

Remarks: The elements of this species are larger and thicker than those of *T. operculata*. The spheres lack a large circular opening.
Dimensions: diameter of sphere: 20–30 μ.
Distribution: Spain: *B. sparsus* Zone – *T. orthostylus* Zone; Israel: *P. dimorphosus* Zone – *T. orthostylus* Zone; Scandinavia: *B. sparsus* Zone – *C. tenuis* Zone.

Genus **Neocrepidolithus** nov. gen.

Type species: *Crepidolithus neocrassus* Perch-Nielsen
Diagnosis: This genus is introduced for elliptical coccoliths composed of a margin with slightly (subvertical) to strongly clockwise imbricating elements (rim) and a relatively thin basal cycle of elements (wall).

The extinction lines are dextrogyre in distal view.
Differential diagnosis: *Neocrepidolithus* differs from the Jurassic genus *Crepidolithus* (Noël, 1968) in the imbrication of the elements in the wall.

Neocrepidolithus neocrassus (Perch-Nielsen) nov. comb.
(pl. 1, fig. 6)

Crepidolithus neocrassus Perch-Nielsen, 1968, p. 36, pl. 2, fig. 9; text-fig. 11.
Crepidolithus cohenii Perch-Nielsen, 1968, p. 37, pl. 2, figs. 7, 10; text-fig. 12; Hoffman, 1970, p. 852, pl. 2, figs. 1, 2.
Crepidolithus sp. Perch-Nielsen, 1968, p. 38, pl. 2, figs. 8, 16.
Crepidolithus sp. Perch-Nielsen, 1969b, partim, p. 58, pl. 4, figs. 3, 4; non pl. 4, figs. 1, 5.

Remarks: The margin of this species is composed of 30 to 40 elements, which show a strong clockwise imbrication in distal view. The central area is closed by an inner cycle of elements. In the upper part of the *C. primus* Zone and in the *P. dimorphosus* Zone specimens occur in which the elements of the inner cycle form a cross-like structure. This structur is orientated along the major axes of the ellipse in early specimens, but in later specimens it makes an angle of about 10° with these axes in clockwise direction in distal view.
Dimensions: length: 4–7 μ.
Distribution: Spain: *C. primus* Zone – *C. tenuis* Zone; Israel: *C. primus* Zone – *C. tenuis* Zone; Scandinavia: *B. sparsus* Zone – *E. macellus* Zone.

Neocrepidolithus fossus (Romein) nov. comb.
(pl. 1, figs. 4, 5)

Crepidolithus sp. Perch-Nielsen, 1969, partim, p. 58, pl. 4, fig. 5, non pl. 4, figs. 3, 4.
Crepidolithus fossus Romein, 1977, p. 273, pl. 1, fig. 8.

Remarks: This broad elliptical species consists of a single cycle of 17 to 35 wedge-like elements, which slightly imbricate clockwise in distal view. The elements meet in the centre in such a way that several irregularly spaced pores are formed. *N. fossus* lacks the proximal cycle of elements that can be found in *N. neocrassus*. "*Discolithina*" *rimosa* shows anti-clockwise imbricating elements in its margin.

Dimensions: length: 5–7 μ.
Distribution: Spain: *C. primus* Zone – *E. macellus* Zone; Israel: *C. primus* Zone – *E. macellus* Zone; Scandinavia: *C. primus* Zone – *C. tenuis* Zone.

Genus **Micula** Vekshina, 1959

Type species: *Micula decussata* Vekshina, 1959

Micula decussata Vekshina

Micula decussata Vekshina, 1959, p. 71, pl. 1, fig. 6; pl. 2, fig. 11; Bukry, 1969, p. 67, pl. 40, figs. 5, 6; Verbeek, 1977, p. 119, pl. 11, fig. 12.

Remarks: The species has the form of a cube with depressed faces. It is composed of at least eight elements. Two of the six faces show subdiagonal dextrogyre sutures, the other four faces show diagonal sutures. The faces with dextrogyre sutures are regarded as the distal and the proximal side.

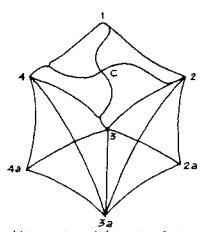

oblique distal/proximal view

Micula

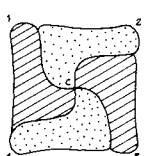

high focus
+-nicols, 1λ, standard orientation

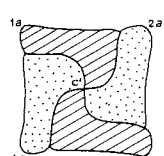

low focus
+-nicols, 1λ, standard orientation

For the standard orientation for distal (proximal) view, the sides with the straight sutures are placed parallel to the cross-hairs. In order to faciliate the description the corners in the upper face are numbered 1 to 4 in clockwise direction in distal view; the underlying corners in the lower face are numbered 1a to 4a. The centre of the upper face is referred to as C, that of the lower face as C'.

In the standard orientation, and when the focus is on the upper face the larger parts of the 1-C-4 and 2-C-3 zones are blue; the other zones are yellow.

When the focus is on the lower face the 1a-C'-2a and 4a-C'-2a zones are blue and the other zones are yellow.
Dimensions: length of edge: 6–10 μ.
Distribution: Spain: *B. sparsus* Zone – *N. fulgens* Zone; Israel: *B. sparsus* Zone – *D. sublodoensis* Zone; Scandinavia: *B. sparsus* Zone – *E. macellus* Zone.

Genus **Octolithus** nov. gen.

Type species: *Tetralithus multiplus* Perch-Nielsen, 1973
Derivation of name: from octo (gr.), eight, and lithos (gr.), stone.
Diagnosis: This genus is introduced for nannoliths consisting of a single layer of eight elements. Four of these elements are larger than the other four.
Differential diagnosis: *Octolithus* differs from *Tetralithus* in the arrangement of the elements in a single layer, instead of in two superposed ones.

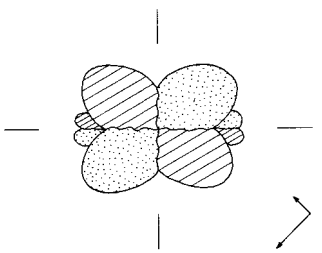

Octolithus multiplus (Perch-Nielsen) nov. comb.

Tetralithus? sp. Perch-Nielsen, 1969b, p. 64, pl. 6, figs. 4, 5.
Tetralithus multiplus Perch-Nielsen, 1973, p. 326, pl. 9, figs. 6, 7; pl. 10, figs. 17, 18; Romein, 1977, p. 276, pl. 2, fig. 7.

Remarks: This slightly vaulted species shows an irregular oval outline. The four larger elements are radially arranged; the four smaller ones are inserted two by two at opposite sides of the fossil in the outer angles formed by two adjacent larger elements.
Dimensions: length: 5–7 μ.
Distribution: Spain: *B. sparsus* Zone – *E. macellus* Zone; Scandinavia: *B. sparsus* Zone – *E. macellus* Zone.

Genus **Goniolithus** Deflandre, 1957

Type species: *Goniolithus fluckigeri* Deflandre, 1957

Remarks: The pentagonal nannoliths of this genus can easily be distinguished from those of *Braarudosphaera* and *Micrantolithus*; they are composed not of five larger elements, but of a large number of regularly arranged, smaller crystals.

Goniolithus fluckigeri Deflandre

Goniolithus fluckigeri Deflandre, 1957, p. 2539, figs. 1–4; Stradner and Edwards, 1968, p. 42, pl. 41; text-figs. 8/1, 2, A-F; Perch-Nielsen, 1969b, p. 62, pl. 6, figs. 7, 8.
Goniolithus cf. *G. fluckigeri* Deflandre, Hay and Mohler, 1967a, p. 1536, pl. 202, figs. 4, 5.

Remarks: An excellent description of this species has been given by Stradner and Edwards (1968). Due to its low relief and low interference the species is hard to detect in the L.M.
Dimensions: 6–7 μ.
Distribution: Spain: *B. sparsus* Zone – *E. macellus* Zone; Israel: *C. tenuis* Zone; Scandinavia: *C. tenuis* Zone.

Genus **Biantholithus** Bramlette and Martini, 1964

Type species: *Biantholithus sparsus* Bramlette and Martini, 1964

Biantholithus sparsus Bramlette and Martini
(pl. 1, fig. 9)

Biantholithus sparsus Bramlette and Martini, 1964, p. 305, pl. 4, figs. 12–14; Perch-Nielsen, 1969b, p. 56, pl. 6, figs. 1–3, 10; pl. 7, figs. 3–10; Romein, 1977, p. 269, pl. 1, figs. 3, 5.
Biantholithus aff. *B. sparsus* Bramlette and Martini, Perch-Nielsen, 1969a, p. 329, pl. 37, fig. 7.

Remarks: The number of elements in the closely appressed cycles varies from 6 to 12. The clockwise imbricating elements of the convex, distal cycle are separated by anti-clockwise oblique sutures, those of concave proximal cycle, by radial sutures. The outer margin of the elements may be straight, outward convex or pointed.
Dimensions: diameter: 10–14 μ.
Distribution: Spain: *B. sparsus* Zone – *E. macellus* Zone; Israel: *B. sparsus* Zone – *C. primus* Zone; Scandinavia: *B. sparsus* Zone – *C. primus* Zone.

Genus **Lapideacassis** Black, 1971

Type species: *Lapideacassis mariae* Black, 1971

Lapideacassis blackii Perch-Nielsen
(pl. 7, fig. 8; pl. 9, fig. 11)

Lapideacassis blackii Perch-Nielsen, 1977, p. 850, pl. 2, figs. 7, 8; text-figs. 3, 5.

Remarks: The few specimens we found lack a distinct proximal tier and collar. The first and the second distal tier, and the centro-distal spine show an equal number of segments (about 12).
Dimensions: height: 26–30 μ., diameter: 8 μ.
Distribution: Spain: *P. dimorphosus* Zone, *D. mohleri* Zone, *D. multiradiatus* Zone.

Genus **Scampanella** Forchheimer and Stradner, 1973

Type species: *Scampanella cornuta* Forchheimer and Stradner, 1973

Scampanella asymmetrica Perch-Nielsen

Scampanella asymmetrica Perch-Nielsen, 1977, p. 853, pl. 2, figs. 3–6, 9, 10.

Remarks: This rare species is characterized by its single, asymmetric spine.
Dimensions: height: 11 μ., diameter: 6 μ.
Distribution: Spain: *P. dimorphosus* Zone.

Scampanella sp.

Description: The specimens are composed of only a first distal tier and a low apical one. Spines or processes are absent.
Dimensions: height: 8–10 μ., diameter: 7 μ.
Distribution: Israel: *E. macellus* Zone, *D. binodosus* Zone.

Scampanella bispinosa Perch-Nielsen

Scampanella bispinosa Perch-Nielsen, 1977, p. 853, pl. 3, figs. 1–7; pl. 6, figs. 12–17; text-fig. 3/14.

Remarks: The single specimen we found has two short apical spines, which are almost perpendicular to each other.
Dimensions: height: 17 μ., diameter: 6 μ.
Distribution: Spain: *D. mohleri* Zone.

Genus **Scapholithus** Deflandre, 1954

Type species: *Scapholithus fossilis* Deflandre, 1954

Scapholithus apertus Hay and Mohler
(pl. 6, fig. 6)

Scapholithus apertus Hay and Mohler, 1967a, p. 1534, pl. 201, figs. 11, 12, 14.
Scapholithus rhombiformis Hay and Mohler, 1967, p. 1534, pl. 201, figs. 13, 16–18; Perch-Nielsen, 1972, pl. 8, figs. 3, 4.
"Scapholithus" apertus Hay and Mohler, Edwards, 1973, pl. 11, fig. 6.

Remarks: Hay and Mohler separated *S. rhombiformis* from *S. apertus* because of the absence of a central rod; in our opinion, the micrographs of the former species represent the proximal side of the latter species.
Dimensions: length along the longer diagonal: 5 μ.
Distribution: Spain: *C. tenuis* Zone, *H. kleinpellii* Zone, *D. multiradiatus* Zone; Israel: *D. mohleri* Zone.

Genus **Ellipsolithus** Sullivan, 1964

Type species: *Coccolithites macellus* Bramlette and Sullivan, 1961

Ellipsolithus macellus (Bramlette and Sullivan) Sullivan

Coccolithites macellus Bramlette and Sullivan, 1961, p. 152, pl. 7, figs. 11–13.
Coccolithus macellus (Bramlette and Sullivan) Stradner, in Gohrbandt, 1963, p. 75, pl. 8, figs. 7–9; text-figs. 3a, b.
Ellipsolithus macellus (Bramlette and Sullivan) Sullivan, 1964, p. 184, pl. 5, fig. 3; Perch-Nielsen, 1977, pl. 42, figs. 1–6; pl. 43, fig. 9.

Remarks: In plane view the species has a long elliptical outline with almost parallel sides. The margin is composed of 55 to 65 elements, which imbricate clockwise in distal view. The central area is closed by two rows of elements, one at each side of the X-axis. Early specimens of this species are smaller than later ones.
Dimensions: length: 7–15 μ.
Distribution: Spain: *E. macellus* Zone – *D. binodosus* Zone; Israel: *E. macellus* Zone – *T. orthostylus* Zone.

Ellipsolithus distichus (Bramlette and Sullivan) Sullivan

Coccolithites distichus Bramlette and Sullivan, 1961, p. 152, pl. 7, fig. 8; Stradner, in Gohrbandt, 1963, p. 76, pl. 9, figs. 3, 4.
Ellipsolithus distichus (Bramlette and Sullivan) Sullivan, 1964, p. 184, pl. 5, figs. 4–6; Edwards and Perch-Nielsen, 1975, pl. 8, fig. 1; Perch-Nielsen, 1977, pl. 43, figs. 1, 2, 4, 8.

Remarks: The species differs from *E. macellus* in the presence of openings in the central area. Their number varies from 7 to 18.
Dimensions: length: 6–12 μ.

Distribution: Spain: *T. contortus* Zone; Israel: *E. macellus* Zone – *T. contortus* Zone.

Genus **Discolithina** Loeblich and Tappan, 1963

Type species: *Discolithus vigintiforatus* Kamptner, 1948

Discolithina rimosa (Bramlette and Sullivan) Levin and Joerger (pl. 6, fig. 5)

Discolithus rimosus Bramlette and Sullivan, 1961, p. 143, pl. 3, figs. 12, 13; Sullivan, 1964, p. 183, pl. 4, fig. 9.

Discolithina rimosa (Bramlette and Sullivan) Levin and Joerger, 1967, p. 167, pl. 2, figs. 9, 10; Radomski, 1968, p. 571, pl. 46, figs. 5, 6.

Remarks: This elliptical species is composed of a thin proximal cycle and a thick distal cycle. The proximal cycle consists of plate-like elements separated by subradial sutures. The elements either extend to the centre and close it, or they give rise to an elliptical or slit-like central opening.

The distal cycle is built up of 50 to 60, in distal view strongly counterclockwise imbricating elements. These elements are high marginally and slope inwards towards the centre. *D. rimosa* can easily be distinguished from species of *Neocrepidolithus* by the opposite direction of imbrication. The extinction lines are laevogyre in distal view.

The species is provisionally placed in the "dust-bin" genus *Discolithina* (elliptical coccoliths with a thickened margin).

Dimensions: length: 5–10 μ.

Distribution: Spain: *F. tympaniformis* Zone – *D. lodoensis* Zone; Israel: *F. tympaniformis* Zone – *T. orthostylus* Zone.

Genus **Hornibrookina** Edwards, 1973

Type species: *Hornibrookina teurensis* Edwards, 1973

Hornibrookina australis Edwards and Perch-Nielsen

Hornibrookina sp. Edwards, 1973, p. 77, fig. 82.

Hornibrookina n. sp. Edwards, 1973, pl. 9, figs. 1–3.

Hornibrookina australis Edwards and Perch-Nielsen, 1975, p. 485, pl. 2, figs. 1–3, 6, 9, 12; pl. 5, figs. 6, 9, 12; pl. 21, figs. 7–14; Wind and Wise, 1977, p. 296, pl. 7, figs. 2–6.

Remarks: The pointed elliptical outline is typical for this rare species.

Dimensions: length: 4–5 μ.

Distribution: Spain: *D. mohleri* Zone – *T. contortus* Zone; Israel: *T. contortus* Zone.

Genus **Rhomboaster** Bramlette and Sullivan, 1961

Type species: *Rhomboaster cuspis* Bramlette and Sullivan, 1961
Description:

Shape: Basically, the species have the form of a rhombohedron with depressed faces.

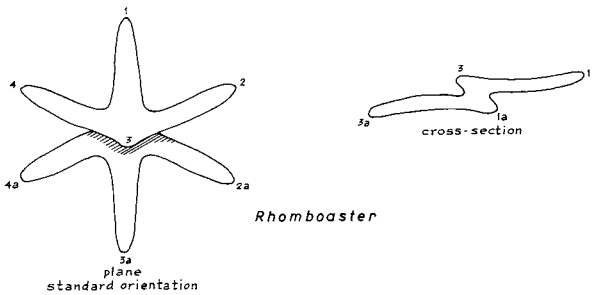

Construction: The specimens consist of a single calcite block.
Specific criteria: The species are based on the outline of the calcite blocks.
Extinction: In cross-polarized light the species show a low birefringence.
Standard orientation: For the description of the species the same number code is applied as was introduced for species of *Micula*; for the standard orientation for plane view the 1–3 diagonal is placed parallel to the Y-cross-hair.
Differential diagnosis: *Rhomboaster* differs from *Micula* in its rhomboid shape.

Rhomboaster intermedia nov. sp.
(pl. 10, figs. 7–9)

Description: The rare representatives of this species are intermediate between *Micula* and *Rhomboaster*. They have a rhomboid shape but are composed of different crystallographic units. The faces are depressed, and six of the twelve edges are thickened: the edges 3–2, 3–4, 3–3a, and the edges 1a–1, 1a–2a, 1a–4a.
Differential diagnosis: *R. intermedia* can be distinguished from *R. bitrifida* by the presence of more than one calcite unit.
Dimensions: diameter: 8–10 μ.
Holotype: T 370a, pl. 10, fig. 7, from sample SP624, *D. multiradiatus* Zone.
Derivation of name: from inter-medius (lat.), intermediate.
Type locality: Barranco del Gredero.

Stratum: Jorquera Formation, Member C.
Age: Late Paleocene.
Paratypoid: T 370b, pl. 10, fig. 9, sample SP624.
Distribution: Spain: *D. multiradiatus* Zone.

Rhomboaster bitrifida nov. sp.
(pl. 7, figs. 3, 4; pl. 10, figs. 10–13)

Rhomboaster cuspis Bramlette and Sullivan, 1961, partim, p. 166, pl. 14, fig. 17, non pl. 14, figs. 18, 19.

Derviation of name: bi (lat.), two; trifida (lat.), with three feet.
Description: The species has the shape of a high rhombohedron with strongly depressed faces, so that cuspate corners are formed. Four arms are visible in the upper face: three longer ones, pointing in the direction of the corners 1, 2 and 4, and a shorter one pointing in the direction of corner 3. The configuration in the lower face is the mirror image of that in the upper face.

In early specimens the arms 1a and 3 are somewhat more pronounced than in later specimens.
Differential diagnosis: The species differs from *R. calcitrapa* in its shorter arms.
Dimensions: diameter: 6–10 μ.
Holotype: T 363, pl. 7, fig. 4 from sample SP630, *D. multiradiatus* Zone.
Type locality: Barranco del Gredero.
Stratum: Jorquera Formation, Member D.
Age: Late Paleocene.
Paratypoid: T 371a, pl. 10, figs. 10, 11, sample SP630.
Distribution: Spain: *D. multiradiatus* Zone – *T. contortus* Zone; Israel: *T. contortus* Zone.

Rhomboaster calcitrapa Gartner
(pl. 7, fig. 5)

Rhomboaster calcitrapa Gartner, 1971, partim, p. 114, pl. 4, figs. 3, 5, 6, non pl. 4, figs. 2, 4.
Marthasterites spineus Shafik and Stradner, 1971, partim, p. 93, text-fig. 7a, non text-figs. 6, 7b, c, d.

Remarks: This species differs from *R. bitrifida* in its longer, spine-like arms. These arms taper outwards to sharply pointed tips. Intermediate forms between this species and *R. bitrifida* were observed in the *D. multiradiatus* Zone.
Dimensions: diameter: 10–18 μ.
Distribution: Spain: *D. multiradiatus* Zone.

Genus **Semihololithus** Perch-Nielsen, 1971

Type species: *Semihololithus biskayae* Perch-Nielsen, 1971
Remarks: Perch-Nielsen introduced this genus for nannoliths which are constructed partly as holococcoliths and partly as heterococcoliths.

Semihololithus kerabyi Perch-Nielsen

Semihololithus kerabyi Perch-Nielsen, 1971c, p. 357, pl. 9, figs. 5–7; pl. 10, figs. 1–6; pl. 14, figs. 19–21.
"*Semihololithus*" *kerabyi* Perch-Nielsen, Edwards, 1973, pl. 13, fig. 3.

Remarks: The species is composed of a thick, proximally tapering base surmounted by a distal rod. The base is fully or partly constructed of small crystals. The rod shows four blades, which make an angle of about 45° with the axes of the elliptical base. In most specimens the base has broken off.
Dimensions: height: 4–14 μ.
Distribution: Spain: *D. multiradiatus* Zone – *T. contortus* Zone.

Semihololithus biskayae Perch-Nielsen
(pl. 7, fig. 7)

Semihololithus biskayae Perch-Nielsen, 1971c, p. 356, pl. 11, figs. 7–11; pl. 14, figs. 10–12.

Remarks: This hollow, beehive-shaped species is composed of varying amounts of smaller crystals and larger elements; in our material all kinds of transitions between specimens consisting entirely of smaller crystals and forms composed entirely of larger elements were observed. It seems that the species has a holococcolithinid "frame", which may be covered by larger elements in later ontogenetic stages or by secondary calcification.

Holococcolithinid variants show a proximally tapering base superposed by a dome with two rows of holes.

Heterococcolithinid variants have a fasciculith-like appearance; in distal view, they show about 9 radially arranged wedges, rounded marginally.
Dimensions: height: 5–7 μ.
Distribution: Spain: *D. multiradiatus* Zone.

Genus **Tribrachiatus** Shamrai, 1963 emend. this paper

Type species: *Tribrachiatus orthostylus* (Bramlette and Riedel) Shamrai (= *Discoaster tribrachiatus* Bramlette and Riedel)
Remarks: Shamrai (1963) introduced this genus for nannoliths consisting of a single calcite unit and having three regularly spaced arms. The genus

is emended here to include forms with six arms. These forms have been assigned to the genus *Marthasterites* by most authors, but in our opinion this genus is restricted to the Cretaceous.

Description:

Shape: The species are three- or hexaradiate in plane view.

Construction: The species consist of a single, modified calcite crystal. In three-rayed species the arms form angles of 120°; six-rayed species are composed of two superposed triplets. The angles between the upper and the lower triplet are variable.

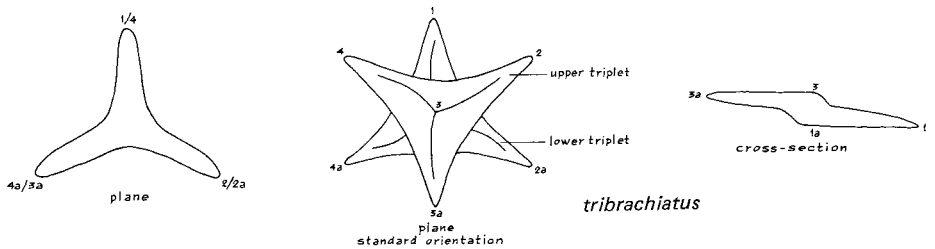

Specific criteria: The species are based on the angles between the arms in the upper and lower triplet and on the length of the arms.

Standard orientation: For the standard orientation for plane view, one of the arms of the lower triplet is placed parallel to the Y-cross-hair in such a way that it points in the positive direction of this cross-hair.

Differential diagnosis: In the closely related genus *Rhomboaster* the arms of the triplets are not regularly spaced.

Tribrachiatus spineus (Shafik and Stradner) nov. comb.
(pl. 7, fig. 6)

Marthasterites spineus Shafik and Stradner, 1971, partim, p. 93, text-figs. 6, 7b, c, d, non text-fig. 7a.
Rhomboaster calcitrapa Gartner, 1971, partim, p. 114, pl. 4, fig. 4, non pl. 4, figs. 2, 3, 5, 6.

Remarks: The species shows six regularly spaced spine-like arms. These arms unite in the centre in such a way that three of them lie in an upper level and the other three in a lower level. The arms show central ribs, which are slightly convex clockwise, near the centre. The arms may show one or more notches at about half of their length. The species differs from *T. nunnii* in its longer arms.

Dimensions: diameter: 10–22 μ.

Distribution: Spain: *D. multiradiatus* Zone.

Tribrachiatus nunnii (Brönnimann and Stradner) nov. comb.

Marthasterites bramlettei Brönnimann and Stradner, 1960, p. 366, figs. 17–20, 23, 24; Stradner and Papp, 1961, p. 113, pl. 11, fig. 9; pl. 19, figs. 5, 6.
Rhomboaster cuspis Bramlette and Sullivan, 1961, partim, p. 166, pl. 14, figs. 18, 19, non pl. 14, fig. 17.
Marthasterites nunnii (Brönnimann and Stradner) Gartner, 1971, p. 116.

Remarks: The relatively wide central body shows six, regularly placed, spine-like arms. The ridges on the arms are convex clockwise in the upper triplet.
Dimensions: diameter: 10–16 μ.
Distribution: Spain: *T. contortus* Zone; Israel: *T. contortus* Zone.

Tribrachiatus contortus (Stradner) Bukry
(pl. 10, fig. 15)

Discoaster contortus Stradner, 1958, p. 187, text-figs. 35, 36.
Marthasterites contortus (Stradner) Deflandre, 1959, p. 139; Stradner and Papp, 1961, p. 112, pl. 36, figs. 1–8; text-figs. 11/8, 20/3.
Tribrachiatus contortus (Stradner) Bukry, 1972, p. 1081.

Remarks: The angles between the arms of the upper and the lower triplet are not equal; smaller and larger angles alternate.

The ridges on the arms are curved in the same manner as in *T. nunnii*.
Dimensions: diameter: 11–15 μ.
Distribution: Israel: *T. contortus* Zone.

Tribrachiatus orthostylus Shamrai

Discoaster tribrachiatus Bramlette and Riedel, 1954, p. 397, pl. 38, fig. 11.
Marthasterites tribrachiatus (Bramlette and Riedel) Deflandre, 1959, p. 138, pl. 2, fig. 1.
Discoaster tribrachiatus robustus Stradner, 1959, p. 477, figs. 4, 9.
Marthasterites robustus (Stradner) Stradner and Papp, 1961, p. 109, pl. 34, fig. 7; text-figs. 11/4, 20/1.
Tribrachiatus orthostylus Shamrai, 1963, p. 38, pl. 2, figs. 13, 14 (nom. subst. pro *Discoaster tribrachiatus* Bramlette and Riedel, I.C.B.N., art. 55).

Remarks: This triradiate species is slightly arched. The arms may be straight or slightly curved; they can be slender and parallel-sided, or wide and tapering. The tips of the arms may be pointed, blunt or notched.
Dimensions: diameter: 6–9 μ.
Distribution: Spain: *T. contortus* Zone – *T. orthostylus* Zone; Israel: *T. contortus* Zone – *T. orthostylus* Zone.

Genus **Zygrhablithus** Deflandre, 1959

Type species: *Zygolithus bijugatus* Deflandre, 1954

Zygrhablithus bijugatus (Deflandre) Deflandre

Zygolithus bijugatus Deflandre, in Deflandre and Fert, 1954, p. 148, pl. 11, figs. 20, 21.
Zygrhablithus bijugatus (Deflandre) Deflandre, 1959, p. 135; Stradner and Edwards, 1966, p. 44–46, pl. 42, 43; Gartner and Bukry, 1969, p. 1218, pl. 140, figs. 3–6; pl. 142, figs. 1, 2; Perch-Nielsen, 1971d, p. 58, pl. 58, figs. 7–9; pl. 59, fig. 10.
Isthmolithus claviformis Brönnimann and Stradner, 1960, p. 368, text-figs. 25–43.
Rhabdosphaera? semiformis Bramlette and Sullivan, 1961, p. 147, pl. 5, figs. 8–10.
Sujkowskiella enigmatica Hay, Mohler and Wade, 1966, p. 397, pl. 13, figs. 6, 7.
Zygrhablithus bijugatus crassus Locker, 1967, p. 764, pl. 1, fig. 7; pl. 2, figs. 7, 8.

Remarks: Variants having a quadrangular outline in side view have been observed in the *D. sublodoensis* Zone.
Dimensions: length of base: 6–8 μ., height: 13–19 μ.
Distribution: Spain: *T. contortus* Zone – *N. fulgens* Zone; Israel: *T. contortus* Zone – *D. sublodoensis* Zone.

Genus **Pedinocyclus** Bukry and Bramlette, 1971

Type species: *Pedinocyclus larvalis* (Bukry and Bramlette) Loeblich and Tappan, 1973

Pedinocyclus larvalis (Bukry and Bramlette) Loeblich and Tappan (pl. 8, fig. 1)

Leptodiscus larvalis Bukry and Bramlette, 1969, p. 134, pl. 2, figs. 8–11.
Pedinocyclus larvalis (Bukry and Bramlette) Loeblich and Tappan, 1973, p. 738; Perch-Nielsen, 1977, pl. 14, fig. 3.

Remarks: The species is probably composed of two superposed shields, which readily separate. Complete specimens show a bright zone around the central opening in cross-polarized light, while the loose shields show low interference colours.

The side where the diameter of the central opening is largest is considered to be distal. In distal view the sutures between the 23 to 35 elements are slightly laevogyre; in proximal view they are subradial.

When the focus is somewhat above a specimen, straight extinction lines can be observed, which make an angle of about 30° with the cross-hairs in clockwise direction in distal view. The second and fourth quadrants of the shields are blue when the gypsum plate is inserted.
Dimensions: diameter: 6–13 μ.
Distribution: Spain: *T. orthostylus* Zone – *D. sublodoensis* Zone; Israel: *T. orthostylus* Zone.

Genus **Chiphragmalithus** Bramlette and Sullivan, 1961

Type species: *Chiphragmalithus calathus* Bramlette and Sullivan, 1961

Chiphragmalithus calathus Bramlette and Sullivan

Chiphragmalithus calathus Bramlette and Sullivan, 1961, p. 156, pl. 10, figs. 7, 8–10; Perch-Nielsen, 1971, p. 47, pl. 39, fig. 4.

Remarks: The height of this species is equal to, or larger than the width of the distal side. The bars of the central cross are parallel to the sides at the distal side, but they are almost diagonal at the proximal side.
Dimensions: width of distal side: 5–10 μ.
Distribution: Spain: *T. orthostylus* Zone; Israel: *T. orthostylus* Zone.

Genus **Cyclolithella** Loeblich and Tappan, 1963

Type species: *Cyclolithus inflexus* Kamptner, 1952

Cyclolithella pactilis Bukry and Percival

Cyclolithella pactilis Bukry and Percival, 1971, p. 126, pl. 2, figs. 4–6.

Remarks: The species has the form of a centrally open, truncated cone. The side with the smallest diameter is considered to be proximal. Distally and proximally the cone shows a flange. The cone is composed of 12 to 22 elements.

The sutures in the proximal flange are oblique clockwise in proximal view; in the distal flange they are subradial.

Early specimens are smaller than later ones, and elliptical variants have been observed.

The extinction lines are slightly laevogyre in distal view.
Dimensions: diameter (length): 6–8 μ.
Distribution: Spain: *T. orthostylus* Zone – *D. sublodoensis* Zone; Israel: *T. orthostylus* Zone – *D. sublodoensis* Zone.

Genus **Scyphosphaera** Lohmann, 1902

Type species: *Scyphosphaera apsteini* Lohmann, 1902

Scyphosphaera columella Stradner

"Lopadolith from Lodo 39" Bramlette and Sullivan, 1961, pl. 5, fig. 19.
Scyphosphaera columella Stradner, 1969, p. 416, pl. 88, figs. 4–8; text-fig. 2/7–9.

Remarks: The nannoliths have the form of a vase with slightly concave sides. In our material the "bottom" is mostly absent. The inner layer is considerably thicker than the outer one.
Dimensions: height: 8–21 μ., diameter: 5–9 μ.
Distribution: Spain: *T. orthostylus* Zone; Israel: *T. orthostylus* Zone.

Scyphosphaera apsteinii Lohmann

Scyphosphaera apsteini Lohmann, 1902, p. 132, pl. 4, figs. 26–30; Stradner, 1969, p. 416, pl. 89, figs. 1–3; text-fig. 2/1–6; Perch-Nielsen, 1977, pl. 29, fig. 16.

Remarks: The inner and the outer layer of this rare, barrel-shaped species are about the same thickness. Very small perforations in the margin could be observed in the L.M.
Dimensions: height: 11 μ., diameter: 11 μ.
Distribution: Israel: *T. orthostylus* Zone – *D. lodoensis* Zone.

Scyphosphaera? expansa Bukry and Percival

Scyphosphaera expansa Bukry and Percival, 1971, p. 138, pl. 6, figs. 10–13.
Scyphosphaera? expansa Bukry and Percival, Perch-Nielsen, 1977, pl. 37, figs. 13, 14.

Remarks: The species has the form of a hollow truncated cone, closed at the side with the smallest diameter. In our material this basal plate is generally absent.

The assignment to the genus *Scyphosphaera* is questionable, as the margin consists of only a single layer.
Dimensions: height: 9–14 μ., diameter: 5–7 μ.
Distribution: Spain: *D. lodoensis* Zone – *N. fulgens* Zone; Israel: *D. lodoensis* Zone – *D. sublodoensis* Zone.

Genus Pseudotriquetrorhabdulus Wise and Constans, 1976

Type species: *Pseudotriquetrorhabdulus inversus* (Bukry and Bramlette) Wise and Constans, 1976

Pseudotriquetrorhabdulus inversus (Bukry and Bramlette) Wise and Constans

Triquetrorhabdulus inversus Bukry and Bramlette, 1969, p. 142, pl. 1, figs. 9–14.
Pseudotriquetrorhabdulus inversus (Bukry and Bramlette) Wise and Constans, 1976, p. 154, pl. 4, figs. 1–9; Perch-Nielsen, 1977, pl. 37, figs. 2–5.

Remarks: In most specimens one end of the rod is blunt, the other acute, but we also observed specimens with two acute ends. In side view the rods

are evenly yellow when they make an angle of 45° in anti-clockwise direction with the Y-cross-hair, and evenly blue when rotated over 90° in clockwise direction.
Dimensions: length: 24–26 μ.
Distribution: Spain: *D. sublodoensis* Zone – *N. fulgens* Zone; Israel: *D. sublodoensis* Zone.

Genus **Nannotetrina** Achuthan and Stradner, 1969

Type species: *Nannotetraster fulgens* Stradner, 1960
Description:
Shape: The nannoliths of this genus have the form of a hollow, four-sided pyramid, which has protrusions at its base. The top of the pyramid is considered to be distal.

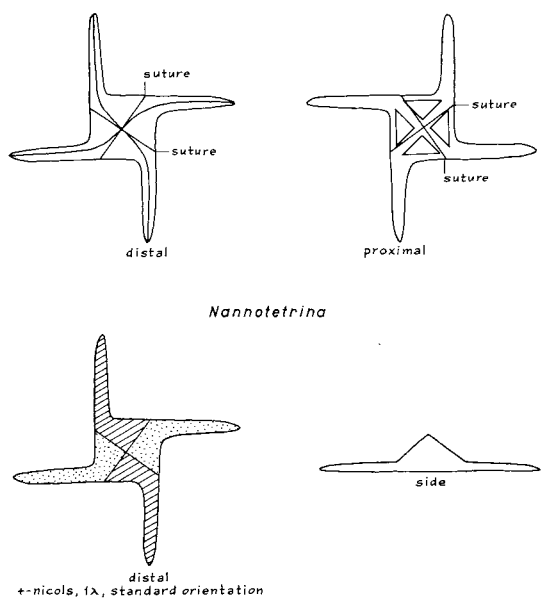

Construction: The pyramids are composed of four units, separated by sutures. The sutures may or may not lie along the edges of the pyramid. The proximal side is partly filled with a cross-like structure, which may or may not be orientated along the diagonals of the base of the pyramid.
Specific criteria: The species are based on the shape and the orientation of the protrusions of the base.
Standard orientation for distal view: Top of pyramid lying upwards; sides

of the base parallel to the cross-hairs.
Extinction lines: In the standard orientation for distal view, the slightly laevogyre or straight extinction lines make a small angle in anti-clockwise direction with the diagonals of the base.
Colour distribution: In the standard orientation for distal view, the second and fourth quadrants are blue, the others are yellow.
Differential diagnosis: *Nannotetrina* differs from *Micula* in its pyramidal shape.

Nannotetrina cristata (Martini) Perch-Nielsen

Trochoaster cristatus Martini, 1958, p. 368, pl. 5, fig. 26; Stradner, 1959, p. 481, text-figs. 56, 58.
Nannotetraster cristatus (Martini) Martini and Stradner, 1960, p. 266; Stradner and Papp, 1961, p. 104, pl. 31, figs. 8, 10; text-fig. 10/10.
Chiphragmalithus cristatus (Martini) Bramlette and Sullivan, 1961, p. 156, pl. 10, figs. 11–13; Radomski, 1968, p. 557, pl. 48, figs. 10, 11.
Nannotetrina cristata (Martini) Perch-Nielsen, 1971d, p. 66, pl. 56, figs. 9–12; Perch-Nielsen, 1977, pl. 47, figs. 1–12.

Remarks: The pyramids of this species show 8 spine-like protrusions. The bars of the central cross-structure lie along the diagonals; centrally they are somewhat higher than the margin. The sutures are slightly laevogyre in distal view; they terminate marginally at some distance from the corners (anti-clockwise).
Dimensions: length of edge: 10–11 μ.
Distribution: Spain: *D. sublodoensis* Zone – *N. fulgens* Zone.

Nannotetrina fulgens (Stradner) Stradner

Nannotetraster fulgens Stradner, in Martini and Stradner, 1960, p. 268, text-figs. 10, 16.
Chiphragmalithus? quadratus Bramlette and Sullivan, 1961, p. 157, pl. 10, figs. 14, 15.
Nannotetrina fulgens (Stradner) Achuthan and Stradner, 1969, p. 7, pl. 5, figs. 4–6; Perch-Nielsen, 1971d, p. 66, pl. 55, figs. 1–7.

Remarks: The species is characterized by four long, spine-like elongations of the basal sides of the pyramid in clockwise direction in distal view. Variants were observed having a strongly reduced pyramid (= *N. alata*).
Dimensions: diameter: 20–25 μ.
Distribution: Spain: *N. fulgens* Zone.

Nannotetrina pappii (Stradner) Perch-Nielsen

Troachoaster pappi Stradner, 1959, p. 480, fig. 54.
Nannotetraster pappi (Stradner) Martini and Stradner, 1960, p. 266, fig. 5; Stradner and Papp, 1961, p. 106, pl. 32, figs. 4, 5; text-fig. 10/7.
Nannotetrina pappi (Stradner) Perch-Nielsen, 1971d, p. 67, pl. 54, figs. 1–6; pl. 57, fig. 9.

Remarks: In this species the sutures coincide with the diagonals of the almost square base. The bars of the central cross make a low angle in counterclockwise direction with the sutures in proximal view. At the intersection points of the bars and the margin, outward projecting, short spines occur, normal to the margin. These spines correspond to ridges on the distal side of the margin.
Dimensions: distance of spine from tip to tip: 10–21 μ.
Distribution: Spain: *N. fulgens* Zone.

Genus **Lanternithus** Stradner, 1962

Type species: *Lanternithus minutus* Stradner, 1962

Lanternithus minutus Stradner

Lanternithus minutus Stradner, 1962, p. 375, pl. 2, figs. 12–15; Gartner and Bukry, 1969, p. 1217, pl. 139, figs. 4–6; pl. 142, figs. 8, 9.

Remarks: This hollow, box-like species is easily recognized by its hexagonal or trapezoidal outline.
Dimensions: length: 4–6 μ.
Distribution: Spain: *N. fulgens* Zone.

REFERENCES

Abtahi, M. (1975). Stratigraphische und mikropaläontologische Untersuchungen der Kreide/Alttertiär Grenze im Barranco del Gredero (Caravaca, Prov. Murcia SE Spanien). Technische Universität Berlin, Thesis.

Achuthan, M. V. and Stradner, H. (1969). Calcareous nannoplankton from the Wemmelian stratotype. Proc. First Internat. Conf. Plankt. Microfos., Geneve, 1967, 1, pp. 1–13.

Adelseck, C. G., Geehan, G. W. and Roth, P. H. (1973). Experimental evidence for the selective dissolution and overgrowth of calcareous nannofossils during diagenesis. Bull. Geol. Soc. America, 84, pp. 2755–2762.

Arkin, Y., Nathan, Y. and Starinsky, A. (1972). Paleocene – Early Eocene environments of deposition in the Northern Negev (Southern Israel). Geol. Surv. Israel Bull., 56, pp. 1–18.

Bang, I. et al. (1977). Excursion guide of the XVth European Micropaleontological Colloquium. Copenhagen.

Bartov, J., Eyal, Y., Garfunkel, Z. and Steinitz, G. (1972). Late Cretaceous and Tertiary stratigraphy and Paleogeography of Southern Israel. Israel Journal Earth Sciences, 21, pp. 69–97.

Bentor, Y. K. (1966). The clays of Israel, guide book to the excursions of the international clay conference, Jerusalem, 1966.

– and Vroman, A. (1964). The geological map of Israel, Nitsana, sheet 17 on scale 1 : 100.000. Geol. Surv. Israel, Jerusalem.

Berggren, W. A. (1962). Some planktonic foraminifera from the Maastrichtian and type Danian stages of Southern Scandinavia. Stockh. Contr. Geol., 9, pp. 1–106.

– (1969). Paleogene biostratigraphy and planktonic foraminifera of Northern Europe. Proc. First Internat. Conf. Plankt. Microfos., Geneva, 1967, 1, pp. 121–160.

Bilgütay, U., Jafar, S. A., Stradner, H. and Szöts, E. (1969). Calcareous nannoplankton from the Eocene of Biarritz, France. Proc. First Internat. Conf. Plankt. Microfos., Geneva, 1967, 1, pp. 167–178.

Black, M. (1962). Fossil coccospheres from a Tertiary outcrop on the continental slope. Geol. Mag., 99, pp. 123–127.

– (1964). Cretaceous and Tertiary coccoliths from atlantic seamounts. Paleontology, 7, pp. 306–316.

– (1965). Coccoliths. Endeavour, 24, pp. 131–137.

– (1967). New names for some coccolith taxa. Proc. Geol. Soc. London, 1640, pp. 139–145.

– (1971). Problematical microfossils from the Gault Clay. Geol. Mag., 108, pp. 325–327.

– and Barnes, B. (1959). The structure of coccoliths from the English Chalk. Geol. Mag., 96, pp. 321–328.

Braarud, T. et al. (1964). *Rhabdosphaera* Haeckel, 1894 (Coccolithophorida) proposed validation under the plenary powers and designation of a lectotype for *Coccolithus oceanicus* Schwarz, 1894. Bull. Zool. Nomencl., 21, pp. 379–400.

Brabb, E. E., Bukry, D. and Pierce, R. L. (1971). Eocene (Refugian) nannoplankton in the Church Creek Formation near Monterey, Central California. Geol. Surv. Res., Chapter C, pp. 44–48.

Bramlette, M. N., and Martini, E. (1968). The great change in calcareous nannoplankton fossils between Maastrichtian and Danian. Micropal., 10, pp. 291–322.

– and Riedel, W. R. (1954). Stratigraphic value of discoasters and some other microfossils related to recent coccolithophores. Journ. Paleont., 28, pp. 385–403.

– and Sullivan, F. R. (1961). Coccolithophorids and related nannoplankton of the Early Tertiary in California. Micropal., 7, pp. 129–188.

– and Wilcoxon, J. A. (1967). Middle Tertiary calcareous nannoplankton of the Cipero section, Trinidad, W. I. Tulane Studies in Geol., 5, pp. 93–132.

Braun, M. (1967). Type sections of Avedat Group, Eocene formations in the Negev (southern Israel). Israel Geol. Surv. Strat. sections, 4, pp. 1–14.

Brönnimann, P. and Rigassi, D. (1963). Contribution to the geology and paleontology of the area of the city of la Habana, Cuba, and its surroundings. Eclog. Geol. Helv., 56, pp. 193–480.
– and Stradner, H. (1960). Die Foraminiferen und Discoasteridenzonen von Cuba. Erdoel Zeitschr., 10, pp. 1–18.
Brotzen, F. (1948). The Swedish Paleocene and its Foraminiferal fauna. Sveriges Geol. Undersökn. Arsbok, 42, pp. 1–140.
– (1959). On *Tylocidaris* species (Echinoidea) and the stratigraphy of the Danian of Sweden. Sveriges Geol. Undersökn., C, 571.
Bukry, D. (1971a). Discoaster evolutionary trends. Micropal., 17, pp. 43–52.
– (1971b). Cenozoic calcareous nannofossils from the Pacific Ocean. San Diego Soc. Nat. Hist. Trans., 16, pp. 303–328.
– (1971c). Coccolith stratigraphy, Leg 6, Deep Sea Drilling Project. *In* Fischer, A. G. et al., Initial Repts. D.S.D.P., Washington, 6, pp. 965–1012.
– (1973). Low-latitude coccolith biostratigraphic zonation. *In* Edgar, N. T., Saunders, J. B. et al., Initial Repts. D.S.D.P., Washington, 15, pp. 685–703.
– (1975). Coccolith and silicoflagellate stratigraphy, Northwestern Pacific Ocean, D.S.D.P. Leg 32. *In* Larson, R. L., Moberly, R. et al., Initial Repts. D.S.D.P., Washington, 32, pp. 677–701.
– and Bramlette, M. N. (1969a). Some new and stratigraphically useful calcareous nannofossils of the Cenozoic. Tulane Studies Geol. Pal., 7, pp. 131–142.
– and – (1969b). Coccolith age determinations, Leg 1, Deep Sea Drilling Project. *In* Ewing, J. I. et al., Initial Repts. D.S.D.P., Washington, 1, pp. 369–387.
– and Percival, S. F. (1971). New Tertiary calcareous nannofossils. Tulane Studies Geol. Pal., 8, pp. 123–146.
Bybell, L. and Gartner, S. (1972). Provincialism among mid-Eocene calcareous nannofossils. Micropal., 18, pp. 319–336.
Caron, Y., Luterbacher, H., Perch-Nielsen, K., Premoli-Silva, I., Riedel, W. R. and Sanfilippo, A. (1975). Zonations à l'aide de microfossiles pélagiques du Paléocène supérieur et de l'Eocène inférieur. B.S.G.F., 17, pp. 125–224.
Cepek, P. and Hay, W. W. (1969a). Calcareous nannoplankton and biostratigraphic subdivision of the Upper Cretaceous. Trans. Gulf Coast Assoc. Geol. Soc., 19, pp. 323–336.
– and – (1969b). Zonation of the Upper Cretaceous using calcareous nannoplankton. XXIII Internat. Geol. Congr. (Prague), Proc. Paleobot. Sect., pp. 333–340.
Christensen, T. (1966). Systematisk Botanik Algen. Botanik, 2, pp. 1–180.
Deflandre, G. (1959). Sur les nannofossiles calcaires et leur systématique. Rev. de Micropal., 2, pp. 127–152.
– and Fert, C. (1954). Observations sur les coccolithophoridés actuels et fossiles en microscopie ordinaire et électronique. Ann. de Paleont., 40, pp. 115–176.
Durand Delga, M. and Magné, J. (1959). Données stratigraphiques et micropaleontologiques sur le nummulitique de l'est des Cordilleres Bétiques (Espagne). Rev. de Micropal., 1, pp. 155–175.
Edwards, A. R. (1966). Calcareous nannoplankton from the Uppermost Cretaceous and the Lowermost Tertiary of the Mid-Waipara section, South Island, New Zealand, N.Z.J. Geol. Geophys., 9, pp. 481–490.
– (1971). A calcareous nannoplankton zonation of the New Zealand Paleogene. Proc. Second Plankt. Conf., Rome, 1970, pp. 381–419.
– (1973a). Calcareous nannofossils from the Southwest Pacific, Deep Sea Drilling Project, Leg 21. *In* Burns, R. E., Andrews, J. E. et al., Initial Repts. D.S.D.P., Washington, 21, pp. 641–691.
– (1973b). Key species of New Zealand calcareous nannofossils. N.Z.J. Geol. Geophys., 16, pp. 68–89.
– and Perch-Nielsen, K. (1975). Calcareous nannofossils from the Southern Southwest Pacific, D.S.D.P., Leg 29. *In* Kennett, J. P., Houtz, R. A. et al., Initial Repts. D.S.D.P., Washington, 29, pp. 469–539.

Eldredge, N. and Gould, S. J. (1972). Punctuated equilibria: an alternative to phyletic gradualism. *In* Models in Paleobiology, Schopf, T. J. M., Freeman, Cooper Eds., San Francisco, pp. 82–115.
– and – (1977). Evolutionary models and biostratigraphic strategies. *In* Concepts and methods of biostratigraphy, Kaufmann, E. G. and Hazel, J. E., Eds. Dowden, Hutchinson and Ross, Strodsburg, pp. 25–40.
Ellis, H. C. and Lohman, W. H. (1973). *Toweius petalosus*, new species, a Paleocene calcareous nannofossil from Alabama. Tulane studies Geol. Pal., 10, pp. 107–110.
Fallot, P., Durand Delga, M., Busnardo, M. and Sigal, J. (1958). El Cretaceo superior del sur de Caravaca (Provincia de Murcia). Notas Com. Inst. Geol. Min. España, 50, pp. 283–299.
Farinacci, A. (1969–1974). Catalogue of calcareous nannofossils, I–IV. Ed. Tecnoscienza, Roma.
– (1971). Round table on calcareous nannoplankton. Proc. Second Plankt. Conf., Rome, 1970, pp. 1343–1369.
Gartner, S. (1969). Two new calcareous nannofossils from the Gulf Coast Eocene. Micropal., 15, pp. 31–34.
– (1970). Phylogenetic lineages in the Lower Tertiary coccolith genus *Chiasmolithus*. Proc. N. Am. Pal. Conv., 1969, Part G, pp. 930–957.
– (1971). Calcareous nannofossils from the Joides Blake Plateau cores, and revision of Paleogene nannofossil zonation. Tulane Studies Geol. Pal., 8, pp. 101–121.
– (1972). Remarks on Late Cretaceous to Pleistocene coccoliths from the North Atlantic. *In* Laughton, A. S., Berggren, W. A. et al., Initial Repts. D.S.D.P., Washington, 12, pp. 1003–1069.
– (1977). Nannofossils and biostratigraphy: an overview. Earth. Sc. Rev., 13, pp. 227–250.
– and Bukry, D. (1969). Tertiary holococcoliths. J. of Paleont., 43, pp. 1213–1221.
– and Keany, J. (1978). The terminal Cretaceous event: a geologic problem with an oceanographic solution. Geology, 6, pp. 708–712.
– and Smith, L. A. (1967). Coccoliths and related calcareous nannoplankton from the Yazoo Formation (Jackson, Late Eocene) of Louisiana. Univ. Kansas Paleont. Contr., 20, pp. 1–7.
Hamaoui, M. and Reiss, Z. (1963). Microfaunas of the Taqyie Formation and Hafir Member. Report Pal/3/63, Pal. Division Geol. Surv. Israel, Jerusalem.
Hansen, H. J., Schmidt, R. R. and Mikkelsen, N. (1975). Convertible techniques for the study of the same nannoplankton specimen. Proc. Kon. Ned. Akad. Wet., ser. B, 78, pp. 226–230.
– (1968a). Electron microscope studies on some Upper Eocene calcareous nannoplankton from Syria. Stockh. Contr. Geol., 15, pp. 23–37.
Haq, B. U., (1968b). Studies on some Upper Eocene calcareous nannoplankton from NW Germany. Stockh. Contr. Geol., 18, pp. 13–74.
– (1969). The structure of Eocene coccoliths and discoasters from a Tertiary deep-sea core in the Central Pacific. Stockh. Contr. Geol., 21, pp. 1–19.
– (1971a). Paleogene calcareous nannoflora. Part I: The Paleocene of West-Central Persia and the Upper Paleocene-Eocene of West Pakistan. Stockh. Contr. Geol., 25, pp. 1–56.
– (1971b). Paleogene calcareous nannoflora. Part II: Oligocene of Western Germany. Stockh. Contr. Geol., 25, pp. 57–97.
– (1971c). Paleogene calcareous nannoflora. Part III: Oligocene of Syria. Stockh. Contr. Geol., 25, pp. 99–127.
– (1971d). Paleogene calcareous nannoflora. Part IV: Paleogene nannoplankton biostratigraphy and evolutionary rates in Cenozoic calcareous nannoplankton. Stockh. Contr. Geol., 25, pp. 129–158.
– (1973a). Transgressions, climatic change and the diversity of calcareous nannoplankton. Marine Geol., 15, pp. 25–30.
– (1973b). Evolutionary trends in the Cenozoic coccolithophore genus *Helicopontosphaera*. Micropal., 19, pp. 32–52.
– and Boersma, A. (1978). Introduction to marine micropaleontology. Elsevier, 1978.

– and Lohmann, G. P. (1976). Early Cenozoic calcareous nannoplankton biogeography of the Atlantic Ocean. Marine Micropal., 1, pp. 119–194.
–, Premoli-Silva, I., and Lohmann, G. P. (1977). Calcareous plankton paleobiogeographic evidence for major climatic fluctuations in the Early Cenozoic Atlantic Ocean. J. of Geoph. Res., 82, pp. 3861–3876.
Hay, W. W. (1964). Utilisation stratigraphique des Discoastéridés pour la zonation du Paléocène et de l'Eocène inférieur. Mem. B.R.G.M., 28, pp. 885–889.
– and Mohler, H. P. (1967). Calcareous nannoplankton from Early Tertiary rocks at Pont Labau France, and Paleocene-Early Eocene correlations, Journ. of Pal., 41, pp. 1505–1541.
–, Mohler, H. P., Roth, P. H. and Schmidt, R. R. (1967). Calcareous nannoplankton zonation of the Cenozoic of the Gulf Coast and Carribean-Antillean area and transoceanic correlation. Trans. Gulf Coast Assoc. Geol. Soc., 27, pp. 428–480.
–, Mohler, H. P. and Wade, M. E. (1966). Calcareous nannofossils from Nal'chik (Northwest Caucasus). Eclog. Geol. Helv., 59, pp. 379–399.
– and Schaub, H. W. (1960). Discoasterids from the Schlierenflysch, Switzerland. Bull. Geol. Soc. Am., 71, p. 1885.
– and Towe, K. M. (1962). Electronmicroscopic examination of some coccoliths from Donzacq (France). Eclog. Geol. Helv., 55, pp. 497–517.
Hekel, H. (1968). Nannoplanktonhorizonte und tektonische Strukturen in den Flyschzone nördlich von Wien (Bisambergzug). Jahrb. Geol. Bundesanstalt Wien, 11, pp. 293–338.
Hillebrandt, A. von. (1974). Biostratigrafía del Paleogeno en el Sureste de España (Provincias de Murcia y Alicante). Cuad. Geol., 5, pp. 135–153.
– (1976). Los foraminiferos planctonicos, nummulitidos y coccolithophoridos de la zona de *Globorotalia palmerae* del Cuisiense (Eoceno Inferior) en el S. E. de España (Provincias de Murcia y Alicante). Rev. Esp. Micropal., 8, pp. 323–394.
Hoek, J. van den (1978). Algen: Einführung in die Phycologie. Thieme Verlag, Stuttgart.
Hoffmann, N. (1970). *Placozygus* n. gen. (Coccolithineen) aus der Oberkreide des Nördlichen Mitteleuropas. Geologie, 19, pp. 1004–1007.
Hofker, J. (1966). Maastrichtian, Danian and Paleocene foraminifera. Paleontographica, Suppl. 10.
Honjo, S. and Okada, H. (1974). Community structure of coccolithophores in the photic layer of the mid-Pacific. Micropal., 20, pp. 209–230.
I.N.A. (1979). Newsletter of the International Nannofossil Association, 1.
Jafar, S. A. and Martini, E. (1974). On the retention of the generic name *Cyclococcolithus* Kamptner, 1954, ex Kamptner, 1956, and the rejection of the generic name *Cyclococcolithina* Wilcoxon, 1970. Micropal., 20, pp. 367–368.
– and – (1975). On the validity of the calcareous nannoplankton genus *Helicosphaera*. Senck. Leth., 56, pp. 381–397.
Jerković, M. L. (1970). *Noëlaerhabdus* nov. gen. type d'une nouvelle famille de Coccolithophoridés fossiles: Noëlaerhabdaceae du Miocène supérieur de Yougoslavie. Compt. Rend. Hebd. Séances Acad., Sci., 270, pp. 468–470.
Kamptner, E. (1956). *Thoracosphaera deflandrei* nov. spec., ein bemerkenwertes Kalkflagellaten-Gehäuse aus dem Eozän von Donzacq (Dep. Landes, Frankreich). Osterr. Bot. Zeitschr., 103, pp. 448–456.
Kapellos, C. (1973). Biostratigraphie des Gurnigelflysches mit besonderer Berücksichtigung der Nummuliten und des Nannoplanktons, unter Einbeziehung des paläogenen Nannoplanktons der Krim (U.D.S.S.R.). Mém. Suisse Paleont., 96.
– (1974). Uber das Nannoplankton im Alttertiär des Profils von Zumaya-Gueteria (Provinz Guipúzcoa, Nordspanien). Eclog. Geol. Helv., 67, pp. 435–444.
– and Schaub, H. (1973). Zur Korrelation von Biozonierungen mit Grossforaminiferen und Nannoplankton im Paläogen der Pyrenäen. Eclog. Geol. Helv., 66, pp. 687–737.
Klaveness, D. (1972). *Coccolithus huxleyi* (Lohmann) Kamptner, II. The flagellate cell, aberrant cell types, vegetative propagation and life cycles. Br. Phyc. J., 7, pp. 309–318.

– and Paasche, E. (1971). Two different *Coccolithus huxleyi* cell types incapable of coccolith formation. Arch. Mikrobiol., 75, pp. 382–385.
Klumpp, B. (1953). Beitrag zur Kenntnis der Mikrofossilien des Mittleren und Oberen Eozän. Paleontographica, 103a, pp. 377–406.
Levin, H. L. (1965). Coccolithophoridae and related microfossils from the Yazoo Formation (Eocene) of Mississippi. Journ. Pal., 39, pp. 265–272.
Locker, S. (1965). Coccolithophoriden aus Eozänschollen Mecklenburgs. Geologie, 14, pp. 1252–1261.
– (1967). Neue, stratigraphisch wichtige Coccolithophoriden (Flagellata) aus dem norddeutschen Alttertiär. Monatsb. Deutsche Akad. Wiss. Berlin, 9, pp. 758–768.
– (1968). Biostratigraphie des Alttertiärs von Norddeutschland mit Coccolithophoriden. Monatsb. Deutsche Akad. Wiss. Berlin, 10, pp. 220–229.
Loeblich, A. R. and Tappan, H. (1963). Type fixation and validation of certain calcareous nannoplankton genera. Biol. Soc. Washington, Proc. 76, pp. 191–196.
Loeblich, A. R. and Tappan, H. (1966). Annotated index and bibliography of the calcareous nannoplankton. Phycologia, 5, pp. 81–216.
– and – (1968). ibid. II, Journ. Pal., 42, pp. 584–598.
– and – (1969). ibid. III, Journ. Pal., 43, pp. 568–588.
– and – (1970). ibid. IV, Journ. Pal., 44, pp. 558–574.
– and – (1970). ibid. V, Phycologia, 9, pp. 157–174.
– and – (1971). ibid. VI, Phycologia, 10, pp. 315–339.
– and – (1973). ibid. VII, Journ. Pal., 47, pp. 715–759.
Malmgren, B. (1974). Morphometric studies of planktonic foraminifers from the type Danian of southern Scandinavia. Stockh. Contr. Geol., 29.
Marshall, H. G. (1966). Observations on the vertical distribution of coccolithophores in the Northwestern Sargasso Sea. Limn. Oceanogr., 11, pp. 432–435.
Martini, E. (1959a). Der stratigraphische Wert von Nannofossilien im nordwestdeutschen Tertiär. Erdoel und Kohle, 12, pp. 137–140.
– (1959b). Discoasteriden und verwandte Formen in N.W. deutschen Eozän (Coccolithophorida). II Stratigraphische Auswertung. Senck. Leth., 40, pp. 137–157.
– (1961). Nannoplankton aus dem Tertiär und der obersten Kreide von SW-Frankreich. Senck. Leth., 42, pp. 1–41.
– (1964). Ein vollständiges Gehäuse von *Goniolithus fluckigeri* Deflandre, N. Jb. Geol. Pal. Abh., 119, pp. 19–21.
– (1965). Mid-Tertiary calcareous nannoplankton from Pacific deep-sea cores. *In* Whittard, W. F. and Bradshaw, R. B., Submarine geology and geophysics. Proc. 17th Symp. Colston Res. Soc., pp. 393–411.
– (1971). Standard Tertiary and Quaternary calcareous nannoplankton zonation. Proc. Second Plankt. Conf., Rome, 1970, 2, pp. 739–777.
– (1976). Cretaceous to recent calcareous nannoplankton from the central Pacific Ocean (D.S.D.P. Leg 33). *In* Schlanger, S. O., Jackson, E. D. et al., Initial Repts. D.S.D.P., Washington, 33, pp. 383–423.
– (1977). Neue Daten zum Paläozän und Unter-Eozän im südlichen Nordseebecken. Newsl. Stratigr., 6, pp. 97–105.
– and Bramlette, M. N. (1963). Calcareous nannoplankton from the experimental Mohole drilling. Journ. Pal., 37, pp. 845–856.
– and Stradner, H. (1960). *Nannotetraster,* eine stratigrafisch bedeutsame neue Discoasteridengattung. Erdoel Zeitschr., 76, pp. 266–270.
Moshkovitz, S. (1967). First report on the occurrence of nannoplankton in Upper Cretaceous-Paleocene sediments of Israel. Jb. Geol. B.A., 110, pp. 135–168.
– (1974). A new method for observing the same nannofossil specimens both by light microscope and scanning electron microscope and preservation of types. Israel J. Earth sc., 23, pp. 145–147.

Müller, C. (1974). Calcareous nannoplankton, Leg 25 (Western Indian Ocean). *In* Simpson, E. S. W., Schlich, R. et al., Initial Repts. D.S.D.P., Washington, 25, pp. 579–633.
Noël, D. (1960). Revision du genre *Discoaster*. Bull. Soc. d'hist. Nat. l'Afr. Nord, 51, pp. 201–229.
– (1968). Sur les coccolithes du Jurassique Européen et d'Afrique du Nord. Essai de classification des coccolithes fossiles. Ed. C.N.R.S., Paris.
– (1970). Coccolithes Crétacés, la Craie Campanienne du Basin de Paris. C.N.R.S., Paris.
Outka, D. E. and Williams, D. C. (1971). Sequential coccolith morphogenesis in *Hymenomenas carterae*. Journ. Protozool., 18, pp. 285–297.
Paquet, J. (1962). Observaciones geologicas en la Loma de Solana (Sur de Cehegin, Murcia). Notas, Com. Inst. Geol. Min. España, 67, pp. 147–158.
– (1967). Etude géologique de l'Ouest de la province de Murcie (Espagne). Thèse, Lille.
Parke, M. and Adams, I. (1960). The motile (*Crystallolithus hyalinus* Gaarder and Markali) and non-motile phases in the life history of *Coccolithus pelagicus* (Wallich) Schiller. Journ. Mar. Biol. Soc. Ass. U.K., 39, pp. 263–274.
Perch-Nielsen, K. (1967a). Nannofossilien aus dem Eozän von Dänemark. Eclog. Geol. Helv., 60, pp. 19–32.
– (1967b). Eine Präparationstechnik zur Untersuchung von Nannoplankton im Lichtmikroskop. Medd. Dansk Geol. Foren., 17, pp. 129–130.
– (1968). Der Feinbau und die Klassifikation der Coccolithen aus dem Maastrichtien von Dänemark. Kong. Danske Vidensk. Selsk., Biol. Skr., 16, pp. 1–96.
– (1969a). Elektronenmikroskopische Untersuchungen der Coccolithophoriden der Dan-Scholle von Katharinenhof (Fehmarn). N. Jb. Geol. Pal. Abh., 132, pp. 317–332.
– (1969b). Die Coccolithen einiger danischer Maastrichtien- und Danienlokalitäten. Medd. Dansk Geol. Foren., 19, pp. 51–68.
– (1971a). Durchsicht Tertiärer Coccolithen. Proc. Second Plankt. Conf. Rome, 1970, 2, pp. 939–981.
– (1971b). Neue Coccolithen aus dem Paleozän von Dänemark, der Bucht von Biskaya und der Eozän der Labrador See. Bull. Geol. Soc. Denmark, 21, pp. 51–66.
– (1971c). Einige neue Coccolithen aus dem Paleozän der Bucht von Biskaya. Bull. Geol. Soc. Denmark, 20, pp. 347–361.
– (1971d). Elektronmikroskopische Untersuchungen an Coccolithen und verwandte Formen aus dem Eozän von Dänemark. Kong. Danske Vidensk. Selsk. Biol. Skr., 18, pp. 1–76.
– (1972). Remarks on Late Cretaceous to Pleistocene coccoliths from the North Atlantic. *In* Laughton, A. S., Berggren, W. A. et al., Initial Repts. D.S.D.P., Washington, 12, pp. 1003–1069.
– (1973). Danian and Campanian/Maastrichtian Coccoliths from Nûgssuaq, West Greenland. Medd. Dansk Geol. Foren., 22, pp. 79–82.
– (1977). Albian to Pleistocene calcareous nannofossils from the Western South Atlantic, D.S.D.P. Leg 39. *In* Supko, P. R., Perch-Nielsen, K. et al., Initial Repts. D.S.D.P., Washington, 39, pp. 699–823.
– and Franz, H. E. (1977). *Lapideacassis* and *Scampanella,* calcareous nannofossils from the Paleocene at sites 354 and 356, D.S.D.P. Leg 39. *In* Supko, P. R., Perch-Nielsen, K. et al., Initial Repts, D.S.D.P., Washington, 39, pp. 849–862.
– and Pomerol, M. C. (1973). Nannoplancton calcaire à la limite Crétacé-Tertiaire dans le bassin de Mayunga (Madagascar). C.R. Acad. Sc. Paris, 276, pp. 2435–2440.
Percival, S. F. and Fischer, A. G. (1977). Changes in calcareous nannoplankton in the Cretaceous-Tertiary biotic crisis at Zumaya, Spain. Evol. Theory, 2, pp. 1–35.
Prins, B. (1971). Speculations on relations, evolution, and stratigraphic distribution of Discoasters. Proc. Second Plankt. Conf., Rome, 1970, 2, pp. 1017–1039.
Proto Decima, F., Roth, P. H. and Todesco, L. (1975). Nannoplancton calcareo del Paleoceno e dell' Eoceno della Sezione di Possagno. Schweiz. Pal. Abh., 97, pp. 35–161.
–, Medizza, F. and Todesco, L. (1978). Southeastern Atlantic Leg 40 calcareous nannofossils. *In* Bolli, H. M., Ryan, W. B. F. et al., Initial Repts. D.S.D.P., Washington, 40, pp. 571–634.

Radomski, A. (1968). Calcareous nannoplankton zones in the Paleogene of the Western Polish Carpathians. Rocz. Polsk, Towarz. Geol., 38, pp. 544–605.
Reinhardt, P. (1966). Zur Taxionomie und Biostratigraphie des fossilen Nannoplanktons aus dem Malm, der Kreide und dem Alttertiär Mitteleuropas. Freib. Forschungsh., C196, pp. 43–46.
– (1967). Zur Taxionomie und Biostratigraphie der Coccolithineen (Coccolithophoriden) aus dem Eozän Norddeutschlands. Freib. Forsch. H., C 213, pp. 201–241.
Romein, A. J. T. (1975). Lower Cretaceous calcareous nannoplankton from the Calderon and Parra Formations (SE Spain). GUA Papers Geol., 1, 7, pp. 77–88.
– (1977). Calcareous nannofossils from the Cretaceous/Tertiary boundary interval in the Barranco del Gredero (Caravaca, prov. Murcia, S.E. Spain). Proc. Kon. Ned. Akad. Wetensch., B, 80, pp. 256–279.
– (1979). Calcareous nannofossils from the Cretaceous/Tertiary boundary interval in the Nahal Avdat section, Israel. *In* Birkelund, T. and Bromley, R. G., eds., Cretaceous/Tertiary boundary events symposium, Proceed., 2, pp. 202–206.
Rozenkrantz, A. and Rasmussen, H. W. (1960). Guide to excursions nos. A 42 and C 37. Internat. Geol. Congr., Norden, 1960. Th. Sorgenfrei Ed., Copenhagen, 1960.
Roth, P. H. (1973). Calcareous nannofossils – Leg 17, D.S.D.P. *In* Winterer, E. L., Ewing, J. I. et al., Initial Repts. D.S.D.P., Washington, 17, pp. 695–795.
–, Franz, H. E. and Wise, S. W. (1971). Morphological study of selected members of the genus *Spheno-lithus* Deflandre (Incertae Sedis, Tertiary). Proc. Second Plankt. Conf., Rome, 1970, 2, pp. 1099–1119.
– and Berger, W. H. (1975). Distribution and dissolution of coccoliths in the South and Central Pacific. *In* Sliter, W., Bé, A. W. H. and Berger, W. H. (eds.), Dissolution of deep sea carbonates. Spec. Publ. Cushm. Found. Foramin. Res., 13, pp. 87–113.
Round, F. E. (1973). The biology of the algae. Edward Arnold Publ., London, pp. 1–278.
Shafik, S. and Stradner, H. (1971). Nannofossils from the Eastern Desert, Egypt, with reference to Maastrichtian nannofossils from the U.S.S.R. Jb. Geol. B. A., Sonderb. 17, pp. 69–104.
Shaw, S. H. (1947). Southern Palestine, Geological Map, Sheet 3, scale 1 : 250.000 with explanatory notes. Government of Palestine.
Shumenko, S. I. (1976). Mesozoic calcareous nannoplankton of the European part of the U.S.S.R. Ac. Sc. U.S.S.R., Pal. Inst., Publ. office "Nauka", Moscow.
Smit, J. (1977). Discovery of a planktonic foraminiferal association between the *A. mayaroensis* Zone and the *G. eugubina* Zone at the Cretaceous/Tertiary boundary in the Barranco del Gredero (Caravaca, S.E. Spain): a preliminary report. Proc. Kon. Ned. Akad. Wetensch., B, 80, pp. 280–301.
Sorgenfrei, T. (1957). Lexique Stratigraphique International, 1, 2D, Denmark.
Stradner, H. (1959a). Die fossilen Discoasteriden Österreichs, II Teil, Erdoel Zeitschr., 12, pp. 1–19.
– (1959b). First report on the discoasters of the Tertiary of Austria and their stratigraphic use. 5th World Petr. Congr., I, paper 60, pp. 1081–1095.
– (1961). Vorkommen von Nannofossilien in Mesozoicum und Alttertiär. Erdoel Zeitschr., 77, pp. 77–88.
– (1962). Uber neue und wenig bekannte Nannofossilien aus Kreide und Alttertiär. Verh. Geol. B.A., pp. 363–377.
– in Gohrbandt, K. (1963). Zur Gliederung des Paläogen im Helvetikum nördlich Salzburg nach planktonischen Foraminiferen. Mitt. Geol. Ges. Wien, 56, pp. 72–81.
– (1969). The nannofossils of the Eocene Flysch in the Hagenbach Valley (Northern Vienna Woods) Austria. Rocz. Polsk. Towarz. Geol., 39, pp. 403–432.
– and Edwards, R. (1968). Electron microscopic studies on Upper Eocene coccoliths from the Oamaru diatomite, New Zealand. Jb. Geol. B. A., Sonderband, 13, pp. 1–66.
– and Papp, A. (1961). Tertiäre Discoasteriden aus Österreich und deren stratigraphische Bedeutung. Jb. Geol. B. A., Sonderband, 7, pp. 1–160.

Sullivan, F. R. (1964). Lower Tertiary nannoplankton from the California Coast ranges. I. Paleocene. Univ. Calif. Publ. Geol. Sc., 44, pp. 163–228.
– (1965). Lower Tertiary nannoplankton from the California Coast ranges. II Eocene. Univ. Calif. Publ. Geol. Sc., 53, pp. 1–52.
Sylvester-Bradley, P. C. (1977). Biostratigraphical tests of evolutionary theory. *In* Concepts and methods of biostratigraphy, Kauffmann, E. G. and Hazel, J. E., Eds. Dowden, Hutchinson and Ross, Strodsburg, pp. 41–64.
Tan Sin Hok (1927). Over de samenstelling en het ontstaan van krijt en mergelgesteenten van de Molukken. Jaarb. Mijnw. Ned. Indië, 55, pp. 111–122.
– (1927b). Discoasteridae incertae sedis. Kon. Akad. Wetensch., Afd. Natuurk., 36, pp. 1–9.
– (1931). Discoasteridae, Coccolithinae and Radiolaria. Leid. Geol. Med., 5, pp. 92–95.
Thierstein, H. R. and Berger, W. H. (1978). Injection events in Ocean history. Nature, 276, pp. 461–466.
Veen, G. W. van (1969). Geological investigations in the region West of Caravaca, South-Eastern Spain. Thesis, University of Amsterdam.
Verbeek, J. W. (1977). Calcareous nannoplankton biostratigraphy of Middle and Upper Cretaceous deposits in Tunisia, Southern Spain and France. Utrecht Micropal. Bull., 16.
Watabe, N. (1967). Crystallographic analysis of the coccolith of *Coccolithus huxleyi.* Calc. Tiss. Res., 1, pp. 114–121.
– and Wilbur, K. M. (1966). Effects of temperature on growth, calcification, and coccolith form in *Coccolithus huxleyi* (Coccolithineae). Limn. Ocean., 11, pp. 567–575.
Wind, F. H. (1974). Calcareous nannoplankton of the Salt Mountain Limestone (Jackson, Alabama). Trans. Gulf Coast Assoc. Geol. Soc., 24, pp. 327–334.
Wise, S. W. and Constans, R. E. (1976). Mid Eocene planktonic correlations: Northern Italy-Jamaica, W.I. Trans. Gulf Coast Assoc. Geol. Soc., 26, pp. 144–155.
– and Wind, F. H. (1977). Mesozoic and Cenozoic calcareous nannofossils recovered by D.S.D.P. Leg 36 drilling in the Falkland Plateau, Southwest Atlantic sector of the Southern Ocean. *In* Barker, P. F., Dalziel, I. W. D. et al., Initial Repts. D.S.D.P., Washington, 36, pp. 269–503.
Worsley, T. R. (1974). The Cretaceous – Tertiary boundary event in the ocean. Soc. Econ. Pal. Min., Spec. Publ., 20, pp. 94–125.
– and Martini, E. (1970). Late Maastrichtian nannoplankton provinces. Nature, 225, pp. 1242–1243.

Plate 1

Fig. 1 — *Thoracosphaera operculata* Bramlette and Martini, DN 75, Utrecht slide CH 6024, location V –3, –3, sphere without an operculum, 3500 X.

Figs. 2, 3 — *Biscutum castrorum* Black, DN 49, Utrecht slide CH 6025, 2, distal view, location V +5, + 1, 5000 X, 3, proximal view, location V +4, +5, 5000 X.

Figs. 4, 5 — *Neocrepidolithus fossus* (Romein), nov. comb., DN 72, Utrecht slide CH 6026, 4, proximal view, location V +1, +5, 6000 X, 5, distal view, location V +2, –3, 3000 X.

Fig. 6 — *Neocrepidolithus neocrassus* (Perch-Nielsen), nov. comb., DN 55, Utrecht slide CH 6027, location V +2, –7, side view, 6000 X.

Fig. 7 — *Markalius astroporus* (Stradner) Hay and Mohler, SP 590, Utrecht slide T 362, location V +3, +7, proximal view, 6000 X.

Fig. 8 — *Placozygus sigmoides* (Bramlette and Sullivan) nov. comb., SP 590, Utrecht slide CH 6028, location V +6, +2, proximal view, 6000 X.

Fig. 9 — *Biantholithus sparsus* Bramlette and Martini, DN 49, Utrecht slide CH 6025, location V –7, +2, distal view, 3000 X.

Fig. 10 — *Biscutum parvulum* nov. sp., SP 566, Utrecht slide CH 6029, location V –3, –6, partly overgrown coccosphere, 8000 X.

The locations of the specimens are based on an x-y coordinate system from the central V-marking of a 200 mesh copper grid (Hansen et al., 1975).

Plate 1

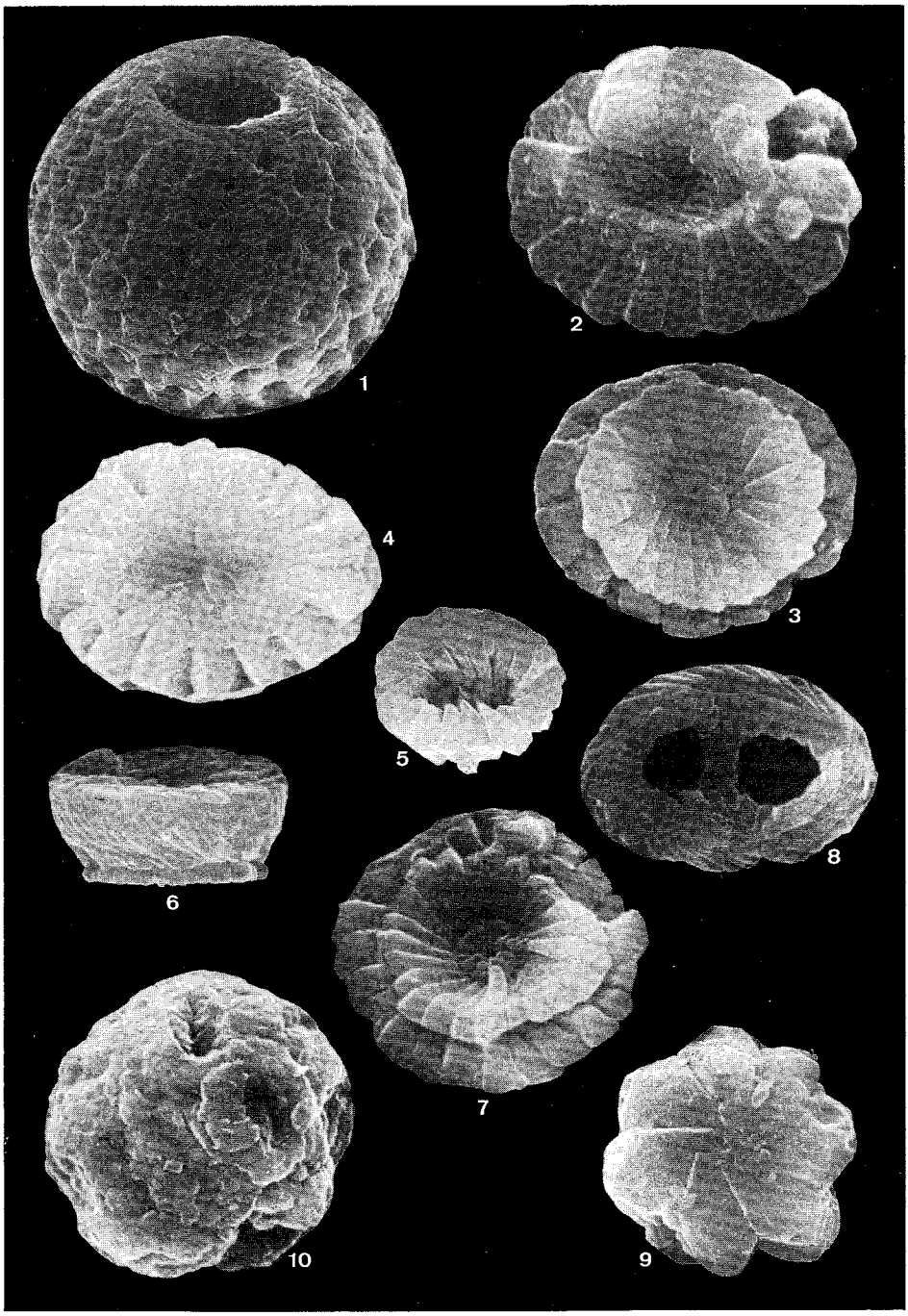

Plate 2

Figs. 1, 2 — *Biscutum parvulum* nov. sp., SP 566, 1, holotype T 359a, Utrecht slide T 359, location V +5, −2, distal view, 14000 X, 2, paratypoid, T 359b, Utrecht slide T 359, location V −3, +4, distal view, 14000 X.

Fig. 3 — *Braarudosphaera alta* nov. sp., SP 566, holotype T 360, Utrecht slide T 360, location V +1, −6, oblique distal (proximal) view, 6000 X.

Figs. 4, 5 — *Ericsonia cava* (Hay and Mohler) Perch-Nielsen, 4, SP 601, Utrecht slide CH 6030, location V +4, +6, distal view, 6000 X, 5, DN 79, Utrecht slide CH 5816, location V + 5, −1, proximal view, 6000 X.

Fig. 6 — *Ericsonia subpertusa* Hay and Mohler, SP 626, Utrecht slide CH 6032, location V +7, −1, distal view, 6000 X.

Fig. 7, 8 — *Cruciplacolithus edwardsii* nov. sp., 7, SP 590, holotype T 361, Utrecht slide T 361, location V +3, −2, distal view, 8000 X, 8, SP 590, paratypoid, T 362, Utrecht slide T 362, location V +7, +1, proximal view, 8000 X.

Plate 2

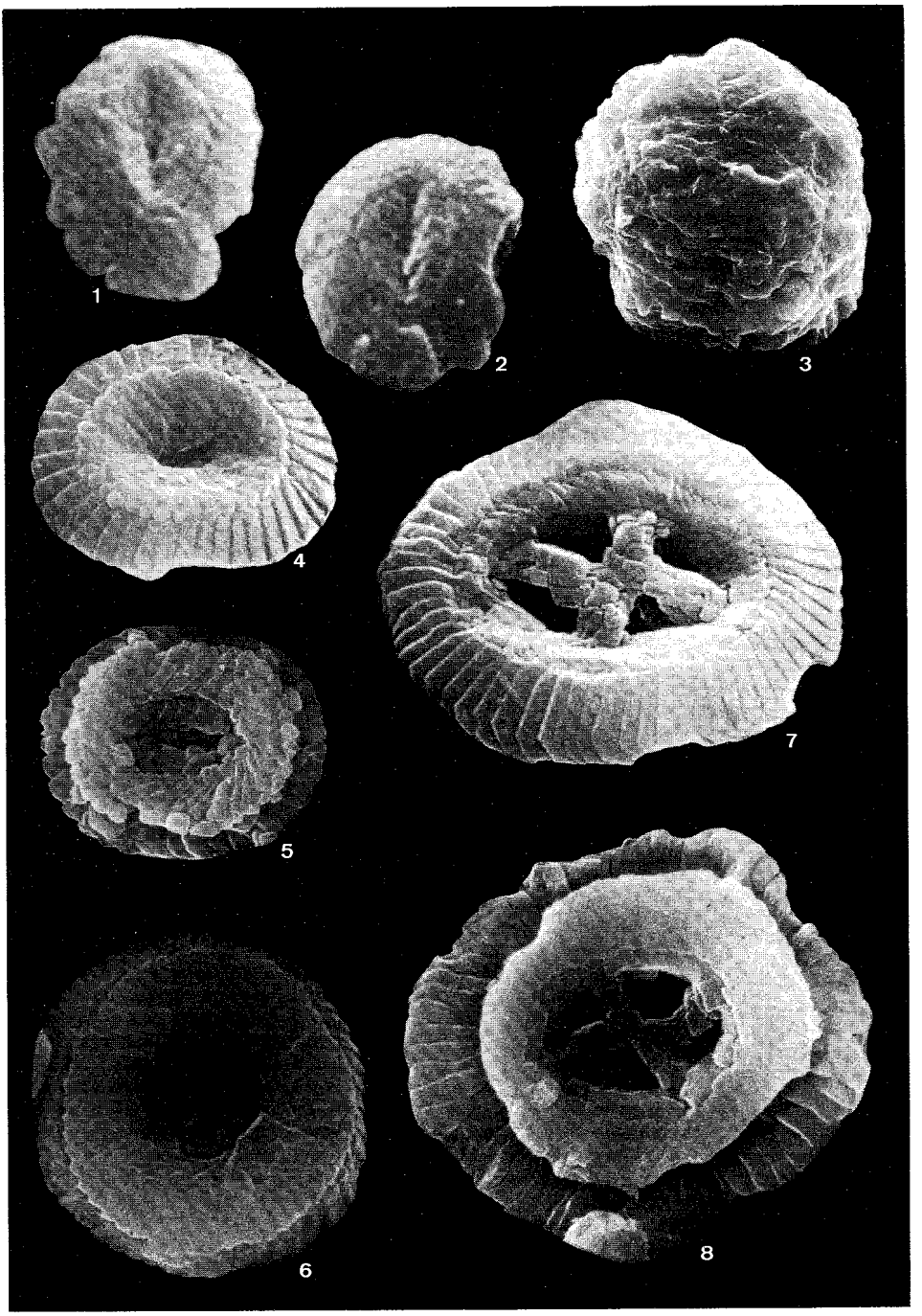

Plate 3

Fig. 1 — *Chiasmolithus danicus* (Brotzen) Bramlette and Martini, DN 75, Utrecht slide CH 6024, location V +7, –2, distal view, 6000 X.

Fig. 2 — *Chiasmolithus eograndis* Perch-Nielsen, IR 131, Utrecht slide CH 6033, location V +1, –1, proximal view, 5000 X.

Figs. 3–6 — *Prinsius dimorphosus* (Perch-Nielsen) Perch-Nielsen, 3, SP 590, Utrecht slide CH 6034, location V +1, +1, coccosphere of *P. dimorphosus* type 1, 5000 X, 4, SP 590, Utrecht slide T 361, location V +4, –1, coccosphere of *P. dimorphosus* type 1, centro-distal cycle broken out in several coccoliths, 3500 X, 5, DN 79, Utrecht slide CH 6031, location V +3, +1, distal view of specimen of *P. dimorphosus* type 2, 14000 X, 6, SP 566, Utrecht slide T 361, location V –3, +6, proximal view, note the presence of three cycles, 12000 X.

Figs. 7, 8 — *Prinsius martinii* (Perch-Nielsen) Haq, DN 79, 7, Utrecht slide CH 6031, location V –2, +2, distal view, 6000 X, 8, Utrecht slide CH 6031, location V +7, +2, proximal view, 10.000 X.

Fig. 9 — *Toweius pertusus* (Sullivan) nov. comb., SP 626, Utrecht slide CH 6035, location V +2, +7, proximal view, 6000 X.

Plate 3

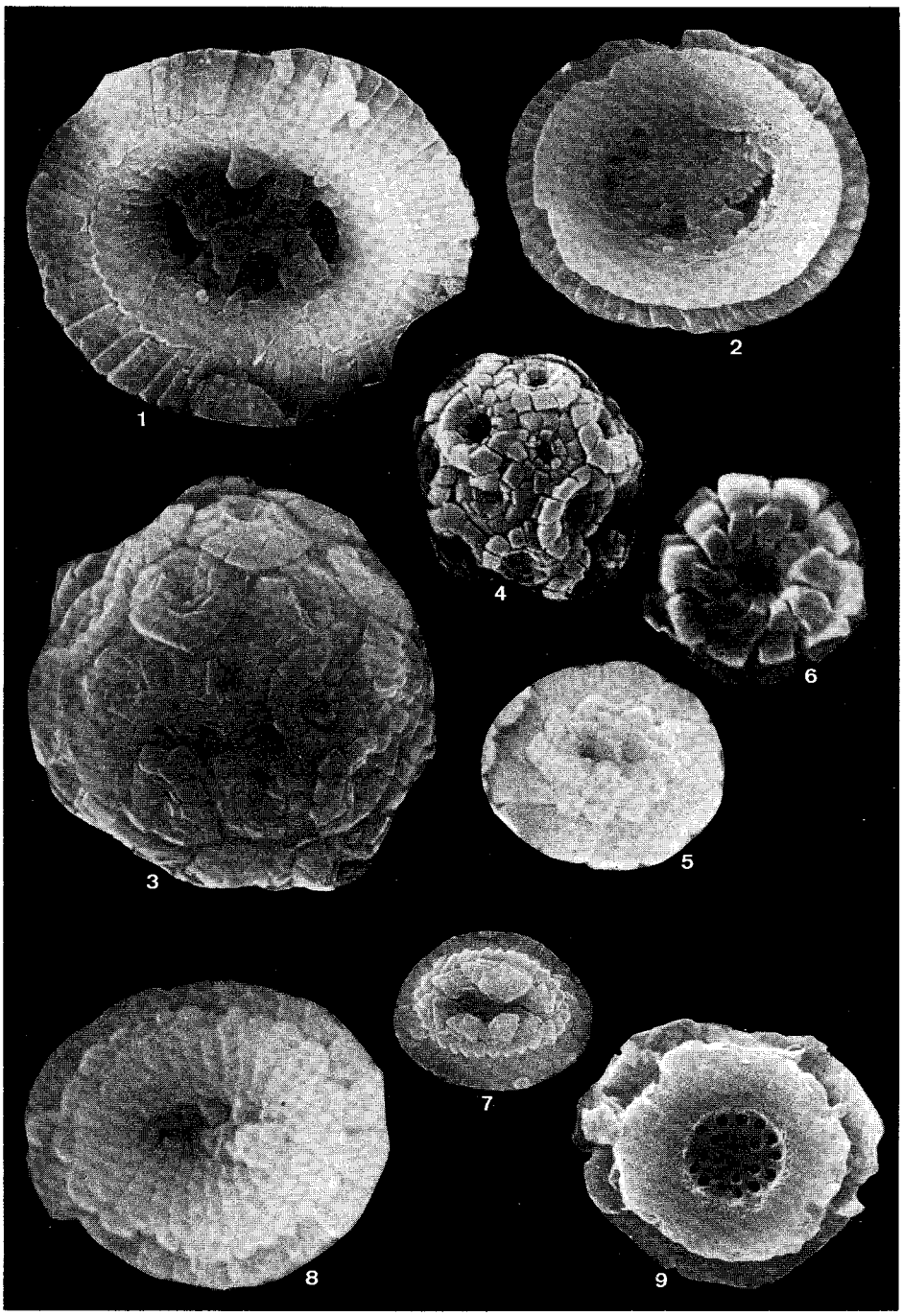

Plate 4

Fig. 1 *Toweius eminens* (Bramlette and Sullivan) Gartner s.l., SP 626, Utrecht slide CH 6035, location V +2, +7, proximal view, 10.000 X.

Figs. 2, 3 *Toweius magnicrassus* (Bukry) nov. comb., 2, SP 653, Utrecht slide CH 6036, location V −8, +2, distal view, 6000 X, 3, SP 638, Utrecht slide CH 6037, location V −1, +3, proximal view, 6000 X.

Figs. 4, 5 *Toweius gammation* (Bramlette and Sullivan) nov. comb., 4, IR 132, Utrecht slide CH 6038, location V +3, +3, distal view, 6000 X, 5, IR 135, Utrecht slide CH 6039, location V −4, −3, proximal view, 6000 X.

Fig. 6 *Reticulofenestra dictyoda* (Deflandre and Fert) Stradner, SP 674, Utrecht slide CH 6040, location V −1, +3, distal view, central area overgrown, note the bend in the sutures in the distal shield, 6000 X.

Fig. 7 *Fasciculithus ulii* Perch-Nielsen, SP 612, Utrecht slide CH 6041, location V +2, −6, oblique distal view, 6000 X.

Plate 4

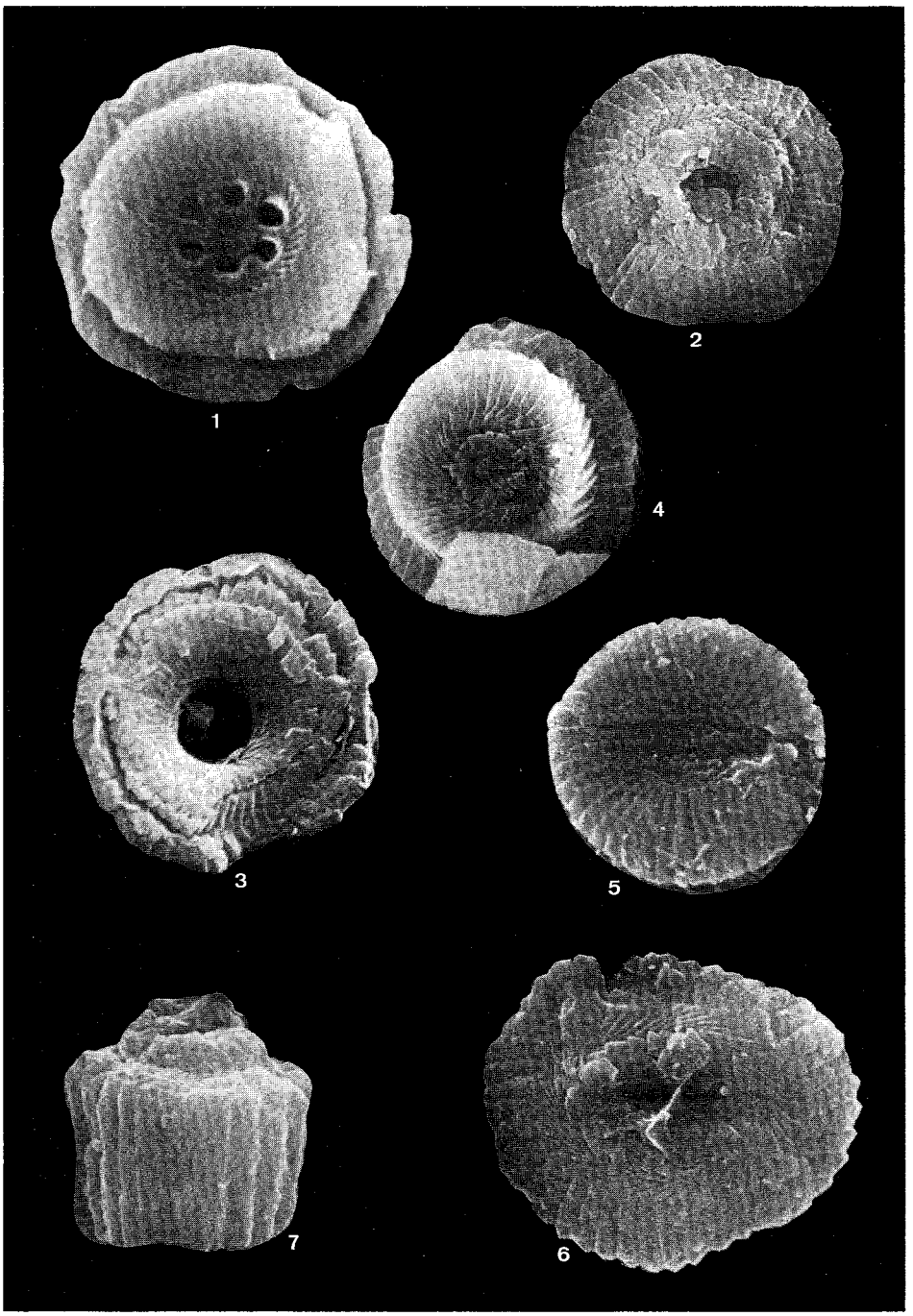

Plate 5

Fig. 1 — *Fasciculithus janii* Perch-Nielsen, SP 624, Utrecht slide CH 6042, location V –8, –4, oblique distal view, 6000 X.

Fig. 2 — *Fasciculithus schaubii* Hay and Mohler, SP 626, Utrecht slide CH 6043, location V +6, +4, interior of a damaged specimen in side view, 6000 X.

Fig. 3 — *Fasciculithus lillianae* Perch-Nielsen, SP 626, Utrecht slide CH 6032, location V +5, –3, side view, 6000 X.

Figs. 4, 5 — *Fasciculithus involutus* Bramlette and Sullivan, SP 626, Utrecht slide CH 6035, location V –4, –2, 4, oblique distal view, 6000 X, 5, distal view of the same specimen, 6000 X.

Fig. 6 — *Heliolithus elegans* (Roth) nov. comb., SP 615, Utrecht slide CH 6044, location V +7, +1, side view, 5000 X.

Figs. 7, 8 — *Heliolithus megastypus* (Bramlette and Sullivan) nov. comb., IR 101, Utrecht slide CH 6045, location V +1, –1, 7, oblique distal view, 6000 X, 8, distal view of the same specimen, 6000 X.

Fig. 9 — *Discoaster mohleri* Bukry and Percival, SP 623, Utrecht slide CH 6046, location V +5, +3, proximal view, 6000 X.

Plate 5

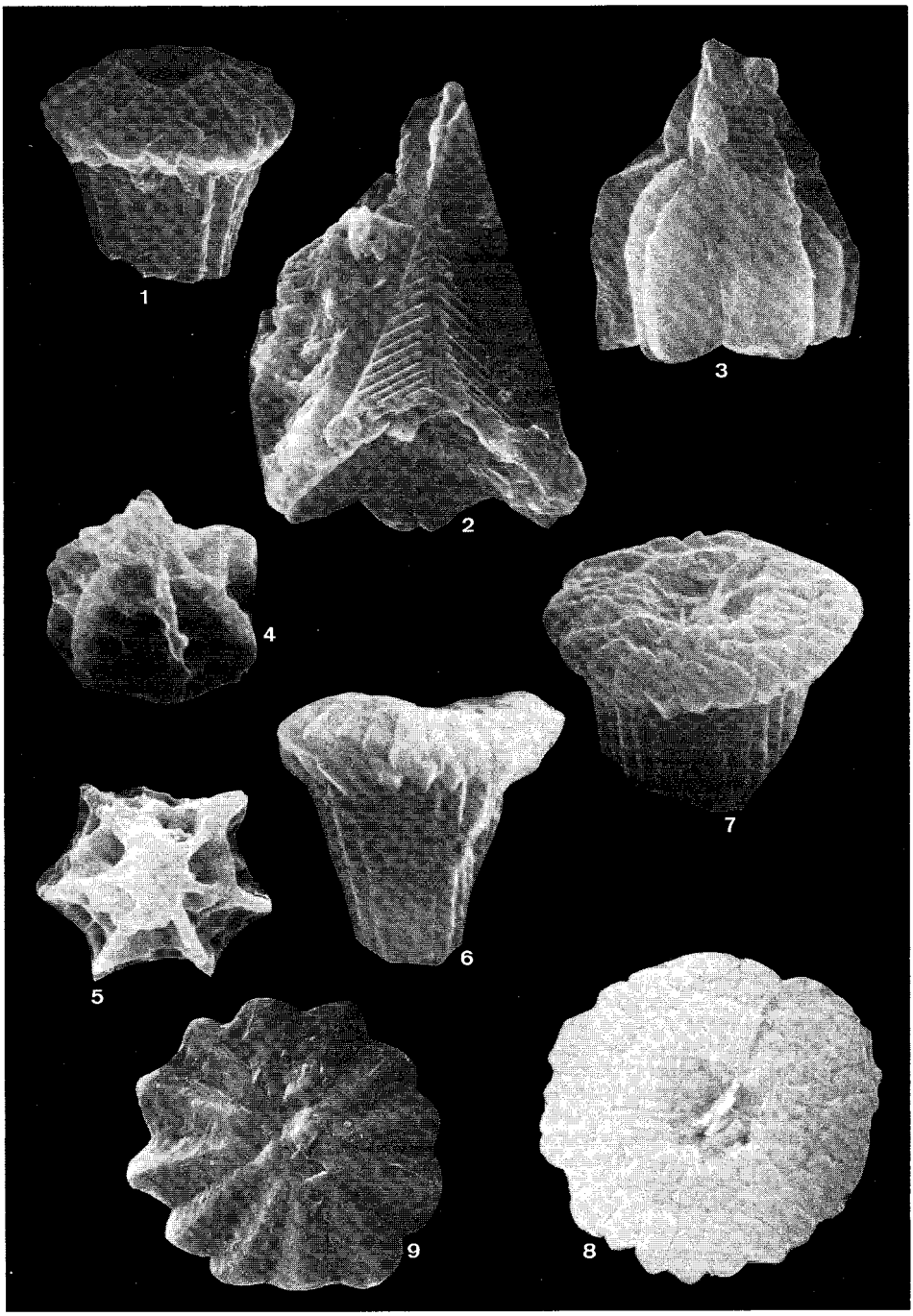

Plate 6

Figs. 1–3 *Discoaster multiradiatus* Bramlette and Riedel, 1, SP 626, Utrecht slide CH 6047, location V +4, –3, distal view, 6000 X, 2, SP 626, Utrecht slide CH 6048, location V +4, +3, distal view, 6000 X, 3, SP 630, Utrecht slide CH 6049, location V –4, –2, oblique distal view, 6000 X.

Fig. 4 *Discoaster perpolitus* Martini, SP 626, Utrecht slide CH 6050, location V +1, +1, proximal view, 6000 X.

Fig. 5 *Discolithina rimosa* (Bramlette and Sullivan) Levin and Joerger, SP 626, Utrecht slide CH 6043, location V –5, –2, distal view, 5000 X.

Fig. 6 *Scapholithus apertus* Hay and Mohler, SP 626, Utrecht slide CH 6050, location V +7, +1, proximal, view, 6000 X.

Figs. 7, 8 *Discoaster araneus* Bukry, 7, SP 630, Utrecht slide CH 6049, location V +2, +2, 3000 X, 8, SP 629, Utrecht slide CH 6051, location V +5, +4, 3000 X.

Plate 6

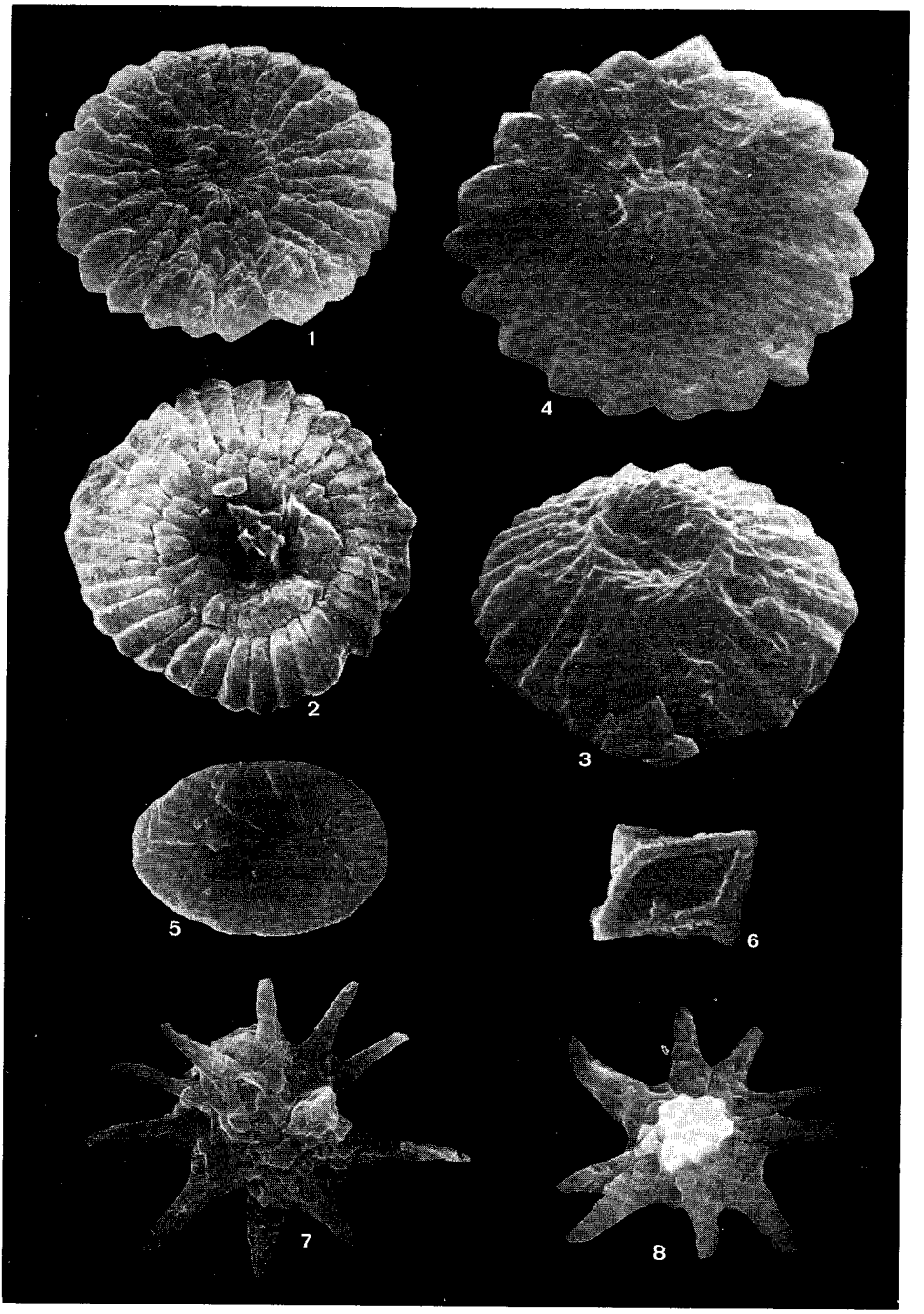

Plate 7

Fig. 1 — *Discoaster barbadiensis* Tan Sin Hok, SP 653, Utrecht slide CH 6052, location V −4, +6, proximal view, 5000 X.

Fig. 2 — *Discoaster binodosus* Martini, IR 132, Utrecht slide CH 6047, location V −1, −3, distal view, 3000 X.

Figs. 3, 4 — *Rhomboaster bitrifida* nov. sp., 3, IR 107, Utrecht slide CH 6053, location V −2, −4, early type, 5000 X, 4, SP 630, Utrecht slide T 363, location V +5, +3, holotype T 363, 3000 X.

Fig. 5 — *Rhomboaster calcitrapa* Gartner, SP 629, Utrecht slide CH 6051, location V +5, +7, 4000 X.

Fig. 6 — *Tribrachiatus spineus* (Shafik and Stradner) nov. comb., SP 629, Utrecht slide CH 6051, location V +4, +6, 2500 X.

Fig. 7 — *Semiholodithus biskayae* Perch-Nielsen, SP 626, Utrecht slide CH 6054, location V −3, −4, side view, 5000 X.

Fig. 8 — *Lapideacassis blackii* Perch-Nielsen, SP 626, Utrecht slide CH 6043, location V +4, −4, side view, 1200 X.

Fig. 9 — *Sphenolithus radians* Deflandre, IR 132, Utrecht slide CH 6038, location V −1, +6, side view, 6000 X.

Plate 7

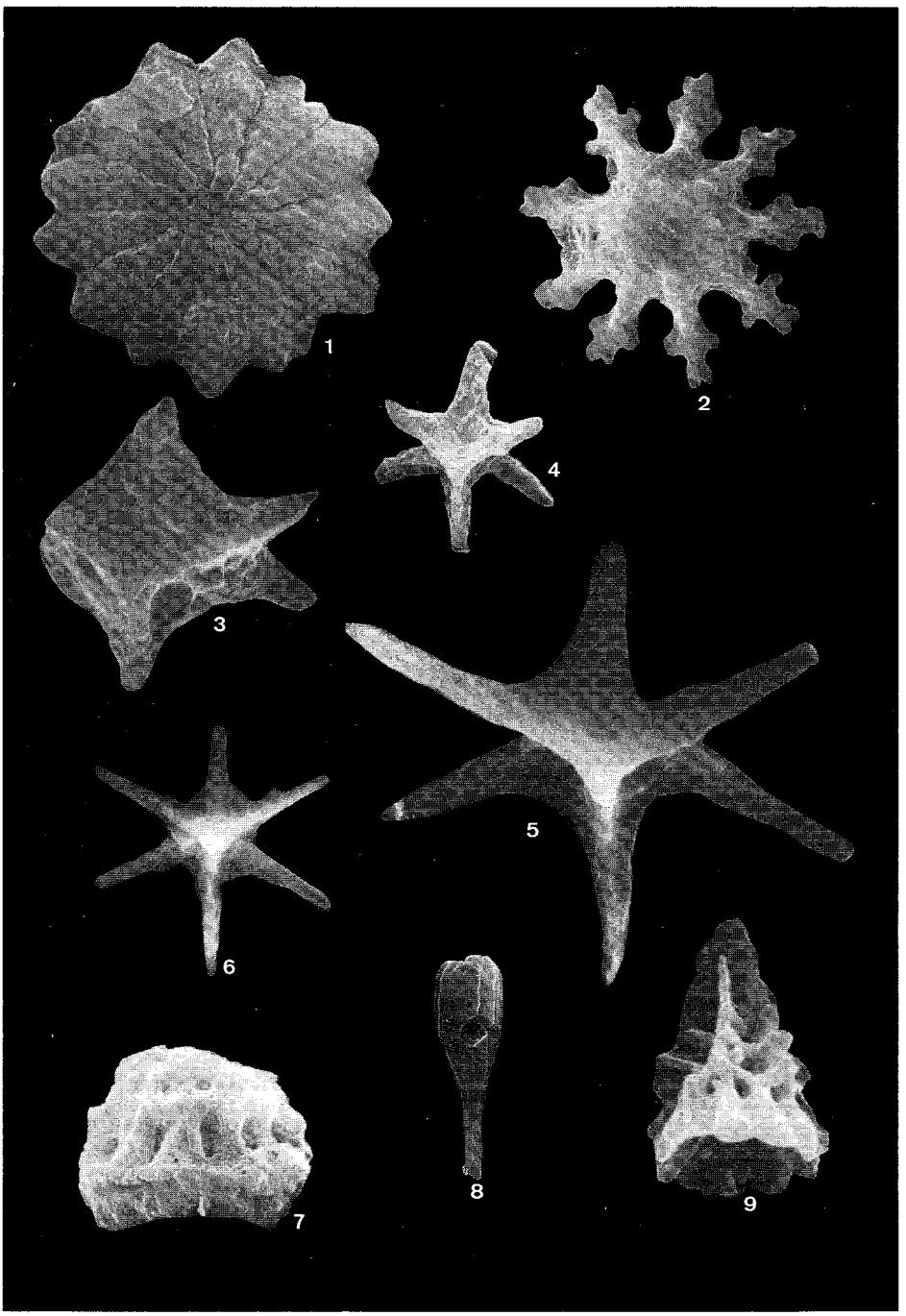

Plate 8

Fig. 1 *Pedinocyclus larvalis* (Bukry and Bramlette) Loeblich and Tappan, SP 673, Utrecht slide CH 6055, location V +5, +5, 6000 X.

Fig. 2 *Pontosphaera pulchra* (Deflandre) nov. comb., IR 132, Utrecht slide CH 6038, location V −3, +3, proximal view, 6000 X.

Fig. 3 *Cyclolithella pactilis* Bukry and Percival, SP 648, Utrecht slide CH 6056, location V +4, −7, distal view, 6000 X.

Fig. 4 *Lophodolithus nascens* Bramlette and Sullivan, IR 131, Utrecht slide CH 6033, location V +7, −5, proximal view, 6000 X.

Fig. 5 *Chiphragmalithus?* sp., SP 653, Utrecht slide CH 6036, location V +5, +7, side view, 6000 X.

Plate 8

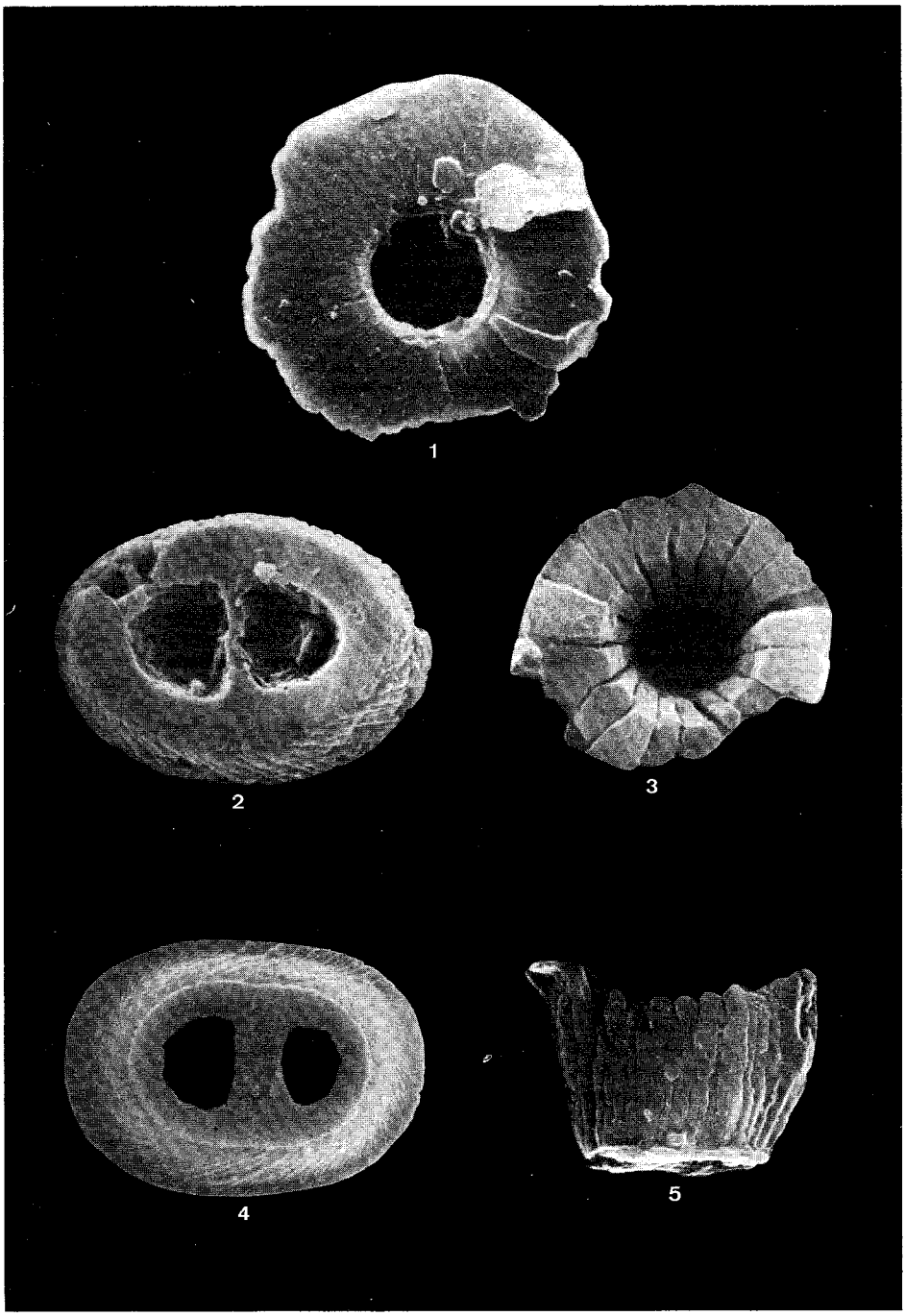

Plate 9

Fig. 1 *Biscutum castrorum* Black, DN 49, Utrecht slide CH 6057, distal view, 2500 X.

Figs. 2, 3 *Braarudosphaera alta* nov. sp., SP 566, 2, Utrecht slide T 364, location 1FK4, paratypoid T 364a, distal (proximal view), 2000 X, 3, Utrecht slide T 364, location 2GS2, paratypoid T 364b, side view, 2000 X.

Fig. 4 *Neocrepidolithus fossus* (Romein), nov. comb., DN 76, Utrecht slide CH 6058, proximal view, 3500 X.

Fig. 5 *Neocrepidolithus neocrassus* (Perch-Nielsen), nov. comb., SP 573, Utrecht slide CH 6059, proximal view of a specimen with a cross-like central structure, 1500 X.

Fig. 6 *Cruciplacolithus frequens* (Perch-Nielsen), nov. comb., IR 104, Utrecht slide CH 6060, proximal view, 1500 X.

Figs. 7, 8 *Cruciplacolithus latipons* nov. sp., SP 614, 7, Utrecht slide T 365, location 6QP3, holotype T 365a, distal view, 2500 X, 8, Utrecht slide T 365, location 7JC2, paratypoid T 365b, proximal view, 1800 X.

Figs. 9, 10 *Cruciplacolithus edwardsii* nov. sp., SP 590, 9, Utrecht slide T 366, location 8OR4, paratypoid T 366a, proximal view, 2500 X, 10, Utrecht slide T 366, location 3FG4, paratypoid T 366b, distal view, 2500 X.

Fig. 11 *Lapideacassis blackii* Perch-Nielsen, SP 623, Utrecht slide CH 6061, side view, 1500 X.

Figs. 12, 13 *Fasciculithus magnicordis* nov. sp., SP 609, 12, Utrecht slide T 367, location 9VQ4, holotype T 367a, side view, 1500 X, 13, Utrecht slide T 367, location 9VQ4, paratypoid T 367b, side view, 2500 X.

Fig. 14 *Fasciculithus magnus* Bukry and Percival, SP 608, Utrecht slide CH 6062, side view, 2500 X.

Fig. 15 *Fasciculithus bitectus* nov. sp., IR 85, Utrecht slide T 368, location 10 QO4, holotype T 368a, side view, 25000 X.

The locations of the specimens are based on a "cell finder culture slide" coordinate system (model Leiden 1974, microlab. Holland).

Plate 9

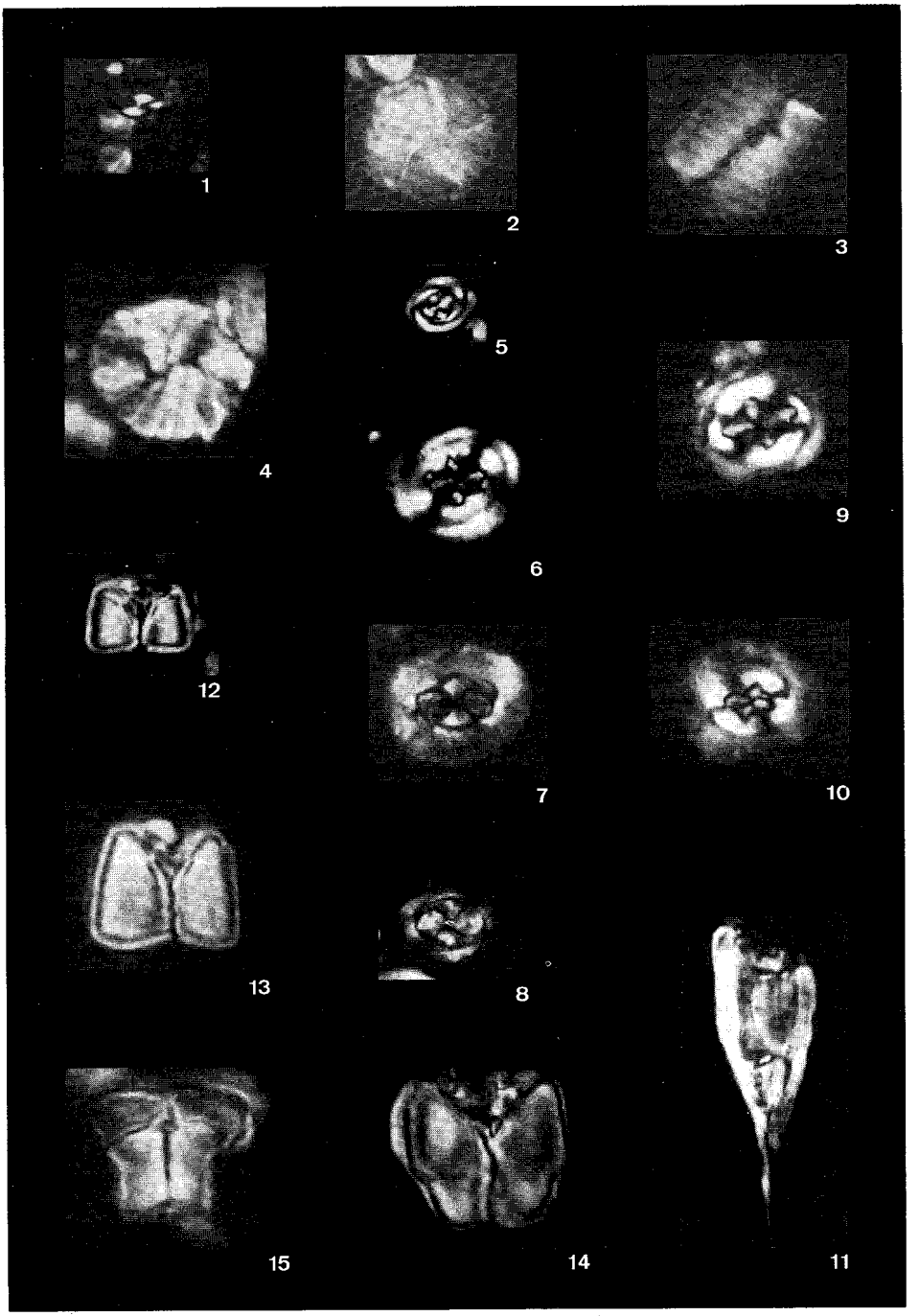

Plate 10

Fig. 1 — *Heliolithus elegans* (Roth) nov. comb., IR 106, Utrecht slide CH 6063, side view, 1500 X.

Fig. 2 — *Heliolithus cantabriae* Perch-Nielsen, IR 102, Utrecht slide CH 6064, side view, 1500 X.

Figs. 3, 4 — *Zygodiscus clausus* nov. sp., SP 619, 3, Utrecht slide T 369, location 5PO3, holotype T 369a, distal view, 1000 X, 4, SP 619, Utrecht slide T 369, location 6ZO4, paratypoid T 369b, distal view, 15000 X.

Fig. 5 — *Zygodiscus adamas* Bramlette and Sullivan, SP 619, Utrecht slide CH 6065, distal view, 1500 X.

Fig. 6 — *Zygodiscus plectopons* Bramlette and Sullivan, IR 123, Utrecht slide CH 6066, proximal view, 1500 X.

Figs. 7–9 — *Rhomboaster intermedia* nov. sp., SP 624, 7, Utrecht slide T 370, location 8ZR4, holotype T 370a, high focus, 2500 X, 8, same specimen, low focus, 2500 X, 9, Utrecht slide T 370, location 8ZE1, paratypoid T 370b, high focus, 2500 X.

Figs. 10–13 — *Rhomboaster bitrifida* nov. sp., SP 630, 10, Utrecht slide T 371, location 7QK2, paratypoid T 371a, high focus, 3000 X, 11, same specimen, low focus, 3000 X, 12, Utrecht slide T 371, location 6HJ3, paratypoid, specimen with relatively short arms, high focus, 3000 X, 13, same specimen, low focus, 3000 X.

Fig. 14 — *Ericsonia universa* (Wind and Wise) nov. comb., IR 100, Utrecht slide CH 6067, proximal view, 1500 X.

Fig. 15 — *Tribrachiatus contortus* (Stradner) Bukry, IR111, Utrecht slide CH 6068, 1500 X.

Plate 10

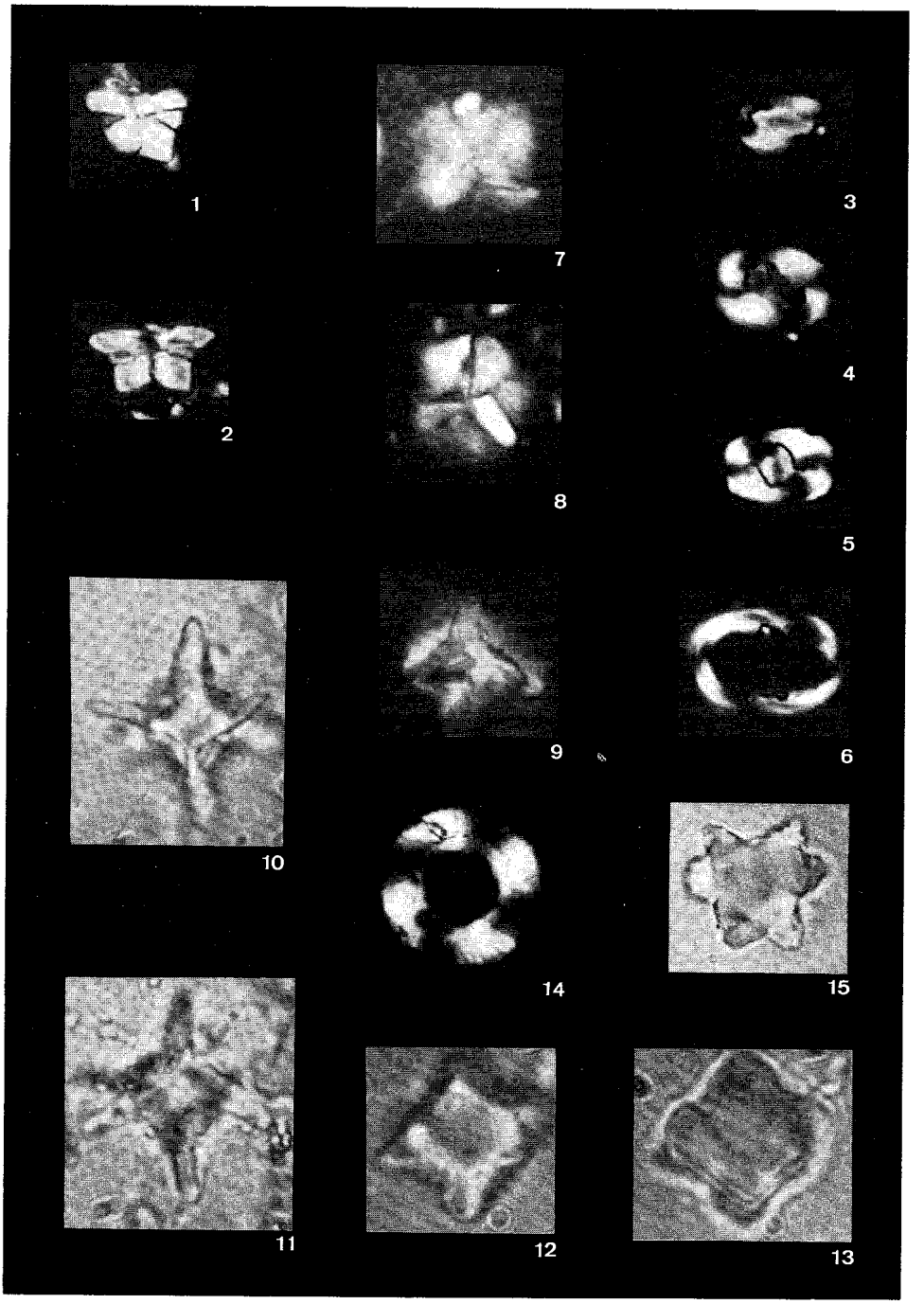

INDEX

Species listed in alphabetical order

Bull. 15. Z. REISS, S. LEUTENEGGER, L. HOTTINGER, W. J. J. FERMONT, J. E. MEULENKAMP, E. THOMAS, H. J. HANSEN, B. BUCHARDT, A. R. LARSEN and C. W. DROOGER – Depth-relations of Recent larger foraminifera in the Gulf of Aqaba-Elat. 244 p., 3 pl., 117 figs. (1977) *f* 53,–

Bull. 16. J. W. VERBEEK – Calcareous nannoplankton biostratigraphy of Middle and Upper Cretaceous deposits in Tunisia, Southern Spain and France. 157 p., 12 pl., 22 figs. (1977) *f* 51,–

Bull. 17. W. J. ZACHARIASSE, W. R. RIEDEL, A. SANFILIPPO, R. R. SCHMIDT, M. J. BROLSMA, H. J. SCHRADER, R. GERSONDE, M. M. DROOGER and J. A. BROEKMAN – Micropaleontological counting methods and techniques – an exercise on an eight metres section of the Lower Pliocene of Capo Rossello, Sicily. 265 p., 23 pl., 95 figs. (1978) *f* 59,–

Bull. 18. M. J. BROLSMA – Quantitative foraminiferal analysis and environmental interpretation of the Pliocene and topmost Miocene on the south coast of Sicily. 159 p., 8 pl., 50 figs. (1978) *f* 49,–

Bull. 19. E. J. VAN VESSEM – Study of Lepidocyclinidae from South-East Asia, particularly from Java and Borneo. 163 p., 10 pl., 84 figs. (1978) *f* 53,–

Bull. 20. J. HAGEMAN – Benthic foraminiferal assemblages from the Plio-Pleistocene open bay to lagoonal sediments of the Western Peloponnesus (Greece). 171 p., 10 pl., 28 figs. (1979) *f* 54,–

Bull. 21. C. W. DROOGER, J. E. MEULENKAMP, C. G. LANGEREIS, A. A. H. WONDERS, G. J. VAN DER ZWAAN, M. M. DROOGER, D. S. N. RAJU, P. H. DOEVEN, W. J. ZACHARIASSE, R. R. SCHMIDT and J. D. A. ZIJDERVELD – Problems of detailed biostratigraphic and magnetostratigraphic correlations in the Potamidha and Apostoli sections of the Cretan Miocene. 222 p., 7 pl., 74 figs. (1979) *f* 57,–

Bull. 22. A. J. T. ROMEIN – Evolutionary lineages in Early Paleogene calcareous nannoplankton. 231 pp., 10 pl., 50 figs. (1979) *f* 64,–

Bull. 23. E. THOMAS – Details of *Uvigerina* development in the Cretan Mio-Pliocene. (1980) price not yet established

Bull. 24. A. A. H. WONDERS – Planktonic foraminifera of the Middle and Late Cretaceous of the Western Mediterranean area. (1980) price not yet established

Spec. Publ. 1. A. A. BOSMA – Rodent biostratigraphy of the Eocene-Oligocene transitional strata of the Isle of Wight. 128 p., 7 pl., 38 figs. (1974) *f* 43,–

Spec. Publ. 2. A. VAN DE WEERD – Rodent faunas of the Mio-Pliocene continental sediments of the Teruel – Alfambra region, Spain. 217 p., 16 pl., 30 figs. (1976) *f* 63,–

Sales office U.M.B.: Singel 105, 3984 NX Odijk, Netherlands
Postal account: 3028890, T. van Schaik, Odijk
Bank account: 55 89 19 855, Alg. Bank Nederland, T. van Schaik, Odijk

After *prepayment* to the sales office on one of the above accounts, the books will be sent by surface mail without further charges. Orders for these books not directly from the purchaser to the sales office may cause much higher costs to the purchaser.